ISSN 0021-9673

VOL. 586 NO. 2 NOVEMBER 22, 1991

JOURNAL OF CHROMATOGRAPHY

INCLUDING ELECTROPHORESIS AND OTHER SEPARATION METHODS

ELSEVIER

JOURNAL OF CHROMATOGRAPHY

INCLUDING ELECTROPHORESIS AND OTHER SEPARATION METHODS

Scope. The *Journal of Chromatography* publishes papers on all aspects of chromatography, electrophoresis and related methods. Contributions consist mainly of research papers dealing with chromatographic theory, instrumental development and their applications. The section *Biomedical Applications*, which is under separate editorship, deals with the following aspects: developments in and applications of chromatographic and electrophoretic techniques related to clinical diagnosis or alterations during medical treatment; screening and profiling of body fluids or tissues with special reference to metabolic disorders; results from basic medical research with direct consequences in clinical practice; drug level monitoring and pharmacokinetic studies; clinical toxicology; analytical studies in occupational medicine.

Submission of Papers. Manuscripts (in English; *four* copies are required) should be submitted to: Editorial Office of *Journal of Chromatography*, P.O. Box 681, 1000 AR Amsterdam, Netherlands, Telefax (+31-20) 5862 304, or to: The Editor of *Journal of Chromatography, Biomedical Applications*, P.O. Box 681, 1000 AR Amsterdam, Netherlands. Review articles are invited or proposed by letter to the Editors. An outline of the proposed review should first be forwarded to the Editors for preliminary discussion prior to preparation. Submission of an article is understood to imply that the article is original and unpublished and is not being considered for publication elsewhere. For copyright regulations, see below.

Publication. The *Journal of Chromatography* (incl. *Biomedical Applications*) has 39 volumes in 1992. The subscription prices for 1992 are:

J. Chromatogr. (incl. *Cum. Indexes, Vols. 551–600*) + *Biomed. Appl.* (Vols. 573–611):
Dfl. 7722.00 plus Dfl. 1209.00 (p.p.h.) (total *ca.* US$ 4421.25)

J. Chromatogr. (incl. *Cum. Indexes, Vols. 551–600*) only (Vols. 585–611):
Dfl. 6210.00 plus Dfl. 837.00 (p.p.h.) (total *ca.* US$ 3488.50)

Biomed. Appl. only (Vols. 573–584):
Dfl. 2760.00 plus Dfl. 372.00 (p.p.h.) (total *ca.* US$ 1550.50).

Subscription Orders. The Dutch guilder price is definitive. The US$ price is subject to exchange-rate fluctuations and is given as a guide. Subscriptions are accepted on a prepaid basis only, unless different terms have been previously agreed upon. Subscriptions orders can be entered only by calender year (Jan.–Dec.) and should be sent to Elsevier Science Publishers, Journal Department, P.O. Box 211, 1000 AE Amsterdam, Netherlands, Tel. (+31-20) 5803 642, Telefax (+31-20) 5803 598, or to your usual subscription agent. Postage and handling charges include surface delivery except to the following countries where air delivery via SAL (Surface Air Lift) mail is ensured: Argentina, Australia, Brazil, Canada, Hong Kong, India, Israel, Japan*, Malaysia, Mexico, New Zealand, Pakistan, PR CHina, Singapore, South Africa, South Korea, Taiwan, Thailand, USA. *For Japan air delivery (SAL) requires 25% additional charge of the normal postage and handling charge. For all other countries airmail rates are available upon request. Claims for missing issues must be made within three months of our publication (mailing) date, otherwise such claims cannot be honoured free of charge. Back volumes of the *Journal of Chromatography* (Vols. 1–572) are available at Dfl. 208.00 (plus postage). Customers in the USA and Canada wishing information on this and other Elsevier journals, please contact Journal Information Center, Elsevier Science Publishing Co. Inc., 655 Avenue of the Americas, New York, NY 10010, USA, Tel. (+1-212) 633 3750, Telefax (+1-212) 633 3990.

Abstracts/Contents Lists published in Analytical Abstracts, Biochemical Abstracts, Biological Abstracts, Chemical Abstracts, Chemical Titles, Chromatography Abstracts, Clinical Chemistry Lookout, Current Contents/Life Sciences, Current Contents/Physical, Chemical & Earth Sciences, Deep-Sea Research/Part B: Oceanographic Literature Review, Excerpta Medica, Index Medicus, Mass Spectrometry Bulletin, PASCAL-CNRS, Pharmaceutical Abstracts, Referativnyi Zhurnal, Research Alert, Science Citation Index and Trends in Biotechnology.

See inside back cover for Publication Schedule, Information for Authors and information on Advertisements.

0021-9673/91/$03.50

This issue is printed on acid-free paper.

Printed in the Netherlands

CONTENTS

(Abstracts/Contents Lists published in Analytical Abstracts, Biochemical Abstracts, Biological Abstracts, Chemical Abstracts, Chemical Titles, Chromatography Abstracts, Current Contents/Life Sciences, Current Contents/Physical, Chemical & Earth Sciences, Deep-Sea Research/Part B: Oceanographic Literature Review, Excerpta Medica, Index Medicus, Mass Spectrometry Bulletin, PASCAL-CRNS, Referativnyi Zhurnal, Research Alert and Science Citation Index)

REVIEWS

REGULAR PAPERS

Column Liquid Chromatography

Gas Chromatography

(Continued overleaf)

In articles with more than one author, the name of the author to whom correspondence should be addressed is indicated in the article heading by a 6-pointed asterisk (*).

Journal of Chromatography Library, 50

Liquid Chromatography in Biomedical Analysis

edited by **T. Hanai,** *International Institute of Technological Analysis, Health Research Foundation, Kyoto, Japan*

This book presents a guide for the analysis of biomedically important compounds using modern liquid chromatographic techniques. After a brief summary of basic liquid chromatographic methods and optimization strategies, the main part of the book focuses on the various classes of biomedically important compounds: amino acids, catecholamines, carbohydrates, fatty acids, nucleotides, porphyrins, prostaglandins and steroid hormones. The different chapters discuss specialized techniques pertaining to each class of compounds, such as sample pretreatment, pre- and post-column derivatization, detection and quantification.

1991 xii + 296 pages
Price: US $ 138.50 / Dfl. 270.00
ISBN 0-444-87451-8

Contents:

Elsevier Science Publishers

P.O. Box 211, 1000 AE Amsterdam, The Netherlands
P.O. Box 882, Madison Square Station, New York, NY 10159, USA

Selective Sample Handling and Detection in High-Performance Liquid Chromatography

Journal of Chromatography Library, 39

part A

edited by **R.W. Frei**†, *Free University, Amsterdam, The Netherlands, and* **K. Zech**, *Byk Gulden Pharmaceuticals, Konstanz, FRG*

Part A of this two-volume project attempts to treat the sample handling and detection processes in a liquid chromatographic system in an integrated fashion. The need for more selective and sensitive chromatographic methods to help solve the numerous trace analysis problems in complex samples is undisputed. However, few workers realize the strong interdependence of the various steps - sample handling, separation and detection - which must be considered if one wants to arrive at an optimal solution. By introducing a strong element of selectivity and trace enrich- ment in the sample preparation step, fewer demands are placed on the quality of the chromatography and often a simple UV detector can be used. By using a selective detection mode, i.e. a reaction detector, the sample handling step can frequently be simplified and more easily automated. The impact of such a "total system" approach on handling series of highly complex samples such as environmental specimens or biological fluids can be easily imagined.

1988 xii + 458 pages
US$ 123.00 / Dfl. 240.00
ISBN 0-444-42881-X

part B

edited by **K. Zech**, *Byk Gulden Pharmaceuticals, Konstanz, FRG, and* **R.W. Frei**†, *Free University, Amsterdam, The Netherlands*

Part B completes the treatment of the handling, separation and detection of complex samples as an integrated, interconnected process. On the basis of this philosophy the editors have selected those contributions which demonstrate that optimal sample preparation leads to a simplification of detection or reduced demands on the separation process. Throughout the book emphasis is on chemical principles with minimum discussion of the equipment required - an approach which reflects the editors' view that the limiting factor in the analysis of complex samples is an incomplete knowledge of the underlying chemistry rather than the hardware available. This lack of knowledge becomes more evident as the demands for lower detection limits grow, as solving complex matrix problems requires a greater understanding of the chemical interaction between the substance to be analysed and the stationary phase.

1989 xii + 394 pages
US$ 136.00 / Dfl. 265.00
ISBN 0-444-88327-4

Written by experienced practitioners, these volumes will be of interest to investigators in many areas of application, including environmental scientists and those active in the clinical, pharmaceutical and bioanalytical fields.

For more information, please write to:

Elsevier Science Publishers
P.O. Box 211, 1000 AE Amsterdam, The Netherlands
P.O. Box 882, Madison Square Station, New York, NY 10159, USA

Journal of Chromatography, 586 (1991) 181–197
Elsevier Science Publishers B.V., Amsterdam

CHROM. 23 548

Review

Beaded polymer supports and gels

I. Manufacturing techniques

Reza Arshady

Department of Chemistry, Imperial College of Science, Technology and Medicine, London SW7 2AY (UK)

(First received March 13th, 1991; revised manuscript received June 11th, 1991)

ABSTRACT

A general review of preparative aspects of beaded polymer supports and gels (microbeads) is presented. Basic features of manufacturing processes employed for the production of beaded organic and inorganic polymers and gels are discussed. Typical procedures for the synthesis of beaded silica, polysaccharides, polyacrylamides, polymethacrylates and polystyrene are described. Preparative aspects of microspherical products based on inorganic–organic composites, interpenetrating networks, pellicular particles, core–shell grafts and recently introduced amphiphilic copolymer resins are also discussed.

CONTENTS

1. INTRODUCTION

Beaded polymer supports and gels (gel microspheres, microbeads; see Fig. 1) are widely used as packing materials for various chromatographic techniques [1–5]. Microspherical polymer products are also employed for a number of related applications, including biochemical transformations [6], immunology [7], water treatment [8] and the extraction of precious metals [9]. Reviews of the use of polymer supports for solid-phase peptide synthesis, catalysis and other chemical applications are cited in Part II [10].

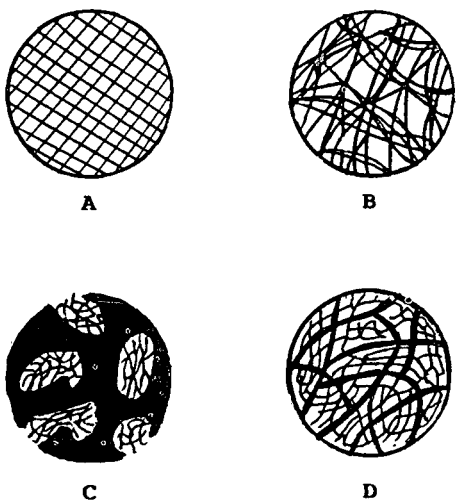

Fig. 1. Schematic presentation of typical particle morphologies of beaded polymer supports and gels used for chromatography. A = Homogeneous matrix (isoporous); B = heterogeneous matrix (macroporous); C = pore-matrix composite; D = interpenetrating network.

Beaded polymer supports and gels are produced from a wide range of natural and synthetic sources (Fig. 2) and by numerous manufacturing processes and technologies. For example, beaded polystyrene resins are produced by oil-in-water (o/w) suspension polymerization, whereas polyacrylamide gels are obtained by water-in-oil (w/o) suspension polymerization. Microspherical poducts based on polysaccharides and silica are manufactured by a number of

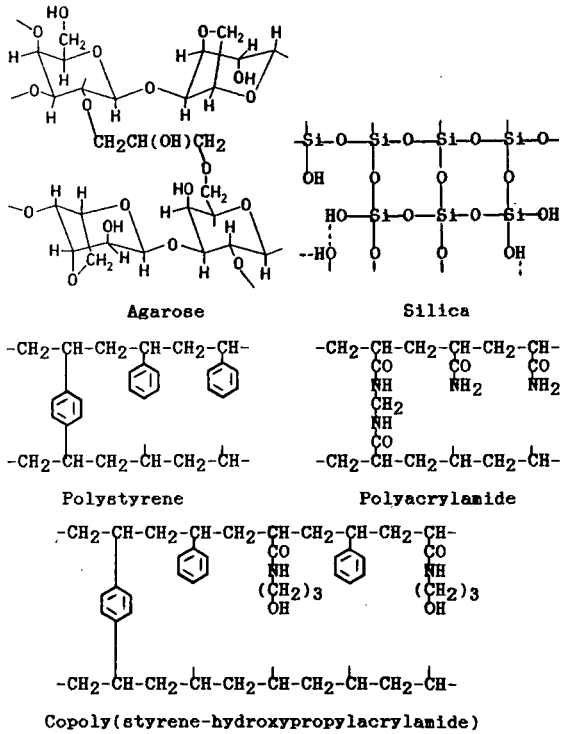

Fig. 2. Structures of different types of beaded polymer supports and gels.

related processes, the details of which are not frequently reported in the literature. In either case, manufacturing parameters are controlled to obtain the beaded product with a relatively narrow particle size distribution within the range of about 5–500 μm. A variety of particle morphologies may also be produced, as indicated in Fig. 1. The products thus obtained may be hydrophilic or hydrophobic, gelatinous or rigid, or they may have low or high porosity and surface area, depending on their chemical structure, degree of cross-linking and manufacturing conditions. Following their production, the microbeads may carry reactive groups, or they may be derivatized and activated by an extensive array of synthetic routes and reagents.

Despite widespread use of microspherical polymer products as packing materials for chromatography [1–5], systematic coverage of the preparation of these materials is lacking in the literature. This two-part review is therefore intended to provide a general picture of the manufacturing aspects of beaded polymer supports and gels. Part I discusses various polymerization and particle formation processes employed for the manufacture of both inorganic and organic polymer and gel microbeads. It covers the preparation of all major packing materials, including silica, polysaccharides, polyacrylamides, polymethacrylates and polystyrene, and also composites and copolymers. Chemical structure, derivatization and the control of physicochemical criteria (*i.e.* particle size, swelling behaviour, porosity and surface area) are discussed in Part II.

It is hoped that this two-part discussion will stimulate a better appreciation of the behaviour and performance of microspherical packing materials on the basis of their chemical structure and synthetic methodology. It should also provide a useful guide and source information for those who may be interested in preparing tailor-made microbeads in the laboratory. For this purpose, a full coverage of more recently introduced beaded polymers, copolymers and composites is provided.

2. BASIC FEATURES OF TWO-PHASE SUSPENSION PROCESSES

2.1. Definitions and criteria [11,12]

Beaded polymer supports, whether silica, agarose, cellulose, polyacrylamide or polystyrene, are all produced by different variations of two-phase suspension processes. Therefore, it is instructive here to define the term "suspension process" as a two-phase system in which "liquid microdroplets" are converted to the corresponding "solid microbeads".

Suspension polymerization of water-insoluble monomers (*e.g.* styrene and methyl methacrylate) involves the formation of a droplet suspension of the monomer in water and direct conversion of the individual monomer droplets into the corresponding polymer beads. Preparation of beaded polymers from water-soluble monomers (*e.g.* acrylamide) is similar, except that an aqueous solution of the monomer is dispersed in an oil to form a water-in-oil (w/o) droplet suspension. Subsequent polymerization of the resulting monomer droplets produces the corresponding swollen polyacrylamide beads. This process is often referred to as inverse suspension polymerization, but this terminology should not be used because it implies a restrictive definition of the term "suspension". Beaded silica gel is produced by, *inter alia*, suspension polycondensation and suspension gelation, while polysaccharide-based polymer supports are mostly obtained by suspension gelation and suspension cross-linking.

Among the various suspension systems mentioned above, the details of o/w suspension polymerization are more fully known [13–15]. Accordingly, the following discussion is based on this system. However, it will become abundantly clear throughout the subsequent sections that the criteria of "droplet formation", "droplet stabilization" and "droplet hardening", as discussed below for o/w suspension polymerization, apply equally to the preparation of beaded polymer supports in general.

2.2. Droplet formation

The most important feature of o/w suspension polymerization is the formation of a droplet suspension of the monomer in water (the suspension medium) and the maintenance of the individual droplets throughout the polymerization process. Droplet formation in an oil–water mixture is most appropriately accomplished by mechanical stirring, although other forms of mixing can also be employed. For most practical purposes, the volume ratio of the monomer phase to water is smaller than unity (usually 1:10–1:2), although stable suspen-

sions with o/w ratios of >1 can also be produced.

In a non-polymerizing suspension system [16], the suspended droplets collide with each other, coalesce into larger ones and rapidly redivide into smaller ones again. Under these conditions the system is in a state of dynamic equilibrium and remains apparently stable upon continued mixing. In a polymerizing suspension system, although the same principles apply initially, redivision of the coalesced (larger) monomer droplets becomes gradually more difficult as a result of polymerization and increased viscosity. This means that at a certain stage of the polymerization (beginning of the sticky period), re-division of the partially polymerized droplets becomes almost impossible and continued droplet coalescence leads to coagulation of the entire bulk of the monomer phase. However, assuming that the individuality of the partially polymerized droplets can be maintained by one means or another, progress of the polymerization reaction leads to gradual hardening of the droplets. Again at a certain stage (end of the sticky period), the hardened droplets will no longer coalesce in the event of any collision. The period during which the partially polymerized droplets can combine but not redivide is termed the sticky period, and is usually observed between 25 and 75% conversion, depending on the nature and composition of the monomer mixture.

2.3. Droplet/particle stabilization

Mass coagulation during the sticky period can be prevented by reducing the surface tension of the droplets and minimizing the force with which they collide. The latter is a matter of apparatus design (principally of the distribution of the stirring force), and the former is achieved by using a small amount of a suitable droplet stabilizer (suspension agent or coagulation inhibitor).

In o/w suspension polymerization, the addition of a small amount of a water-insoluble inorganic salt to the suspension system causes the formation of a very thin film around the monomer droplets and thus greatly reduces the danger of coagulation. Organic polymers which are insoluble in the monomer droplets and have relatively low solubility in the suspension medium are also highly effective as droplet stabilizers. Organic polymers are usually preferred to insoluble inorganic salts because they are more easily removed from the surface of the beads by aqueous stripping.

Examples of inorganic droplet stabilizers used for o/w suspension polymerization include talc, bentonite, calcium sulphate and calcium orthophosphate. Among the most commonly used organic stabilizers for o/w suspension systems are polyvinylpyrrolidone and poly(vinyl alcohol) (75–98% hydrolysed). A wide range of other water-soluble polymers such as methylcellulose, gelatin, acacia and other natural gums are also used. In general, a relatively low concentration of the stabilizer (*ca.* 0.1–1%)) is sufficient to maintain a stable suspension system under constant stirring conditions. It is noteworthy, however, that droplet stabilization is a surface phenomenon. Therefore, the minimum stabilizer concentration required for a full monolayer coverage of the droplets increases with decreasing particle size.

The relationship between particle size and the concentration of droplet stabilizer and other manufacturing parameters will be discussed in Part II. Here it should be mentioned that the use of unnecessarily high concentrations of stabilizer should be avoided, because they lead to increased monomer solubilization, lower yields and poorer quality of the beaded polymer product. In practice, both the type and concentration of stabilizer are arrived at empirically. Similarly, the design of the suspension polymerization reactor plays an important role in the stabilization of the suspension system and the quality of the beaded polymer product. Fig. 3 shows a cylindrical suspension polymerization reactor vessel especially designed [13,17] for laboratory preparation of beaded polymer supports.

3. SYNTHETIC ORGANIC POLYMERS

Synthetic organic polymers used as polymer supports or polymeric reagents are mainly based on polystyrene and polyacrylamides. Polymethacrylates and poly(vinyl alcohol) are also used to a lesser extent. Beaded polycondensates such as phenolic and polycarbonate resins can be produced readily by suspension polycondensation [18], but polycondensates are generally less suitable for the development of polymer supports.

3.1. Polystyrene

Styrene-based polymer supports are produced by o/w suspension copolymerization of styrene and

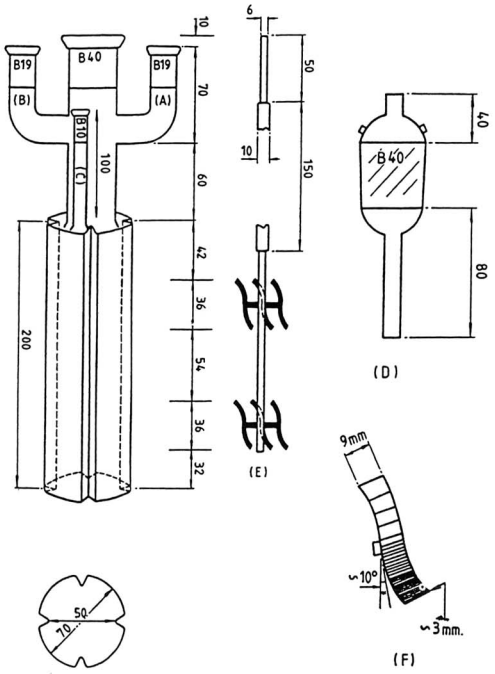

Fig. 3. Laboratory-scale suspension polymerization apparatus. A and B = accession points for a reflux condenser and nitrogen inlet; C = sampling arm; D = a stirrer guide; E = stirrer with its position indicated for full-scale operation; F = expanded drawing of a single stirrer blade indicating the curvature at both ends and the position and angle of attachment to the stirrer rod. All dimensions are in mm.

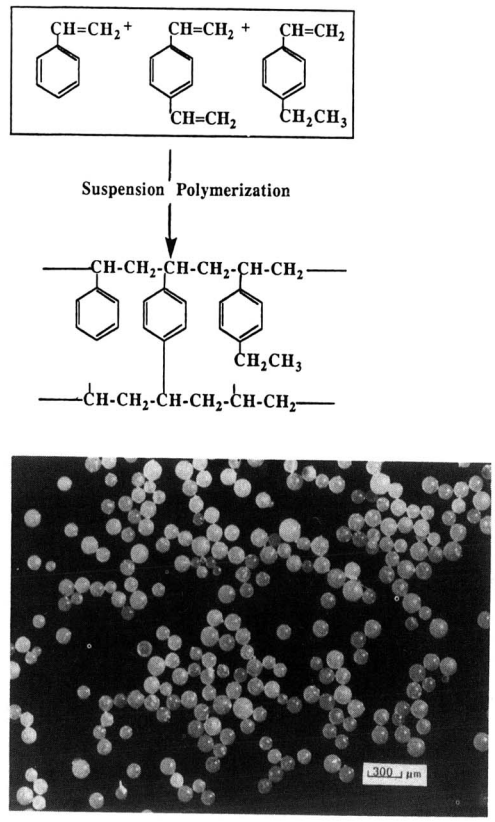

Fig. 4. Synthesis of styrene-based polymer supports by copolymerization of styrene, divinylbenzene and ethylvinylbenzene.

divinylbenzene (DVB), as indicated in Fig. 4. The DVB monomer commonly used for this purpose is a technical mixture composed of divinylbenzene isomers (*ca.* 60%, mainly *meta* and *para*), ethylvinylbenzenes (*ca.* 36%) and small percentages of related aromatic compounds. Suspension polymerization is usually carried out by using a monomer-soluble initiator such as benzoyl peroxide (BP) or 2,2′-azo-bis-2-methylpropionitrile (AIBN), at a temperature of 60–80°C. A relatively high initiator concentration [1–2% (w/w) based on monomer] is used, and the polymerization is allowed to proceed to completion (98–100%). The time required for complete monomer conversion must be determined by preliminary experiments, but is usually between 5 and 15 h, depending on the initiator concentration, temperature and the exact composition of the monomer mixture (see Table 1).

In addition to the monomers and the initiator, an inert liquid (referred to as a monomer diluent or porogen) may also be added to the monomer phase to influence the pore structure and swelling behaviour of the beaded resin product. The monomer diluent (not to be confused with the water used as the suspension medium) is usually a hydrophobic liquid such as toluene, dodecane or pentanol (see Table 1). These liquids represent examples of good, poor and non-solvents, respectively, for polystyrene, and their use leads to the formation of isoporous, microporous or macroporous beads [27,28], as discussed in Part II.

It is noteworthy that the nature and percentage of

TABLE 1

TYPICAL PROCEDURES FOR OIL-IN-WATER (O/W) SUSPENSION POLYMERIZATION REPORTED FOR THE PREPARATION OF BEADED COPOLYMERS OF STYRENE AND DIVINYLBENZENE

Monomer diluent	o/w vol. ratio	Droplet stabilizer[a]	Remarks	Ref.
Toluene, xylene or diphenylmethane	1:2	A	Early synthesis and study of porous resins	19
Toluene, dodecane or isoamyl alcohol	?	?	Synthesis and evaluation of porous resins for gel permeation chromatography	20
None or chlorobenzene	1:10	B	Functionalized polymer supports	21
None	1:5	A	Systematic study of suspension polymerization	22
None	?	C	Reduction in the amount of emulsified polymer	23
Ethylhexanoic acid	1:1	D	Study of pore formation	24
Hexane–toluene	1:4	E	Study of pore formation	25
None	1:1.5	F	Chloromethylated supports	26

[a] A = Poly(vinyl alcohol); B = a mixture of polyvinylpyrrolidone, calcium orthophosphate and calcium sulphate; C = hydrophobically modified polyethylene glycol or hydroxyethylcellulose; D = copoly(styrene–maleic acid) ammonium salt; E = bentonite and gelatin; F = gelatin and poly(allyldimethylammonium chloride).

the monomer diluent also influence the rate of polymerization. This may be mainly a concentration or precipitation effect, depending on whether the diluent is a solvent or precipitant for the polymer. For example, when the diluent is a good solvent, such as toluene or chlorobenzene, the polymerization proceeds at a correspondingly slower rate, whereas with a non-solvent such as pentanol the opposite is true.

Following the completion of the polymerization process, the beaded polymer product is recovered from the suspension mixture and freed from the stabilizer, diluent and traces of monomers and initiator. In industry, this is usually accomplished by steam stripping [29,30]. For laboratory preparations, repeated washing with water, a chlorinated solvent (*e.g.* chloroform) and methanol, respectively, is more appropriate [13]. Complete removal of the monomer diluent, especially from macroporous resins, may require long equilibration times with methanol, and some workers use a Soxhlet apparatus at the final stage of the recovery process.

Monodisperse polystyrene beads are produced by a special mode of seeded polymerization developed by Elingsen *et al.* [31]. According to this method, an aqueous polystyrene latex is equilibrated, first with a suitable oligomer and then with styrene and DVB. Under carefully controlled experimental conditions, the monomers are absorbed uniformly by the seed latex particles. Subsequent polymerization of the swollen particles (*i.e.* monomer droplets in the aqueous medium) produces the corresponding polymer beads. The size and cross-linking of the resulting particles are determined by the amount of the monomers used for swelling. This method is generally applicable, but is especially useful for producing uniform particles in the range 2–20 μm.

Beaded polystyrene resins can also be produced by suspension cross-linking of preformed soluble polystyrene. For example [32], a solution of the polymer, the cross-linking agent, 3,6-dimethyl-1,4-dichloromethylbenzene and a Friedel–Crafts catalyst ($SbCl_5$) in dichloroethane is dispersed in silicone oil (oil-in-oil suspension). The polystyrene droplets obtained in this way are then converted to the corresponding swollen polymer beads by effecting the cross-linking reaction at 70°C. This procedure is basically similar to those used for the preparation of beaded polysaccharides, as will be discussed in section 4.

3.2. Polyacrylamides

Literature on the synthesis of acrylamide resins for chromatography can be traced back to the late 1950s [33]. Early workers [33–37] produced bulk cross-linked polymers by homogeneous copolymerization of acrylamide and methanediacrylamide (methylenebisacrylamide, Bis), followed by grinding of the bulk polymer to obtain small gel particles. Hjerten and Mosbach [38] passed the swollen acryl-

TABLE 2

TYPICAL PROCEDURES REPORTED FOR THE SYNTHESIS OF BEADED POLYACRYLAMIDES BY WATER-IN-OIL (W/O) SUSPENSION COPOLYMERIZATION OF ACRYLAMIDES WITH BISACRYLAMIDE

Beaded polymer	Monomer diluent	Oil phase	Droplet stabilizer[a]	Remarks	Ref.
Polyacrylamide (Bio-Gel)	0.1 *M* sodium acetate	1,2-Dichloro-ethane	CAB	Early example of beaded hydrophilic gels	39
	Water	Toluene	A	Use of methacrylamide and hydroxymethylacrylamide	40
	0.1 *M* sodium acetate	Chloro-benzene	CAB	Alternative cross-linking monomers	41
Polyacryloylmorpholine (Enzacryl gel)	Water	Liquid paraffin	Span 85	Resins for gel permeation chromatography	42
Polyacryloyltrihydroxymethyl-acrylamide (Trisacryl gel)	Water	Petroleum	?	Resin for enzyme immobilization	43
Polydimethylacrylamide (Pepsyn)	Water–DMF[b]	1,2-Dichloro-ethane	CAB	Functional resins for peptide synthesis and catalysis	44, 45
	Water	?	CMC	Resin for gel permeation chromatography	46, 47

[a] CAB = Cellulose acetate butyrate; A = calcium stearate and dodecylphenoxypolyethoxyethanol; CMC = carboxymethylcellulose.
[b] DMF = Dimethylformamide.

amide gel through a pressurized jet to obtain a granular product. However, in a patent issued in 1964, Flodin [39] described a suspension polymerization procedure for the preparation of beaded acrylamide resins, which has remained the basis of much of the later work in this area.

Beaded acrylamide resins are generally produced by w/o suspension polymerization. This involves the dispersion of an aqueous solution of the monomer and an initiator (*e.g.* ammonium peroxodisulphate) in an immiscible liquid (the oil phase, see Table 2). A polymerization catalyst, usually N,N′-tetramethylethylenediamine (TEMED) or riboflavin, may also be added to the monomer mixture. Under these conditions, the polymerization of most acrylamides proceeds at substantially faster rates than that of styrene in o/w suspension polymerization. For this reason, preparation of beaded acrylamide resins is carried out at relatively low temperatures (20–50°C), and the polymerization is complete within relatively short periods (1–5 h). All of these conditions reduce the risk of droplet coagulation during the suspension polymerization. Accordingly, the problem of droplet coagulation during the synthesis of beaded polyacrylamides by w/o suspension polymerization is less critical than that of styrene-based resins.

Recently Patel *et al.* [48] described an interesting method for the preparation of beaded polyacrylamide gels involving droplet formation by a vibrating needle. Thus, the aqueous monomer solution (containing the initiator and catalyst, TEMED) is dropped into the suspension medium (chlorobenzene–xylene) from an 18-gauge needle at a rate of 0.5–7 g/min. The use of a catalyst and a temperature of 75°C leads to a relatively high rate of polymerization. Under these conditions, the polymerization is complete probably within 5–10 min, and the polymer beads (300–1000 μm) settle at the bottom of the polymerization tube. This procedure provides a particularly versatile method for producing small amounts of polymer, and is also adaptable for large-scale preparations.

3.3. Other synthetic polymers

In an early publication, Heitz *et al.* [49] described the preparation of beaded poly(methyl methacrylate) cross-linked with ethanedimethacrylate, and poly(vinyl acetate) cross-linked with butanediol divinyl ether. The latter polymer is the basis of the Merckogel series of gel permeation chromatographic packings, and its hydrolysed derivative, poly(vinyl alcohol), is marketed as Fractogel and Toyopearls. Beaded methacrylic polymers, poly(hydroxy-

ethyl methacrylate) (Spheron, Separon) [50] and poly(glycidyl methacrylate) (Eupergit) [51,52], have been introduced and extensively studied at the Czechoslovak Academy of Macromolecular Sciences. The most recent addition to the range of beaded polymer supports is poly(oligooxyethylene dimethacrylate)s, described by Trijasson *et al.* [53].

4. POLYSACCHARIDES

Beaded polysaccharide resins (gels) are produced by a variety of closely related suspension processes, one example of which for non-cross-linked cellulose beads is shown schematically in Fig. 5. Most of the techniques developed for the preparation of beaded polysaccharide resins are based on droplet formation processes more or less similar to w/o suspension polymerization, but they differ in the conversion of the droplets to the corresponding solid particles. This may involve a simple gelation or chelation process, solvent extraction, covalent cross-linking, or in the case of allyldextran, suspension copolymerization with bisacrylamide. Representative examples of different processes used for the preparation of beaded polysaccharide gels are described below.

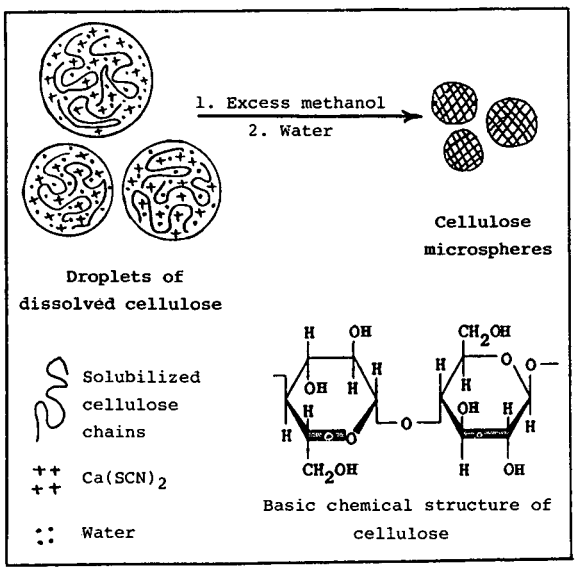

Fig. 5. Schematic presentation of solvent extraction process used for the preparation of beaded cellulose.

TABLE 3

PREPARATION OF AGAROSE BEADS BY SUSPENSION GELATION (ADAPTED FROM REF. 56)

Agarose in 300 ml of solution (g)	Oil phase, toluene-CCl_4 (ml)	Droplet stabilizer (g)[a]	Stirrer speed (rpm)	Bead size (US mesh)
3	490–110	SSO (0.5)	250	30–60
9	470–130	SSO (0.5)	1150	100–170
18	450–150	SSO (1)	1700	100–170
18	450–150	SSO (1.5)	1700	170–300
24	455–155	PSO (5)	1500	60–100
24	455–155	PSO (12)	1700	170–300
30	440–160	PSO (15)	1700	170–300
45	420–180	PSO (35)	1700	170–300

[a] SSO = Sorbitan sesqui-oleate; PSO = polyethylene oxide derivative of sorbitan monooleate.

4.1. Agarose

Agarose is obtained from a variety of marine algae [54,55]. It is a linear alternating copolymer of (1→3)-β-D-galactopyranose and (1→4)-3,6-anhydro-α-L-galactopyranose, and usually contains a small percentage of sulphate groups (<0.2% sulphur). Agarose is soluble in water at above 50°C up to a concentration of 20% or more, and the solution gels readily when cooled to room temperature. This favourable sol–gel behaviour is the basis of a relatively simple process for the preparation of non-cross-linked beaded agarose (Sepharose), as described by Hjerten in 1964 [56].

Thus, an aqueous solution of 1–5% agarose is stirred in a mixture of toluene and carbon tetrachloride at 50°C, in the presence of a droplet stabilizer. The resulting droplet suspension is then cooled to room temperature under continuous stirring to effect gelation, and hence the formation of non-cross-linked agarose beads (*cf.* Sepharose B). Table 3 provides quantative details of a series of beaded agarose gels obtained according to this procedure [56].

For the preparation of cross-linked agarose beads (*cf.* Sepharose CL-B), the non-cross-linked gels described above are treated with epichlorohydrin, diepoxides, 2,3-dibromopropanol or divinyl sulphone at high pH and 60°C for 2 h. The resulting cross-linked beads are then desulphatized at a higher temperature (120°C). These reactions are usually carried out in the presence of small amounts of a

reducing agent (sodium borohydride) to avoid oxidative degradation of the polymer [57,58].

More recently, agarose gels containing two types of cross-linking have been described [59]. Thus, the aqueous agarose droplets are prepared as described above. The w/o droplet suspension is treated with a diepoxide, *e.g.*

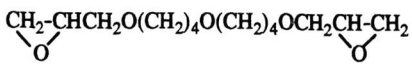

which is soluble in the organic phase, followed by reaction with epichlorohydrin. This cross-linking procedure probably results in the formation of microcapsular particles in which the outer shells are more hydrophobic and more highly cross-linked than the inner cores.

4.2. Cellulose

Cellulose has long atrracted interest as a suitable column packing material for liquid chromatography and other chromatographic separations. However, conventionally produced cellulose powders (known as microcrystalline cellulose) consist of irregularly shaped fibrous particles, and as such do not meet the requirements of modern chromatographic techniques.

Regularly sized cellulose microspheres (referred to as regenerated cellulose) are produced by dissolution of cellulose powder in a suitable solvent (see below), followed by droplet formation in a suspension medium, and subsequent solvent extraction or covalent cross-linking.

Early examples of the preparation of cellulose beads by solvent extraction are those described by O'Neill and Reichart [60] and Determan and Wieland [61]. In the last example, linter cellulose is dissolved in Schweitzer solvent (aqueous ammonium cuprate) and the solution is then stirred in benzene in the presence of a suspension stabilizer (Emulphor EL) to form the desired aqueous cellulose droplets. Addition of the resulting suspension mixture to a large volume of benzene containing acetic or benzoic acid results in solvent extraction, and hence the formation of the corresponding cellulose beads.

Two more recent reports on the preparations of non-cross-linked cellulose beads, by Peska *et al.* [62] and by Kuga [63], are also based on solvent extraction procedures. In the latter work, cellulose (Whatman CF-1, DP 180 or cotton linter, DP 1620) is dissolved in a highly concentrated solution of calcium thiocyanate at 120–140°C. The polymer solution is then stirred in dichlorobenzene at above its gel point (*ca.* 80°C). The resulting droplet suspension is added to cold methanol to effect solvent extraction and to form the corresponding cellulose beads as indicated in Fig. 5. If the dichlorobenzene suspension is prepared below the gel point of the cellulose solution, only irregular cellulose particles are obtained. Fig. 6 shows photomicrographs of both spherical and irregular cellulose particles produced from a 6% solution of cellulose CF-1.

Preparation of cross-linked cellulose beads by suspension cross-linking has been studied by Chitumbo and Brown [64]. In this work, a viscose solution (9.2% cellulose, 7.5% sodium hydroxide and 28% carbon disulphide) is vigorously stirred in dichloroethane containing a suitable suspension stabilizer (*e.g.* Cremophor EL) and a small percentage of sodium borohydride. The temperature of the droplet suspension is brought to 40°C, epichlorohydrin is added, and the stirring is continued until the desired degree of cross-linking is reached (14 h).

4.3. Dextran

Dextran, a branched homopolymer of D-glucose, lacks the structural rigidity which is the basis of the favourable sol–gel transformations in agarose and cellulose. Accordingly, all dextran-based polymer supports are cross-linked. Preparation of Sephadex [65] by cross-linking of dextran with epichlorohydrin or 2,3-dibromopropanol is similar to that of Sepharose, as described above. In the case of Sephacryl [66], bead formation is accomplished by w/o suspension copolymerization of allyldextran with bisacrylamide (*cf.* section 3.2).

4.4. Other polysaccharides

The preparation of cyclodextrin beads has been described in some detail by Fenyvesi *et al.* [67]. The cross-linking agent used in this work is a diepoxide similar to that used in the two-stage cross-linking of agarose beads [59]. Epichlorohydrin cross-linked starch microspheres [68] and bisacrylamide cross-linked acrylstarch microspheres [69] are produced in basically the same way as those of Sephadex [65] and Sephacryl [66], respectively. Chibata *et al.* [70] have

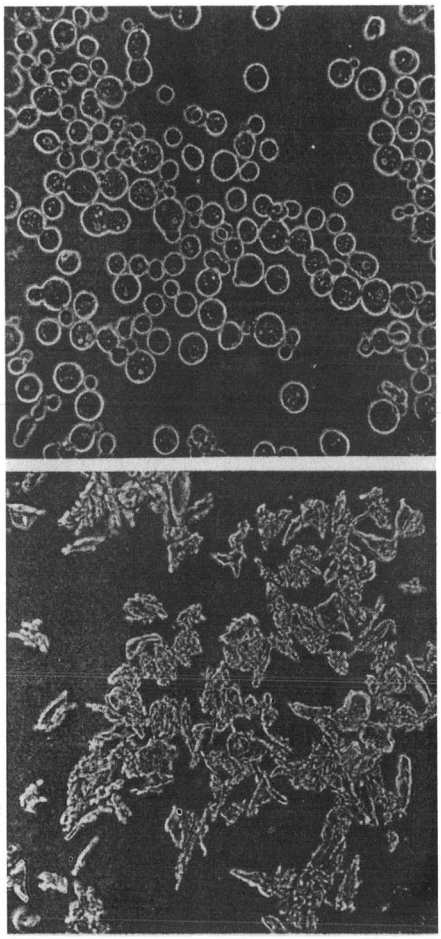

Fig. 6. Phase contrast micrograph of beaded and irregular particles of cellulose produced by solvent extraction (from ref. 63).

described the preparation of κ-carrageenan beads by suspension cross-linking with epichlorohydrin in a fashion similar to that described for agarose [56,57].

5. INORGANIC SUPPORTS

Porous silica (silica gel) is widely used as a sorbent, catalyst and polymer support. Related sorbents such as alumina, titania and zirconia are also used to a lesser extent. Controlled pore glass (CPG) has attracted considerable interest in recent years for enzyme immobilization and affinity chromatography. Zeolites are also extensively used as catalysts and sorbents, but do not fall within the scope of this review. This section discusses the production technology of porous silica in general, and those of microspherical and pellicular silica supports in particular. A brief section is also devoted to CPG for the sake of completeness.

5.1. Granular silica gel

The term "silica" in the specific sense refers to SiO_2 as a stoichiometric compound. However, silica-based supports to be discussed here contain various proportions of bound water [*i.e.* $SiO_2(H_2O)_x$]. Granular silica is produced by the conventional sol–gel process, as outlined in Fig. 7. The process involves the formation of a series of silica intermediates, including sodium silicate solution (obtained from caustic dissolution of sand), silicic acids, "silica sol", "silica hydrogel" and "silica xerogel".

5.1.1. Silica sol. The term "silica sol" is used to describe an aqueous dispersion of nanometre-sized silica particles (10–100 nm, colloidal silica), obtained by controlled polycondensation of silicic acid. Thus, acidification of a solution of sodium silicate leads to polycondensation and the formation of poly(silicic acid)s. As the polycondensation proceeds, precipitation takes place and silica nuclei (or primary particles) are formed. These nuclei subsequently grow to colloidal size, and hence the formation of "silica sol" [71]. This process is reminiscent of dispersion polymerization [11].

5.1.2. Silica hydrogel. The growth of the colloidal silica particles in the silica sol can be controlled by a number of parameters, notably silicate concentration, pH, temperature and stabilization by electrolytes [71]. As the number and size of the particles increase, they coagulate and form larger (micrometre sized) particles as a result of interparticle bonding. The continuation of this process (ageing) gradually leads to mass coagulation, and hence the formation of aqueous silica gel (or silica hydrogel).

5.1.3. Silica xerogel. The bulk hydrated gel produced in the sol–gel process is converted to porous dry silica (xerogel) by thermal dehydration. An interesting observation related to the dehydration process is that when the swelling water in the hydrogel is replaced with an organic solvent, and the latter is removed by heat treatment, relatively more

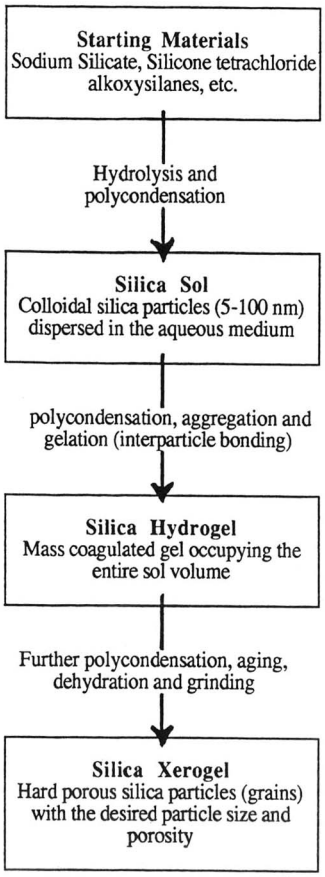

Fig 7. Different steps and intermediates involved in the preparation of irregular silica particles by the conventional sol–gel process.

highly porous particles are obtained [72]. This effect is similar to the diluent effect observed in the synthesis of organic polymer supports in the presence of a monomer diluent (*cf.* section 3.1). The silica gel obtained at the end of the drying stage may be soaked in a salt solution, followed by sintering for further adjustment of particle rigidity and pore structure [73]. The product is finally milled and sieved to produce several particle size ranges (*ca.* 5 μm–5 mm).

5.2. *Silica microbeads*

The introduction of beaded silica supports (silica microbeads) in the late 1960s and early 1970s [74] followed the popularity of beaded organic polymer supports in chromatography. Accordingly, different suspension systems initially developed for the production of beaded organic polymer supports are also the basis of most of the procedures described for the manufacture of beaded silica. Typical examples of these procedures are outlined below.

5.2.1. Suspension gelation. This procedure is basically similar to the sol–gel process (Fig. 7), except that "gelation" is effected while the silica sol is suspended in the form of small droplets in an organic liquid (suspension medium). Following the sol–gel conversion, the resulting "silica hydrogel beads" are separated, washed, dried and calcined to obtain the corresponding dry silica microbeads [75].

5.2.2. Suspension polycondensation. According to this method [76], a low-molecular-weight polyethoxysilane (PES) is first prepared by partial hydrolysis of tetraethoxysilane. The PES oligomer is then stirred in a water–methanol mixture to form a droplet suspension, followed by addition of a catalyst (*e.g.* ammonia) to effect polycondensation and the formation of the corresponding silica microbeads. This procedure represents an interesting quasi-suspension system in which a single liquid apparently serves both as a solvent (monomer diluent) within the monomer droplets and as a suspension medium in which the droplets are formed.

5.2.3. Microencapsulation. This method involves the entrapment of silica sol particles within an organic polymer matrix, followed by sintering and burning of the organic polymer. For example [77, 78], formaldehyde and urea are added to a well dispersed silica sol, followed by adjustment of the pH to effect the simultaneous polycondensations of silica sol and the organic monomers. This is basically a "dispersion polycondensation" process [18], in which a network of nanometre-sized silica particles are encapsulated within a micronmetre-sized network of the organic polycondensate. The resulting microcapsules are then subjected to heat treatment, first at 500°C to burn the organic polymer, and then at 1000°C to effect a slight sintering of the final silica microbeads.

5.2.4. Spray drying. According to this procedure [79], small droplets of silica sol are sprayed into an oven at 400°C. This results in the evaporation of water and simultaneous polycondensation within

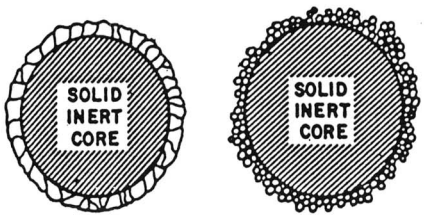

Fig. 8. Schematic presentation of (left) pellicular and (right) superficially porous polymer supports.

the droplets. The semispherical particles obtained in this way are then subjected to a hydrothermal treatment for the adjustment of porosity.

5.3. Pellicular silica

Pellicular and superficially porous silica supports are composed of a compact core and a porous shell or coat, as shown schematically in Fig. 8. The preparation of pellicular silica supports was first introduced by Halász and Horváth in 1964 [80], and a number of modified procedures have since been reported, as outlined below.

5.3.1. Single-step aerosil coating. According to the original method reported by Halász and Horváth [80], clean glass beads are shaken with a dispersion of colloidal silica (Aerosil, 5–50-nm particles) in an organic liquid. The liquid is then removed, and the silica coat is cemented around the glass core by heat treatment.

5.3.2. Multi-step aerosil coating. In this procedure [81], the core particles are first coated with a monolayer of colloidal silica (see above), and then with a positively charged organic polymer such as poly(methacryloxyethyldimethylammonium acetate), followed by drying. This alternating silica–organic coating is then repeated until the desired coat layer thickness (0.5–1 μm) is reached. The coated microbeads are finally subjected to a two-stage heat treatment to burn off the organic polymer and to adjust the pore structure and mechanical stability of the silica coat.

5.3.3. Polycondensation coating. This method [82] involves the formation of a silica layer around the glass particles by direct polycondensation of polyethoxysilane (PES). Thus, cleaned glass beads are dipped in a solution of PES in a low-boiling solvent, followed by evaporation of the solvent. The PES-coated particles are then suspended in a mixture of ethanol and water, and polycondensation of the adsorbed PES is effected by addition of a catalyst (*e.g.* ammonia). The resulting product is allowed to age before washing and drying.

5.4. Controlled pore glass

CPG is obtained from borosilicate glass (SiO_2, B_2O_3, Na_2O) by acid treatment. The process is based on the observation that, on heat treatment, certain borosilicate compositions from two-phase systems in which tiny borate-rich particles exist within a continuous silicate-rich matrix [83]. When this material is treated with acid, the borate phase is leached out and a porous product is thus obtained.

The pores formed by acid leaching are relatively small (30–60 Å). For the preparation of larger pore glasses, the acid leaching is followed by a mild caustic treatment [84,85]. This results in controlled dissolution of silicate from the interior of the pores, and hence the formation of larger pores. The initial phase separation process of borosilicate glass, as well as acid and base treatments, can be carefully "controlled" to produce relatively narrow pore sizes of up to about 3000 Å (300 nm) or larger (Fig. 9). CPG produced in this way typically contains about 95–96% silica glass, 3–5% B_2O_3 and traces of related metal oxides.

6. COMPOSITE SUPPORTS

The variety of polymer supports described in the preceding sections cover a wide range of chemical

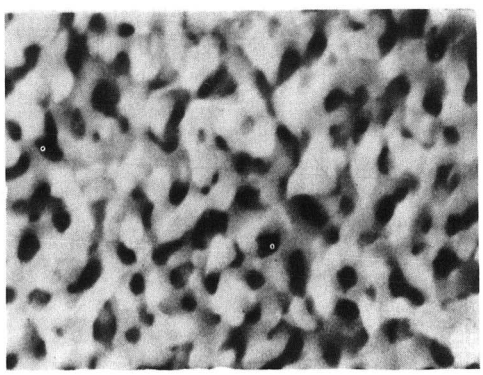

Fig. 9. Scanning electron micrograph of controlled pore glass (magnification 10 500) (adapted from ref. 85).

structures, solvent compatibility, mechanical rigidity and thermal stability. However, most of these polymers have well defined characteristics within relatively sharp boundaries. For example, polystyrene is strongly hydrophobic and is not suitable for aqueous applications, whereas simple polyacrylamide is strongly hydrophilic and not suitable for use in organic media. Some of the more recently introduced products (*e.g.* Enzacryl and Spheron) have intermediate properties, and hence a wider range of applications.

Silica-based supports are rigid (do not swell), but most polyacrylamides and polysaccharides form soft gels in the swollen state. Mechanical rigidity of the support is an important advantage in, for example, high-performance liquid chromatography, especially when a high capacity is not essential. On the other hand, soft gels provide high capacity and increased site accessibility, but they collapse under high pressure.

Most of the supports described here are chemically stable under most operating conditions. However, silica and (to a lesser extent) methacrylate supports are not stable under strongly alkaline conditions. Polysaccharides are prone to degradation by strong acids, oxidants and microorganisms. The methylenebisacrylamide bridges in acrylamide resins are also labile towards strong acids.

In order to benefit from the desirable features of different polymer types, and at the same time minimize their shortcomings, attempts have been directed towards the design of composite and multicomponent polymer supports. The variety of composite polymer supports described in the literature can be divided into four broad categories: (1) pore–matrix composites, (2) interpenetrating networks, (3) cores–shell grafts and (4) pellicular supports.

6.1. *Pore–matrix composites*

This category of composite supports has attracted considerable interest owing to its simple design and ease of production, as illustrated in Fig. 10. Thus, a porous inorganic support (*e.g.* porous silica or CPG) is soaked in a solution of the organic monomer mixture, usually containing a cross-linker and an initiator. Subsequent polymerization under carefully controlled conditions leads to the formation of the desired organic polymer within the pores of the beaded inorganic support [86–88].

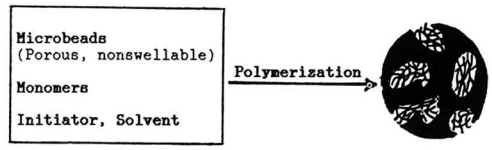

Fig. 10. Preparation of pore–matrix composite supports.

It should be emphasized, however, that the organic polymer must usually be sufficiently cross-linked to be permanently "entrapped" within the pores of the inorganic matrix. Alternatively, a less highly cross-linked organic polymer may be covalently "anchored" to the pore surface. Covalent attachment can be accomplished either by copolymerization with vinyl residues attached to the pore surface [89] or by reaction between appropriately chosen reactive groups on the organic polymer and the inorganic matrix [90].

Another example of pore–matrix type composite supports is that of polyacrylamide–agarose (Ultragel) described by Uriel [91] and Monsigny *et al.* [92]. Here, the composite beads are obtained by suspension polymerization in the same way as polyacrylamide beads (section 3.2), except that the required percentage of agarose is also dissolved in the monomer mixture. Thus, suspension copolymerization of acrylamide and bisacrylamide produces polyacrylamide beads which entrap the agarose chains initially present in the monomer droplets. A scanning electron micrograph of a partially dried Ultragel bead obtained from 4% acrylamides and 4% agarose is presented in Fig. 11 [92]. The micrograph shows a loose network of polyacrylamide rods (*ca.* 100–500 nm thick) and relatively large loops filled with collapsed agarose particles.

6.2. *Interpenetrating networks*

Beaded polymer supports composed of two interpenetrating networks are produced according to the general scheme shown in Fig. 12 [93]. This method involves the formation of one cross-linked polymer network within the matrix of a preformed beaded polymer. An interesting example of beaded interpenetrating networks is provided by the recently reported molecular organometallic composites [94]. Fig. 13 shows an X-ray microprobe image of a copolymer of vinylferrocene formed within a beaded polydimethylacrylamide matrix [94]. This image

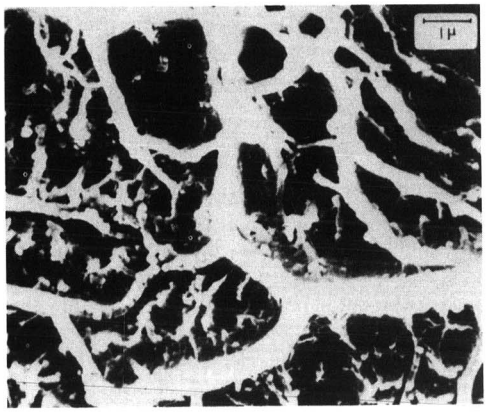

Fig. 11. Scanning electron micrograph of partially dried agarose–polyacrylamide composite supports (from ref. 92).

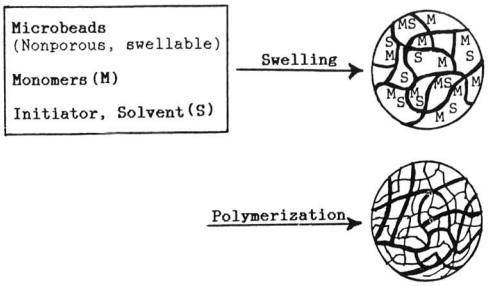

Fig. 12. Preparation of beaded interpenetrating networks.

shows that the organometallic network is homogeneously distributed throughout the initial polyacrylamide network.

6.3. *Core–shell grafts*

An ideal model of a core–shell graft composite, having a rigid core and relatively long flexible graft chains, is shown in Fig. 14A. The rigid core may be an inorganic material (*e.g.* glass) or an organic polymer (*e.g.* polystyrene). Such an ideally grafted surface can be produced by attaching specifically monofunctionalized linear chains to suitably activated surfaces. A more practical approach is, however, the attachment of initiator groups [95] or vinyl residues [96] to the surface, followed by direct graft polymerization. Graft polymerization onto the surface of the core produces a different shell structure

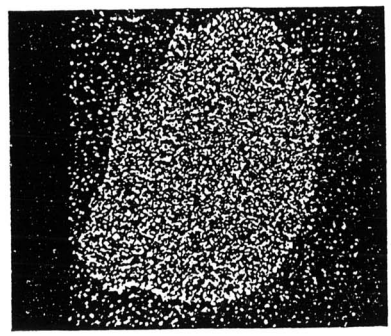

Fig. 13. X-ray microprobe image of a cross-linked (network) copolymer of dimethylacrylamide and vinylferrocene formed within a preformed network of cross-linked polydimethylacrylamide [94].

(Fig. 14B) as a result of chain transfer and termination reactions. Note that when the core particles are porous, the illustrations in Fig. 14 still apply, albeit the overall morphology approaches that of pore–matrix composites shown in Fig. 10. For representative examples of these preparations, see refs. 97–100 and section 5.4 in Part II.

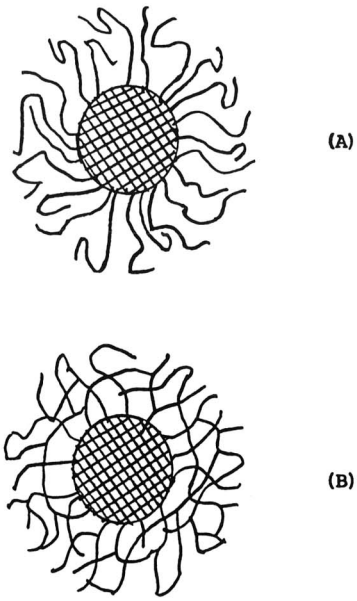

Fig. 14. Schematic presentation of core–shell grafts. (A) Ideal structure; (B) typical structure available via attachment of monomer on the surface, followed by graft polymerization.

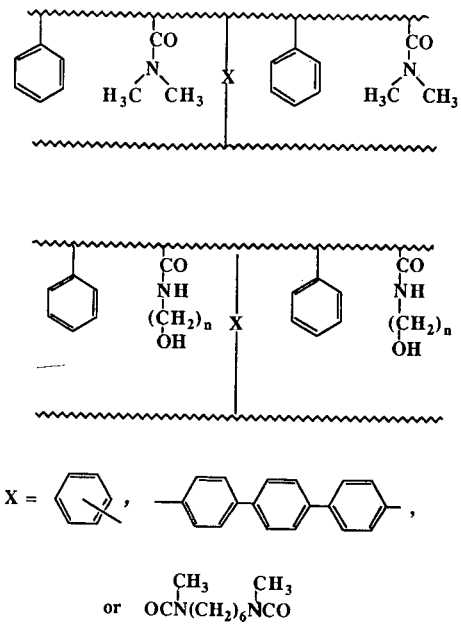

Fig. 15. Amphiphilic polymer supports with copoly(styrene–acrylamide) structures.

6.4. *Pellicular supports*

Pellicular supports are essentially similar to core–shell grafts shown in Fig. 14B. However, the term "pellicular" is used to describe materials in which the outer shell is relatively thicker than that in core–shell supports. In addition, in pellicular supports the shell is deliberately cross-linked by the inclusion of a cross-linking monomer, and the shell may or may not be covalently attached to the core. Here again, the pellicular terminology is equally used whether the core is rigid or porous. The topic of pellicular supports has been reviewed thoroughly by Horváth [101].

7. COPOLYMER SUPPORTS

A logical extension of the concept of composite supports is the development of copolymer supports. In a formal sense, all of the cross-linked beaded resins and most of the composite supports described above are copolymers. In addition, activated (functionalized) polymer supports (see Part II) may also be regarded as copolymers. However, in all of these, the main repeating units on the polymer *backbone* have essentially the same structure. The term "copolymer support" is here meant to describe a copolymer structure incorporating two (or more) distinctly different types of monomeric units in the polymer *backbone*.

An interesting class of copolymer supports is the alternating copoly(styrene–acrylamide) structures shown in Fig. 15. These copolymers combine the structural units of polystyrene with those of polydimethylacrylamide or polyhydroxyalkylacrylamide. As a result, they cover the solvent and substrate compatibility ranges of both hydrophobic and hydrophilic polymer supports, and hence are suitable for general use in aqueous media and in polar and non-polar organic solvents. The new copolymer supports are also ideally suitable for multi-step processes involving the use of aqueous and non-aqueous solvents at different stages.

It is interesting that beaded copolymer supports of the type shown in Fig. 15 cannot be produced by suspension copolymerization of the respective comonomers. This is because the two comonomers have opposite water solubilities and unfavourable copolymerization reactivity ratios. These copolymer supports are, however, obtained readily by a new synthetic method based on the chemistry of "activated esters" or "leaving group substitution" [102, 103].

REFERENCES

1 P. D. G. Dean, W. S. Johnson and F. A. Middle (Editors), *Affinity Chromatography*, IRL Press, Oxford, 1985.
2 S. G. Allenmark, *Chromatographic Enantioseparations*, Ellis Horwood, Chichester, 1988.
3 R. Epton (Editor), *Chromatography of Synthetic and Biological Macromolecules*, Vols. 1 and 2, Ellis Horwood, Chichester, 1978.
4 T. Kremmer and L. Boross, *Gel Chromatography*, Wiley-Interscience, New York, and Akadémiai Kiadó, Budapest, 1979.
5 D. Ishii, *Introduction to High-Performance Liquid Chromatography*, Verlag Chemie, Weinheim, 1988.
6 K. Mosbach (Editor), *Methods in Enzymology*, Vol. 112, Academic Press, New York, 1985.
7 A. Rembaum and Z. A. Tokes (Editors), *Microspheres: Medical and Biological Applications*, CRC Press, Boca Raton, FL, 1988.
8 D. Bohnsack, W. Hoell, E. Klein, W. Koelle and K. Soine, *DVGW Schriftenr. Wasser*, 6 (1989) 51.
9 M. Streat and D. Naden (Editors), *Ion-Exchange and Sorption Processes in Hydrometallurgy*, Wiley, Chichester, 1987.
10 R. Arshady, *J. Chromatogr.*, 586 (1991) 199.

11 R. Arshady, *J. Microencapsulation*, 5 (1988) 101.
12 R. Arshady, *Polym. Eng. Sci.*, 29 (1989) 1746.
13 R. Arshady and A. Ledwith, *React. Polym.*, 1 (1983) 159.
14 M. Munzer and E. Trammsdorf, *High Polym.*, 29 (1977) 106.
15 H. Warson, *Polym. Paint Colour J.*, Aug. 10/24 (1983) 541.
16 I. S. Pavlushenko and A. V. Yanishevski, *J. Appl. Chem. USSR*, 32 (1959) 1529.
17 R. Arshady, G. W. Kenner and A. Ledwith, *J. Polym. Sci.*, 12 (1974) 2017.
18 R. Arshady, *J. Microencapsulation*, 6 (1989) 1.
19 J. R. Millar, D. G. Smith and T. R. E. Kressman, *J. Chem. Soc.*, (1965) 304.
20 J. C. Moore, *J. Polym. Sci., Part A-2*, (1964) 835.
21 R. Arshady, *Chim. Ind. (Milan)*, 70, No. 9 (1988) 70.
22 F. Wolf and S. Eckert, *Plaste Kautsch.*, 18 (1971) 650 and 890; 19 (1972) 26.
23 S. M. Ahmed, *J. Disp. Sci. Technol.*, 5 (1984) 421.
24 H. Jacobelli, M. Bartholin and A. Guyot, *J. Appl. Polym. Sci.*, 23 (1979) 927.
25 W. L. Sederel and G. J. de Jong, *J. Appl. Polym. Sci.*, 17 (1973) 2835.
26 M. Tomoi and W. T. Ford, *J. Am. Chem. Soc.*, 103 (1981) 821.
27 A. Guyot, *Pure Appl. Chem.*, 60 (1988) 365.
28 J. Seidl, J. Malinsky, K. Dusek and W. Heitz, *Adv. Polym. Sci.*, 5 (1967) 113.
29 J. M. Church, *Chem. Eng.*, Aug. 1 (1966) 79.
30 R. B. Bishop, *Practical Polymerization for Polystyrene*, Cahners, New York, 1971.
31 T. Elingsen, O. Aune, J. Ugelstad and S. Hogan, *J. Chromatogr.*, 535 (1990) 147.
32 F. P. Regas and C. G. Papadoyanis, *Polym. Bull.*, 3 (1980) 279.
33 W. H. Schuller, J. A. Price, S. T. Moore and W. M. Thomas, *J. Chem. Eng. Data*, 4 (1959) 273.
34 S. Hjerten, *Arch. Biochem. Biophys., Suppl.*, 1 (1962) 174.
35 D. J. Lea and A. H. Sehan, *Can. J. Chem.*, 40 (1962) 159.
36 K. Sun and A. H. Sehan, *Can. J. Chem.*, 43 (1965) 969.
37 J. S. Fawcet and C. J. O. R. Morris, *Sep. Sci.*, 1 (1966) 9.
38 S. Hjerten and R. Mosbach, *Anal. Biochem.*, 3 (1962) 109.
39 P. Flodin, *Fr. Pat.*, 1 363 978 (1964); *C.A.*, 62 (1965) P6640e.
40 J. Ingemar, H. Joustra and K. Marius, *Ger. Offen.*, 1 954 349 (1970); *C.A.*, 73 (1970) P15906f.
41 K. Mizutani, *US Pat.*, 3 880 814 (1975); *C.A.*, 83 (1975) P115710n.
42 R. Epton, S. R. Holding and J. V. McLaren, *Polymer*, 17 (1976) 843.
43 E. Brown and J. Tuet, *J. Chem. Res. (S)*, 9 (1979) 290.
44 R. Arshady, *J. Colloid Polym. Sci.*, 268 (1990) 948.
45 R. Arshady, B. Corain, M. Roncato, M. Zecca, L. D. Guistina, S. Lora and G. Palma, *J. Mol. Catal.*, 53 (1989) 111.
46 C. Hyrayama, K. Yamaguchi, K. Masumoto and Y. Motozata, *Kobunshi Ronbunshu*, 40 (1983) 441; *C.A.*, 99 (1983) 123700e.
47 C. Hyrayama, K. Yamaguchi, K. Masumoto and Y. Motozata, *Kobunshi Ronbunshu*, 40 (1983) 547; *C.A.*, 99 (1983) 195796p.
48 S. K. Patel, F. Rodriguez and E. Cohen, *Polymer*, 30 (1990) 2198.
49 W. Heitz, H. Ulliner and H. Hoeker, *Makromol. Chem.*, 98 (1966) 42.
50 J. Coupek, M. Krivakova and S. Pokorny, *J. Polym. Sci., Polym. Symp.*, 42 (1973) 185.
51 F. Svec, J. Hradil, J. Coupek and J. Kalal, *Angew. Makromol. Chem.*. 48 (1975) 135.
52 D. Horak, F. Svec, M. Bleha and J. Kalal, *Angew. Makromol. Chem.*, 95 (1981) 109.
53 P. Trijasson, Y. Ferere and P. Gramain, *Makromol. Chem. Rapid Commun.*, 11 (1990) 235.
54 T. Araki, in *Proceedings of the 5th International Seaweed Symposium*, Halifax, Canada, 1965.
55 J. Tramper, *Chem. Anal. (Warsaw)*, 66 (1983) 393.
56 S. Hjerten, *Biochim. Biophys. Acta*, 79 (1964) 393.
57 J. Porath, J. C. Johnson and T. Laas, *J. Chromatogr. Sci.*, 60 (1971) 167.
58 J. Porath and J. C. Janson, *Ger. Offen.*, 2 131 139 (1971); *C.A.*, 76 (1972) 115174w.
59 T. Andersson, M. Carlsson, L. Hagel, P.-A. Parnemalm and J.-C. Janson, *Eur. Pat. Appl.*, 84850215.9, 1984.
60 J. J. O'Neill, Jr. and E. R. Reichart, *US Pat.*, 2 543 928 (1951); *C.A.*, 45 (1951) 4927c.
61 H. Determan and T. Wieland, *Makromol. Chem.*, 114 (1968) 263.
62 J. Peska, J. Stamberg and J. Hradil, *Angew. Makromol. Chem.*, 53 (1976) 73.
63 S. Kuga, *J. Chromatogr.*, 195 (1980) 221.
64 K. Chitumbo and W. Brown, *J. Polym. Sci.*, Part C, 36 (1971) 279.
65 *Gel Filtration: Theory and Practice*, Pharmacia, Uppsala.
66 H.I. Johansson, D. T. Lindstrom and J. L. Soderberg, *Ger. Offen.*, 2 655 292 (1977).
67 E. Fenyvesi, B. Zsadon, J. Szejtli and F. Tudos, *Ann. Univ. Sci. Budap. Rolando Eotvos Nominatae Sect. Chim.*, 15 (1979) 13 (essential details are reviewed in ref. 18).
68 U. Rothman and B. Lindberg, *Ger. Pat.*, 2 524 279 (1976); *C.A.*, 85 (1976) 99172x.
69 B. Ekman and J. Sjoeholm, *J. Pharm. Sci.*, 67 (1978) 693.
70 I. Chibata, T. Tosa and T. Sato, *J. Chromatogr.*, 215 (1981) 93.
71 R. K. Iller, in E. Matijevic (Editor), *Surface and Colloid Science*, Vol. 6, Wiley, Chichester, 1973, pp. 1–100.
72 F. Wolf and H. Beyer, *Kolloid-Z.*, 165 (1959) 151.
73 K. F. Krebs and H. Heinz, *Ger. Pat.*, 2 042 910 (1970).
74 W. A. Dark and R. M. Limpert, *J. Chromatogr. Sci.*, 11 (1973) 114.
75 I. Sebastian and I. Halász, *Ger. Pat.*, 2 155 045 (1975).
76 K. Unger, J. Schick-Kalb and B. Straube, *J. Polym. Colloid Sci.*, 253 (1974) 658.
77 J. J. Kirkland, *US Pat.*, 3 782 075 (1974).
78 R. K. Iller and H. J. McQueston, *US Pat.*, 3 855 172 (1974).
79 A. V. Kiselev, G. L. Kunstowa, B. A. Lipkind and J. S. Nikitin, *Ger. Pat.*, 2 225 452 (1972).
80 I. Halász and Cs. Horváth, *Anal. Chem.*, 36 (1964) 1178 and 2226.
81 J. J. Kirkland, *US Pat.*, 3 505 785 (1970).
82 H. W. Kohlschütter, K. Unger and J. Schick-Kalb, *Ger. Pat.*, 2 225 973 (1973).

83 M. E. Norderg, *J. Am. Ceram. Soc.*, 27 (1944) 299.
84 M. L. Hair and A. M. Filbert, *Res. Dev.*, 20, No. 12 (1969) 30.
85 M. Lynn and A. M. Filbert, in E. Grushka (Editor), *Bonded Stationary Phases in Chromatography*, Ann Arbor Sci. Publ., Ann Arbor, MI, 1974, pp. 1–11.
86 A. J. Alpert and P. E. Regnier, *J. Chromatogr.*, 185 (1979) 375.
87 G. Heinemann, J. Koehler and G. Schomburg, *Chromatographia*, 23 (1987) 435.
88 P. Kolla, J. Koehler and G. Schomburg, *Chromatographia*, 23 (1987) 465.
89 G. Wulf, D. Oberkobush and M. Minarik, *React. Polym.*, 3 (1985) 261.
90 J. Schutyser, T. Buser, D. Van Olden and H. Tomas, in T. C. J. Gribnau, J. Visar and R. J. F. Nivard (Editors), *Affinity Chromatography and Related Techniques*, Elsevier, Amsterdam, 1982, p. 143.
91 J. Uriel, *Bull. Soc. Chim. Biol.*, 48 (1966) 969.
92 M. Monsigny, M. Cornet, R. Tixier, M. Corgier and P. Girot, in R. Epton (Editor), *Chromatography of Synthetic and Biological Molecules*, Vol. 1, Ellis Horwood, Chichester, 1978, p. 57.
93 R. Arshady, *Polymer*, 23 (1982) 947 and 1870.
94 R. Arshady, B. Corain, S. Lora, G. Palma, U. Rosso, F. Okan and M. Zecca, *Adv. Mater.*, 2 (1990) 412.
95 G. Challa, *J. Mol. Catal.*, 21 (1983) 1.
96 J. L. Garnet, R. Levot and M. A. Long, *J. Polym. Sci., Polym. Lett. Ed.*, 19 (1981) 23.
97 B. B. Wheals, *J. Chromatogr.*, 107 (1975) 402.
98 K. Klatyk, *US Pat.*, 3 549 525 (1970); *C.A.*, 74 (1971) 91636d.
99 N. Fery, R. Hoene and K. Haman, *Angew. Chem., Int. Ed. Engl.*, 11 (1972) 337.
100 S. A. Barker and P. J. Sommers, *Br. Pat.*, 1 456 865 (1976), *C.A.*, 86 (1977) 190835.
101 Cs. Horváth, in E. Grushka (Editor), *Bonded Stationary Phases in Chromatography*, Ann Arbor Sci. Publ., Ann Arbor, MI, 1974, p. 59.
102 R. Arshady, *Adv. Mater.*, 3 (1991) 182.
103 R. Arshady, *Makromol. Chem.*, 185 (1984) 2383.

Journal of Chromatography, 586 (1991) 199–219
Elsevier Science Publishers B.V., Amsterdam

CHROM. 23 549

Review

Beaded polymer supports and gels

II. Physico-chemical criteria and functionalization

Reza Arshady

Department of Chemistry, Imperial College of Science, Technology and Medicine, University of London, London SW7 2AY (UK)

(First received March 13th, 1991; revised manuscript received June 11th, 1991)

ABSTRACT

A systematic description of morphology, physicochemical criteria, functionalization and activation of beaded polymer supports and gels is presented. The products covered include polystyrene, polyacrylamides, copoly(styrene-acrylamide)s, polysaccharides, polymethacrylates and silica gel. Morphological aspects of beaded polymer products (i.e. bead size, porosity and surface area) and swelling behaviour are discussed. Various chemical reactions employed for derivatization and activation of polymer supports and gels are charted and their limitations and side reactions are outlined. The significance of physicochemical criteria such as matrix architecture, chemical structure of the polymer backbone, site accessibility and spacer arm are also briefly covered.

CONTENTS

1. INTRODUCTION

Microspherical polymer products (beaded polymer supports and gels, both organic and inorganic) are widely used as packing materials for chromatography and a variety of other applications (see Table 1) [1–20]. Gel (permeation) chromatography (or gel filtration) [1–3] is based on the pore structure of the

polymer microbeads. Porosity and surface area also play an important role in other applications such as ion-exchange and affinity chromatography and polymer-supported catalysis. However, in these and most other uses of polymer supports listed in Table 1, the "function" of the polymer is based essentially on specific functional residues (or reactive sites). In either case, the size of the microbeads, the swelling behaviour and the chemical structure of the polymer backbone strongly influence the overall performance of the product.

This review follows the general introduction and preparative details of beaded polymer products discussed in Part I [21]. The present discussion focuses on morphological, chemical and physicochemical aspects of beaded polymer supports and gels, including polystyrene, polyacrylamides, polymethacrylates, polysaccharides, silica gel and copoly(styrene–acrylamide)s. The manufacturing basis of bead size, porosity, surface area and bulk expanded volume are discussed. Various chemical reactions employed for the functionalization and activation of beaded polymer supports and gels are systematically reviewed. The significance of physico-chemical criteria, such as the chemical structure of the polymer backbone, architecture of the polymer matrix, site accessibility and spacer arm are also pointed out.

2. PARTICLE SIZE

Beaded polymer supports and gels are produced by two-phase suspension processes in which "microdroplets" of a monomer or polymer solution are directly converted to the corresponding "microbeads" (see Part I). The size of the microdroplets (and hence that of the microbeads) is determined by a number of interrelated manufacturing parameters, including reactor design, the rate of mixing (stirring), ratio of the monomer (or polymer) phase to the suspension medium, viscosity of both phases and type and concentration of the droplet stabilizer [22–24].

The size distribution of the polymer beads obtained by two-phase suspension systems depends mainly on the configuration of the reactor and "artful" management of the suspension process. With the cylindrical apparatus introduced in Part I, it is possible to obtain relatively uniform beads in which the deviation from the average size is not greater than about 100% (see Figs. 3 and 4 in Part I) [22]. More generally, however, two-phase suspension systems produce beaded products with considerably broader particle size distributions (e.g., 5–50 or 20–200 μm). Such products are usually separated (graded) into a series of relatively narrow particle size ranges as desired. The actual classifica-

TABLE 1

MAJOR APPLICATIONS OF BEADED POLYMER SUPPORTS AND GELS

Application	Bead functionality needed or preferred[a]	Ref.
Chromatography:		
Gel (permeation) or size exclusion	Porosity	1–3
Ion-exchange	SO_3H (Na), CO_2H (Na), NR_3X	4–6
Affinity	OH, NH_2, CHO COOH, COOAr	7–9
Enantioselective	Asymmetric centers (*e.g.*, *C)	10
Biotransformations (immobilized enzymes/cells)	OH, NH_2, COOH, porosity	11, 12
Solid-phase peptide synthesis	OH, NH_2	13, 14
General organic synthesis	Various	15, 16
Chemical catalysis	PPh_3, NC, CN, others	15–17
Hydrometallurgy (metal ion extraction)	Various	18
Diagnostics and immunoassay	OH, NH_2, CHO, COOH	19, 20

[a] R = alkyl; X = Br, Cl, OH; Ar = activating/leaving group; Ph = phenyl.

tion process depends on the size range involved, the nature of the beaded product and its intended application. Relatively large (> 50 μm) and mechanically stable particles can be easily sieved in the dry state. Smaller particles are processed more conveniently in the swollen (or wet) state. Highly porous particles may be fragile and irregular in the dry state. For these, and also for very fine particles (< 20 μm), classification is accomplished by wet sedimentation, counterflow settling (elutriation) or counterflow centrifugation [25–27] (see also ref. 1, pp. 109–112). Fig. 1 shows the particle size distribution of a typical polystyrene resin and those of its fractions obtained by the counterflow centrifugation method.

Among various factors influencing particle size, stirring speed (or more generally, the power of mixing) provides a relatively convenient means of particle size control for most practical purposes. Fig. 2 illustrates a typical example [28] of the effect of stirrer speed on the size of polystyrene particles obtained by suspension polymerization. The pattern of particle size variation *versus* stirrer speed indicated in Fig. 2 applies equally to beaded polymers obtained by other two-phase suspension systems discussed in Part I.

It must be emphasized, however, that there are limits within which particle size can be controlled by the adjustment of the stirring speed. These limits

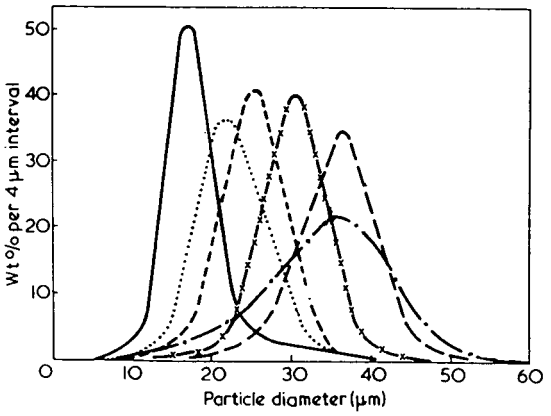

Fig. 1. Particle size distribution of a typical polystyrene–DVB resin produced by suspension polymerization (— · —), and its fractionation by an Alpine Zig-Zag Centrifugal Separator. Particle size: (———) 10–15 μm; (.....) 16–20 μm; (– – –) 20–24 μm; (– × –) 25–28 μm; (– – –) >28 μm (adapted from ref. 27).

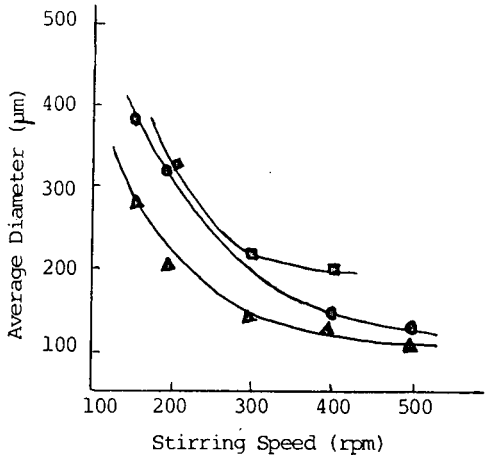

Fig. 2. Effect of stirring speed on the size of polystyrene particles produced by suspension polymerization; stabilizer: (■) 0.2%; (●) 0.3%; (▲) 0.4% (adapted from ref. 28).

depend on the size and the configuration of the polymerization reactor (including its stirring arrangement). For laboratory preparations involving a total volume of about 500 ml (see Fig. 3 in Part I), the stirring speed can be varied between about 200 and 800 rpm. Lower stirring speeds may not be sufficient to establish a steady-state droplet size distribution, whereas too vigorous stirring may exceed the shear tolerance of the whole set-up.

Another practically important consideration about the dependence of particle size on stirring speed is that smaller droplets/particles produced by faster mixing require correspondingly increased concentrations of the droplet stabilizer. In the absence of sufficient stabilizer, the smaller droplets coalesce easily during the hardening stage. This produces larger (and irregularly sized) particles, and may also lead to partial or full coagulation of the microbeads. For example, in the case of experiments indicated in Fig. 2, at a stabilizer concentration of 0.1%, an increased rate of stirring leads to the formation of much larger particles.

In principle, two-phase suspension systems can be employed to produce polymer particles within the range of about 0.2–2000 μm. In suspension polymerization of vinyl monomers, however, the production of very small particles (< 20 μm) is difficult owing to emulsification and latex formation by emulsion polymerization. This problem does not arise when the particles are formed by solvent

TABLE 2

DEPENDENCE OF SURFACE AREA AND POROSITY OF SILICA GEL ON THE CONDITIONS OF HYDROTHERMAL TREATMENT (ADAPTED FROM REF. 32)

Sample	Treatment conditions			Surface area and porosity		
	Temperature (°C)	Time (h)	Pressure (bar)	Surface area (m^2/g)	Pore volume (ml/g)	Mean pore diameter (nn)
1a	–	–	–	210	0.73	10.0
1b	110	4	2	121	0.70	22.0
1c	180	4	10	39	0.72	74.0
1d	250	4	50	20	0.78	290
1e	300	4	100	1.4	0.70	1420
2a	–	–	–	330	1.07	10.5
2b	250	5	50	63	1.09	68.0
2c	250	10	50	51	1.06	88.5
2d	250	15	50	48	1.15	88.0
2e	250	20	50	38	1.06	88.5
3a	–	–	–	498	0.63	5.1
3b	100	0.5	1	432	0.93	7.2
3c	100	1.0	1	395	0.94	8.0
3d	100	1.5	1	356	0.94	8.6

extraction and suspension cross-linking (*e.g.* polysaccharide gels). Small particles of vinyl-based polymers can be obtained by dispersion polymerization or by more elaborate two-step processes involving the enlargement of monodisperse seed particles [29].

3. POROSITY AND SURFACE AREA

Traditional sorbents such as charcoal [30,31] and silica gel [32] have rigid three-dimensional structures with tightly fixed matrices. Accordingly, surface area and porosity in inorganic supports represent real structural criteria, and often the limits of support characterization. In contrast, organic gels are based on relatively flexible matrix structures (see Fig. 2 in Part I). Here, porosity and surface area represent tertiary and higher orders of macromolecular structure, rather than the limits of structural characterization.

Porosity and surface area in both inorganic and organic supports can be controlled easily during production. In silica gel, the pore structure is dependent on hydrothermal treatment (Table 2) [32,33] and on other manufacturing parameters discussed in Part I. In the case of organic resins, porosity is determined by gelation and/or precipitation processes that take place during the conversion of liquid microdroplets to solid microbeads. For example, polystyrene beads produced in the presence of 1–2% divinylbenzene (DVB) without a monomer diluent have very low surface area (<1 m^2/g) with no real porosity or very small pores. However, by using higher DVB concentrations and a monomer diluent, polymer beads with a wide range of porosities can be produced, depending on the proportions of DVB and monomer diluent.

Fig. 3 shows scanning electron micrographs of two samples of beaded copolymers of styrene with 2,4,5-trichlorophenyl acrylate and DVB, obtained in the presence of either chlorobenzene or chlorobenzene–octane [34]. In the presence of chlorobenzene (a good solvent for this polymer), the polymer chains remain solvated throughout the matrix formation. This produces a relatively homogeneous matrix with very low porosity (micrograph a). On the other hand, polymerization in the presence of chlorobenzene–octane (a poor solvent) leads to phase separation and the formation of polymer "nuclei" within the polymerizing droplets. Accordingly, each individual polymer bead produced in this

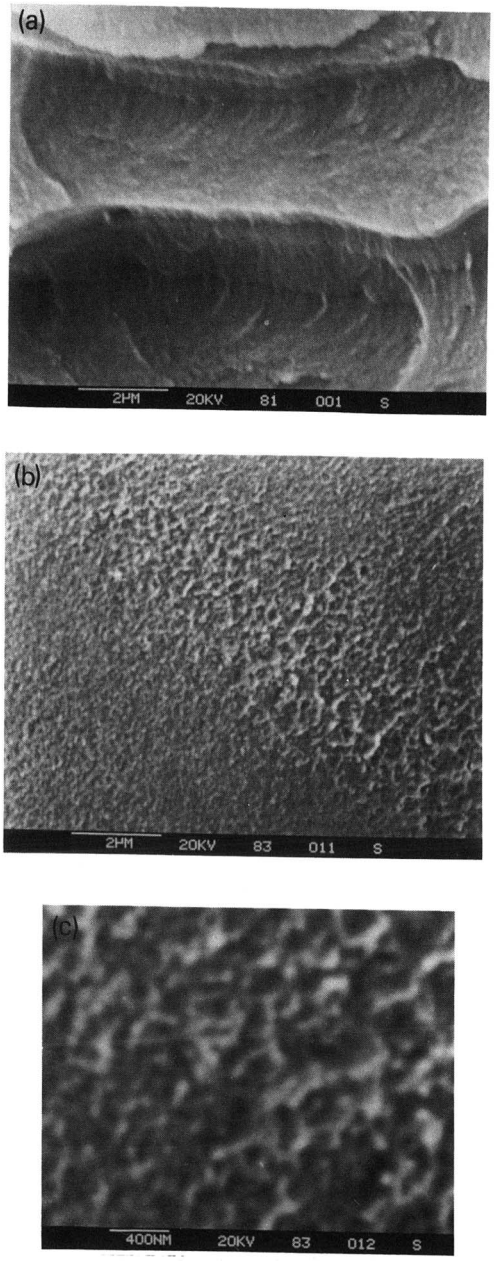

Fig. 3. Scanning electron micrographs of cross-sections of beaded copolymers of styrene with 2,4,5-trichlorophenyl acrylate and DVB obtained in the presence of chlorobenzene (a) (a good solvent) or (b and c) chlorobenzene–*n*-octane (a poor solvent); (c) is the same as (b) but with higher magnification (from ref. 34).

way consists of a mass of aggregated polymer nodules or "grains" evident at a magnification of 10 000 (micrograph b). At a higher magnification of 40 000 (micrograph c), the inter-grain spaces (*i.e.* pores) with dimensions of about 20–200 nm are also clearly visible. It must be emphasized again, however, that porosity in organic polymer supports may not represent a strictly invariable criterion [35].

Control of porosity by means of a monomer diluent (or porogen) has been extensively studied for polystyrene [35–38] and polymethacrylates [39–42]. For polyacrylamides, a detailed electron microscopic study of gels produced in bulk was reported by Ruchel and Brager [43]. A recent illustration of the dependence of pore size distribution on the nature and percentage of monomer diluent is provided in Fig. 4 [44]. The surface areas of the resins indicated in Fig. 4 range between 5 and 145 m^2/g.

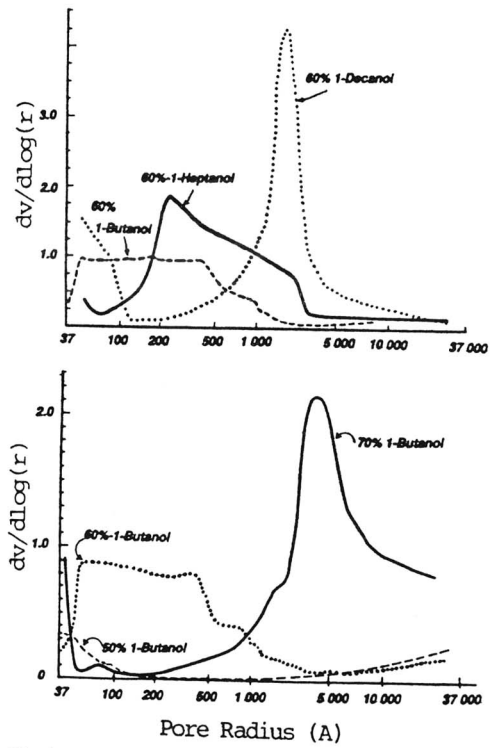

Fig. 4. Dependence of porosity of phenolic resins on the nature and proportion of monomer diluent. r = Pore radius; v = pore volume (adapted from ref. 44).

Surface area and porosity are routinely measured by nitrogen adsorption–desorption (BET and BJH methods), mercury intrusion and low-angle X-ray scattering [45–48]. Specific pore volume can be estimated from the apparent density of the microbeads or the gain of an inert liquid (a non-solvent for the polymer). These methods are generally convenient and suitable for comparison of samples produced under related experimental conditions. However, the absolute values of the data obtained by these methods are subjective to some extent. Electron microscopy (EM) provides directly visual evidence of pore size and pore size distribution (see Fig. 3), but it is less practicable for routine use. Thus, a combination of EM and conventional methods of pore size measurement should provide reliable information on the pore structure of the polymer.

Matrix porosity is the basis of support characteristics in gel (permeation) chromatography, and determines the fractionation range of the support. Resin porosity may also affect the support performance in other applications such as affinity chromatography, catalysis and solid-phase synthesis. However, in all of the above applications, the support functions in a solvent in which the matrix may swell to various extents. Under these conditions, the specific pore volume and pore size distribution in the swollen state [49] may be substantially different from those measured in the dry state. Accordingly, the support performance is strongly dependent on its swellability in the solvent used.

4. POLYMER SWELLABILITY

Resin swellability (or bulk expanded volume) in a given solvent is a multifaceted property reflecting the chemical structure of the polymer backbone, degree of cross-linking and the architecture of the polymer matrix. The three-dimensional structure of the polymer matrix (or network) *takes shape* according to the conditions prevailing during the formation of the polymer microbeads. For beaded poly-

TABLE 3

EFFECTS OF CROSS-LINKING AND MONOMER DILUENT ON THE SWELLING BEHAVIOUR OF STYRENE-BASED RESINS[a]

Cross-linking (mol%)	Monomer diluent (ml/g)[b]	Bulk expanded volume (ml/g) in solvent[c]					
		None	MET	DMF	EAC	DOX	DCM
0.5	0.0	nm[d]	2.5	6.2	6.5	10	11
1.4	0.0	1.6	2.2	4.2	4.8	5.0	5.2
2.2	0.0	1.4	2.0	2.3	2.6	3.6	3.5
5.0	0.0	1.4	nm	1.8	nm	nm	2.1
10	0.0	1.4	nm	1.7	nm	nm	1.9
2.1	A(1.0)	1.6	2.4	5.4	6.1	9.6	10
2.1	B(1.0)	6	6	10	20	20	22
2.1	C(1.0)	4.4	5.1	6.8	7.0	8.5	8.5
2.1	D(1.0)	1.6	1.6	4.2	4.5	5.7	6.2
5.8	A(3.3)	1.6	1.8	6.1	8.5	9.5	11
5.8	B(3.3)	14	16	17	15	14	25
5.8	C(3.3)	7	nm	nm	nm	nm	11
5.8	E(2.5)	2.1	3.4	5.5	5.5	7.0	8.5
5.8	F(3.0)	6	nm	nm	nm	nm	11
5.8	A(5.0)	nm	Soluble	Soluble	Soluble	Soluble	Soluble

[a] Produced [50] by suspension copolymerization of styrene and approximately equal concentrations of 2(3)-ethylvinylbenzene and 2(3)-divinylbenzene.

[b] Monomer diluent (ml/g monomer); A = chlorobenzene; B = dodecane; C = pentanol; D = carbon tetrachloride; E = A + B (2:3); F = B + C (2:1).

[c] MET = Methanol; DMF = dimethylformamide; EAC = ethyl acetate; DOX = dioxane; DCM = dichloromethane.

[d] nm = Not measured.

mer supports obtained by suspension polymerization, the type and percentage of the monomer diluent strongly influence the shape of the three-dimensional polymer network. For polysaccharide gels produced by suspension cross-linking, the nature and proportion of the polymer solvent have a similar role. In either case, polymer molecular weights (degree of polymerization, DP) also contribute to matrix architecture. In general terms, these criteria also apply to inorganic gels, although the process is more complicated in this case (see Part I).

Table 3 [50] shows the swelling behaviour of a series of copoly(styrene–divinylbenzene) resins in a number of commonly used organic solvents, including methanol (MET), dimethylformamide (DMF), dioxane (DOX), ethyl acetate (EAC) and dichloromethane (DCM).

A full interpretation of the swelling data in Table 3 is beyond the scope of the present discussion. However, a number of general conclusions can be drawn from the swelling patterns of different samples. For example, under a given set of experimental conditions, the extent of polymer swelling (bulk expanded volume) decreases as the nominal degree of cross-linking increases. It is also evident that, for a given degree of cross-linking, the bulk expanded volume is strongly dependent on the nature and proportion of the monomer diluent used during matrix formation. In general, the higher the percentage of the monomer diluent, the larger the bulk expanded volume of the resin, but different diluents affect polymer swelling to different extents.

An interesting implication of these observations is that the bulk expanded volume of the gel can be maintained at a relatively constant level by simultaneously increasing both the degree of polymer cross-linking and the percentage of the monomer diluent. However, this process has a far-reaching effect on the gelation and precipitation of the polymer "grains" within the microbeads (see Fig. 3). The pattern of gelation and precipitation, in turn, affects the porosity and surface area of the beads, as discussed in the preceding section.

Another practically important aspect of resin swellability is the pattern of polymer–solvent compatibility, *i.e.* the relative measure of polymer swelling in different solvents. Polymer–solvent compatibility is determined by the chemical structure of the polymer backbone. An interesting illustration of this structure–property relationship is provided by the swellability data in Table 4 [32]. These data show the swelling behaviour of a series of copoly(styrene–

TABLE 4

SWELLING BEHAVIOUR OF DIFFERENT TYPES OF POLYMER SUPPORTS

Polymer type[a]	Swellability (ml/g) in different solvents[b]								
	TOL	EAC	THF	DCM	DMF	DMSO	MeOH	AcOH	Water
Polystyrene:									
(1a)	5.1	4.8	5.0	5.2	4.2	–[c]	–	–	–
(1b)	10.0	8.5	10.0	11.0	6.2	–	–	–	–
Polydimethylacrylamide:									
(2a)	–	–	–	9.5	9.1	10	12	12	9.0
(2b)	–	–	–	20	20	20	23	35	19
Copoly(styrene–dimethylacrylamide)									
(12b)	7.1	6.0	7.5	7.3	6.0	5.1	6.1	6.9	3.9
(12c)	4.7	4.0	5.3	5.8	5.2	4.6	5.5	5.5	3.7
(12d)	18	16	21	27	16	13	13	21	8.9

[a] For details of polymer types 1 and 2, see refs. 51 and 52, respectively. Polymers 12b, 12c and 12d were obtained from three different samples of copoly(styrene–2,4,5-trichlorophenyl acrylate) according to Fig. 17.

[b] TOL = Toluene; EAC = ethyl acetate; THF = tetrahydrofuran; DCM = dichloromethane; DMF = dimethylformamide; DMSO = dimethyl sulphoxide; MeOH = methanol; AcOH = acetic acid.

[c] Dashes indicate polymer–solvent incompatibility.

dimethylacrylamide)s as compared with those of the corresponding homopolymers, polystyrene and polydimethylacrylamide.

The hydrophobic resin (polystyrene) [51] and the hydrophilic resin (polydimethylacrylamide) [52] are compatible with, respectively, the first five and the last six solvents listed in Table 4. The copolymer resins, copoly(styrene–dimethylacrylamide)s, incorporate the structural units of both homopolymers, and have an amphiphilic structure. As a result, they are compatible with all of the solvents listed in Table 4, ranging from toluene and ethyl acetate on the one hand to dimethyl sulphoxide and water on the other. This general solvent compatibility is related to the actual solvation of the polymer backbone, and should not be confused with the uptake of non-solvents by porous gels (see below). Swellability data for other polymers covered by this review have been reported by Pharmacia [53] for Sephacryl, Peska *et al.* [54] for cellulose ion exchangers, Smrz and Viska [55] for Spheron, Fenyvesi *et al.* [56] for polycyclodextrins, Epton and co-workers [57,58] for Enzacryl and related polymers and Birr [59] for low-cross-linked polystyrene.

It should be emphasized that the extent of apparent polymer swelling (bulk expanded volume) and the solvation of the polymer chains do not necessarily coincide. The distinction between "polymer swelling" and "solvation of the polymer chains" is particularly relevant in any discussion of the reactivity (or site accessibility) of polymer-bound reactive sites. When a low-cross-linked polymer (whether porous or not) swells in a "good solvent", individual polymer chain segments become solvated. Under these conditions, the polymer-bound reactive sites are rendered potentially accessible to the soluble reagent. On the other hand, highly cross-linked porous gels generally "suck up" certain volumes of various liquids, whether good or poor solvents [60,61]. Here, the liquid is stored in the pores (*cf.* the channels between the precipitated grains in Fig. 3), without necessarily contributing to polymer solvation and site accessibility. For non-porous polymer beads, the extent of swelling is closely related to solubility parameters [62], that is, the closer the solubility parameters of the polymer and the solvent, the greater the extent of polymer swelling.

In practice, highly swollen gels may not be desirable, because they collapse under pressure and are difficult to filter. In addition, a highly swollen gel behaves as a viscous polymer solution, with the consequence of poor substrate diffusion and transport within the polymer matrix. Accordingly, it is often necessary to employ relatively more cross-linked porous gels, in which site accessibility is judiciously compromised at the expense of handling convenience and rapid diffusion. This topic is further discussed in section 6.1.

5. ACTIVATION AND FUNCTIONALIZATION

The discussion on the activation and functionalization of polymer supports and gels is organized under separate subheadings for major polymer types, including polystyrene, polyacrylamides, polysaccharides, porous silica and the recently introduced amphiphilic copolymers. Other polymer types commonly used for chromatography and related applications include poly(vinyl alcohol), poly(hydroxyethyl methacrylate) (Separon), poly(glycidyl methacrylate) (Eupergit) and Ultragel. The first two resins contain hydroxy groups, and can be activated and derivatized in basically the same way as described for polysaccharides. Polymer supports carrying glycidyl (oxirane or epoxide) functionality react with nucleophiles in a manner similar to oxirane derivatives of polysaccharides and silica gel. Ultragel contains both hydroxy and amide residues, and can be derivatized by the same procedures as described for polysaccharides and polyamide. Activation of organic and inorganic supports by complexation/chelation of titanium and related metals (for enzyme immobilization) has been reviewed recently [63], and will not be covered here. For derivatization of fluorocarbon polymers (Kel-F beads) by organometallic reagents, see refs. 64 and 65.

5.1. Polystyrene

Beaded copolymers of styrene and divinylbenzene are most widely used for the manufacture of strongly acidic [66] and strongly basic [67] ion-exchange resins [68,69]. Commercially important polystyrene ion exchangers are produced in one or two steps, as depicted in Fig. 5. A variety of related chelating agents [18] can also be produced from the chloromethylated polystyrene by processes basically similar to that of the ammonium resins shown in Figure 5.

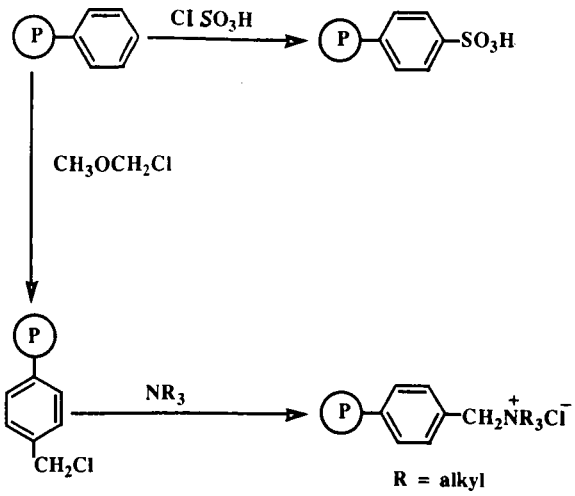

Fig. 5. Basic chemical reactions employed for the synthesis of styrene-based ion exchangers.

On the basis of its chemical structure, polystyrene is more inert than other commonly available polymer supports. Largely for this reason, and also owing to compatibility with organic solvents, styrene-based polymer supports have been generally adapted for solid-phase peptide synthesis [13,14]. They are also being studied for a wide range of other analytical, catalytic and synthetic uses [15–17].Chloromethylation (see Fig. 5) [66–72] and bromination [73,74] of beaded polystyrene provide two of the most useful intermediates for the synthesis of styrene-based polymer supports [15–17]. It must be borne in mind, however, that both chloromethylation and bromination involve a variety of side-reactions and complications [75], depending on the experimental conditions and the desired level of functionalization.

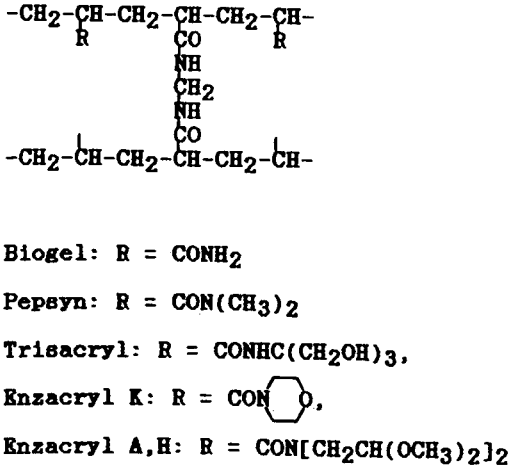

Fig. 6. Structures of different acrylamide gels.

5.2. *Polyacrylamides*

There are five different types of acrylamide-based polymer supports and gels commercially available, including polyacrylamide (Bio-Gel), polyacryloylaminomethyldimethylacetal (Enzacryl A and H), polyacryloylmorpholine (Enzacryl K), poly[(trishydroxymethyl)methylacrylamide] (Trisacryl) and polydimethylacrylamide (Pepsyn). The structures of different polyacrylamides are shown in Fig. 6.

Derivatization of Bio-Gel, as elaborated by Inman and Dintzis [76], is outlined in Fig. 7. The functionalized gels obtained in this way can be further derivatized and activated (*i.e.* for enzyme and ligand attachment) by reagents such as nitrous acid, carbodiimide and glutaraldehyde [76]. Isocyano derivatives of Bio-Gel have also been produced by Goldstein [77] for enzyme immobilization via four-component condensation (4CC). For a review of these and other isocyano polymer supports, see ref. 78.

Trisacryl gels contain an abundance of hydroxy groups and can be activated in basically the same way as described for polysaccharide gels (see below). Enzacryl A and H are produced by reaction of the dimethylacetyl resin with tartaric acid dihydrazide

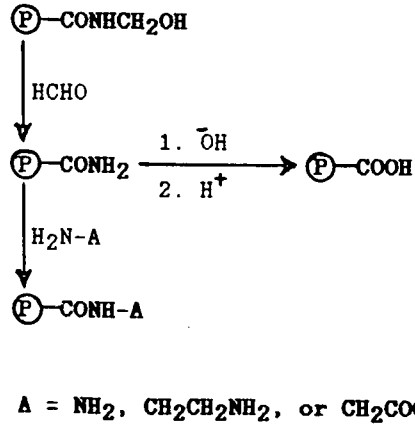

Fig. 7. Functionalization of polyacrylamide (Bio-Gel).

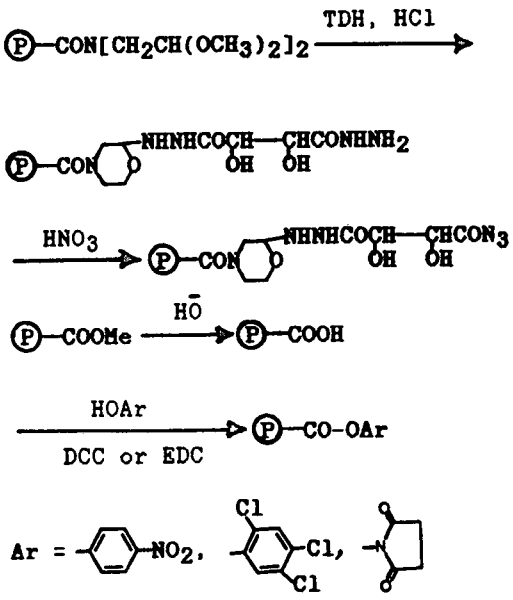

Fig. 8. Preparation of activated derivatives of substituted acrylamide gels. Enzacryl (adapted from ref. 79) and Pepsyn (adapted from ref. 52). TDH = Tartaric acid dihydrazide; DCC = dicyclohexylcarbodiimide; EDC = 3-(dimethylaminopropyl)ethylcarbodiimide; Me = methyl.

and nitrous acid, as depicted in Fig. 8 [79]. Dimethylacrylamide resins have been developed for solid-phase peptide synthesis [80] (hence the acronym Pepsyn). Details of the synthesis and derivatization of these resins, including those carrying free amino or carboxy functionality, have been discussed recently [52]. Preparation of carboxyl–activated dimethylacrylamide resins is also outlined in Fig. 8 [52].

Enzacryl K was introduced by Epton for gel permeation chromatography (ref. 2, pp. 70–90). Derivatization of this polymer via treatment with diamines at relatively high temperatures has been reported by Narang *et al.* [81] and Arshady *et al.* [82,83]. Their work represents an interesting functionalization route in which the reactive sites on the polymer are the "cross-linking units", as indicated in Fig. 9 [82,83]. Accordingly, the result of the functionalization depends strongly on the structure of the diamine and the reaction conditions employed (usually DMF or ethylene glycol solvent, 150–200°C, 2–24 h).

With symmetrical diamines, initially derivatized gels with free amino groups are produced, followed by the gradual formation of highly rigid resins if the reaction is continued. When unsymmetrical diamines, such as 1-(2-aminoethyl)piperazine, are used, gradual de-cross-linking of the gel leads to the formation of completely soluble polymers.

5.3. Polysaccharides

Polysaccharide gels are produced from cellulose, agarose (Sepharose) and dextran (Sephadex), and they are widely used for chromatography and enzyme immobilization. All of these polymers contain hydroxy groups available for activation and further derivatization. A small number of hydroxy groups in native agarose are sulphated ($-CH_2OSO_3^-$), but these sulphate groups are usually removed during the manufacture of the beaded polymer. Dextran-based gels may contain some carboxyl groups. It is also noteworthy that the basic polysaccharide structures of these gels is preserved only in the case of non-cross-linked products. In cross-linked polysaccharide gels, the chemical structure is often substantially altered, depending on the nature and extent of the cross-linking units. Two examples, namely those of agarose gels produced by epichlorohydrin cross-linking and Sephacryl obtained by cross-linking (copolymerization) of allyldextran with bisacrylamide, are shown in Fig. 10.

It is also evident from Fig. 10 that cross-linked polysaccharide gels may carry primary and/or secondary hydroxy groups. The proportions of different OH groups on the polymer are determined by the type of polysaccharide, and the structure and the percentage of the cross-linking units. This must be borne in mind when planning the activation and utilization of polysaccharide gels. Primary hydroxy groups are, for the purpose of the present discussion, substantially more reactive than secondary and tertiary ones. This order of reactivity also applies to the corresponding activated derivatives such as sulphonates (see below).

Chemically modified polysaccharide gels can be divided into two broad categories, namely ion-exchange resins and activated intermediates used for affinity chromatography and enzyme immobilization. Preparation of various cellulosic ion exchangers was described by Peterson and Sober in the late 1950s [84,85], Determan and Wieland in the 1960s

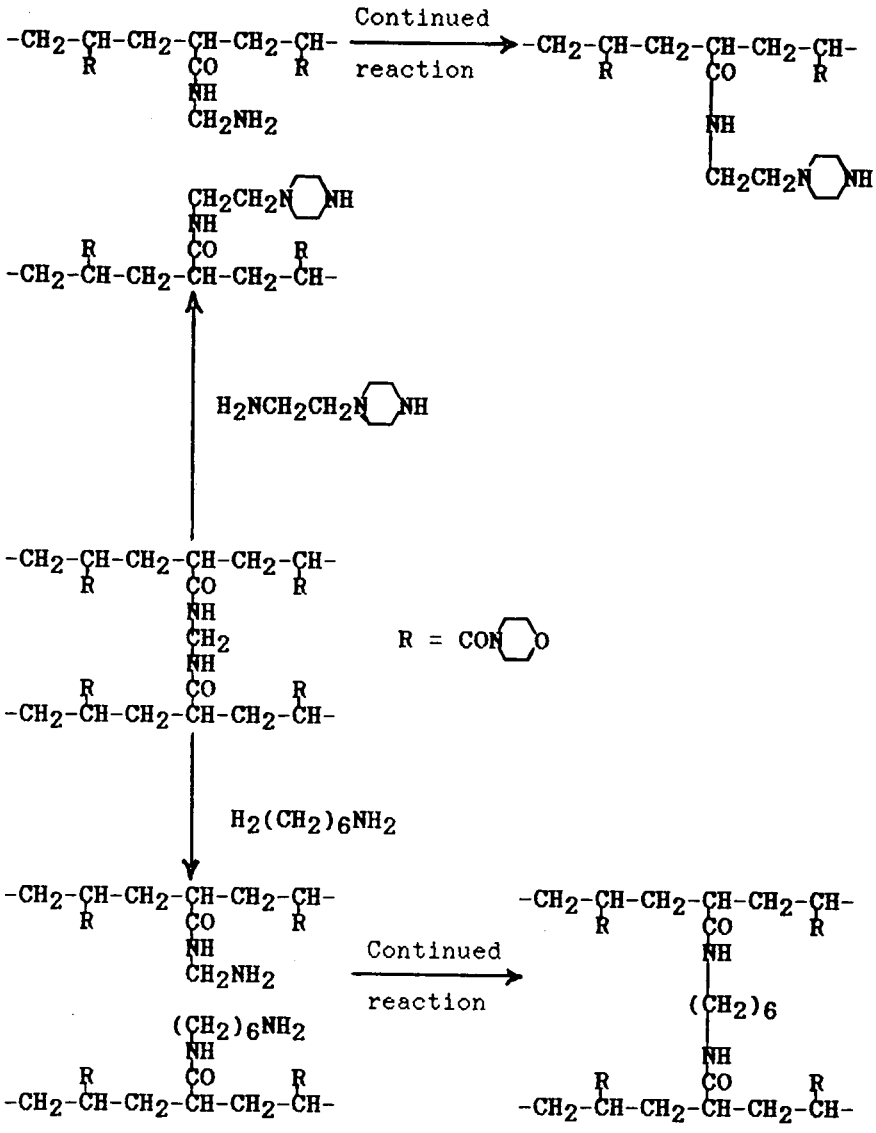

Fig. 9. Functionalization of Enzacryl K via treatment with diamines [82].

[86], and more recently by Peska *et al.* [54]. The basic chemistry of these preparations is illustrated in Fig. 11.

The use of polysaccharide-based polymer supports for affinity chromatography and enzyme immobilization involves the preparation of "activated" gels, followed by the attachment of the affinity ligand or enzyme via NH_2, SH and/or OH groups. One generally useful type of activated intermediate for this purpose is the "active ester derivative" obtained by succinylation, followed by reaction with a phenolic or N-hydroxy compound, as indicated in Fig. 12. The succinylation reaction is carried out in basically the same way as the reactions shown in Fig. 11. A wide range of other commonly used activation methods are outlined in Fig. 13 [87–101]. It should be evident that most of the chemical reactions indicated in Figs. 12 and 13 are

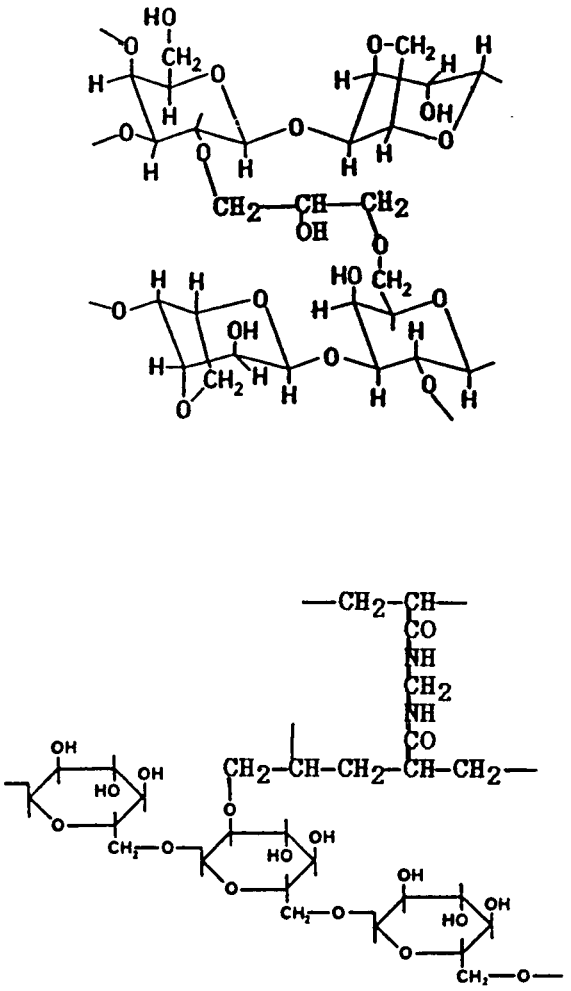

Fig. 10. Structures of Sepharose (cross-linked agarose) (top) and Sephacryl (copolymer of allyldextran and bisacrylamide) (bottom).

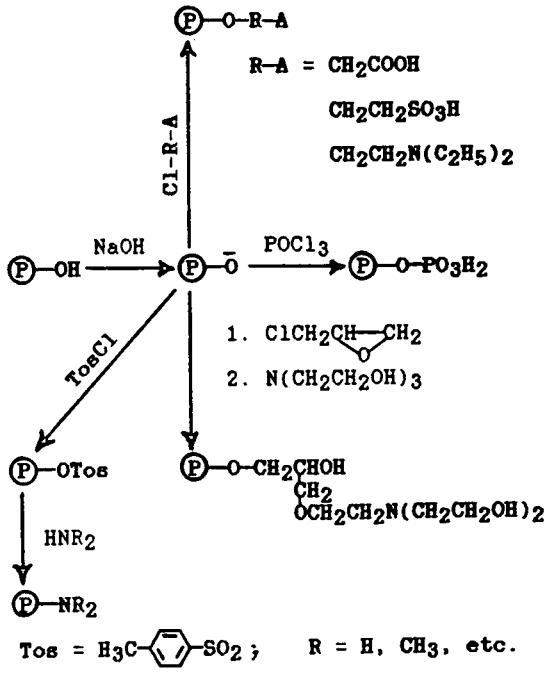

Fig. 11. Preparation of cellulose-based ion exchangers.

also applicable to other hydroxyl-bearing polymers such as Trisacryl, Separon, poly(vinyl alcohol) and hydroxy derivatives of silica gel and glass beads.

Among the reactions represented in Fig. 13, cyanation with cyanogen bromide was first introduced by Axen *et al.* [87] in 1967 and is still widely used. The popularity of this activation route is largely due to the simplicity of the method and the low cost of the reagent. However, the procedure usually requires a large excess of the toxic reagent (cyanogen bromide). Furthermore, the linkage formed between the cyanyl-activated gel and the ligand (or enzyme) is not completely stable, and hence gradual leakage and decreased capacity (or activity) of the gel occur.

Wilchek [91] studied the mechanistic details of cyanogen bromide activation. He introduced less toxic cyanylating reagents, such as triethylamine–cyanogen bromide complex and 4-nitrophenyl cyanate. However, the reduction in toxicity achieved by

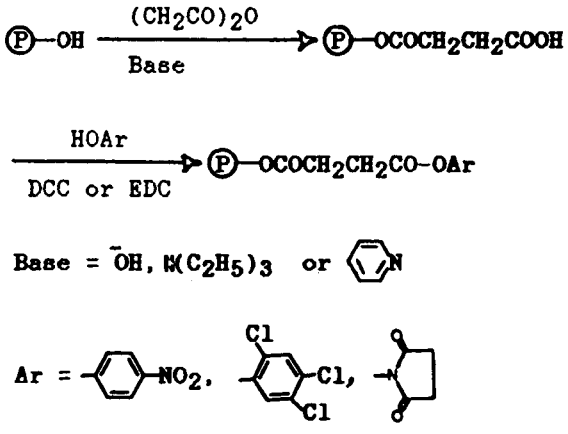

Fig. 12. Preparation of succinyl-activated polysaccharides.

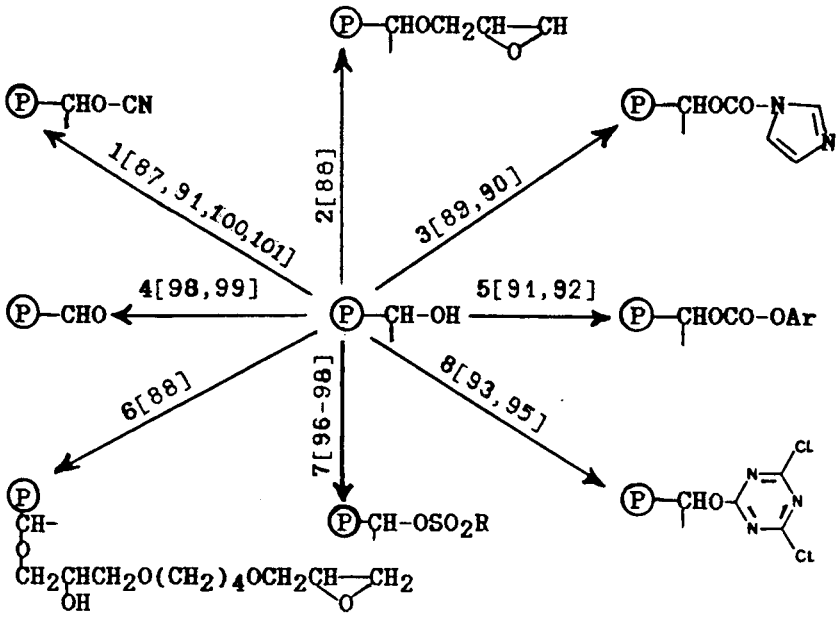

1 = CNBr or O_2N-⟨⟩-OCN; 2 = $ClCH_2CH—CH_2$;

3 = Carbonyldiimidazole, 4 = $I\bar{O}_4$

5 = Cl-CO-OAr (Ar, see Figure 12);

6 = $H_2C—CHCH_2O(CH_2)_4OCH_2CH—CH_2$;

7 = $ClSO_2R$, R = CH_2CF_3, -⟨⟩-CH_3, N=N-⟨⟩-$N(CH_3)_2$;

8 = Cyanuric chloride (2,4,6-trichloro-1,3,5-triazine)

Fig. 13. Activation of polysaccharide gels.

the use of these reagents is offset by substantially increased reagent cost and additional labour.

Activation of polysaccharide gels by cyanogen bromide and most other reagents indicated in Fig. 13 often involves a variety of side-reactions and complications, some of which are outlined in Fig. 14. For example, O-cyanyl activated gels, in addition to hydrolysis, undergo intra-resin transformation with neighbouring (including spatially nearby) hydroxy groups, leading to the formation of cyclic or inter-chain carbonate and imidocarbonate bridges [90].

Activation by sulphonyl chlorides produces primary and secondary sulphonates, depending on the reaction conditions employed. Only primary sulphonates are sufficiently reactive under the mild conditions desired for ligand/enzyme attachment. Residual sulphonate groups on the polymer increase gel hydrophobicity. It is also possible that secondary

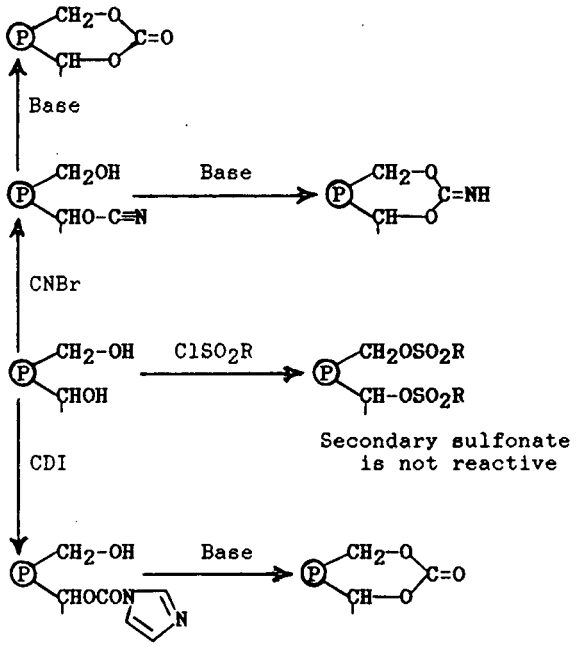

Fig. 14. Possible side-reactions associated with the activation of polysaccharide gels.

sulphonate residues may gradually hydrolyse or react with the soluble or polymer-bound enzyme (or substrate) during the utilization of the gel.

It should also be noted that the reaction of highly functionalized polymer supports with symmetrical difunctional reagents (*e.g.*, diamines or diepoxides) generally leads to extensive intra-resin cross-linking (*cf.* Fig. 9 and ref. 52). The large excess of reagents usually employed for these reactions is not effective because of the intra-resin proximity of the reactive sites. This means that functionalization of polymer supports via symmetrical difunctional reagents may produce gels with lower than expected functionality, higher degrees of cross-linking, increased rigidity and correspondingly altered (reduced) porosity.

5.4. Porous silica and glass beads

Functionalization of siliceous gels is based on the chemistry of surface silanol groups. The silanol function can be derivatized via several reaction pathways [32], including condensation with alcohols and trichloro- and trialkoxysilanes. In particular, reaction with triethoxysilanes [32,102–106] provides a highly versatile route for the production of stable functionalized silica supports in a single step (Fig. 15). Silylating reactions according to Fig. 15 are carried out by refluxing the silica particles in a solution of the reagent in pure toluene [103,104], in toluene contaminated with (traces of) water [104,105] or in aqueous media [106]. In either case, the chemistry of the reaction is complicated because the OH groups may be free or hydrogen bonded, depending on the thermal history of the particles [104,107]. The silylation reaction shown in Fig. 15 is also applicable to metal oxide supports such as titania and zirconia, as reported recently by Truedinger *et al.* [108].

The theoretical silanol content of porous silica varies with porosity and surface area, but is usually about 3–4 mmol (mequiv.) per gram of dry sample. However, most of these OH groups are either buried within the silica grains (isolated small pores), or are otherwise strongly hydrogen bonded and inaccessible. The presence of water in the reaction mixture reduces the level of hydrogen bonding and creates additional silanol sites via hydrolysis of surface Si–O–Si bonds. In this way, the reaction conditions can be empirically adjusted to produce a so-called monolayer functionality of up to about 0.2–0.3 mmol/g. In strictly rigid supports, functionality may also be expressed in units of μmol/m^2.

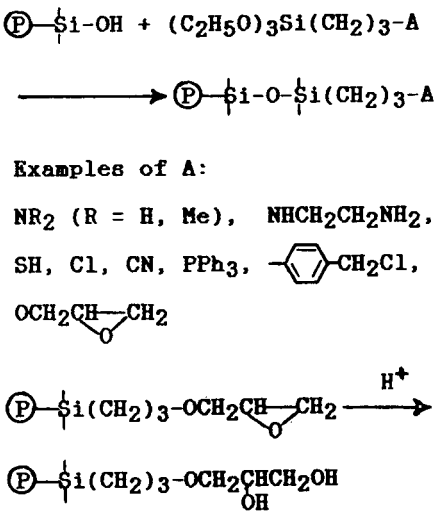

Fig. 15. Derivatization of silica gel via reaction with triethoxysilanes.

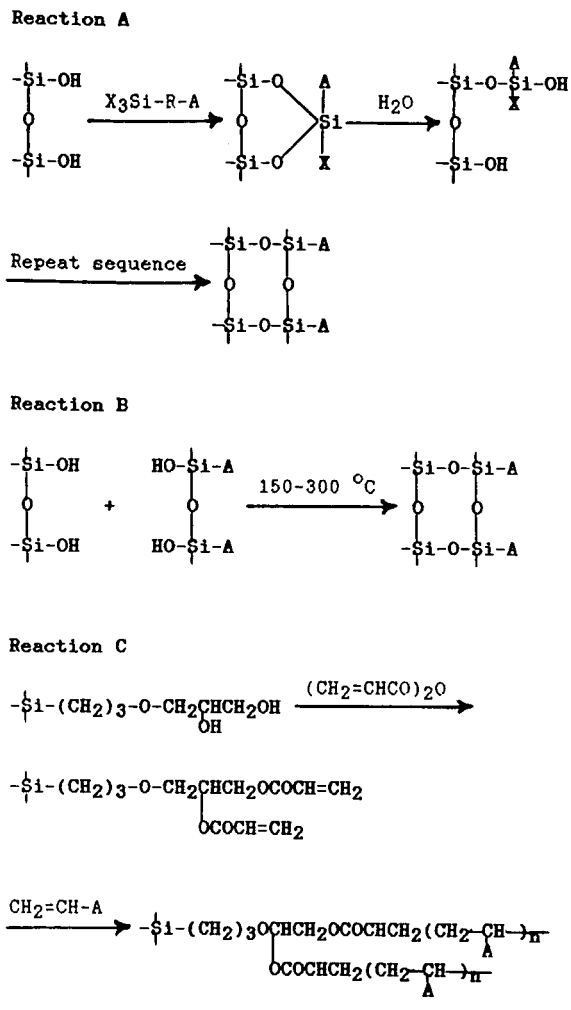

Fig. 16. Preparation of highly functionalized silica gel by surface polycondensation of alkoxy or chlorosilanes (Reaction A), polymeric alkoxysilanes (Reaction B) or surface polymerization of organic monomers (Reaction C).

Once this primary derivatization has been accomplished, the resulting functional groups can be activated or further derivatized as necessary [109,110]. One particularly useful reaction is the acid hydrolysis [106,111] of the oxirane (epoxide) functionality to obtain the corresponding diol derivative. Here again, the accessibility of the initially generated functional groups depends on sample porosity and reaction conditions. Surface modification of colloidal silica particles by organic polymers has been recently reviewed by Ryan [112].

Silica particles with relatively higher degrees of functionality can be produced by forming, or attaching (grafting), polymeric species onto the initially generated functional groups. Three different routes for the formation of polymeric species on porous silica are depicted in Fig. 16.

In the stepwise condensation of chloro- or alkoxysilanes on the silica surface (Fig. 16, Reaction A) [113], the stoichiometry of the reaction is very difficult to control. On the other hand, according to Kirkland and Yates [114], the reaction of silica with preformed polyethoxysilanes (Reaction B) can be easily controlled to obtain a multilayer thickness of about 3–1000 nm. Graft polymerization of vinyl monomers on appropriately functionalized silica surfaces (Reaction C) [115] is essentially similar to the formation of core–shell grafts discussed in Part I. This method usually leads to the formation of cross-linked (entrapped) organic polymer within the pore structure of the silica.

5.5. *Amphiphilic copolymers*

In recent years, a new synthetic approach has been introduced [116–118] whereby both the functionality and the chemical structure of the polymer can be tailored for optimum performance. The method is based on a new class of activated polymer intermediates and the chemistry of active esters (active ester synthesis or leaving group substitution) (Fig. 17) [119–121].

According to the new method, the activating (or leaving) groups on the polymer are displaced by suitably chosen nucleophiles carrying the desired structure (A^1) or functionality (A). As can be seen in Fig. 17, the functional residue (A) is positioned at the end of a spacer arm (B). In addition, the choice of the structural residue (A^1) offers the possibility of "tailoring" the composition of the polymer support for any specific application. In particular, the new method provides a uniquely versatile route for the synthesis of amphiphilic polymer supports carrying the desired functionality (Table 5).

The range of functional groups which can be introduced into the polymer according to Fig. 17 is virtually unlimited. For polymer supports with low degrees of functionality (< 1 mmol/g), the reaction

sequence (1) HA^1, (2) HBA is more convenient, except when HA^1 is a volatile compound (*e.g.* dimethylamine). There is a possibility that a fractionation of the reactive sites generated on the resin initially may be relatively more accessible than those introduced at the end. Accordingly, the reaction sequence (1) HBA, (2) HA^1 should be preferred in principle. However, the practical significance of this differential accessibility would appear to depend on the particular application involved. The possibility of generating reactive sites with relatively low accessibility is of special interest in the design and study of site isolation on the polymer support.

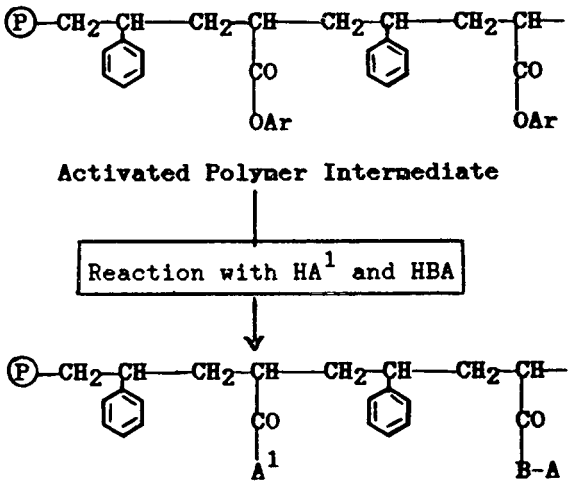

Fig. 17 Synthesis of amphiphilic polymer supports via activated polymer intermediates (active ester synthesis or leaving group substitution) [116–118].

TABLE 5

EXAMPLES OF AMPHIPHILIC POLYMER SUPPORTS AVAILABLE VIA ACTIVE ESTER SYNTHESIS ACCORDING TO FIG. 17

A^1	B–A
$NHCH_2CH_2N(CH_3)_2$	$NHCH_2CH_2N(CH_3)_2$
$NHCH_2CH_2SO_3H$	$NHCH_2CH_2SO_3H$
$NHCH_2CH_2CH_2OH$	$NHCH_2CH_2CH_2OH$
$N(CH_3)_2$	$N(CH_3)_2$
$N(CH_3)_2$	$NHCH_2CH(OH)CH_2OH$
$N(CH_3)_2$	$NH(CH_2)_6OH$
$N(CH_2)_2$	$NH(CH_2)_5COOH$
$N(CH_3)_2$	$NH(CH_2)_6NH_2$
$N(CH_3)_2$	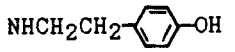
$N(CH_3)_2$	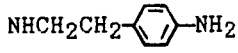
$N(CH_3)_2$	$O(CH_2CH_2O)_nOH$
$N(CH_3)_2$	$O(CH_2)_6NHCHO$[a]
$N(CH_3)_2$	$O(CH_2)_6PPh_2$
$NHCH_2CH_2CH_2OH$	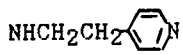
$N(CH_3)_2$	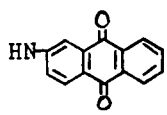

[a] The –NHCHO group can be dehydrated to the corresponding isocyano (–NC) group, useful for metal complexation or enzyme/ligand attachment by four-component condensation.

6. POLYMER MATRIX AND CHEMICAL STRUCTURE

6.1. Polymer matrix

The term "polymer matrix" is employed here to refer to the macromolecular (or *secondary*) structure of the polymer chains within the individual microbeads. A schematic illustration of this structure for a lightly cross-linked non-porous gel matrix is provided in Fig. 18 [122]. Such a polymer matrix is expected to result from the "random coil" nature of the polymer chains and the conditions under which the microbeads are usually formed.

When a low-cross-linked gel swells in a good solvent (see Tables 3 and 4), the matrix expands and a certain degree of short-range re-organization of the loose and tight chain segments may take place. Long-range conformational changes are, however, prohibited by the cross-link bridges between the

Fig. 18. Schematic presentation of the macromolecular (or matrix) structure of a lightly cross-linked polymer bead.

chains. In addition, extensive non-covalent cross-linking (*e.g.* hydrophobic interaction in polystyrene, or hydrogen bonding in polyacrylamides and polysaccharides) may restrict even the short-range mobility of the chain segments. In other words, polymer supports and gels have a heterogeneous matrix structure which is largely preserved even in the swollen state.

Routine experience indicates that when non-porous gels swell in a "good" solvent to a minimum of about 5 ml/g, all of the polymer-bound reactive sites are usually accessible within a reactivity range of 1–2 orders of magnitude. That is, in fully swollen gels some of the reactive sites on a single polymer microbead may be 10–100 times less reactive than others. In highly cross-linked and porous gels, the degree of site heterogeneity is correspondingly higher. In the extreme case, and where the polymer does not swell, only the surface reactive groups may be accessible. Even some of the surface groups may have reduced accessibility because of strong non-covalent interactions with the neighbouring groups and/or the polymer backbone.

To this end, it should be stressed that the overall efficiency of a given polymer support is not necessarily determined by full site accessibility. In general, chromatographic and catalytic applications of polymer supports and gels require rapid diffusion of the substrate to, and from, the polymer matrix. Here, accessibility of all of the reactive sites is by no means essential. On the other hand, for organic chemical applications, and notably for solid-phase peptide synthesis, it is essential that all of the polymer-bound reactive sites are more or less equally accessible. In this case, high reaction rates are desirable, but not critical. Accordingly, the architecture of the polymer matrix should be designed for either rapid diffusion or maximum site accessibility, depending on the requirement of the intended application.

6.2. Chemical structure

Traditionally, structure–performance relationships in polymer supports and gels are studied on the basis of porosity and surface area (or *tertiary structure*). The significance of the polymer matrix (or *secondary structure*) is also generally recognized, as outlined above. An even deeper level of gel structure, which may critically influence the overall gel performance, is the chemical (or *primary*) structure of the polymer backbone. This level of structure–performance relationship originates from the fact that the "function" of the polymer support, whether in chromatography, catalysis or synthesis, is invariably based on "direct molecular contacts" between the polymer backbone and the soluble substrate.

Experimental evidence on the relationship between the chemical structure of the polymer backbone and overall polymer performance abounds in the literature. However, the significance of these observations is not always appreciated, and hence they may be left "unexplained", or reported as "thermodynamic" or "microenvironment" effects. Notable examples where explanation in terms of chemical structure has been offered include the role of chemical structure in gel permeation chromatography [123], aqueous hydrolysis of species bound to hydrophobic polymer supports [124], polymer-supported hydrogenation catalysts [125,126], and in peptide synthesis [34]. Some of these observations have been briefly reviewed recently [117]. The conclusion is that, in many instances, the overall efficiency of a given gel may depend critically on the chemical compatibility of the polymer backbone with the polymer-bound substrate or the soluble reagent.

6.3. Site accessibility and spacer arm

Functional groups attached to cross-linked polymer matrices usually have reduced accessibility compared with those of analogous low-molecular-weight compounds. This decreased site accessibility is partly due to reduced mobility of the cross-linked chain segments and partly the result of "spatial" hindrance within the cross-linked matrix. The term "spatial" (rather than steric) is employed to emphasize the effect of "through-space" interactions *versus* steric effects of neighbouring residues observed in small molecules.

Both segmental mobility of the polymer chains and spatial hindrance (matrix architecture) are closely related to polymer cross-linking and swellability, but they represent two different aspects of matrix structure. Spatial hindrance cannot be easily measured and quantified, whereas segmental mobility can be quantified by, for example, electron spin resonance [127,128] and NMR spectroscopy [129].

Reduced site accessibility caused by low mobility of the polymer chains can, in principle, be remedied by introducing a spacer arm between the polymer backbone and the functional groups. In practice, the degree by which a given spacer arm may enhance site accessibility depends largely on the size and nature of the soluble reagent. However, a five- or six-bond spacer arm is usually considered useful for most applications of polymer supports, including affinity chromatography, immobilized enzymes and solid-phase synthesis and catalysis.

Typical spacer molecules employed in conjunction with different polymer supports are indicated in Fig. 19. In conventionally produced polymers, the positioning of functional groups at the end of such spacer arms usually involves a multi-step synthesis.

$H_2N(CH_2)_nNH_2$ (n = 6 or 12)

$H_2NCH_2CH_2NHCH_2CH_2NH_2$

$OHC(CH_2)_4CHO$

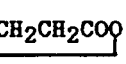

$Br(CH_2)_nBr$

$H_2N(CH_2)_5COOH$

Fig. 19. Structures of typical spacer molecules employed in conjunction with the use of different polymer supports and gels.

For the recently introduced amphiphilic copolymer resins, the desired functionality, already positioned at the end of a four- to nine-bond spacer arm (see Table 5), is introduced into the polymer in a single step.

7. CONCLUSIONS AND GENERAL REMARKS

Beaded polymer supports and gels, including polystyrene, polyacrylamides, polymethacrylates, polysaccharides, porous silica, copoly(styrene–acrylamide)s and composites, are produced by various modes of two-phase suspension systems. The main feature of these two-phase systems is the formation of "microdroplets" of the desired monomer or polymer solution, followed by their conversion to the corresponding "microbeads". The conversion of the liquid droplets to solid polymer particles may involve a polymerization or polycondensation process, or it may require solvent extraction or covalent cross-linking of the dissolved polymer.

The size, porosity and surface area of the polymer beads obtained by two-phase suspension processes can be easily controlled by various manufacturing parameters. The relationship between these parameters and bead characteristics is fairly well established for synthetic organic polymers (*e.g.* polystyrene, polymethacrylates and polyacrylamides), but they are less fully documented for polysaccharides and silica gel. An extensive array of chemical reactions and reagents are available for functionalization and activation of various polymer types considered above. However, chemical transformation of polymer supports and gels may often involve undesirable side-reactions, and sufficient care must be exercized to avoid or minimize such complications.

Structure–performance relationships in polymer supports and gels are traditionally studied on the basis of surface area and porosity (*i.e. tertiary structure*). The effect of the polymer matrix (or *secondary structure*) is also being increasingly recognized. However, the "function" of the polymer support, whether in chromatography, catalysis or synthesis, is invariably based on "direct molecular contacts" between the polymer backbone and the soluble substrate. Thus, in addition to surface area, porosity and matrix structure, an appreciation of the chemical (or *primary*) structure of the polymer backbone is suggested to be essential for a better

understanding of the behaviour of polymer supports and gels. By the same token, our knowledge of "chemical structure" and "polymer–solvent–substrate" interactions can be employed to design and tailor polymer supports and gels for optimum performance.

A number of interesting new polymer supports, including inorganic–organic composites, interpenetrating networks, core–shell grafts and amphiphilic copoly(styrene–acrylamide)s with general solvent and substrate compatibility, have been introduced in recent years. Further development of these new materials along the above lines is expected to attract increasing interest in the future.

REFERENCES

1 T. Kremmer and L. Boros, *Gel Chromatography*, Wiley, New York, and Acadèmiai Kiadó, Budapest, 1979.
2 R. Epton (Editor), *Chromatography of Synthetic and Biological Macromolecules*, Vols. 1 and 2, Ellis Horwood, Chichester, 1978.
3 J. J. Kirkland (Editor), *Modern Practice of Liquid Chromatography*, Wiley, New York, 1971.
4 F. C. Frank and R. C. Chang, *The Practice of Ion Exchange Chromatography*, Wiley, New York, 1983.
5 C. Calmon, *AIChE Symp. Ser.*, 80 (1984) 84.
6 J. Inczedy, *Analytical Applications of Ion Exchangers*, Pergamon Press, Oxford, 1966.
7 T. C. J. Gribnau, J. Visa and R. J. F. Nivard, *Affinity Chromatography and Related Techniques*, Elsevier, Amsterdam, 1982.
8 P. D. G. Dean, W. S. Johnson and F. A. Middle (Editor), *Affinity Chromatography: a Practical Approach*, IRL Press, Oxford, 1985.
9 L. Jervis, in D. C. Sherrington and P. Hodge (Editors), *Syntheses and Separations Using Functional Polymers*, Wiley, Chichester, 1988, pp. 265–303.
10 S. G. Allenmark, *Chromatographic Enantioseparations*, Ellis Horwood, Chichester, 1988.
11 K. Mosbach (Editor), *Methods in Enzymology*, Vol. 112, Academic Press, New York, 1985.
12 J. Woodward, *Immobilized Cells and Enzymes: a Practical Approach*, IRL Press, Oxford, 1985.
13 R. B. Merrifield, *Makromol. Chem. Makromol. Symp.*, 19 (1988) 31.
14 J. M. Stewart and J. D. Young, *Solid Phase Peptide Synthesis*, Pierce, Rockford, IL, 2nd ed., 1984.
15 W. T. Ford (Editor), *Polymeric Reagents and Catalysts*, American Chemical Society, Washington, DC, 1986.
16 *Pure Appl. Chem.*, 60 (1988) 353.
17 D. C. Sherrington and P. Hodge (Editors), *Syntheses and Separations Using Functional Polymers*, Wiley, Chichester, 1988.
18 A. Warshawsky, in M. Streat and D. Naden (Editors), *Ion Exchange and Sorption Processes in Hydrometallurgy*, Wiley, New York, 1987, pp. 127–225.
19 A. Rembaum and Z. A. Tokes (Editors), *Microspheres: Medical and Biological Applications*, CRC Press, Boca Raton, FL, 1988.
20 K. Nustad, L. Johansen, J. Ugelstadt, T. Elingsen and A. Berge, *Eur. Surg. Res.*, 16, Suppl. 2 (1984) 80.
21 R. Arshady, *J. Chromatogr.*, 586 (1991) 181.
22 R. Arshady and A. Ledwith, *React. Polym.*, 1 (1983) 159.
23 H. Hopff, H. Lussi and E. Hammer, *Makromol. Chem.*, 82 (1965) 175 and 184.
24 F. Wolf and S. Eckert, *Plaste Kautsch.*, 18 (1971) 650 and 890; 19 (1972) 26.
25 T. Allen, *Particle Size Measurement*, Chapman & Hall, London, 2nd ed., 1975.
26 C. D. Scott, *Anal. Biochem.*, 42 (1968) 292.
27 J. V. Dawkins, T. Stone and G. Yeadon, *Polymer*, 18 (1977) 1179.
28 S. M. Ahmed, *Dispersion Sci. Technol.*, 5 (1984) 421.
29 R. Arshady, *Colloid Polym. Sci.*, in preparation.
30 J. W. Hassler, *Purification with Activated Carbon*, Chemical Publishing, New York, 1971.
31 J. S. Mattson and H. B. Mark, *Activated Carbon*, Marcel Dekker, New York, 1971.
32 K. K. Unger, *Porous Silica*, Elsevier, Amsterdam, 1979.
33 N. V. Akshinaskaya, A. V. Kiselev and Y. S. Nikitin, *Russ. J. Phys. Chem.*, 37 (1963) 927 (reported in ref. 32).
34 R. Arshady, *Adv. Mater.*, 3 (1991) 182.
35 H. Galina, N. B. Colaz, P. P. Wiezorek and M. Wojszynska, *Br. Polym. J.*, 17 (1985) 215.
36 W. Heitz, *Adv. Polym. Sci.*, 23 (1977) 1.
37 A. Guyot and M. Bartholin, *Prog. Polym. Sci.*, 8 (1982) 277.
38 J. C. Moore, *J. Polym. Sci., Part A-2*, (1969) 835.
39 D. Horak, Z. Pelzbauer, M. Bleha, M. Ilavsky, F. Svec and J. Kalal, *J. Appl. Polym. Sci.*, 26 (1980) 411.
40 D. Horak, F. Svec, M. Bleha and J. Kalal, *Angew. Makromol. Chem.*, 95 (1981) 109.
41 D. Horak, F. Svec, M. Ilavsky, M. Bleha and J. Kalal, *Angew. Makromol. Chem.*, 95 (1981) 117.
42 J. Coupek, M. Krivakova and S. Pokorny, *J. Polym. Sci., Polym. Symp.*, 42 (1973) 185.
43 R. Ruchel and M. D. Brager, *Anal. Biochem.*, 68 (1975) 415.
44 W. Rolls, F. Svec and J. M. J. Frechet, *Polymer*, 31 (1990) 165.
45 S. Brunauer, P. Emmet and E. Teller, *J. Am. Chem. Soc.*, 60 (1938) 309.
46 E. P. Barret, L. J. Joyner and P. P. Halenda, *J. Am. Chem. Soc.*, 73 (1951) 373.
47 J. Gregg and K. S. W. Sing, *Adsorption, Surface Area and Porosity*, Academic Press, London, 1982.
48 B. H. Davis, *Appl. Catal.*, 10 (1984) 185.
49 M. Brun, J. F. Quinson, R. Blanc, M. Negre, C. Eyrand and M. Bartholin, *Makromol. Chem.*, 182 (1981) 873.
50 R. Arshady, unpublished results; *cf.* ref. 22.
51 R. Arshady, *Makromol. Chem.*, 189 (1988) 1295.
52 R. Arshady, *Colloid Polym. Sci.*, 268 (1990) 948.
53 *Gel Filtration: Theory and Practice*, Pharmacia, Uppsala.
54 J. Peska, J. Stamberg and J. Hradil, *Angew. Makromol. Chem.*, 53 (1976) 73.
55 M. Smrz and J. Viska, in R. Epton (Editor), *Chromatography of Synthetic and Biological Macromolecules*, Vol. 1, Ellis Horwood, Chichester, 1978, pp. 91–108.

56 E. Fenyvesi, B. Szadon, J. Szejtli and F. Tudos, *Ann. Univ. Sci. Budap. Rolando Eotvos Nominatae Sect. Chim.*, 15 (1979) 13.
57 A. V. J. Brough, R. Epton, G. Marr, A. T. Shackley and G. A. Sniezko-Blocki, in R. Epton (Editor), *Chromatography of Synthetic and Biological Macromolecules*, Vol. 1, Ellis Horwood, Chichester, 1978, pp. 70–90.
58 A. V. J. Brough, R. Epton, J. V. McLaren, *Polymer*, 18 (1977) 1208.
59 C. Birr, *Aspects of Merrifield Peptide Synthesis*, Springer, Berlin, 1978.
60 M. Negre, M. Bartholin and A. Guyot, *Angew. Makromol. Chem.*, 106 (1982) 79.
61 D. G. Barer, K. P. Staller and N. A. Peppas, *Ind. Eng. Chem., Prod. Res. Dev.*, 22 (1983) 161.
62 E. A. Grulke, in J. Brandrup and E. H. Immergut (Editors), *Polymer Handbook*, Wiley, New York, 3rd ed., 1989, pp. VII/519–559.
63 J. F. Kennedy and J. M. S. Cabral, *Trans. Met. Chem.*, 11 (1986) 41; 12 (1987) 481.
64 R. W. Siergiej and N. D. Danielson, *Anal. Chem.*, 55 (1983) 17.
65 A. Dias and T. J. McCarty, *Macromolecules*, 18(1985) 1826.
66 R. Millar, D. G. Smith, W. E. Marr and T. R. E. Kressman, *J. Chem. Soc.*, (1963) 218.
67 K. W. Pepper, H. M. Paisely and M. A. Young, *J. Chem. Soc.*, (1953) 4097.
68 M. J. Hudson (Editor), *Recent Developments in Ion Exchange*, Elsevier Applied Science, Barking, 1987.
69 J. A. Malinsky (Editor), *Ion Exchange*, Marcel Dekker, New York, 1969.
70 R. S. Feinberg and R. B. Merrifield, *Tetrahedron*, 30 (1974) 3209.
71 J. T. Sparrow, *Tetrahedron Lett.*, 1975 (1975) 4637.
72 R. E. Barron and J. S. Fritz, *React. Polym.*, 1 (1983) 215.
73 M. J. Farral and J. M. J. Frechet, *J. Org. Chem.*, 41 (1976) 3877.
74 G. A. Crosby, N. M. Weinshenker and H. S. Uh, *J. Am. Chem. Soc.*, 97 (1975) 2232.
75 D. C. Sherrington, in P. Hodge and D. C. Sherrington (Editors), *Polymer-Supported Organic Synthesis*, Wiley, Chichester, 1980, pp. 1–82.
76 J. K. Inman and H. M. Dintzis, *Biochemistry*, 8 (1969) 4047.
77 L. Goldstein, *Methods Enzymol.*, 135 (1987) 90.
78 R. Arshady and I. Ugi, *Polymer*, 31 (1990) 1164.
79 R. Epton, B. L. Hibart and G. Marr, *Polymer*, 16 (1975) 314.
80 R. Arshady, E. Atherton, D. L. J. Clive and R. C. Sheppard, *J. Chem. Soc., Perkin Trans. 1*, (1981) 529.
81 C. K. Narang, K. Brunfeldt and K. E. Norris, *Tetrahedron Lett.*, (1977) 1819.
82 R. Arshady, E. Atherton and R. C. Sheppard, *Tetrahedron Lett.*, 1979 (1979) 1521.
83 R. Arshady, unpublished results.
84 E. A. Peterson and H. A. Sober, *J. Am. Chem. Soc.*, 78 (1956) 751.
85 E. A. Peterson and H. A. Sober, *Biochem. Prep.*, 8 (61) 39 and 43.
86 H. Determan and T. Wieland, *Makromol. Chem.*, 114 (1968) 263.
87 R. Axen, J. Porath and S. Earnback, *Nature (London)*, 214 (1967) 1302.
88 L. Sundberg and J. Porath, *J. Chromatogr.*, 171 (1974) 87.
89 G. S. Bethell, J. S. Ayers, M. T. W. Hearn and W. S. Hancock, *J. Chromatogr.*, 219 (1981) 353 and 361.
90 M. T. W. Hearn, L. E. Harris, G. S. Bethell, W. S. Hancock and J. S. Ayers, *J. Chromatogr.*, 219 (1981) 509.
91 M. Wilchek, *Angew. Makromol. Chem.*, 123/124 (1984) 175.
92 L. Drobnik, J. Labsky, H. Kudlvasrova, U. Sandec and F. Svec, *Biotechnol. Bioeng.*, 24 (1982) 487.
93 G. Kay and E. M. Crook, *Nature (London)*, 216 (1967) 514.
94 C. Longstoff, in P. D. G. Dean, W. S. Johnson and F. A. Middle (Editors), *Affinity Chromatography: a Practical Approach*, IRL Press, Oxford, 1985, pp. 37–38.
95 J. S. Ayers, M. J. Peterson, B. E. Sheerin and G. S. Bethel, *J. Chromatogr.*, 294 (1984) 195.
96 K. Nilsson and K. Mosbach, *Methods Enzymol.*, 104 (1984) 56.
97 W. H. Scouten and W. van der Tweel, in I. M. Chaiken, M. Wilchek and J. Parikh (Editors), *Affinity Chromatography and Biological Recognition*, Academic Press, New York, 1983, pp. 229–302.
98 N. Weliky and H. H. Weetall, *Immunochemistry*, 2 (1965) 293.
99 T. Miron and M. Wilchek, *J. Chromatogr.*, 215 (1981) 55.
100 J. Kohn and M. Wilchek, *Chem. Anal. (Warsaw)*, 66 (1983) 599.
101 J. Kohn and M. Wilchek, *Biochem. Biophys. Res. Commun.*, 107 (1982) 878.
102 E. Grushka (Editor), *Bonded Stationary Phases in Chromatography*, Ann Arbor Sci. Publ., Ann Arbor, MI, 1974.
103 H. Engelhardt and D. Mathes, *J. Chromatogr.*, 142 (1977) 311.
104 M. Lynn and A. M. Filbert, in E. Grushka (Editor), *Bonded Stationary Phases in Chromatography*, Ann Arbor Sci. Publ., Ann Arbor, MI, 1974, pp. 1—11.
105 K. G. Allum, R. D. Hancock, I. V. Howell, S. McKenzie, R. C. Pikethly and P. J. Robinson, *J. Organomet. Chem.*, 87 (1975) 203.
106 R. R. Walters in P. D. G. Dean, W. S. Johnson and F. A. Middle (Editors), *Affinity Chromatography: a Practical Approach*, IRL Press, Oxford, 1985, pp. 35–39.
107 U. Kittelmann and K. Unger, *Prog. Colloid Polym. Sci.*, 67 (1980) 19.
108 U. Truedinger, G. Mueller and K. K. Unger, *J. Chromatogr.*, 535 (1990) 111.
109 P.-O. Larsson, M. Glad, L. Hansson, S. Ohlson and K. Mosbach, *Adv. Chromatogr.*, 21 (1983) 41.
110 W. Parr and M. Novotny, in E. Grushka (Editor), *Bonded Stationary Phases in Chromatography*, Ann Arbor Sci. Publ., Ann Arbor, MI, 1974, p. 173.
111 F. E. Regnier and R. Noel, *J. Chromatogr. Sci.*, 14 (1976) 316.
112 K. Ryan, *Chem. Ind. (London)*, (1988) 359.
113 R. E. Majors and H. J. Hopper, *J. Chromatogr. Sci.*, 12 (1974) 767.
114 J. J. Kirkland and P. C. Yates, *US Pat.*, 3 722 181 (1973) and 3 795 313 (1974).
115 J. P. J. Verlaan, J. P. C. Bootsma and G. Challa, *J. Mol. Catal.*, 14 (1982) 1211.

116 R. Arshady, B. S. R. Reddy and M. H. George, *Polymer*, 27 (1986) 69.
117 R. Arshady, in preparation.
118 R. Arshady, *Makromol. Chem.*, 185 (1984) 2387.
119 J. Pless and R. A. Biossonas, *Helv. Chim. Acta*, 46 (1963) 1609.
120 M. Bodanszky, *Principles of Peptide Synthesis*, Springer, Heidelberg, 1984.
121 M. Bodanszky, *The Practice of Peptide Synthesis*, Springer, Heidelberg, 1984.
122 R. Arshady, *Chim. Ind. (Milan)*, 70, No. 9 (1988) 70.
123 D. J. Harmon, in R. Epton (Editor), *Chromatography of Synthetic and Biological Macromolecules*, Vol. 1, Ellis Horwood, Chichester, 1978, pp. 122–145.
124 R. Arshady, *Angew. Makromol. Chem.*, 106 (1982) 191.
125 J. K. Stille, *J. Makromol. Sci. Chem., Part A2*, 13–14 (1984) 1689.
126 N. Takashi, H. Imai, C. A. Bertelo and J. K. Stille, *J. Am. Chem. Soc.*, 100 (1978) 264.
127 S. L. Regan, *Macromolecules*, 8 (1975) 689.
128 S. L. Regan, *J. Am. Chem. Soc.*, 96 (1974) 5275.
129 W. T. Ford, M. Peryasamy and H. O. Spivey, *Macromolecules*, 17 (1984) 2881.

Journal of Chromatography, 586 (1991) 221–232
Elsevier Science Publishers B.V., Amsterdam

CHROM. 23 573

Multiparameter optimizations in micellar liquid chromatography using the iterative regression optimization strategy

Joost K. Strasters, Sang-Tae Kim☆ and Morteza G. Khaledi*

North Carolina State University, Department of Chemistry, P.O. Box 8204, Raleigh, NC 27695 (USA)

(First received January 3rd, 1991; revised manuscript received May 29th, 1991)

ABSTRACT

An extension of the iterative regression optimization strategy to multi-parameter optimizations is described and applied to the separation of ionic compounds (amino acids and peptides) by means of micellar liquid chromatography. The parameters examined are the concentration of surfactant, the concentration of 2-propanol and pH. Fairly regular (linear, weakly curved) retention behaviour of the compounds as a function of the parameters results in an efficient optimization using a relatively small number of initial experiments.

INTRODUCTION

The method development scheme in most forms of reversed-phase high-performance liquid chromatography (RP-HPLC) is relatively complex owing to a lack of theoretical relationships to predict retention behaviour under varying experimental conditions. This is especially true if the identity of one or more of the components in a mixture is unknown.

It is for this reason that a large number of approaches using more or less empirical relationships have been developed to obtain a satisfactory separation on the basis of a limited number of experiments, as indicated in a number of excellent reviews [1–3]. In addition, an overview of advances regarding computer applications in this area was published recently [4].

The necessity for an efficient experimental design becomes especially important when dealing with forms of liquid chromatography suitable for the simultaneous analysis of ionic and non-ionic compounds such as ion-pair liquid chromatography (IP-LC) and micellar liquid chromatography (MLC). Here the number of possible parameters can be large, *e.g.*, the type and concentration of surfactant or ion-pairing reagent, the type and concentration of organic modifier(s), pH, temperature and ionic strength. The method development strategy must provide the chromatographer with an answer as to which parameters are the most appropriate ones to use and how to set up initial experiments to search the selected parameter space in an efficient way. The problem of parameter selection in IP-LC and MLC has not been fully addressed as yet, although preliminary investigations in IP-LC have been described [5,6].

Here we are concerned with a multi-parameter experimental design which can be applied in RP-HPLC in general, although the largest gain with respect to finding a better separation can be expected in IP-LC and MLC owing to the large number of relevant parameters, as indicated above. The main difference between these two forms of chromatography is the amount of hydrophobic surfactant in the mobile phase: the concentration used in IP-LC is below the critical micelle concentration (CMC) and consequently only free surfactant

☆ Present address: Hyo-Mox 2-Dong 383-2, Dong-Gu Taegu, 701-032, Seoul, South Korea.

0021-9673/91/$03.50

ions are present in the solution. As the stationary phase is modified with surfactant, a variation in the surfactant concentration will strongly influence the characteristics of the stationary phase. Solutes form ion pairs either in the mobile phase or on the stationary phase and consequently a strong curvature will be observed in plots of ln k' (k' = capacity factor) as a function of the surfactant concentration in the mobile phase. Nonetheless, optimization of these separations is possible and has been described [7–9].

In MLC, on the other hand, the concentration of surfactant is above the CMC and the concentration of free surfactant does not vary nearly as much with the amount of surfactant as in IP-LC. Instead, a variation in the surfactant concentration is translated into an increase in the concentration of micelles in the solution. As a consequence, the characteristics of the modified stationary phase are much more stable, and generally a regular (*i.e.* linear or weakly curved) retention behaviour is observed as a function of both the surfactant and organic modifier concentration [10–15].

Previously we described the successful application of a two-parameter version of the iterative regression optimization strategy in MLC [15]. Owing to unique selectivity effects as a function of the surfactant or organic modifier concentration [13,14], a simultaneous variation of these parameters is required in order to exploit the full separation power of the method. Optimizing these two parameters often results in shorter chromatograms with superior resolution.

Here we are concerned with a further extension of the parameter space with a third variable, *i.e.* pH. As we are often dealing with weakly acidic or basic compounds [5,6], this parameter can play a major role in fine tuning the selectivity. However, one should be cautious owing to the inherent non-linearity in the resulting change in retention behaviour, as discussed below. In order to include an additional parameter in the optimization, an adjusted scheme of the iterative regression optimization strategy was applied which was used previously in IP-LC. Although two parameters usually suffice for samples of moderate complexity to obtain a satisfactory separation, inclusion of the third parameter will often further improve the quality of the obtainable optimum, with respect to both resolution and analysis time. In other words, by including additional, relevant parameters in the optimization, the required peak capacity for a given separation is further reduced [16].

THEORY

Optimization strategy

The iterative regression optimization strategy was originally described by Drouen *et al.* for both the one- and two-parameter cases [17,18]. Applications were mainly found in traditional RP-HPLC, although applications in IP-LC and MLC have also been reported [8,15]. Full details of the method can be found in the above references. In a previous paper [15], the two-parameter optimization in MLC was discussed in detail, and only the basic principles will be given here.

In the two-parameter case, the search for the "optimum" separation can be envisioned in a three-dimensional space: two axes are related to the parameter under investigation and the third dimension is used to express the quality of the separation by means of a criterion (*e.g.*, minimum resolution) observed in the chromatogram. Within the examined region of the parameter space, a chromatogram can be simulated at every combination of the two parameters and consequently a criterion value can be predicted at a given mobile phase composition. This results in a three-dimensional plot (like a mountainous landscape) called the response surface, where the highest (or lowest) peak will be related to the parameter values that produce the best chromatogram. The aim of interpretive optimization strategies is to produce an accurate representation of the response surface with a minimum number of experiments.

The iterative regression strategy assumes that in a first approximation, retention (ln k') is a linear function of the parameters within a selected portion of the parameter space. When represented in a three-dimensional space, with ln k' as the third dimension, this translates into a plane [15]. As three points are required to define a plane, the parameter space will be divided into triangular subspaces (Fig. 1a) [15]. The linear models derived on the basis of three experiments (chromatograms observed for the parameter values on the corners of the triangles) are used to predict the retention for each component for

other experimental conditions (parameter values). The computer is used to go through the parameter space with small steps and to use the predictions of ln k' at each point to reconstruct the chromatogram and consequently calculate the predicted quality of the separation. After calculating the criterion values over the parameter space (*i.e.*, the response surface), the mobile phase compositions for the optimal chromatogram can be predicted.

Subsequent measurements can be used to refine the response surface by a further subdivision of the parameter space into smaller triangles. Again it is assumed that the linear model holds within each subspace. Depending on the location of the additional measurements, a triangular subspace is subdivided either into three or two new triangles. In Fig. 1b, measurement 6 performed after the five initial experiments divides one of the original subspaces,

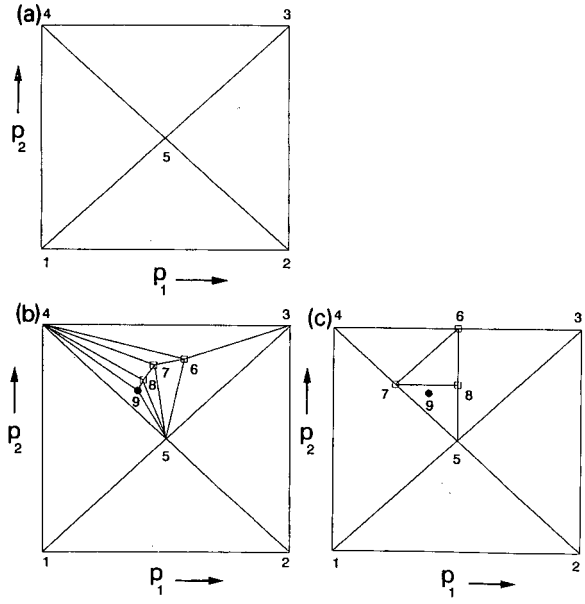

Fig. 1. Experimental design for a two-parameter optimization by means of the iterative regression strategy. The solid lines indicate the subspaces used to define the linear models and the numbers identify the location and order of the experiments. (a) The initial experiments; (b) a possible set of consecutive experiments in the case of a direct measurement of the predicted optimum in combination with a retention behaviour showing a strong curvature as a function of the parameters; (c) a possible set of consecutive experiments when the next measurement is chosen in the subspace containing the predicted optimum and is located as far from the other measurements as possible.

triangle 3,4,5, into three new subspaces: 3,4,6; 3,5,6; and 4,5,6. Measurement 7, located in the triangle 4,5,6, creates three new triangles, etc. In Fig. 1c, measurement 6 is located on the side of the subspace 3,4,5 and consequently divides this subspace in triangles 3,5,6 and 4,5,6. Each additional measurement will further refine the subdivision and consequently the accuracy of the prediction within the affected sections of the parameter space.

The selection of the location of the next measurement is governed by two, sometimes conflicting, considerations: on the one hand, one tries to measure the predicted optimum directly. When the measured and predicted chromatograms coincide, a confirmation of the assumed linearity is obtained in addition to a strong indication that the predicted global optimum actually is the true optimum (this proposition assumes that the observed linearity in the examined portion of the parameter space will also be maintained in the remainder of the parameter space). A disadvantage of this approach is illustrated in Fig. 1b: when strong deviations of the linear model are observed, the subsequent search of the parameter space will provide the location of a new optimum, and the process is repeated until the predicted and measured optima coincide. This will possibly result in an undesirably large number of experiments.

Possible solutions to this problem include the use of higher order models (and consequently a different experimental design with a larger number of initial experiments). Alternatively, one can adhere to the second consideration mentioned above, *i.e.*, try to obtain as much information as possible by means of an additional measurement. This can be relaized by locating the next measurement as far from the other measurements as possible, *i.e.*, on the long side of the triangle (Fig. 1c). In order to converge on the optimum, additonal measurements are always located in the subspace containing the predicted optimum. The procedure is stopped and the predicted optimum measured when the size of the resulting subspaces drops below a given size, dictated by the expected curvature of the retention behaviour as a function of the mobile phase composition. This approach will result in an inefficiently large number of experiments when the retention behaviour (ln k') is fairly linear.

Drouen *et al.* [17,18] proposed an intermediate

solution by shifting the composition of the next measurement in the direction of the point with the largest information content. One could also envision a design where the first additional experiment is performed according to the second consideration, while the locations of further measurements are based on the observed linearity of the retention behaviour. However, it is important to realize that the "best" approach is strongly dependent on the regularity of the observed retention, and will vary with the type of chromatography, the range of parameters examined and possibly also the nature of the solutes.

An inherent assumption in the application of the iterative regression strategy as described above is that deviations from linearity are limited to the extent that the quality of chromatograms in areas not examined and the area near the optimum is not much higher than predicted. This assumption seems to hold much better in MLC [15] than in IP-LC [8]. As indicated in these references, this can be checked by additional experiments.

Adjustments for three-parameter optimization

In order to perform the optimization for three or more parameters, a straightforward extension to a multi-parameter space must be performed [19]. For instance, in the case of a three-parameter optimization, the square in Fig. 1 is replaced by a cube and the triangles are replaced by tetrahedra, as indicated in Fig. 2, where the tetrahedron defined by measurements 2, 5, 8 and 9 has been emphasized. Each side of the cube is a two-parameter design identical with that presented in Fig. 1. Again, in order to obtain an unambiguous subdivision of the cube, the centre of the cube is included in the measurements, which results in a total of 24 tetrahedra. This requires a total of fifteen initial chromatograms. In analogy with the two-parameter optimization, a linear model relating the retention of a solute to the parameter values can be derived for each subspace. The models derived for all components in the mixture can then be used to predict and evaluate the chromatograms. However, as the parameter space is already three-dimensional, it would be difficult to envision a plot of the criterion value as a function of the three parameters, as this constitutes the fourth dimension (one possible way to visualize this is to think of a cube where the quality of the chromatogram in each

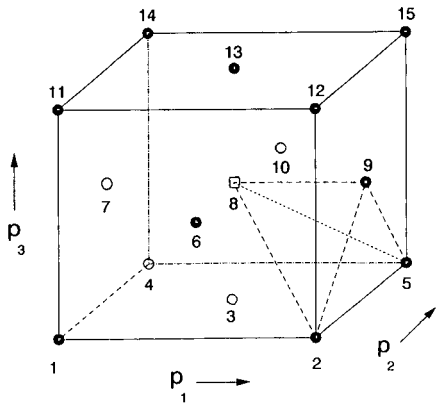

Fig. 2. Initial experiments in the case of a three-parameter iterative regression optimization. The solid dots represent points located on the "visible" outside of the cube, the open dots (3, 4, 7 and 10) are measurements on the "invisible" sides of the cube and the open square (8) is located in the centre of the cube. One of the subspaces, the tetrahedron (2, 5, 8, 9), is indicated by the dashed lines.

point is represented by a colour, ranging from dark blue for a bad separation to light red for good separations: the optimum would be apparent as an intensely coloured red cloud in the cube). The graphical representation is discussed further later.

It is apparent in the rigorous treatment described here that the number of initial experiments increases rapidly with each additional parameter, *i.e.*, two for one parameter, five for two parameters, fifteen for three parameters, etc. Therefore, it seems likely that this will limit the applied dimensionality (the number of parameters taken into consideration), rather than restrictions in calculation time [20]. This again emphasizes the need for efficient selection procedures to be applied before the actual optimization in order to keep the actual amount of experimental work to the minimum [5]. Alternative designs with fewer measurements can be envisioned, but these will require some form of regressiin; for instance, a pyramid described by the centre and four corners of the cube encloses a larger part of the parameter space (equivalent to four tetrahedra) and uses five measurements to derive a linear model with four parameters. As a consequence, deviations from linearity will strongly influence a larger section of the model and thus might require additional measurements in a later stage of the optimization. In addition, it will reduce the certainty in the statement

that the determined optimum in the examined section of the parameter space is the true optimum for that section.

The inclusion of additional experiments in a three-parameter optimization follows the same rules as the two parameter case (Fig. 3). A new measurement on the side of the triangle results in two new triangles (Fig. 1c), while a new measurement on the side of a tetrahedron divides the two sides of that tetrahedron and consequently results in two new tetrahedra (Fig. 3a). A new measurement inside a triangle divides that triangle into three new ones (Fig. 1b), while a new measurement on the side of a tetrahedron (*i.e.*, a triangle) again divides that triangle into three sections, thus creating three new tetrahedra (Fig. 3b). When the new measurement is located in the centre of the tetrahedron, four new tetrahedra will result (Fig. 3c). For each additional parameter, this scheme will be extended with one step, and will be extremely difficult to visualize.

In analogy with the two-parameter optimization, a new retention model is now derived for each compound in each newly created subspace and the chromatograms in these sections are predicted and evaluated.

A separate problem is a simple graphical representation of the quality of the separation as a function of the various parameters. In the software version used for the example described under Experimental, this was done by presenting the user with two-dimensional slices at fixed values of the third parameter. In addition, it is also possible to extend this approach by calculating the slice at a given combination of two or more of the parameters. In this way it will be possible to obtain an impression of the quality of the separation for a more or less "isoeluotropic" set of conditions, although both parameters involved will influence the retention time. Further examples of the graphical representation are given under Results and Discussion.

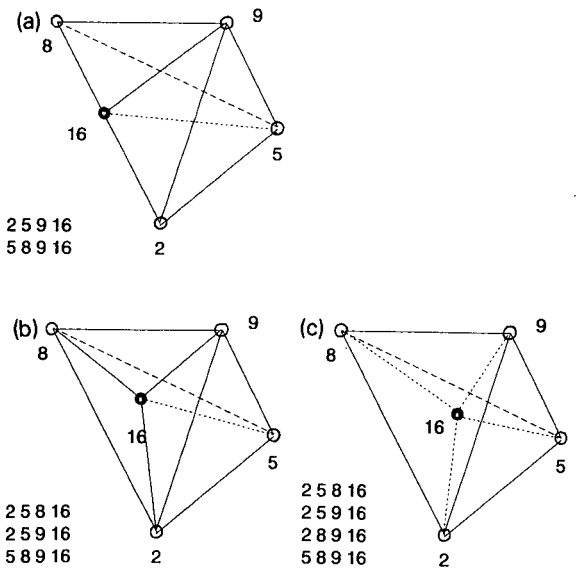

Fig. 3. Possible subdivisions of the tetrahedron shown in Fig. 2 by an additional measurement (16). The newly created tetrahedra are identified by the experiments listed on the lower left side of the figures. (a) Measurement 16 located on the line connecting experiments 2 and 8; (b) measurement 16 located on the plane defined by experiments 2, 8 and 9; (c) measurement 16 located in the centre of the original tetrahedron.

EXPERIMENTAL

In order to illustrate the use and implications of a three-parameter optimization in MLC, the retention of a set of nine amino acids and peptides was examined as a function of pH, the concentration of surfactant and the concentration of organic modifier.

All experiments were performed on a 5-μm particle size LiChroCART C_{18} column (12.5 cm × 4 mm I.D.) (Merck, Darmstadt, Germany). The column was thermostated at 40°C and the flow-rate was 1 ml/min (dead volume 0.86 ml). A silica precolumn was employed to saturate the mobile phase with silicates and to protect the analytical column. The chromatographic equipment consisted of a pump (Model 2350; ISCO, Lincoln, NE, USA) and a V^4 absorbance detector set at 210 nm (ISCO).

The compositions of the mobile phases, the identities of the solutes (checked in the chromatograms by means of separate injection of the standard) and the observed retention times are listed in Table I. The solutes and the surfactant, sodium dodecyl sulphate (SDS), were obtained from Sigma (St. Louis, MO, USA). The surfactant solution was prepared by dissolving the required amount in doubly distilled, deionized water and filtering over a 0.45-μm nylon filter. The pH and ionic strength were adjusted by adding phosphate buffer such that the total buffer concentration of the final solution was 0.02 *M*. After adding the required amount of

TABLE I

CONCENTRATION OF THE SURFACTANT ([SDS]), THE PERCENTAGE OF 2-PROPANOL (PrOH) AND THE pH USED IN THE CHROMATOGRAPHIC EXPERIMENTS REGARDING THE MIXTURE OF NINE AMINO ACIDS AND PEPTIDES, TOGETHER WITH THE IDENTITIES AND RETENTION TIMES [t_r (min)] OF THE SOLUTES

Mobile phase		Composition				
[SDS] (*M*)		0.1	0.1	0.2	0.3	0.3
PrOH (%)		0.0	10.0	5.0	0.0	10.0
pH		2.5	2.5	2.5	2.5	2.5
Components		t_r (min)				
1 Arg	(R)	25.53	13.73	8.17	8.01	4.23
2 His	(H)	20.85	9.60	6.38	6.63	3.33
3 Leu	(L)	26.37	9.79	7.85	9.43	4.19
4 Tyr	(Y)	8.14	3.72	3.18	3.32	2.02
5 Ala–Tyr	(AY)	4.50	3.31	2.35	2.05	1.66
6 Gly–Phe–Leu	(GFL)	53.15	23.10	14.61	17.59	7.62
7 Aso–Phe	(DF)	11.69	7.39	4.89	4.44	2.97
8 Lys–Phe	(KF)	35.50	29.82	13.37	11.01	7.76
9 Leu–Trp	(LW)	32.02	13.65	9.06	11.13	4.78
Mobile phase		Composition				
[SDS] (*M*)		0.1	0.2	0.2	0.2	0.3
PrOH (%)		5.0	0.0	5.0	10.0	5.0
pH		3.0	3.0	3.0	3.0	3.0
Components		t_r (min)				
1 Arg	(R)	15.25	11.85	6.80	4.85	4.45
2 His	(H)	9.93	9.00	4.57	3.33	3.21
3 Leu	(L)	13.05	14.02	7.05	4.65	5.08
4 Tyr	(Y)	4.10	4.50	2.63	1.90	2.12
5 Ala–Tyr	(AY)	3.55	2.70	2.15	1.95	1.70
6 Gly–Phe–Leu	(GFL)	32.57	27.50	15.05	11.10	9.90
7 Asp–Phe	(DF)	8.46	6.38	4.37	3.62	3.16
8 Lys–Phe	(KF)	32.10	17.69	13.35	12.40	8.25
9 Leu–Trp	(LW)	18.75	17.59	9.05	6.73	6.23
Mobile phase		Composition				
[SDS] (*M*)		0.1	0.1	0.2	0.3	0.3
PrOH (%)		0.0	10.0	5.0	0.0	10.0
pH		3.5	3.5	3.5	3.5	3.5
Components		t_r (min)				
1 Arg	(R)	21.78	7.09	5.38	6.64	2.74
2 His	(H)	13.45	4.30	3.43	4.25	2.17
3 Leu	(L)	24.25	5.05	5.75	9.04	3.15
4 Tyr	(Y)	6.21	1.65	2.09	2.85	1.45
5 Ala–Tyr	(AY)	4.25	2.57	1.97	1.92	1.53
6 Gly–Phe–Leu	(GFL)	58.89	22.70	14.82	18.21	7.67
7 Asp–Phe	(DF)	10.27	4.18	3.70	3.92	2.28
8 Lys–Phe	(KF)	38.04	28.80	12.99	11.12	7.60
9 Leu–Trp	(LW)	35.50	12.75	8.85	11.47	4.65

organic modifier, 2-propanol (Fisher Scientific, Pittsburgh, PA, USA), the apparent pH was adjusted to the specified value.

The software to evaluate the separation at different mobile phase compositions was based on an extended version of the iterative regression optimization strategy [19] implemented by means of the Turbo-Pascal compiler version 5.5 (Borland, Scotts Valley, CA, USA). The program runs on a DeskPro 286 (COMPAQ Computer, Houston, TX, USA), equipped with a Model 80287 coprocessor, 640 kbyte of conventional and 1 Mbyte of expanded memory, and an Enhanced Graphics Adapter with colour monitor. The simulated chromatograms are based on a Gaussian peak shape, using the plate count (average 2500) and dead volume observed in the chromatographic experiments.

RESULTS AND DISCUSSION

Fig. 4 shows the parameter space selected for the separation of the mixture of nine peptides and amino acids listed in Table 1. Similarly to described procedure [15], the examined range of concentrations for surfactant and 2-propanol were determined on the basis of chromatographic insight and physical limitations: the minimum surfactant concentration is far above the CMC of SDS and was chosen such that a reasonable retention time for all components was obtained. Although in this instance information from previous experiments was used, a more objective selection on the basis of a micellar gradient will be a valid alternative to determine this concentration [21]. Likewise, the maximum micelle concentration was selected such that the viscosity of the mobile phase was acceptable (*i.e.*, maximum pressure drop over the column within 2000 psi) and all capacity factors were higher than (approximately) 1.0. The upper limit of the propanol concentration was based on considerations regarding retention times, viscosity and micellar integrity: when the concentration of the organic modifier becomes too high, the characteristics of the micellar pseudo-phase change (by creating a micro-emulsion or complete disappearance of the micelles).

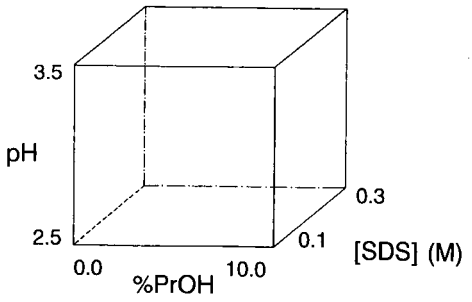

Fig. 4. Parameter space selected for the separation of the nine-component amino acid–peptide mixture. [SDS] indicates the concentration of surfactant (*M*) and %PrOH is the percentage of 2-propanol organic modifier.

The range of pH values examined was intentionally selected to contain only a small portion of the full range between 2.5 and 7.0, *i.e.*, pH 2.5–3.5. This was done to prevent deviations from linearity in the retention behaviour: for larger ranges an S-shaped retention *vs.* pH curve will be observed when the component changes from its acidic to its basic form, which will require at least one additional measurement for an approximation with linear segments.

A number of the initial chromatograms are displayed in Fig. 5. The criterion used here to define the quality of the separation is the minimum resolution, *i.e.*, the resolution of the least separated pair of components in the chromatogram. The following remarks can be made.

None of the initial chromatograms shows sufficient separation of all components in the mixture (sufficient separation is usually defined as resolution between 1.0 and 1.5, where a resolution of 1.5 corresponds to "baseline" separation). This again illustrates the observations presented in previous papers [14,15] where a decrease in elution strength by decreasing the surfactant and/or organic modifier concentration does not automatically result in improved resolution due to the combined selectivity/elution strength observed in MLC.

The overall analysis time is not a function of pH, because the degree of dissociation of the latter components in the chromatograms (KF, GFL) hardly changes in the examined pH range. As a consequence, the pH can be used to fine tune the selectivity without influencing the elution strength of the mobile phase. However, the observation is strongly sample dependent.

The influence of the pH is dependent on the values of the other parameters, in other words, a simultaneous optimization of all variables is required in order to examine the full separation potential. This is

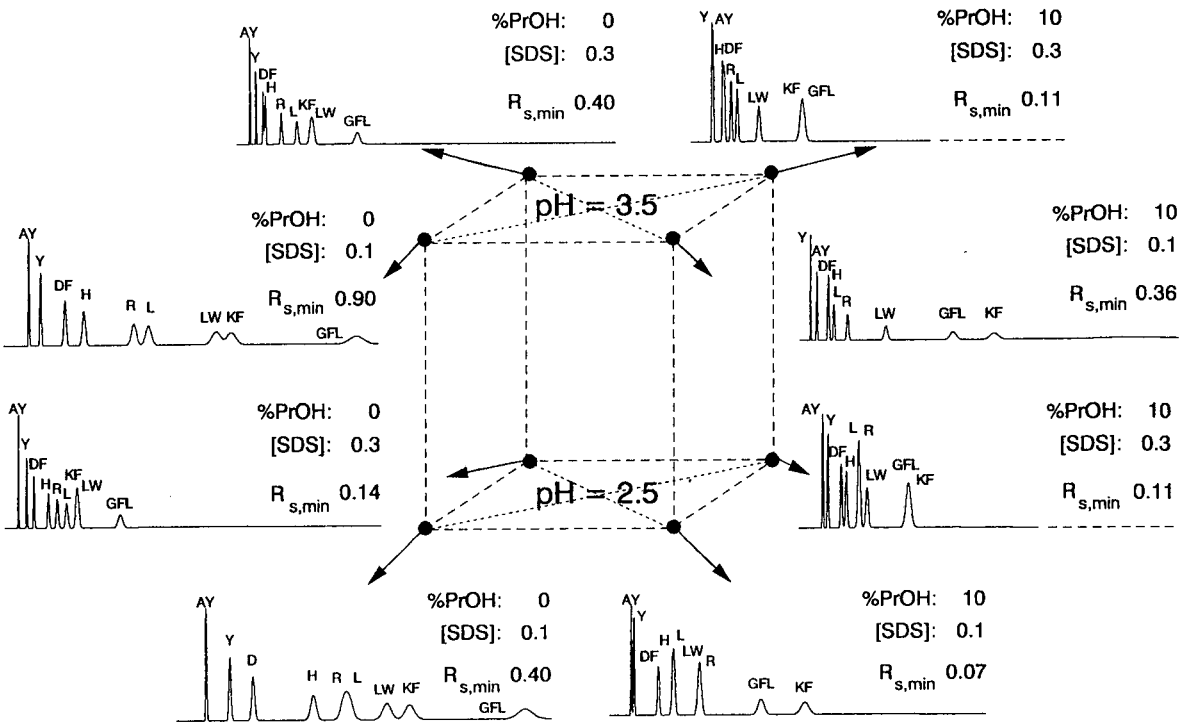

Fig. 5. Set of the initial experiments performed with the nine-component amino acid–peptide mixture, identified in Table 1, relative to their position in the parameter space. The minimum resolution observed in each chromatogram is indicated by $R_{s,min}$.

especially obvious when comparing the chromatograms on the left and the right sides of the cube: on the left side, the order of components AY and Y does not change as a function of pH. On the right side, on the other hand, the order of AY and Y does change on increasing the pH from 2.5 to 3.5. A possible explanation of this phenomenon is the micellar-induced pK_a shift [22], caused by a difference in the partitioning of the undissociated and dissociated species of a solute in the micellar pseudo-phase. As the dissociated form has the same charge as the micelles, the partitioning process will result in a surplus of this form in the aqueous phase with respect to the thermodynamic equilibrium, and consequently a reduction in the amount of dissociation. Hence the apparent pK_a of a solute will increase or, in other words, the S-shaped retention behaviour of a solute will be shifted to the right. Here this shift is more apparent for AY than for Y, such that the decrease in retention for AY as a function of pH is less pronounced at high concentrations of surfactant whereas the decrease in the retention of Y is influenced less by the surfactant concentration.

The above observations are further emphasized in Fig. 6, where the results of the first step of two two-parameter optimizations and the three-parameter optimization are compared. The lower iso-response surface (containing lines which connect points with equal criterion values) refers to pH 2.5. Apparently, a good separation is predicted at 4% propanol, 0.10 *M* SDS. The corresponding chromatogram is displayed on the right. The resolution is more than adequate ($R_{s,min}$ = 1.6) but the analysis time is relatively long (*ca.* 40 min). The same applies to the optimum predicted at pH 3.5, where similar resolution and analysis time are observed at 1% propanol, 0.14 *M* SDS. However, when the full parameter space is taken into consideration, an even better separation is obtained. This is represented by the iso-response surface at the pH where the optimum criterion value for the full parameter space is observed, *i.e.*, pH 3.1. Not only is the resolution

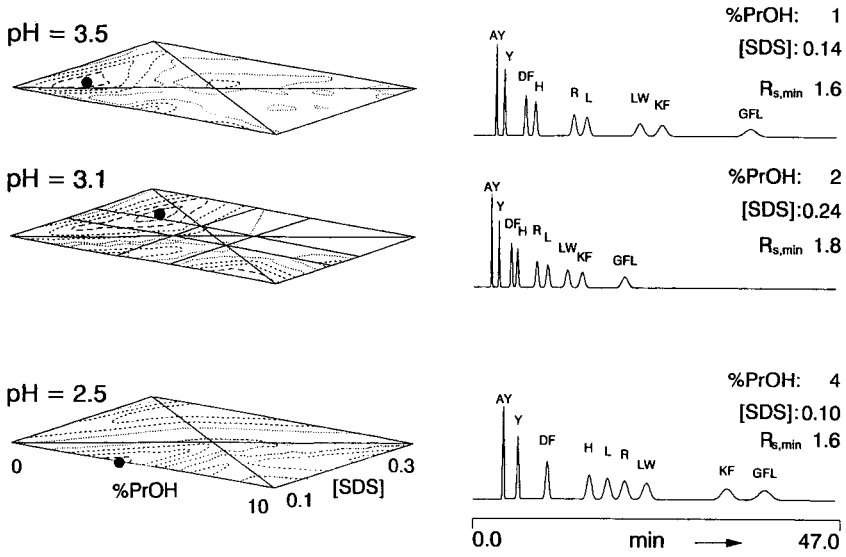

Fig. 6. Three intersections in the original parameter space at the specified pH values. In each intersection, isoresponse lines show the behaviour of the criterion, *i.e.*, the minimum resolution. In addition, the predicted optimum at each pH, location indicated by the solid dot, is displayed on the right. The optimum at pH 3.1 is also the predicted global optimum of the three-parameter optimization.

improved from 1.6 to 1.8 (in fact an unnecessary improvement, as 1.5 is already a sufficient separation for components with approximately equal responses and concentrations) but, more important, the analysis time can be drastically reduced from 38 to 20 min. Hence two parameters are sufficient to obtain a sufficient separation for this mixture but three parameters enable us to achieve a better chromatogram with respect to both separation and analysis time. Further discussion of this topic is presented later.

The full three-parameter optimization predicts an optimum mobile phase composition of 2% propanol, 0.24 *M* SDS and pH 3.1. However, when this chromatogram was actually measured, a slight difference was observed between the predicted and measured chromatograms, resulting in a new location of the predicted global optimum. This is illustrated in Fig. 7: another slice of the full parameter space is shown for a constant value of the surfactant concentration (0.24 *M* SDS). The intersection between this plne and the various tetrahedra is indicated by the solid lines. Chromatogram 16 (2% propanol. 0.24 *M* SDS, pH 3.1) results in the formation of four new tetrahedra within tetrahedron (4, 7, 10, 14) as indicated in the middle left of the square. The measured chromatogram is indicated by the asterisk, and is surrounded by the intersections of tetrahedra (4, 7, 10, 16), (4, 10, 14, 16), (4, 7, 14, 16) and (7, 10, 14, 16) with the plane ([SDS] = 0.24 *M*).

The change in the location of the global optimum and consequently the necessity for an additional

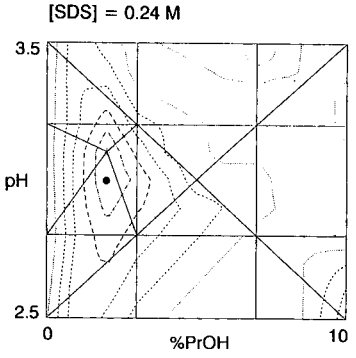

Fig. 7. Intersection of the full parameter space at a surfactant concentration [SDS] = 0.24 *M* after sixteen experiments. The iso-response lines (dashed lines) connect points with identical criterion values. The solid lines show intersections with the various tetrahedra defined by previous experiments. The asterisk indicates the location of experiment 16, and the solid dot defines the location of the predicted optimum, shown in Fig. 8.

measurement are caused by a deviation from the assumed linear retention behaviour (ln k') as a function of the parameters. In this instance the deviation was most noticeable in the direction of varying pH, as was to be expected given the nature of the parameter. The location of the next measurement is indicated by the dot, and is positioned at 2% propanol, 0.24 M SDS and pH 3.0. In addition, the shape of the response surface, described by the dashed lines, indicates a fairly stable optimum (gradual change in the criterion value as a function of the parameters). Of course, this statement only holds here for the two parameters examined in this figure (pH and propanol concentration), but examination of the plane perpendicular to that presented in Fig. 7 at 2% propanol shows a similar behaviour of the response (not shown).

The predicted and observed chromatograms at this mobile phase composition are presented in Fig. 8. Since the predicted chromatogram is the result of a simulation, the impurities (origin unknown) in the beginning of the measured chromatogram in Fig. 8b are absent. In addition, the resolution in the measured chromatogram is slightly less than that in the predicted chromatogram, mostly because of some peak asymmetry, not expressed in the plate count and consequently not taken into consideration in the calculations. Refinement of the criterion by including asymmetry in the resolution calculation [23] will improve the results. Nonetheless, the two chromatograms are very similar, indicating that the linear model applied was sufficient to describe most

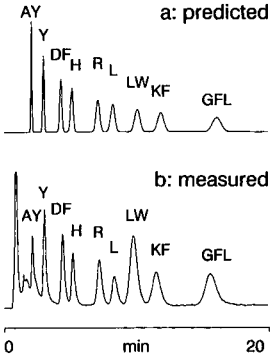

Fig. 8. Predicted and measured chromatograms of the nine-component amino acid–peptide mixture defined in Table 1 at [SDS] = 0.24 M, 2% propanol and pH 3.0.

of the observed retention behaviour. This is indicative of a fairly regular retention behaviour as a function of the examined parameters, which is similar to the conclusion obtained for the two-parameter case [15].

As mentioned before, the use of minimun resolution is not the best criterion if one wants to optimize both separation and analysis time. This is especially true if sufficient separation (R_s = 1.5) is achieved for a number of parameter settings: further improvement of the resolution is not sensible, while improvement in analysis time is not expressed by the criterion (if strongly varying concentrations or detector responses of the components are observed, an adjusted definition of resolution might be applied [24] and the above statement still holds true). In order to circumvent these problems, several solutions have been proposed, *e.g.*, the use of the so-called "multi-criterion decision making" [24]. Alternatively, a much better defined response surface with respect to the goal of the chromatographer is obtained if a so-called threshold criterion is applied [2]: the parameter space is searched for the minimum analysis time, taking into consideration only chromatograms with sufficient separation. The results of using a variation of this criterion (*i.e.*, the inverse of the retention time of the last peak, unless the resolution drops below a critical value in which case the criterion is set to zero) for the peptide–amino acid mixture are presented in Fig. 9. The intersections show that the global optimum is much better defined by this approach, and indeed results in a better chromatogram with respect to analysis time (*ca.* 14 min) compared with those presented in Fig. 6, with sufficient resolution of all components.

CONCLUSIONS

The iterative regression optimization strategy is easily extended to multi-parameter optimizations. However, an inhibitively large number of initial experiments limits the application to three parameters.

The regular retention behaviour of solutes in MLC as a function of the concentration of organic modifier, concentration of surfactant and pH permits the use of the simple linear model, as long as the examined range of pH values is limited. This regularity also allows a direct measurement of the predicted

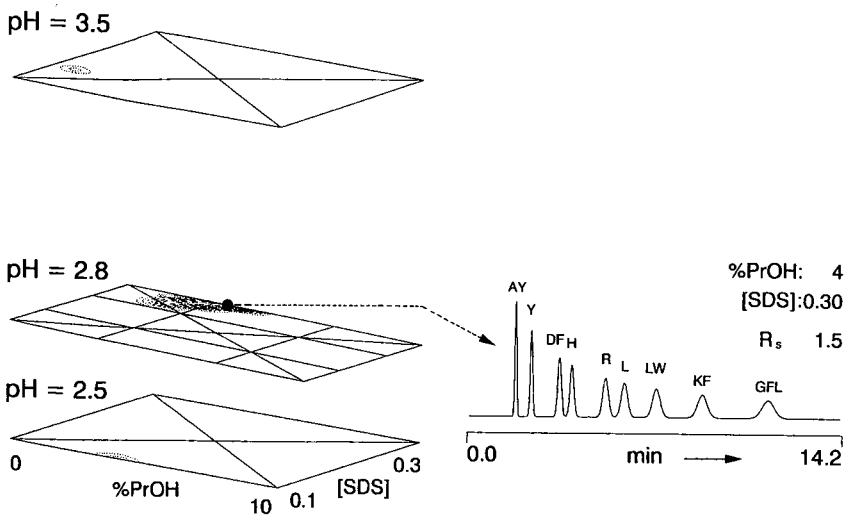

Fig. 9. Three intersections in the original parameter space at the specified pH values. In each intersection, iso-response lines show the behaviour of the criterion, the inverse retention time of the last component unless the minimum resolution is lower than 1.5, in which event the criterion is set to zero. In addition, the predicted global optimum, location indicated by the solid dot, is displayed on the right.

optimum mobile phase composition, resulting in a fast optimization procedure. However, the iterative part of the procedure remains essential to correct for slight deviations in the observed retention behaviour.

Separate optimization of, *e.g.*, pH apart from the other parameters is inefficient and can result in sub-optimum separations owing to the dependence of the response on the values of surfactant and organic modifier concentration. This is inherent in the chromatographic technique, where for instance a change in surfactant concentration influences the overall dissociation of the components.

The next step in the development of a comprehensive optimization strategy for this type of chromatography is an intelligent and efficient selection of the relevant parameters and especially the examined range in the parameter space. In this way the advantages of a fast and easy method development protocol in MLC can overcome some of the disadvantages of this type of chromatography, such as the limited efficiency.

ACKNOWLEDGEMENT

This work was supported by a grant from the National Institutes of Health (FIRST Award, GM38738).

REFERENCES

1 J. C. Berridge, *Techniques for Automated Method Optimization of HPLC Separations*, Wiley, Chichester, 1985.
2 P. J. Schoenmakers, *Optimization of Chromatographic Selectivity —a Guide to Method Development*, Elsevier, Amsterdam, 1986.
3 L. R. Snyder, J. L. Glajch and J. J. Kirkland, *Practical HPLC Method Development*, Wiley, New York, 1988.
4 J. L. Glajch and L. R. Snyder (Editors), *Computer-Assisted Method Development for High-Performance Liquid Chromatography*, Elsevier, Amsterdam, 1990; *J. Chromatogr.*, 485 (1989).
5 G. K.-C. Low, A. Bartha, H. A. H. Billiet and L. de Galan, *J. Chromatogr.*, 478 (1989) 21.
6 A. Bartha, G. Vigh and J. Stahlberg, *J. Chromatogr.*, 485 (1989) 403.
7 A. P. Goldberg, E. Nowakowska, P. E. Antle and L. R. Snyder, *J. Chromatogr.*, 316 (1984) 241.
8 H. A. H. Billiet, J. Vuik, J. K. Strasters and L. de Galan, *J. Chromatogr.*, 384 (1987) 153.
9 P. M. J. Coenegracht, N. V. Tuyen, H. J. Metting and P. J. M. Coenegracht-Lamers, *J. Chromatogr.*, 389 (1987) 351.
10 D. W. Armstrong and F. Nome, *Anal. Chem.*, 53 (1981) 1662.
11 M. Arunyanart and L. J. Cline Love, *Anal. Chem.*, 56 (1984) 1557.
12 J. G. Dorsey, M. T. DeEchegaray and J. S. Landy, *Anal. Chem.*, 55 (1983) 924.
13 M. G. Khaledi, *Anal. Chem.*, 60 (1988) 876.
14 M. G. Khaledi, J. K. Strasters, A. H. Rodgers and E. D. Breyer, *Anal. Chem.*, 62 (1990) 130.
15 J. K. Strasters, E. D. Breyer, A. H. Rodgers and M. G. Khaledi, *J. Chromatogr.*, 511 (1990) 17.

16 D. P. Herman, H. A. H. Billiet and L. de Galan, *Anal. Chem.*, 58 (1986) 2999.
17 A. C. J. H. Drouen, H. A. H. Billiet, P. J. Schoenmakers and L. de Galan, *Chromatographia*, 16 (1982) 48.
18 A. C. J. H. Drouen, *Ph.D. Thesis*, Delft University of Technology, Delft, 1985.
19 A. van Renesse, J. K. Strasters, H. A. H. Billiet and L. de Galan, presented at the *13th Symposium on Column Liquid Chromatography, Stockholm, June 25–30, 1989*, (poster) M/TU-P-164.
20 H. A. H. Billiet and L. de Galan, *J. Chromatogr.*, 485 (1989) 27.
21 L. S. Madamba-Tan, J. K. Strasters and M. G. Khaledi, *Anal. Chem.*, submitted for publication.
22 M. G. Khaledi and A. H. Rodgers, *Anal. Chim. Acta*, 239 (1990) 121.
23 P. J. Schoenmakers, J. K. Strasters and A. Bartha, *J. Chromatogr.*, 458 (1988) 355.
24 P. M. J. Coenegracht, A. K. Smilde, H. J. Metting and D. A. Doornbos, *J. Chromatogr.*, 485 (1989) 195.

Journal of Chromatography, 586 (1991) 233–248
Elsevier Science Publishers B.V., Amsterdam

CHROM. 23 575

Separation of enantiomers using cellulase (CBH I) silica as a chiral stationary phase

I. Marle☆

Department of Analytical Pharmaceutical Chemistry, Biomedical Centre, Uppsala University, P.O. Box 574, S-751 23 Uppsala (Sweden)

P. Erlandsson☆☆

Department of Technical Analytical Chemistry, Chemical Centre, University of Lund, P.O. Box 124, S-221 00 Lund (Sweden)

L. Hansson☆☆☆

Draco AB, P.O. Box 34, S-221 00 Lund (Sweden)

R. Isaksson and C. Pettersson*

Department of Analytical Pharmaceutical Chemistry, Biomedical Centre, Uppsala University, P.O. Box 574, S-751 23 Uppsala (Sweden)

G. Pettersson

Department of Biochemistry, Biomedical Centre, P.O. Box 576, S-751 23 Uppsala (Sweden)

(First received February 13th, 1991; revised manuscript received June 20th, 1991)

ABSTRACT

A new chiral stationary phase for high-performance liquid chromatography based on a glycoprotein (celllulase, CBH I) isolated from a culture filtrate of a fungus, *Trichoderma reesei*, was prepared. Chiral acidic and basic drugs were resolved into their enantiomers on this phase. Compared with other similar chiral phases, high enantioselectivity was obtained for β-blocking agents despite low capacity factors. As much as 200 nmol of propranolol in a single injection could be separated into its enantiomers on an analytical column (250 × 5.0 mm I.D.) without loss of resolution. No significant decrease in enantioselectivity was observed after daily use of the phase during a period of 4 months with varying mobile phase compositions. The retention and enantioselectivity of amines increased with increasing pH of the mobile phase, whereas the opposite effect was observed for acids. Addition of organic solvents to the mobile phase both decreased the retention and increased the enantioselectivity for the analytes.

☆ Present address: Analytical Quality Control. Astra Pharmaceutical Production, S-151 85 Södertälje, Sweden.
☆☆ Present address: Svensk Oljeextraktion AB, P.O. Box 3, S-374 21 Karlshamn, Sweden.
☆☆☆ Present address: Hafslund Nycomed Innovation AB, Ideon, P.O. Box, S-205 12 Malmö, Sweden.

0021-9673/91/$03.50

INTRODUCTION

Mammalian proteins immobilized on a support [1–9] or used as chiral additives to the mobile phase [10] have been utilized successfully as chiral selectors in liquid chromatographic separations of enantiomers. Other proteins, *e.g.*, microbial proteins, might also be of interest as chiral selectors. Recently, a cellulase (CBH I) produced by the fungus *Trichoderma reesei* was immobilized on silica and used as a chiral stationary phase for direct separation of some enantiomeric drugs [11].

We now report on the reproducibility of the preparation of CBH I columns and the sample capacity of the columns. However, our main interest in this study was focused on controlling the enantioselective retention of acidic, basic and uncharged analytes on CBH I–silica by adjusting the pH of the mobile phase and by addition of different kinds and amounts of organic solvents to the mobile phase. A screening of enantiomeric separations of β-blocking agents and analogues and a few other chiral drugs was performed. A brief description of the cellulases and their properties is included.

Cellulase

The degradation of cellulose is a process of major importance in nature [12] and the initial step in the process is effected by enzymes, cellulases, produced mainly by fungi and bacteria. Functionally, cellulases have been divided into two classes, endoglucanases, which attack interior non-crystalline parts of the cellulose chain, and exoglucanases, which attack the chains from the non-reducing end to produce cellobiose. The latter enzymes have also been called cellobiohydrolases. One of the most efficient cellulose-degrading organisms in nature is the mould *Trichoderma reesei*. Some of the *Trichoderma* mutants can produce very large amounts of cellulases in liquid cultures: 20 g/l is not an unusual amount [13]. *T. reesei* produces mainly four different cellulases: two endoglucanases, EG I and EG III, and two cellobiohydrolases, CBH I and CBH II. These four enzymes have a common structural organisation (Fig. 1) with a terminal 36 residue long binding domain connected to the rest of the enzyme (*i.e.*, the core) through a flexible arm. The interconnecting region is rich in serine, threonine and proline residues and is highly glycosylated. The core is catalytically active. The three-dimensional structures of both the binding domain [14] and the CBH II core [15] have been solved. Cellulases are very elongated tadpole-like structures wherein the two functional domains are separated by as much as 100 Å [16].

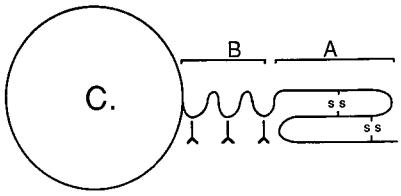

Fig. 1. Structural organization of fungal CBH. Active site is located in the core (C). B is a flexible spacer. A is a 36 amino acids long wedge-shaped peptide that anchors the enzyme to the cellulose fibre, thereby increasing its activity.

CBH I is the quantitatively dominating cellulase of *T. reesei*. It has a molecular weight of 60 000–70 000, an isoelectric point of 3.9, a carbohydrate content of 6% [17] and is stabilized by twelve disulphide bridges [18]. The binding domain of CBH I is located at the C-terminus of the enzyme [19] and the amino terminus of the core is blocked by a pyroglutamoyl moiety [17]. The *Trichoderma* CBH I gene has been characterized [20] and it is therefore possible to produce recombinant proteins with changed properties with the aim of gaining a deeper insight into chiral recognition.

EXPERIMENTAL

Chemicals

Concentrated culture filtrate from the fungus *T. reesei* chain QM9414 was a kind gift from VTT, the Technical Research Centre of Finland (Espoo, Finland). Spherical diol-silica with a particle diameter of 10 μm, pore size 300 Å, area 60 m^2/g and containing 5 $\mu mol/m^2$ of diol was obtained from Perstorp Biolytica (Lund, Sweden). Periodic acid was obtained from Merck (Darmstadt, Germany) and sodium cyanoborohydride from Janssen Chimica (Beerse, Belgium). (*R,S*)-, (*R*)- and (*S*)-propranolol chloride and (*R,S*)-pronethalol were obtained from Imperial Chemical Industries (Macclesfield, UK). (*RR,SS*)- and (*RS,SR*)-labetalol chloride were supplied by Glaxo Group Research (Greenford, UK). Racemic oxprenolol chloride and chlorthalidone

were obtained from Ciba-Geigy (Basle, Switzerland). (*R*)- and (*S*)-alprenolol tartrate, the racemates of the other amino alcohols as chlorides and racemic omeprazole were kindly supplied by Astra Hässle (Mölndal, Sweden). Racemic, (*R*)- and (*S*)-prilocaine chloride, racemic tocainide chloride, mepivacaine chloride and bupivacaine chloride were gifts from Astra Pain Control (Södertälje, Sweden). Racemic mexiletine chloride was obtained from Boehringer Ingelheim (Ingelheim/Rhein, Germany). Racemic benproperine was a gift from Pharmacia (Uppsala, Sweden). (*R,S*)-Warfarin, D- and L-N-CBZ-phenylalanine, D- and L-tryptophan and (*R*)- and (*S*)-1-phenylethanol were purchased from Sigma (St. Louis, MO, USA). (*R*)- and (*S*)-warfarin were kindly supplied by Dr. Istvan Szinai, Central Research Institute for Chemistry of the Hungarian Academy of Sciences (Budapest, Hungary). (*R*)- and (*S*)-ethyl mandelate were from Aldrich (Milwaukee, WI, USA). (+)- and (−)-α-phenylethylsulphamic acid were purchased from ICN Pharmaceuticals (Plainview, NY, USA). (+)- and (−)-trimethylnaphthylethylammonium bromide were a gift from Kabi (Stockholm, Sweden). (*R*)- and (*S*)-naproxen were obtained from Syntex Labs. (Palo Alto, CA, USA). The buffer salts and organic solvents were of analytical or reagent grade. Solute structures are shown in Fig. 2.

Isolation of CBH I from culture filtrate

CBH I was isolated from the crude concentrated culture filtrate of *T. reesei* QM 9414 by gel chromatrography on Sephadex G-25, to remove salts and pigments, followed by two chromatographic steps on DEAE-Sepharose CL-6B at pH 5.0 and 3.7 [17]. After the last chromatographic step the material was analysed by sodium dodecyl sulphate–polyacrylamide gel electrophoresis according to Maizel [21] and the fraction C_1 [17] that contained CBH I displayed no heterogeneity.

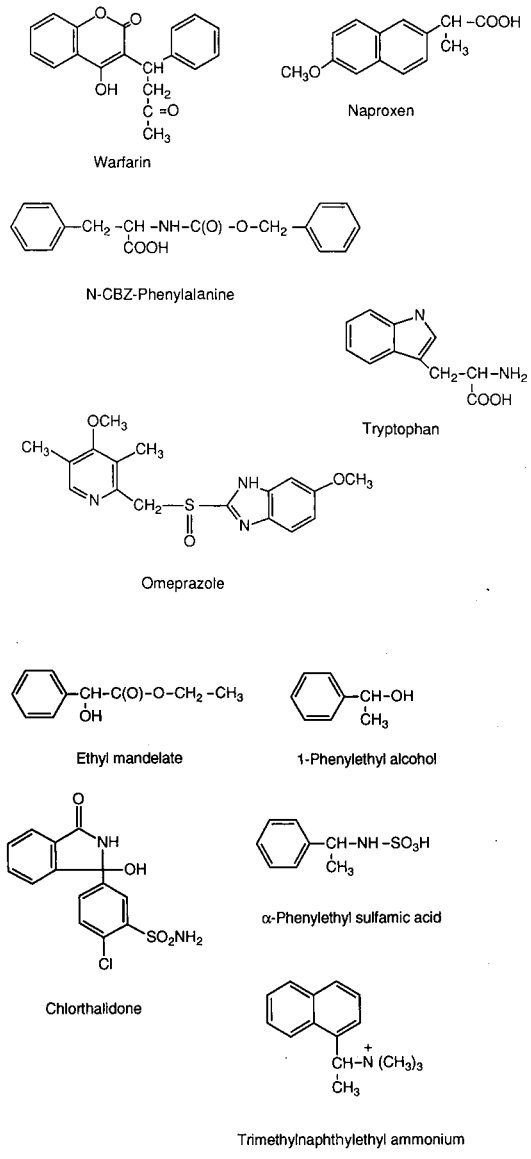

Fig. 2. Solute structures.

Circular dichoroism (CD) experiments

CD measurements were performed by use of samples prepared by diluting 1 ml of a stock solution [obtained by dissolving 52.3 mg of lyophilized CBH I in 10 ml of water purified with a Milli-Q system (Millipore, Bedford, MA, USA)] to a total volume of 5 ml with 0.1 *M* sodium phosphate buffer of pH 2.2, 3.6 or 8.1. After first having recorded the CD spectra of the samples of pH 2.2 and 8.1, the pH of these samples was then adjusted to 3.6 by titration with 1 *M* sodium hydroxide or 1 *M* phosphoric acid, respectively, and the CD measurements were repeated. All CD experiments were performed on a Jasco J-500 A spectropolarimeter (Japan Spectroscopic, Tokyo, Japan) using a 1-mm quartz cell.

Preparation of CBH I columns

A 5-g amount of diol-silica was suspended in 30 ml of water and 0.35 g periodic acid was added. The suspension was first treated on a Sonorex (Berlin, Germany) ultrasonic bath for 1 min and then kept on a rocker table for 2–3 h. The aldehyde silica was washed on a glass filter with water. A 35-ml volume of 0.1 *M* sodium phosphate buffer (pH 7.0) containing 0.75 g of CBH I and 0.13 g of sodium cyanoborohydride was added to the wet aldehyde-silica and the suspension was treated in the ultrasonic bath for 1 min. The resulting slurry was agitated on a rocker table for 2 days and then washed with 0.1 *M* phosphate buffer (pH 7.0). The amount of immobilized CBH I was calculated by determining the UV absorbance of the CBH I solution before and after reaction with the aldehyde-silica using a Shimadzu (Kyoto, Japan) UV-160A spectrophotometer. About 30–50% of the CBH I added to the aldehyde-silica became immobilized.

Diol-silica from a single batch and four different batches of CBH I were used to prepare the solid phases. The stationary phases of columns CBH I-A and CBH I-B were made from the same preparation of CBH I. Another preparation of CBH I was used for the solid phases of columns CBH I-C and -E. The solid phases of columns CBH I-D and -F were made from another two CBH I preparations. The solid phases C and E were made on the same occasion and the other solid phases were prepared one at a time.

Columns were prepared by suspending the CBH I-silica in the phosphate buffer and were packed at 350 bar into PTFE-coated (Svefluor, Uppsala, Sweden) stainless-steel columns from Skandinaviska GeneTec (Kungsbacka, Sweden), using an ascending packing technique [22]. The column dimensions for the solid phases CBH I-A, -B, -D, and -E were 250 × 5.0 mm I.D. and for CBH I-C and -F 100 × 4.6 mm I.D.

Chromatographic apparatus

A Model 2150 dual-piston high-performance liquid chromatographic pump (LKB, Bromma, Sweden) and a Lambda-Max Model 481 LC spectrophotometer (Waters Assoc., Milford, MA, USA) connected to a Model BD 41 recorder (Kipp & Zonen, Delft, Netherlands) were used. Chromatographic data were also collected by a JCL6000 chromatographic data system (Jones Chromatography, Hengoed, UK). The injector was a Rheodyne (Cotati, CA, USA) Model 7125. The volume injected was 20 μl in all experiments except those illustrated in Fig. 3 and Table III.

Chromatographic technique

Acetate buffers were prepared from acetic acid and sodium acetate and phosphate buffers from phosphoric acid and sodium hydroxide. Prior to injection, the solutes were dissolved in the mobile phase at concentrations of about 0.1 m*M* unless stated otherwise. The experiments were performed at ambient temperature (21–25°C). The influence of temperature on retention and enantioselectivity was not studied systematically in this work. Preliminary results indicated, however, that the capacity factors and the enantioselectivity may change by about 5% in the temperature range 20–25°C. A comprehensive temperature study is in progress and will be reported separately.

The capacity factors was calculated as $k' = (V_R - V_0)/V_0$, where V_R and V_0 are the retention volumes of the solute and the non-retained compound, respectively. V_0 was obtained from the inflection point of Milli-Q-purified water unless stated otherwise. The enantioselectivity, α, was calculated as k'_2/k'_1, where k'_2 is the capacity facor of the more retained enantiomer. The peak symmetry was calculated in the following way: two tangents to the peak were drawn, and the projection of the point of intersection divided the baseline into two parts, *a*, the front side, and *b*, the rear side. The asymmetry factor, *asf*, was defined as *b*/*a*. The resolution of incompletely resolved peaks was calculated according to ref. 23. At a right-angle to the baseline a line was drawn from the baseline through the valley (the minimum) between the peaks up to a line joining the maxima of the peaks. This distance is defined as *g*. The distance between the intersection of the two lines and the valley is defined as *f*. According to this definition, the ratio $f/g = 1$ corresponds to complete separation. The resolution of completely resolved peaks was calculated by use of the equation

$$R_s = N^{1/2}k'_2(\alpha - 1)/4(1 + k'_2)\alpha$$

although the peaks were asymmetric. *N*, the peak efficiency, was calculated as $16(t_R/w_t)^2$, where t_R is

the retention time of the solute and w_t is the peak width at the baseline, *i.e.*, $a+b$.

RESULTS AND DISCUSSION

Properties of CBH I silica

Solute structure and enantioselectivity. The enantioselective retention of β-adrenergic blocking

TABLE I

SOLUTE STRUCTURES AND STEREOSELECTIVITY OF β-BLOCKERS

Solid phase: CBH I-B. Mobile phase: 0.065 *M* 2-propanol in phosphate buffer, pH 6.0 (I = 0.01).

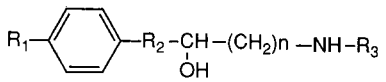

Solute No.	n	R_1	R_2	R_3	k'_1	α	f/g
1[a]	1	$-(CH_2)_2OCH_3$	$-OCH_2$	$-CH(CH_3)_2$	0.82	2.67	3.1[b]
2	2	$-(CH_2)_2OCH_3$	$-OCH_2$	$-CH(CH_3)_2$	0.51	1.90	0.98
3	3	$-(CH_2)_2OCH_3$	$-OCH_2$	$-CH(CH_3)_2$	0.37	1.50	0.89
4	1	$-OH$	$-OCH_2$	$-CH(CH_3)_2$	0.10	3.95	0.99
5	1	$-OCH_3$	$-OCH_2$	$-CH(CH_3)_2$	0.31	3.81	4.4[b]
6	1	$-CH_2CH_3$	$-OCH_2$	$-CH(CH_3)_2$	0.57	2.65	3.4[b]
7	1	$-OCH_2CH=CH_2$	$-OCH_2$	$-CH(CH_3)_2$	0.50	2.41	0.98
8	1	$-O(CH_2)_2OCH_3$	$-OCH_2$	$-CH(CH_3)_2$	0.26	1.41	0.63
9[c]	1	$-CH_2CONH_2$	$-OCH_2$	$-CH(CH_3)_2$	0.05	4.0	0.94
10[d]	1	$-NHCOCH_3$	$-OCH_2$	$-CH(CH_3)_2$	0.20	1.0	
11	1	$-(CH_2)_2OCH_3$	–	$-CH(CH_3)_2$	0.06	1.0	
12	1	$-(CH_2)_2OCH_3$	$-OCH_2$	$-H$	0.38	1.0	

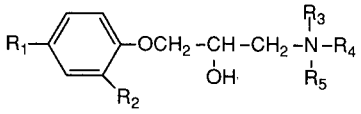

	R_1	R_2	R_3	R_4	R_5	k'_1	α	f/g
13	$-(CH_2)_2C(O)OCH_2CH_3$	$-F$	$-CH(CH_3)_2$	$-H$		1.49	1.0	
14	$-(CH_2)_2OCH_3$	$-Br$	$-(CH_2)_2OC_6H_4$-*p*-$C(O)NH_2$	$-H$		0.70	1.0	
15[e]	$-H$	$-CH_2CH=CH_2$	$-CH(CH_3)_2$	$-H$		0.97	9.88	6.3[b]
16[f]	$-H$	$-OCH_2CH=CH_2$	$-CH(CH_3)_2$	$-H$		0.47	3.27	4.3[b]
17	$-H$	$-Cl$	$-CH_2OC_6H_4$-*p*-$C(O)NH_2$	$-H$		2.96	2.75	4.4[b]
18	$-H$	$-CH_3$	$-(CH_2)_3C_6H_5$	$-H$		1.82	3.77	2.3[b]
19	$-H$	$-H$	$-(CH_2)_2C_6H_4$-*o*-CH_3	$-H$		1.12	1.78	0.92
20	$-H$	$-H$	$-CH(CH_3)_2$	$-CH_3$	$-CH_3$	0.28	1.0	
21	$-H$	$-CH_2CH=CH_2$	$-H$	$-H$		1.56	3.47	4.4[b]
22	$-H$	$-CH_2CH=CH_2$	$-(CH_2)_2OC_6H_4$-*p*-$C(O)NH_2$	$-H$		4.53	4.08	4.7[b]
23	$-H$	$-CH_2CH=CH_2$	$-C_5H_{10}$	see R_3	$-CH_3$	0.41	1.0	
24[g] (*RR/SS*)		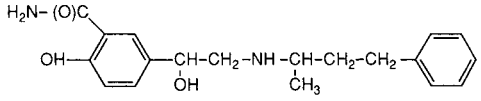				0.78	4.17	3.4[b]
25[g] (*RS/SR*)						0.83	1.0	

(Continued on p. 238)

TABLE I *(continued)*

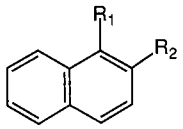

Solute No.	R_1	R_2	k'_1	α	*f/g*
26[h]	$-OCH_2CH(OH)CH_2NHCH(CH_3)_2$	$-H$	2.28	5.18	5.2[b]
27	$-OCH_2CH(OH)CH_2NHCH(CH_3)_2$	$-CH_3$	2.05	1.82	2.1[b]
28[i]	$-H$	$-CH(OH)CH_2NHCH(CH_3)_2$	0.60	1.98	0.97

[a] Metoprolol.
[b] Calculated as R_s.
[c] Atenolol.
[d] Praktolol.
[e] Alprenolol.
[f] Oxprenolol.
[g] Labetalol.
[h] Propranolol.
[i] Pronethalol.

agents and analogues on CBH I-silica is summarized in Table I. An increase in the number of carbon atoms between the hydroxyl and the amino groups resulted in a significant decrease in the enantioselectivity and the capacity factors (Nos. 1–3, Table I). A similar finding with enantioseparations of amino alcohols related to metoprolol on the α_1-AGP phase has been reported by Hermansson and Schill [24]. Complete loss of enantioselectivity was observed for the amino alcohol having four methylene groups between the hydroxylic groups and the amino group. A poorer fit of the solute to the chiral binding site with increasing chain length was suggested as an explanation for the loss of enantioselectivity and this explanation may also hold true for the CBH I-silica. The enantioselectivity of the CBH I-silica is also sensitive to the substitution pattern on the aromatic ring (Nos. 4–10, 13, 15, 16 and 27, Table I). This is illustrated by the difference in enantioselectivity between atenolol (α = 4.0) and praktolol (α = 1.0) (Nos. 9 and 10, Table I). Similar effects were observed on altering the substitution of the amino group of the amino alcohol chain (Nos. 14–23, Table I). The enantioselectivity decreased when the isopropyl group of alprenolol (α = 9.9) was replaced with a hydrogen atom (α = 3.5) (Nos. 15 and 21, Table I).

The enantioselectivities of the local anaesthetic prilocaine and some analogues were also investigated (Nos. 29–34, Table II). Enantioselective retention was observed for a primary or secondary amine with an amide group close to the aromatic ring. No enantioselectivity was observed for tertiary amines in which the chiral carbon atom was contained in a ring structure or when the amide group close to the aromatic ring was replaced with a methoxy group.

The enantiomers of the weak acid warfarin and the sulphoxide omeprazole were separable in pH intervals where these solutes are mainly uncharged (see Table VI). No enantioselective separation was observed for mono- and divalent carboxylic acids and N-phenylalanine derivatives chromatographed under corresponding conditions.

Capacity. A concentration-independent retention and peak symmetry of (*R*)- and (*S*)-propanolol, respectively, were obtained for injected amounts up to 0.01 nmol (Table III). A possible explanation for this low loading capacity might be a heterogeneous adsorbing surface caused by a low coverage of protein on the CBH I-silica phase. The analyte could thus interact not only with the chiral selector but also with some sites on the silica itself, such as unreacted silanol groups, which are characterized by relatively high equilibrium constants [25]. Hermans-

TABLE II

SOLUTE STRUCTURES AND STEREOSELECTIVITY OF PRILOCAINE AND ANALOGUES

Solid phase: CBH I-A. Mobile phase: 0.065 *M* 2-propanol in phosphate buffer, pH 6.7 (I = 0.01).

Solute No.	Formula	k'_1	α	f/g
29[a]	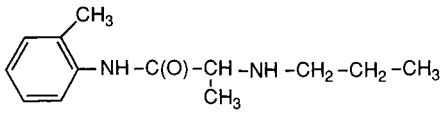	0.29	1.49	0.79
30[b]	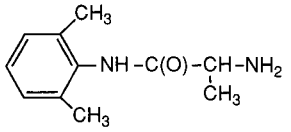	0.49	1.21	0.26
31[c]	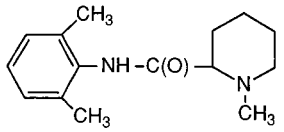	0.38	1.0	
32[d]	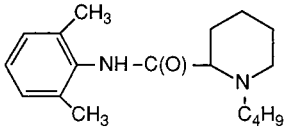	0.78	1.0	
33[e]	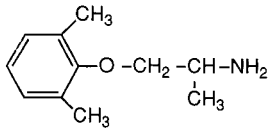	2.18	1.0	
34[f]	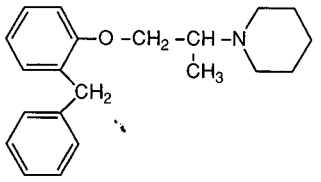	12.0	1.0	

[a] Prilocaine.
[b] Tocainide.
[c] Mepivacaine.
[d] Bupivacaine.
[e] Mexiletine.
[f] Benproperine.

son [26] observed an improvement in peak symmetry when the amount of immobilized α_1-AGP was increased from 76 to 183 mg of protein per gram of silica.

Although the binding isotherm of CBH I-silica is linear only at low sample loads, a large amount of racemic propranolol could be separated into its enantiomers owing to the high enantioselectivity (Fig. 3) (the column contained 75 mg of CBH I per gram of silica). When 10 nmol of racemic propranolol were injected, the retention of (*R*)- and (*S*)-propranolol decreased by 10% compared with the concentration-independent retention. The high selectivity factor for propranolol allowed the injection of as

TABLE III

CAPACITY OF (*R*)- AND (*S*)-PROPRANOLOL ON CBH I-F SOLID PHASE

Mobile phase: 0.065 *M* 2-propanol in acetate buffer, pH 4.7 (I = 0.01). Injected volume: 5 μl. Flow-rate: 1 ml/min. t_0 solute: (+)-norephedrine.

Amount injected (nmol)	(*R*)-		(*S*)-		α	R_s
	k'	*asf*	*k'*	*asf*		
$2.5 \cdot 10^{-3}$	1.06	n.d.	3.21	n.d.	3.03	n.d.
$1.2 \cdot 10^{-2}$	1.06	1.2	3.20	1.2	3.04	4.0
$2.5 \cdot 10^{-2}$	1.03	1.3	3.13	1.3	3.04	4.2
$2.5 \cdot 10^{-1}$	1.01	1.4	3.12	1.5	3.09	4.0

much as 200 nmol (60 μg) of (*R,S*)-propranolol without the loss of peak separation. Retained peak separation at high sample loads is advantageous from an analytical point of view as it increases the detection limit for an enantiomeric impurity in a sample. As the cellulases are also available in large amounts they might therefore afford preparative-scale separations of enantiomers. The retention of both (*R*)- and (*S*)-propranolol decreased at increasing sample loads, the decrease being most pronounced for the more retained enantiomer. On severe overloading, *e.g.*, 500 nmol of racemic propranolol in Fig. 3, the retention of (*S*)-propranolol approaches that of (*R*)-propranolol.

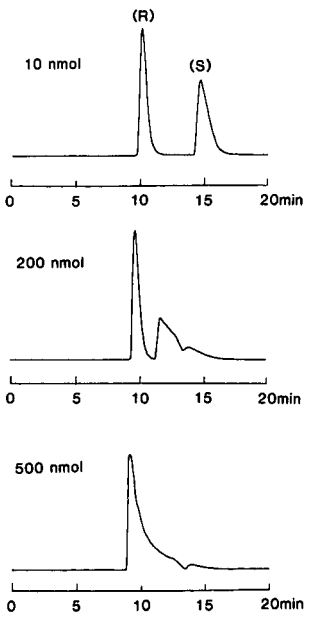

Fig. 3. Loading capacitiy of (*R,S*)-propranolol on the solid phase CBH I-E. Injected volume: 200 μl. Mobile phase: 0.065 *M* 2-propanol in acetate buffer, pH 4.7 (I = 0.01). Flow-rate: 0.5 ml/min.

Reproducibility and stability. Chiral separations obtained on three different CBH I stationary phases are presented in Table IV. Good reproducibility of enantioselectivity, retention and peak symmetry were observed for columns containing CBH I-silica prepared from the same batch of enzyme (columns CBH I-A and CBH I-B) and also from a different batch (column CBH I-E). The retention of the solutes listed in Table IV was low when an acidic mobile phase was used. Small differences in the capacity factors therefore resulted in relatively large differences in the enantioselectivity.

A CBH I column was used daily for 3.5 months at a flow-rate of 1 ml/min and at different pHs (2–8) and with different concentrations of 2-propranol (0.5–6%) in the mobile phase. A 23% change in the capacity factors of warfarin and propranolol was observed during this period, as measured with a reference mobile phase (Table V). The enantioselectivity was almost uninfluenced, but the resolution of propranolol and omeprazole decreased by 4 and 11%, respectively, owing to increased peak tailing. Similar findings were reported recently for an α_1-AGP column [27]. A possible explanation for the retention changes and the decreased peak symmetry might be a gradual loss of CBH I from the support and/or denaturation of the protein by metal ions in the system, as both enantiomers of the solutes were affected equally.

TABLE IV

COMPARISON OF CBH I SOLID PHASES

Mobile phase: 0.065 *M* 2-propanol in acetate buffer, pH 4.7 (I = 0.01). Flow-rate: 0.3 ml/min. V_0 was obtained with (+)-norephedrine.

Solute	CBH I-A				CBH I-B				CBH I-E[a]			
	k'_2	asf_2	α	f/g	k'_2	asf_2	α	f/g	k'_2	asf_2	α	f/g
Propranolol	1.26	1.9	2.6	4.2[b]	1.20	2.4	3.3	5.1[b]	1.21	1.8	2.5	5.0[b]
Alprenolol	0.83	1.9	5.5	4.8[b]	0.87	2.3	7.2	5.8[b]	0.76	2.2	4.6	5.8[b]
(*RR/SS*)-Labetalol	0.47	1.5	1.9	0.94	0.40	2.1	2.5	0.98	0.46	1.9	1.7	0.94
Oxprenolol	0.17	0.9	1.9	0.78	0.16	1.8	2.7	0.90	0.19	n.d.	1.7	0.87
No. 17, Table I	0.82	1.4	2.0	0.98	0.76	1.8	2.5	3.6[b]	0.91	2.0	1.9	3.2[b]
No. 21, Table I	0.48	1.3	2.8	0.99	0.48	1.9	3.0	3.3[b]	0.45	1.8	2.5	2.9[b]

[a] Flow-rate 0.5 ml/min.
[b] Calculated as R_s.

The solid phase used to prepare the CBH I-D column contained about 55 mg of CBH I per gram of silica, whereas the other phases contained about 75 mg/g. The retention and stereoselectivity of the CBH I-D column deviated from those of the other columns, *cf.*, propranolol in Tables IV and V. The retention of propranolol was higher and the stereoselectivity and resolution were lower on the CBH I-D phase than on the other phases. In addition, the enantiomers of warfarin were separable only on the CBH I-D column. CBH I from different batches was, however, used to prepare the solid phases. Variation of CBH I between different batches cannot be excluded as the composition of the culture medium influences the degree of glycosylation of the enzyme. This might account for the differences in the enantioselective retention of propranolol and warfarin.

TABLE V

STABILITY OF CBH I-SILICA

Solid phase: CBH I-D. Mobile phase: phosphate buffer, pH 4.8 (I = 0.01). Flow-rate: 1 ml/min.

Solute	Parameter	Volume of mobile phase (l)				
		Day 12: 5.5	Day 33: 15.5	Day 67: 31.4	Day 88: 41.4	Day 106 49.9
Warfarin	k'_2	6.11	6.05	5.36	4.92	4.65
	asf_2	4.8	4.2	4.5	4.7	5.0
	α	1.26	1.28	1.30	1.28	1.33
	f/g	0.94	0.93	0.94	0.91	0.94
Propranolol	k'_2	4.81	4.88	5.54	5.69	5.85
	asf	3.0	4.2	4.2	4.9	5.4
	α	1.42	1.43	1.42	1.42	1.34
	f/g	1.0	1.0	0.97	0.97	0.96
	R_s	2.1	2.2			
Omeprazole	k'_2	3.47	3.78	3.77	3.64	3.57
	α	1.09	1.10	1.09	1.09	1.09
	f/g	0.36	0.38	0.34	0.32	0.32

TABLE VI

INFLUENCE OF pH

Solid phase: CBH I-D. Mobile phase: phosphate buffer (I = 0.01).

Solute	pK_a[a]	Parameter	pH					
			2.2	3.5	4.7	5.6	6.8	8.1
Acids								
Warfarin	5.0	k'_2	5.58	6.92	6.11	2.45	0.89	0.18
		α	1.27	1.31	1.26	1.14	1.0	1.0
		f/g	0.92	0.94	0.94	0.16		
Naproxen	4.2	k'_2	7.73	8.11	4.24	1.24	0.55	0.14
		α	1.01	1.00	1.00	1.00	1.0	1.0
N-CBZ-phenylalanine	3.7[b]	k'_2	2.61	3.16	1.35	0.50	0.29	0.09
		α	1.00	1.00	1.02	1.0	1.0	1.0
Ampholytes								
Tryptophan	2.38, 9.39[c]	k'_2	0.06	0.15	0.14	0.18	0.24	0.34
		α	1.1	1.0	1.0	1.0	1.0	1.0
Omeprazole	4.0, 8.7[d]	k'_2	0.33	1.47	3.78	4.03	4.01	3.29
		α	1.0	1.0	1.10	1.10	1.06	1.0
		f/g			0.38	0.38	0.16	
Amines								
Prilocaine	7.9	k'_2		0.06	0.28	0.87	1.98	3.72
		α		1.0	1.0	1.0	1.22	1.19
		f/g					0.95	0.87
Propranolol	9.5	k'_2	0.69	1.37	4.81	18.8	106	339
		α	1.0	1.05	1.42	2.34	4.31	3.83
		f/g		0.38	1.0	1.0	1.0	1.0
		R_s			2.1	3.5	5.2	3.2
Uncharged solutes								
Ethyl mandelate		k'_2	0.27	0.30	0.25	0.31	0.37	0.47
		α	1.0	1.0	1.0	1.0	1.0	1.0
1-Phenylethanol		k'_2	0.23	0.26	0.21	0.26	0.34	0.42
		α	1.0	1.0	1.0	1.0	1.0	1.0
Chlorthalidone	9.4	k'_2	1.17	1.29	1.28		1.53	1.60
		α	1.0	1.0	1.0		1.0	1.0
Charged solutes								
α-Phenylethylsulphamic acid	−0.33[e]	k'_2	0.57	0.33	0.03			
		α	1.0	1.0	1.0			
Trimethylnaphthylethylammonium		k'_2	0.43	0.80	1.99		8.97	33.5
		α	1.0	1.0	1.04		1.00	1.02

[a] From ref. 28 unless indicated otherwise.
[b] pK_a of N-acetylalanine [29].
[c] Ref. 30.
[d] Ref. 31.
[e] pK_a of 1-aminoethylsulphonic acid [29].

Further improvement of the CBH I phase requires thorough control of the fermentation conditions and the work-up procedure for CBH I, optimization of the method used to immobilize the protein on the support, the kind of support used and the amount of protein bonded to the support. The influence of the CBH I loading on the chromatographic parameters is under closer investigation.

Influence of mobile phase composition on chiral separation

pH. The influence of mobile phase pH on the enantioselective retention of analytes (amines, carboxylic acids, charged and uncharged solutes) from a CBH I column was investigated (Table VI and Fig. 4). To obtain a variation of the net charge of the protein the study covered a wide pH range, from

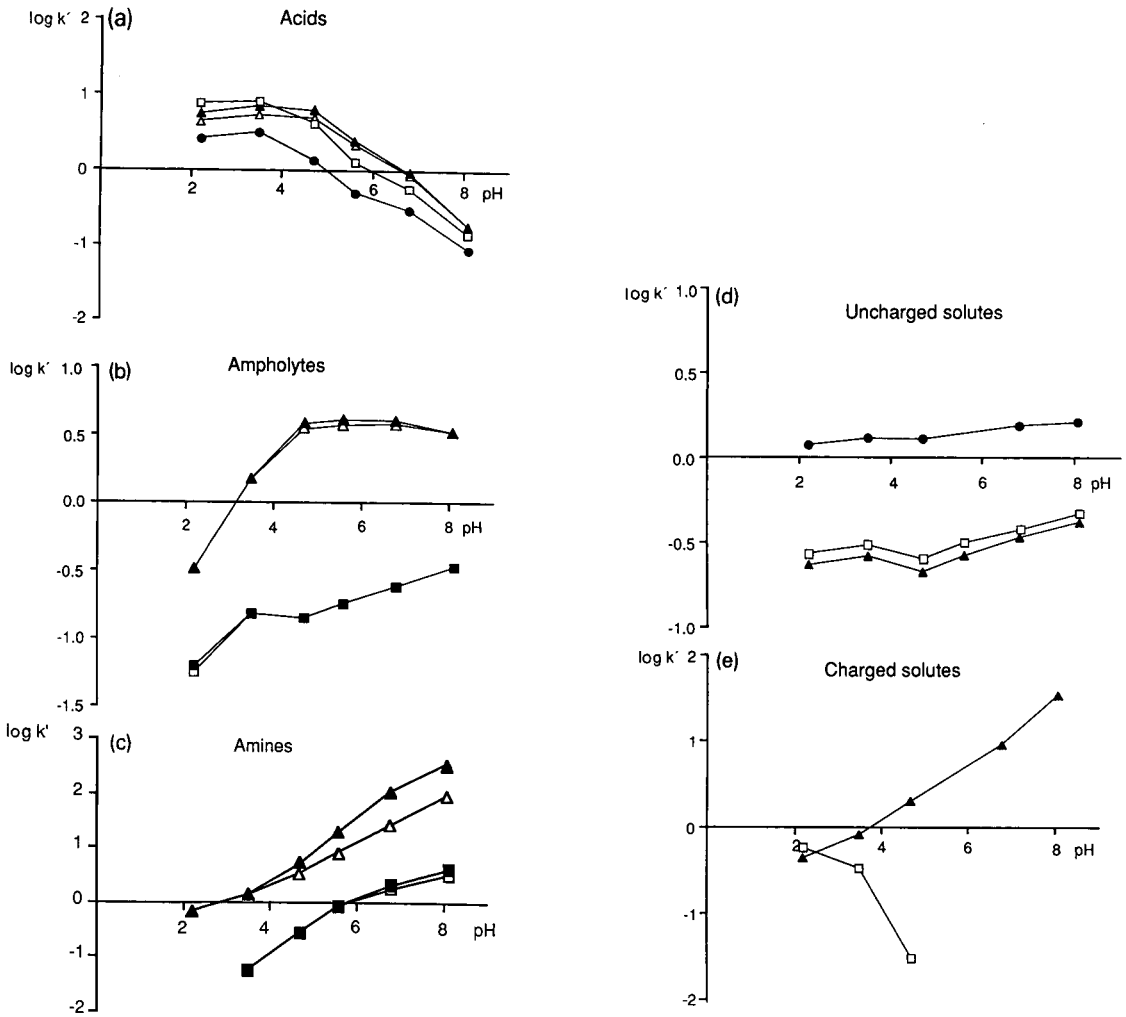

Fig. 4. (a) Influence of pH on retention and enantioselectivity of acids. Solid phase: CBH I-C. Mobile phase: Phosphate buffer (I = 0.01). □ = (*R*)- and (*S*)-naproxen; ● = L- and D-N-CBZ-phenylalanine; ▲ = (*R*)-warfarin; △ = (*S*)-warfarin. (b) Influence of pH on retention and enantioselectivity of ampholytes. Conditions as in (a). ■ = D-Tryptophan; □ = L-tryptophan; ▲ = omeprazole 2; △ = omeprazole 1. (c) Influence of pH on retention and enantioselectivity of amines. Conditions as in (a). ▲ = (*S*)-Propranolol; △ = (*R*)-propranolol; ■ = (*R*)-prilocaine; □ = (*S*)-prilocaine. (d) Influende of pH on retention and enantioselectivity of uncharged solutes. Conditions as in (a). ● = (*R,S*)-Chlorothalidone; □ = (*R*)- and (*S*)-ethyl mandelate; ▲ = (*R*)- and (*S*)-1-phenylethanol. (e) Influence of pH on retention and enantioselectivity of charged solutes. Conditions as in (a). □ = (+)- and (−)-α-phenylethylsulphamic acid; ▲ = (+)- and (−)-trimethylnaphthylethylammonium.

2 to 8. The retention of the acids decreased with increasing pH of the mobile phase. The pH dependence of the retention of the amines and the quaternary amine was opposite to that observed for acids. The retention of the uncharged solutes was almost unaffected by the pH.

The influence of pH on the conformation of CBH I was studied by circular dichroism (CD). The CD spectra showed a significant dependence on pH, indicating conformational changes of the protein (Fig. 5). Different ratios of the CD bands at 210–215 and 230 nm were obtained at pH 2.2, 3.6 and 8.1. After adjustment to pH 3.6 of the samples having initial pH values of 2.2 and 8.1, the CD spectra obtained were identical with that obtained at pH 3.6. The conformational changes occuring in CBH I over this pH range are obviously reversible. It is, open to discussion, however, whether these conformational changes also occur when the CBH I is immobilized on the silica support.

Within the pH range 3.9–8.0, the net charge of the protein is negative, whereas the amines used as analytes are predominantly protonated. The increase in retention observed for the amines and the quaternary amine on increasing the pH of the mobile phase above the isoelectric point of the protein might therefore be partly due to increased attractive electrostatic interactions between the analyte and the protein. As the mobile phase pH approached the pK_a values of the amines (Table VI), their hydrophobicities increases and this might also contribute to increased retention. As was found experimentally, one should have expected less retention of the amines at low pH as compared with that at high pH. At low pH the amines are completely protonated and CBH I also exhibits a positive net charge, *i.e.*, conditions more or less opposite to those obtaining at higher pH. The enantioselectivity of propranolol and prilocaine increasd with pH up to 6.8, but decreased slightly at pH 8.1 despite the increased retention. This behaviour might be ascribed to the kind of conformational changes of CBH I observed in the CD studies of the protein.

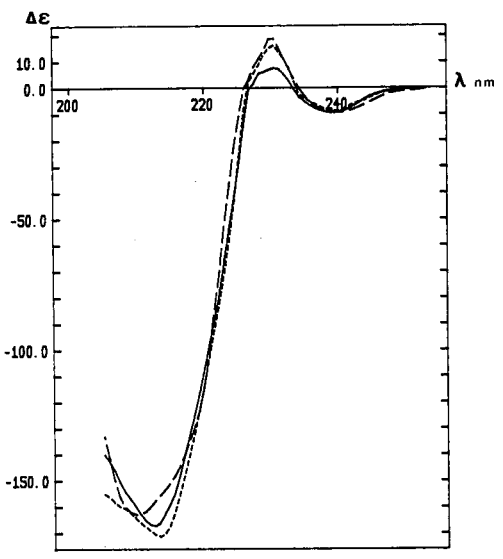

Fig. 5. Circular dicroism spectra of CBH I at (solid line) pH 2.2, (long dashed line) pH 3.6 and (short dashed line) pH 8.1, showing the conformational dependence of pH.

The retention of acids at very low pH is probably due to hydrophobic interactions, but other kinds of interactions, such as hydrogen bonding and various kinds of polar interactions, can, of course, contribute to the net retention. It is not unlikely that the small decrease in retention observed on decreasing the pH from 3.6 to 2.2 is due to conformational changes in the CBH I. The CD studies of CBH I (Fig. 5) confirmed that conformational changes actually occur at low pH values. At high pH the carboxylic groups of the acids exist as carboxylate ions and as the net charge of the CBH I at this pH is also negative a decrease in the retention could be expected. The retention of uncharged solutes, *e.g.*, carboxylic acids, at very low pH, omeprazole in the pH range 5–7.7 or permanently uncharged compounds, was almost independent of mobile phase pH. The highest enantioselectivity of warfarin and omeprazole was obtained at a pH where these solutes are uncharged. In the enantiomeric binding of these solutes to the protein, the presence of a charge on the molecules decreases the enantioselectivity, in contrast to the situation with the chiral separation of amines.

The solute retention on the CBH I silica phase is generally low. By the addition of organic counter ions to the mobile phase it may be possible to increase the retention of ionized acids and amines.

Organic modifier. The influence of the organic solvents 2-propanol, acetonitrile, tetrahydrofuran and methanol on the enantioselective retention and chromatographic performance was studied using

TABLE VII

INFLUENCE OF ORGANIC MODIFIER ON THE SEPARATION OF (*R,S*)-PROPRANOLOL

Solid phase: CBH I-C. Mobile phase: 0.78 *M* organic modifier in acetate buffer, pH 5.5 (I = 0.01). Flow-rate: 1 ml/min. Solute concentration: $5 \cdot 10^{-5}$ *M*.

Organic modifier	k'_1	k'_2	asf_1	asf_2	α	R_s
–	1.27	3.86	3.0	3.1	3.0	3.6
2-Propanol	0.62	2.46	2.3	2.4	3.9	4.0
Acetonitrile	0.62	2.46	2.3	2.6	3.5	3.9
Tetrahydrofuran	0.28	0.94	2.6	2.7	3.4	2.7
Methanol	0.95	3.21	2.6	2.6	3.4	3.7

propranolol as a model compound (Table VII). As might be expected from other studies [32], the retention of (*R*)- and (*S*)-propranolol decreases on addition of an organic solvent to the mobile phase. The enantioselectivity increased irrespective of the solvent used (Table VII) and only minor differences in enantioselectivity could be observed between hydrogen-donating and hydrogen-accepting organic solvents. A slight improvement in the chromatographic performance (*asf*) of (*R*)- and (*S*)-propranolol was observed in the presence of organic solvents (Table VII). Assuming the presence of multiple sites, the solvents probably decrease the overloading of the stationary phase by competing with the analytes for high affinity binding sites [25].

TABLE VIII

INFLUENCE OF CONCENTRATION OF 2-PROPANOL ON THE SEPARATION OF ENANTIOMERS WITH SOLID PHASE CBH I-B

Mobile phase: 2-propanol in phosphate buffer, pH 6.8 (I = 0.01). Flow-rate: 0.9 ml/min.

Solute	Parameter	Concentration of 2-propanol (*M*)			
		0.065	0.26	0.78	1.6
Metroprolol	k'_2	2.62	2.50	2.59	2.09
	asf_2	2.9	2.7	3.4	2.5
	α	2.5	2.7	3.3	4.4
	R_s	4.4	4.1	4.9	5.6
Propranolol	k'_2	33.6[a]		30.7	20.6
	asf_2	3.6		3.7	2.9
	α	4.6		6.1	6.9
	R_s	4.2		5.4	5.9
Prilocaine	k'_2	0.45	0.35	0.29	0.16
	asf_2	1.7	1.7	1.3	1.5
	α	1.8	2.0	2.0	2.1
	f/g	0.96	0.97	0.93	0.70

[a] Solid phase: CBH I-A, flow-rate, 0.3 ml/min.

In a preliminary attempt to optimize the chiral resolution of solutes on the CBH I silica phase, 2-propanol was added to the mobile phase at different concentrations (Tables VIII and IX). The enantioselectivity, the peak symmetry and the efficiency of the amines (Table VIII) were improved on increasing the concentration of the alcohol. The chroma-

TABLE IX

INFLUENCE OF THE CONCENTRATION OF 2-PROPANOL ON THE SEPARATION OF ENANTIOMERS WITH SOLID PHASE CBH I-D

Mobile phase: 2-propanol in phosphate buffer, pH 4.8 (I = 0.01). Flow-rate: 1 ml/min.

Solute		Concentration of 2-propanol (*M*)					
		0	0.13	0.26	0.39	0.52	0.78
Warfarin	k'_2	5.36	3.60	2.95	2.56	2.25	1.80
	asf_2	4.5	2.4	2.6	2.3	2.0	n.d.
	α	1.30	1.33	1.32	1.31	1.31	1.28
	f/g	0.94	0.97	0.97	0.97	0.95	0.90
Omeprazole	k'_2	3.77	2.35	1.87	1.62	1.40	1.10
	α	1.09	1.12	1.14	1.14	1.14	1.13
	f/g	0.34	0.56	0.60	0.58	0.52	0.37

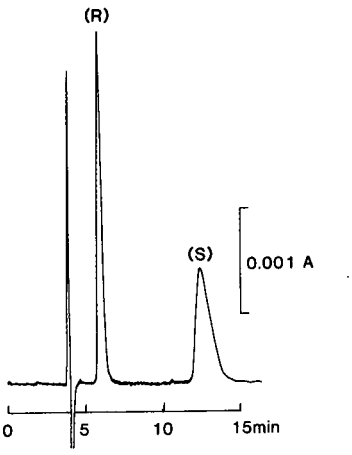

Fig. 6. Separation of (*R,S*)-metoprolol. Solid phase: CBH I-B. Mobile phase: 1.56 *M* 2-propanol in phosphate buffer, pH 6.8 (I = 0.01). Flow-rate: 1 ml/min. Solute concentration: $1.5 \cdot 10^{-4}$ *M*.

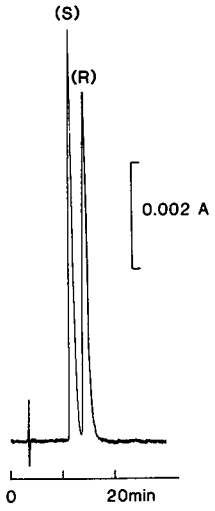

Fig. 8. Separation of (*R,S*)-warfarin. Solid phase: CBH I-C. Mobile phase: 0.26 *M* 2-propanol in phosphate buffer, pH 4.8 (I = 0.01). Flow-rate: 1 ml/min. Solute concentration: $4.6 \cdot 10^{-5}$ *M*.

tographic performance of warfarin and omeprazole (Table IX) was improved by the addition of the organic modifier whereas the enantioselectivity was almost unaffected. This is illustrated by the separation of (*R,S*)-metoprolol, (*R,S*)-prilocaine and (*R,S*)-warfarin in Figs. 6–8. On the α_1-acid glycoprotein column [33,34] the enantioselectivity of solutes generally decreased with increasing concentration of organic solvents in the mobile phase.

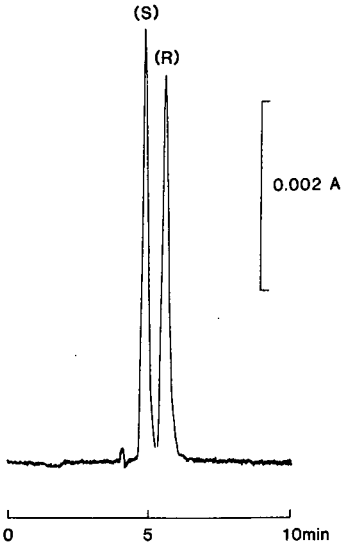

Fig. 7. Separation of (*R,S*)-prilocaine. Solid phase: CBH I-B. Mobile phase: 0.26 *M* 2-propanol in phosphate buffer, pH 6.8 (I = 0.01). Flow-rate: 1 ml/min. Solute concentration: $4.9 \cdot 10^{-5}$ *M*.

Buffer ions and ionic strength. Phosphate buffer (I = 0.01) compared with acetate buffer at pH 4.7 gave a slightly higher stereoselectivity, peak symmetry and resolution (Table X). At pH 4.8, increasing the ionic strength of the phosphate buffer from 0.01

TABLE X

INFLUENCE OF BUFFER IONS ON THE SEPARATION OF ENANTIOMERS

Solid phase: CBH I-D. Mobile phase: buffer, pH 4.7 (I = 0.01). Flow-rate: 1 ml/min. Enantiomer concentration: $2.0 \cdot 10^{-5}$ *M*.

Solute	Parameter	Buffer	
		Acetate	Phosphate
Warfarin	k'_2	5.94	6.11
	asf_2	4.2	4.8
	α	1.26	1.26
	f/g	0.90	0.94
Propranolol	k'_2	4.65	4.81
	asf_2	3.4	3.0
	α	1.37	1.42
	f/g	0.98	1.0

TABLE XI

INFLUENCE OF IONIC STRENGTH ON THE SEPARATION OF ENANTIOMERS

Solid phase: CBH I-D. Mobile phase: phosphate buffer, pH 4.8. Flow-rate: 1 ml/min. Enantiomer concentration: $2.0 \cdot 10^{-5}$ *M*.

Solute	Parameter	Ionic strength	
		0.01	0.1
Warfarin	k'_2	4.92	5.21
	asf_2	4.7	4.5
	α	1.28	1.26
	f/g	0.91	0.91
Propranolol	k'_2	5.69	4.61
	asf_2	4.9	3.4
	α	1.42	1.59
	f/g	0.97	0.97

to 0.1 influenced the retention of the acid and base in different directions but dit not influence the resolution (Table XI). The peak symmetry and the enantioselectivity of the base improved when the ionic strength was increased.

CONCLUSIONS

The enantiomers of β-adrenergic blocking agents were separable with high enantioselectivity on the CBH I-silica phase, *e.g.*, $\alpha = 9.9$ for alprenolol. The observed enantioselectivity factors of β-blocking agents on this phase were higher than those on other similar phases such as α_1-AGP [34] and albumin [35]. The enantiomers of the local anaesthetic prilocaine, the gastric acid inhibitor omeprazole and the anticoagulant warfarin were also separated on this chiral phase.

A CBH I column was used daily for 3.5 months at a flow-rate of 1 ml/min, at different pHs (2–8) and with different concentrations of 2-propanol (0.5–6%) without changes in the enantioselectivity. However, a change in the capacity factors was observed during this period. Further, the column still showed tailing peaks after 3.5 months. Owing to the high enantioselectivity of β-adrenergic blocking agents, the loading capacity for these substances on the CBH I-phase seems to be high. A 60-μg (200-nmol) amount of racemic propranolol was almost completely resolved into the *R* and *S* enantiomers on an analytical column (250 × 5.0 mm I.D.).

The retention and the enantioselectivity of charged analytes were mainly regulated by the pH of the mobile phase. Interestingly, the enantioselectivity of the analytes increased with addition of organic solvents to the mobile phase, although the capacity factors decreased. Increasing the ionic strength from 0.01 to 0.1 improved the enantioselectivity and the peak symmetry and decreased the retention of an amine, whereas the effect on the enantioselective retention of an acid was small.

ACKNOWLEDGEMENTS

VTT, the Technical Research Centre of Finland, is gratefully acknowledged for supplying the culture filtrate from *T. reesei*. This work was supported by grants from the National Swedish Board for Technical Development and the Swedish Natural Science Research Council. Astra Hässle (Mölndal, Sweden) is gratefully acknowledged for the financial support to one of us (I.M.).

REFERENCES

1 K. K. Stewart and R. F. Doherty, *Proc. Natl. Acad. Sci. U.S.A.*, 70 (1973) 2850–2852.
2 S. Allenmark, *J. Liq. Chromatogr.*, 9 (1986) 425–442.
3 E. Domenici, C. Bertucci, P. Salvadori, G. Felix, I. Cahagne, S. Motellier and I. W. Wainer, *Chromatographia*, 29 (1990) 170–176.
4 J. Hermansson, *J. Chromatogr.*, 269 (1983) 71–80.
5 I. W. Wainer, Ph. Jadaud, G. R. Schombaum, S. V. Kadodkar and M. P. Henry, *Chromatographia*, 25 (1988) 903–907.
6 I. Marle and C. Pettersson, poster presented at the *13th International Symposium on Column Liquid Chromatography, Stockholm, June 25–30, 1989.*
7 S. Thelohan, Ph. Jadaud and I. W. Wainer, *Chromatographia*, 28 (1989) 551–555.
8 T. Miwa, M. Ichikawa, M. Tsuno, T. Hattori, T. Miyakawa, M. Kayano and Y. Miyake, *Chem. Pharm. Bull.*, 35 (1987) 682–686.
9 T. Miwa, T. Miyakawa and Y. Miyake, *J. Chromatogr.*, 457 (1988) 227–233.
10 C. Pettersson, T. Arvidsson, A.-L. Karlsson and I. Marle, *J. Pharm. Biomed. Anal.*, 4 (1986) 221–235.
11 P. Erlandsson, I. Marle, L. Hansson, R. Isaksson, C. Pettersson and G. Pettersson, *J. Am. Chem. Soc.*, 112 (1990) 4573–4574.
12 *Kirk–Othmer Encyclopedia of Chemical Technology*, Vol. 5, Wiley, New York, 3rd ed., 1979, pp. 70–86.
13 J. Knowles, P. Lehtovaara and T. Teeri, *TIBTECH*, 5 (1987) 255–261.

14 P. J. Kraulis, G. M. Clore, M. Nilges, T. A. Jones, G. Pettersson, J. Knowles and A. M. Gronenborn, *Biochemistry*, 28 (1989) 7241–7257.
15 J. Rouvinen, T. Bergfors, T. Teeri, J. K. C. Knowles and T. A. Jones, *Science*, (Washington, D.C.), 249 (1990) 380–386.
16 P. M. Abuja, M. Schmuck, I. Pilz, P. Tomme, M. Claeyssens and H. Esterbauer, *Eur. Biophys, J.*, 15 (1988) 339–342.
17 R. Bhikhabhai, G. Johansson and G. Pettersson, *J. Appl. Biochem.*, 6 (1984) 336–345.
18 R. Bhikhabhai and G. Pettersson, *Biochem. J.*, 222 (1984) 729–736.
19 H. Van Tilbeurgh, P. Tomme, M. Claeyssens, R. Bhikhabhai and G. Pettersson, *FEBS Lett.*, 204 (1986) 223–227.
20 S. Shoemaker, V. Schweickart, M. Ladner, D. Gelfand, S. Kwok, K. Myambo and M. Innis, *Bio/Technology*, 1 (1983) 691–696.
21 J.V. Maizel, Jr., in K. Habel and N. P. Salzman (Editors), *Fundamental Techniques in Virology*, Academic Press, New York, 1969, pp. 334-362.
22 P. A. Bristow, P. N. Brittain, C. M. Riley and B. F. Williamson, *J. Chromatogr.*, 131 (1977) 57–64.
23 R. Kaiser, *Chromatographie in der Gasphase, I, Gas-chromatographie*, Bibliographisches Institut, Mannheim, 1960, p. 35.
24 J. Hermansson and G. Schill, in P. R. Brown and R. A. Hartwick (Editors), *High Performance Liquid Chromatography (Chemical Analysis*, Vol. 98), Wiley, New York, 1989, Ch. 8.8.
25 A. Sokolowski and K.-G. Wahlund, *J. Chromatogr.*, 189 (1980) 299–316.
26 J. Hermansson, *J. Chromatogr.*, 298 (1984) 67–78.
27 G. Örn, K. Lahtonen and H. Jalonen, *J. Chromatogr.*, 506 (1990) 627–635.
28 A. C. Moffat, J. V. Jackson, M. S. Moss and B. Widdop (Editors), *Clarke's Isolation and Identification of Drugs*, Pharmaceutical Press, London, 2nd ed., 1986.
29 G. Kortüm, W. Vogel and K. Andrussow (Editors), *IUPAC, Dissociation Constants of Organic Acids in Aqueous Solution*, Butterworths, London, 1961.
30 M. Windholz, S. Budavari, R. F. Blumetti and E. S. Otterbein (Editors), *The Merck Index*, Merck, Rahway, NJ, 10th ed., 1983.
31 A. Brändström, N.-Å. Bergman, I. Grundevik, S. Johansson, L. Tekenbergs-Hjelte and K. Ohlson, *Acta Chem. Scand.*, 43 (1989) 569–576.
32 S. Allenmark, in A. M. Krstulovic (Editor), *Chiral Separations by HPLC*, Ellis Horwood, Chichester, 1989, Ch. 11.
33 M. Enquist and J. Hermansson, *J. Chromatogr.*, 519 (1990) 271–283.
34 M. Enquist and J. Hermansson, *J. Chromatogr.*, 519 (1990) 285–298.
35 E. Küsters and D. Giron, *J. High Resolut. Chromatogr. Chromatogr. Commun.*, 9 (1986) 531–533.

Journal of Chromatography, 586 (1991) 249–254
Elsevier Science Publishers B.V., Amsterdam

CHROM. 23 605

Chiroptical detection during liquid chromatography

III☆. Non-stop acquisition of circular dichroism spectra during liquid chromatography☆☆

Gert Brandl, Fritz Kastner and Albrecht Mannschreck*

Institute of Organic Chemistry, University of Regensburg, W-8400 Regensburg (Germany)

Bengt Nölting

Central Institute of Molecular Biology, O-1115 Berlin-Buch (Germany)

Karl Andert

Central Institute of Cardiovascular Research, O-1155 Berlin-Buch (Germany)

Rolf Wetzel*

Central Institute of Molecular Biology, O-1115 Berlin-Buch (Germany)

(First received March 27th, 1991; revised manuscript received July 4th, 1991)

ABSTRACT

A new type of spectrometer, built in-house, served as a circular dichroism detector for liquid chromatography. It acquired differential absorbances $\Delta A = f(\lambda)$ at all wavelengths, λ, between 208 and 268 nm simultaneously within a time interval of 9 s. Non-stop acquisition of circular dichroism spectra during liquid chromatography is described for the first time. The novel set-up gives automatic access to dichrograms without preparative enrichment of enantiomers, if some analytical separation on an optically active sorbent can be achieved. Like photodiode-array detection, the new technique collects ultraviolet spectra $A = f(\lambda)$, but furnishes positive/negative information $\Delta A = f(\lambda)$ in addition. It was applied to (±)-2,2′-spirobi[2*H*-chromene] as a test sample and microcrystalline tribenzoylcellulose as a sorbent. Future applications of non-stop liquid chromatographic circular dichroic–ultraviolet data are discussed.

INTRODUCTION

Circular dichroism (CD) detection during liquid chromatography (LC) at a fixed wavelength has been performed successfully in the past by several groups [1–6], its advantages [7] compared with polarimetry being the increased selectivity and the possibility of determining absolute molecular chirality. Recording of CD spectra during stoppages [1,8–10] of chromatographic flow represented a considerable progresss, since this procedure gives access to dichrograms without preparative enrichment of enantiomers. On the other hand, CD spectra provide the most important information for the charac-

☆ For Part II see ref. 23.

☆☆ Dedicated to Professor Heinz A. Staab on the occasion of his 65th birthday.

0021-9673/91/$03.50

terization and the structural investigation of chiral molecules.

However, stoppages of eluent flow, besides requiring the attention and activity of the experimenter, generate errors in the apparent retentions of the substrates because the LC pump has to be stopped and restarted. Therefore, an automatic procedure avoiding any stoppage would be very useful for the analysis of LC peaks and for the acquisition of unknown CD spectra. Such a procedure is well known for UV detection: the use of photodiode-array technology [11]. To our knowledge, no technique for non-stop recording of CD spectra during LC has yet been described.

This technique was made possible by a novel spectrometer [12–14] which allows the simultaneous measurement of CD and UV absorptions at all wavelengths within a limited spectral range. In this apparatus, a polychromator and a charge-coupled device serving as a multichannel sensor are arranged behind the flow cell, in contrast to commercial circular dichrographs in which a monochromator is located in front of the cell and a photomultiplier behind it.

EXPERIMENTAL

Microcrystalline tribenzoylcellulose [15,16] (particle sizes 10–15 μm) from Riedel-de Haën (Seelze, Germany) was packed into a Knauer steel column (250 × 8 mm I.D.) using methanol as an eluent at *ca.* 170 bar and a flow-rate of 6 ml/min according to ref. 15. For LC work, the IRICA Σ - 871 pump (Irica Instruments, Kyoto, Japan) produced a pressure of 17 bar at a flow-rate of 0.7 ml/min. Rheodyne 7125 served as an injector and ERC 7210 (ERMA Optical Works, Tokyo, Japan) as a photometric detector at 254 nm. The latter allowed the quality of the separation to be checked and the capacity factors, k', to be determined. The k' values are given relative to 1,3,5-trihydroxybenzene [16] ($k' = 0$).

Following the photometer, a novel spectrometer [12–14] built in-house was connected as a CD and UV detector. A polychromator (holographic concave grating) and a charge-coupled device (L172D; VEB Werk für Fernsehelektronik, Berlin, Germany) were located behind the flow cell of this spectrometer. A schematic set-up is presented in Fig. 1. The home-made cell had a cylindrical form of 1.5

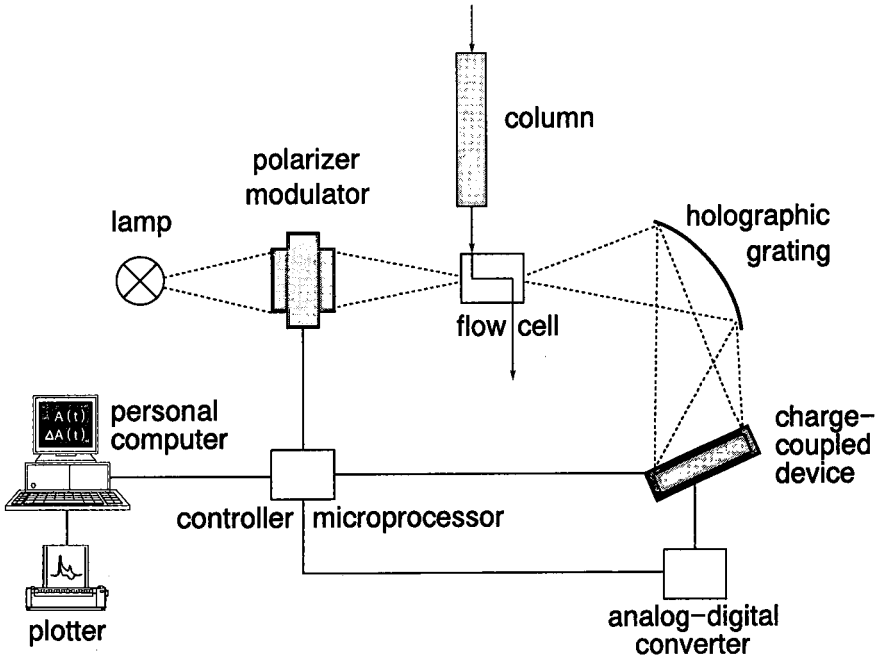

Fig. 1. Schematic set-up for non-stop aquisition of LC–CD–UV data.

mm diameter and 5.8 mm length (light path), resulting in a volume of 10 μl. It was located closely behind the entrance slit of the polychromator. The flow within the cell was in the direction of the light beam. A more detailed description of the whole spectrometer and its operation is given elsewhere [14]. The acquisition time for one spectrum was 9 s, the spectral bandwith being approximately 3 nm. The acquisition time was a consequence of using the available charge-coupled device (see above) and computer (see below). We assume that replacing these items with more efficient ones will reduce the acquisition time to *1 s or less* without significant loss of sensitivity. These modifications should allow application of the detector to more rapid separations. Systematic errors were avoided because there was no time shift between the measurement of CD and UV absorptions and the measurements at different wavelengths within a limited spectral range. The calibration of differential absorbance, ΔA, was performed using the Cotton effect [14] at 220 nm of a solution of D-pantolactone in water (0.165 g/l) in a static cell with a 1.0-mm light path. CAMAC hardware and a Robotron A 7100 personal computer served for instrumental control and data processing, respectively, using specialized programs.

(±)-2,2′-Spirobi[2*H*-chromene] (**1**) was prepared according to ref. 17. Its chromatograms, $A = f(t)$ and $\Delta A = f(t)$ (for example, see Fig. 3), correspond to our earlier results [18]. The UV spectrum $A = f(\lambda)$ (for example, see Fig. 4) is in agreement with the literature [19]. The circular dichrogram $\Delta A = f(\lambda)$ (*e.g.* Fig. 4) corresponds to our spectrum $\Delta\varepsilon = f(\lambda)$, obtained [20] for (+)−**1** [18] (enantiomeric purity $P = 94\%$) at 20°C in methanol and calculated for $P = 100\%$: + 69 (212), −44 (225), +52 (258), +11 l mol^{-1} cm^{-1} (300 nm).

The amount of 0.05 mg of (±) −**1** in 0.05 ml of methanol was chosen to give an absorbance of less than $A = 0.8$ for the peak maximum at $k' = 3.4$ in the measured spectral range. This limit was a consequence of the dataprocessing program mentioned above.

Although some information about signal-to-noise ratios achieved with this detector in its present state is available [14], final experiments concerning the noise level and the limit of detection of the new dichrograph have not yet been performed. Therefore, the experiment reported in Figs. 2–5 does not indicate a limitation of the utility. A preliminary measurement indicates that values of $\Delta A \approx 10^{-4}$ can still be detected above noise.

The experimental data were externally processed and plotted by means of an Acer 910 personal computer and specialized programs [21].

RESULTS

Stopped-flow measurements were performed with several racemates, including (±)-2,2′-bis(methoxycarbonyl)-1,1′-binaphthyl, using the set-up described above. Of these, (±)-spirobi[2*H*-chromene] (**1**) (for formula, see Fig. 2) was the most successful because of its high $\Delta\varepsilon$ values [20] (see Experimental section) and the excellent separation [18] of its enantiomers on microcrystalline tribenzoylcellulose [15,16] as an optically active sorbent. Therefore, (±)-**1** was chosen for non-stop acquisition of spectra during LC. This spirochromene and its enantiomers [18] are of interest in connection with thermal racemization [18] and photochromism [17].

On the other hand, under these conditions the peaks of (+)- and (−)-**1** are relatively broad because of partial racemization [18] during chromatography and because of the particular kinetic properties of the sorbent. Further investigations must include examples with sharper peaks.

The LC–CD data for (±)-**1** (Fig. 2) were obtained by recording dichrograms $\Delta A = f(\lambda)$ at certain retention times t ($t = 0$ upon injection). During the acquisition time of 9 s, the differential absorbance ΔA was recorded at all wavelengths between 208 and 268 nm simultaneously. The dichrograph used measured ΔA values within a λ-window of 76 nm, but the region of low wavelength was lost in the present case because of the UV absorption of methanol serving as an eluent. A visual overview and quantitative evaluation of three-dimensional plots such as in Fig. 2 is not easy. Therefore, we have prepared cross-sections of these data, two of which are presented as a CD-detected chromatogram $\Delta A = f(t)$ of (±)-**1** (Fig. 3, solid line) and as a circular dichrogram $\Delta A = f(\lambda)$ of (±)-**1** (Fig. 4, solid line).

The solid line in Fig. 4 corresponds to (+)-**1**, *i.e.* the enantiomer with positive polarimetric rotation angles [18,20] between 365 and 578 nm. This assignment follows from the CD spectrum $\Delta\varepsilon = f(\lambda)$ given

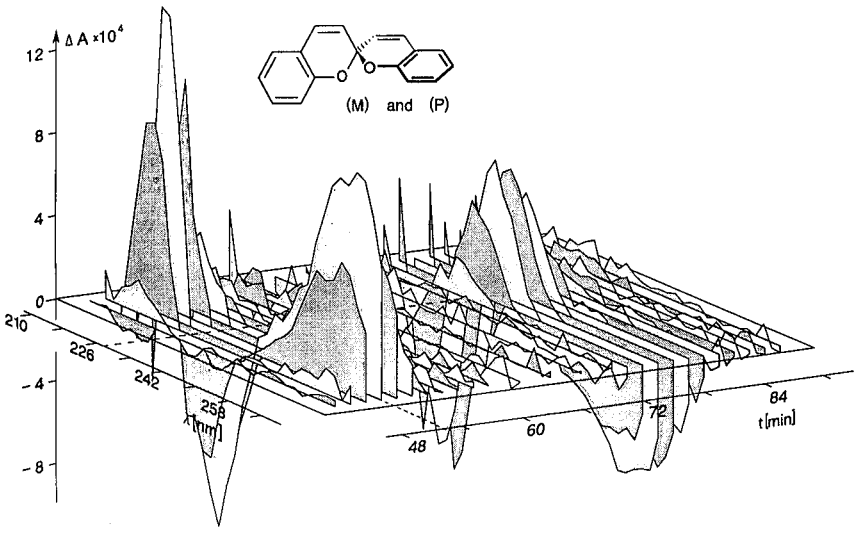

Fig. 2. Non-stop acquisition of circular dichroism (CD) spectra during LC of 0.05 mg of (±)-**1** in methanol on microcrystalline tribenzoylcellulose. Flow-rate 0.7 ml/min, linear velocity 0.35 mm/s, retention time t (t = 0 upon injection), wavelength λ, differential absorbance ΔA. The peaks of the enantiomers at t = 52 and 80 min correspond to the capacity factors k' = 3.4 and 5.7, respectively. The absorptions at λ = 208 nm are due to a Cotton effect around λ = 200 nm. The CD spectra shown for certain times (differing by 1.5 or by 3.0 min) were acquired during time intervals of 9 s each. ----- = Cross-sections used for Figs. 3 and 4.

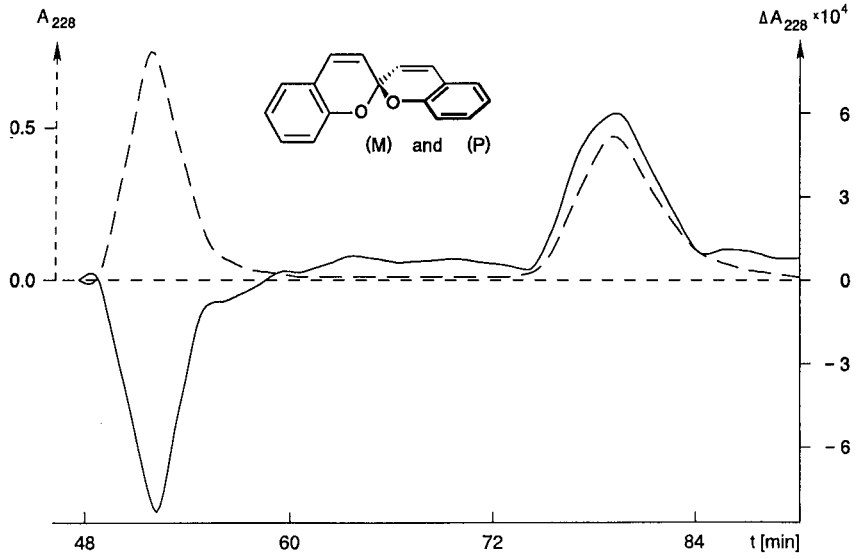

Fig. 3. LC of (±)-**1** on microcrystalline tribenzoylcellulose. The peaks of the enantiomers correspond to the capacity factors k' = 3.4 and 5.7. See Fig. 2 for further experimental details. ——— = Circular dichroism detection ΔA = f(t), obtained as a cross-section at λ = 228 nm of the data ΔA = f(λ,t) in Fig. 2. ----- = UV detection A = f(t), obtained as a cross-section at λ = 228 nm of the data A = f(λ,t) in Fig. 5.

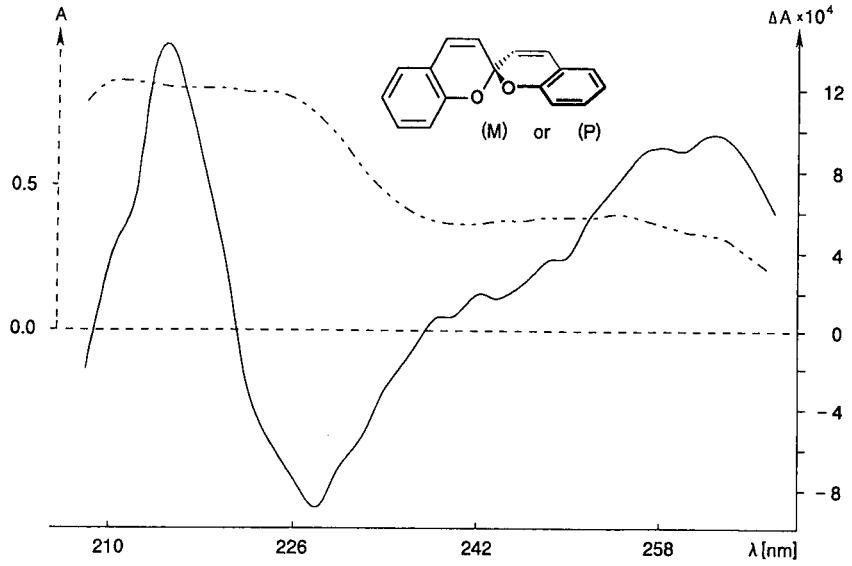

Fig 4. Circular dichroism (CD) and UV spectra of (+)-**1**, recorded during LC of (±)-**1** on microcrystalline tribenzoylcellulose. See text for notation of the enantiomer (+)-**1**; see Fig. 2 for further experimental details. ———— = CD spectrum $\Delta A = f(\lambda)$, obtained as a cross-section at $t = 52$ min of the data $\Delta A = f(\lambda,t)$ in Fig. 2. ----- = UV spectrum $A = f(\lambda)$, obtained as a cross-section at $t = 52$ min of the data $A = f(\lambda,t)$ in Fig. 5.

for preparatively enriched (+)-**1** in the Experimental section. It should be noted that the absolute chiralities [22] (M) and (P) of the enantiomers of **1** are not known (see formula in Fig. 4).

The computer dedicated to the circular dichrograph is also capable [14] of calculating and storing the absorbance A and the ratios $\Delta A/A$ immediately after the measurement of ΔA. The LC–UV data for (±)-**1** (Fig. 5) were obtained in this way. They correspond to the results which would be obtained by a photodiode-array detector [11]. Two cross-sections of these data are presented as a UV-detected chromatogram $A = f(t)$ (Fig. 3, dotted line) and as a UV spectrum $A = f(\lambda)$ (Fig. 4, dotted line).

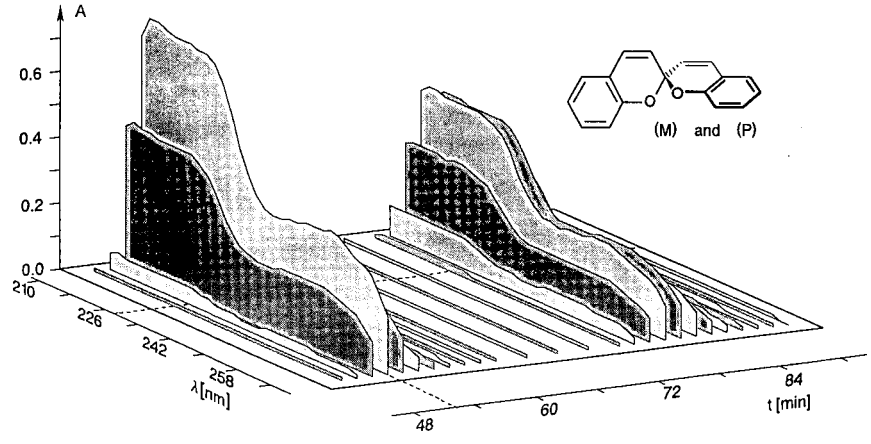

Fig. 5. Non-stop acquisition of UV spectra during LC of (±)-**1** on microcrystalline tribenzoylcellulose. The UV spectra shown for certain times (differing by 1.5 or by 3.0 min) were acquired during time intervals of 9 s each. See Fig. 2 for further experimental details. ----- = Cross-sections used for Figs. 3 and 4.

Similar measurements were successfully performed for (±)-2,2′-bis(methoxycarbonyl)-1,1′-binaphthyl.

DISCUSSION

Non-stop acquisition of LC–CD–UV data has been described above for the first time. It gives automatic access to dichrograms without preparative enrichment of the components of a mixture, provided an LC sorbent accomplishes some analytical separation.

As far as (±)-**1** is concerned, all the information in Figs. 2–5 was known in advance (see Experimental section), which was the reason for choosing it as a test sample. The sensitivity of the dichrograph remains to be demonstrated for compounds which are less ideal than (±)-**1** and for mixtures of compounds.

There are many examples for which the new technique will yield data and conclusions not easily obtainable by other methods. In chemistry, it will be useful for the stereodynamic investigation of enantiomers which cannot be separated because intramolecular processes [1] interconvert them. We have also encountered racemates whose components would have to be enriched on an analytical column by many time-consuming injections because the corresponding preparative column is too expensive. In these cases, the unknown dichrograms can now be measured without preparative enrichment of the enantiomers.

On the other hand, the above technique can also serve for the CD and UV analysis of LC peaks as a means of checking their identity and purity. This is a frequent task [11] in pharmacy, biology and medicine, where chiral drugs and their metabolites and chiral biomolecules or mixtures containing them have to be investigated.

ACKNOWLEDGEMENTS

R. Allmeier Dipl.-Chem. wrote most of the computer programs needed for the external evaluation of data. B. Stephan Dipl.-Chem. prepared and characterized compounds (±)- and (+)-**1**. Preliminary arrangements for the present work were done together with Dr. A. Lebek and R. Korzendorfer. We are grateful to Ing. R. Pittelkow for technical assistance. Support from the Fonds der Chemischen Industrie (Frankfurt, Germany) and from Deutscher Akademischer Austauschdienst (Bonn, Germany) is gratefully acknowledged. The referees kindly drew our attention to some details which were missing in the original manuscript.

REFERENCES

1 A. Mannschreck, D. Andert, A. Eiglsperger, E. Gmahl and H. Buchner, *Chromatographia*, 25 (1988) 182, and references cited therein.
2 A. F. Drake, J. M. Gould and S. F. Mason, *J. Chromatogr.*, 202 (1980) 239.
3 C. Bertucci, E. Domenici, G. Uccello-Barretta and P. Salvadori, *J. Chromatogr.*, 506 (1990), 617, and references cited therein.
4 R. E. Synovec and E. S. Yeung, *J. Chromatogr.*, 368 (1986) 85, and references cited therein.
5 A. F. Drake and G. D. Jonas, *Chromatogr. Anal.*, February (1989) 11.
6 M. Xu and C. D. Tran, *Anal. Chem.*, 62 (1990) 2467.
7 D. K. Lloyd and D. M. Goodall, *Chirality*, 1 (1989) 251.
8 S. A. Westwood, D. E. Games and L. Sheen, *J. Chromatogr.*, 204 (1981) 103.
9 T. Takakuwa, Y. Kurosu, N. Sakayanagi, F. Kaneuchi, N. Takeuchi, A. Wada and M. Senda, *J. Liq. Chromatogr.*, 10 (1987) 2759; Y. Kurosu, T. Sasaki, T. Takakuwa, N. Sakayanagi, K. Hibi and M. Senda, *J. Chromatogr.*, 515 (1990) 407.
10 C. Bertucci, C. Rosini, D. Pini and P. Salvadori in H. Frank, B. Holmstedt and B. Testa (Editors), *Chirality and Biological Activity*, Alan B. Liss, Hitchin, 1990, p. 71.
11 A. F. Fell and B. J. Clark, *Eur. Chromatogr. News*, 1 (1987) 16, and references cited therein.
12 R. Wetzel, U. Plauschin, R. Pittelkow, D. Obst and A. Lebek, *German Pat.*, 216 099 A1 (1983).
13 R. Wetzel, *Optik*, 78 (1987) 43.
14 K. Andert, W. Schälike, B. Nölting, R. Pittelkow, R. Wetzel and G. Snatzke, *Rev. Sci. Instr.*, 62 (1991) 1912; B. Nölting, *Thesis*, in preparation.
15 K.-H. Rimböck, F. Kastner and A. Mannschreck, *J. Chromatogr.*, 351 (1986) 346.
16 A. Mannschreck and R. Wernicke, *Labor-Praxis*, 14 (1990) 730; *C.A.*, 113 (1990) 218 852.
17 E. D. Bergmann, A. Weizmann and E. Fischer, *J. Am. Chem. Soc.*, 72 (1950) 5009.
18 B. Stephan, H. Zinner, F. Kastner and A. Mannschreck, *Chimia*, 44 (1990) 336.
19 P. Appriou, C. Tredaul, J. Brelivet, F. Garnier and R. Guglielmetti, *Bull. Soc. Chim. Fr.*, (1976) 2039.
20 A. Mannschreck and B. Stephan, Regensburg, unpublished result.
21 R. Allmeier and H. Zinner, Regensburg, unpublished computer programs.
22 International Union of Pure and Applied Chemistry, *Pure Appl. Chem.*, 45 (1976) 13.
23 A. Mannschreck and L. Kießl, *Chromatographia*, 28 (1989) 263.

Journal of Chromatography, 586 (1991) 255–258
Elsevier Science Publishers B.V., Amsterdam

CHROM. 23 617

Configuration analysis of unsaturated hydroxy fatty acids

Philip E. Sonnet*, Robert L. Dudley, Stanley Osman, Philip E. Pfeffer and Daniel Schwartz

US Department of Agriculture, ARS, Eastern Regional Research Center, 600 E. Mermaid Lane, Philadelphia, PA 19118 (USA)

(Received June 4th, 1991)

ABSTRACT

Stereoisomers of methyl ricinoleate, methyl isoricinoleate, and related methyl esters of bis-homoallylic hydroxy fatty acids were reacted with (*R*)- and (*S*)-α-naphthylethyl isocyanate to form diastereomeric carbamates that separated well on silica gel high-performance liquid chromatography. Proton nuclear magnetic resonance shifts of the carbomethoxymethyl protons were used to assign configuration to the alcohol component of the carbamate derivative. Combining high-performance liquid chromatography with proton nuclear magnetic resonance spectroscopy may allow one to determine the configuration of naturally occurring hydroxy fatty acids as well as to determine configurational purity.

INTRODUCTION

Separations of selected chiral hydroxy fatty acids and esters by gas–liquid chromatography (GC) and high-performance liquid chromatography (HPLC) has been summarized recently [1]. In particular, α-hydroxy acids, and less frequently β-hydroxy acids, have been resolved using chiral stationary phases or by derivatization with a common chiral derivatizing agent (CDA) to afford separable diastereomers. In addition, chiral allylic [2,3] and propargylic alcohols [4] can be distinguished by conversion to esters of (*R*)- or (*S*)-α-methoxytrifluoromethylphenylacetic acid and observing the shifts of the methoxyl protons.

Ricinoleic acid, (*R*)-12-hydroxy-(*Z*)-9-octadecenoic acid, and isoricinoleic acid, (*S*)-9-hydroxy-(*Z*)-12-octadecenoic acid, are industrially important natural products [5] whose syntheses and stereochemistry have been reviewed [6]. We are unaware of a simple method by which to distinguish or separate enantiomers of such homoallylic and bis-homoallylic structures. We report here that diastereomeric carbamates of the methyl esters of these alcohols formed from (*R*)- or (*S*)-α-naphthylethyl-isocyanate (NEI) as the CDA are cleanly separated by HPLC with a silica gel column. Moreover, the ^{1}H NMR shifts of CH_3O_2C–can be employed to characterize the alcohol's configuration.

EXPERIMENTAL[☆]

GC was performed with a Supelcowax column (30 m × 0.25 mm I.D.) using a Chrompack-Packard Model 438A chromatograph operating with helium carrier gas at 18 cm/s and a 50:1 split ratio (the subject diastereomers were not resolved with this column). HPLC was performed using a Spectra-Physics SP8800 pump, SP8480 XR scanning UV detector and SP4290 integrating recorder with a silica gel column (15 cm × 0.25 in.) from Supelco. Infrared spectra were recorded with a Perkin-Elmer 1310 spectrophotometer using 3% solutions in carbon tetrachloride. Mass spectra were obtained with a Hewlett-Packard HP-5995 GC–mass spectrometry (MS) system using the direct probe. ^{1}H NMR spectra were obtained with a JEOL JNM-GX 400 Fourier transform (FT) NMR spectrometer with [2]

☆ Mention of brand or firm names does not constitute an endorsement by the US Department of Agriculture over others of a similar nature not mentioned.

chloroform as the solvent and tetramethylsilane as internal standard. The solvents employed were HPLC-grade, and the tetrahydrofuran was dried initially over KOH and then distilled from lithium aluminum hydride with storage in a stoppered bottle containing molecular sieve 4A. Thin-layer chromatography (TLC) was performed with standard analytical plates of silica gel from Analtech. Silica gel (60–200 mesh) for open column chromatography was purchased from Baker.

D-Methyl ricinoleate that was >98% pure by GC, was a generous gift of Dr. Robert Benedict of this laboratory, and D-methyl isoricinoleate was islated from the seeds of *Holarrhena antidysenterica* (NU-46607), a gift of Dr. Robert Kleiman of the Northern Regional Research Center, Peoria, IL, USA, using essentially the procedure described previously [7] to obtain GC-pure material. The other bis-homoallylic hydroxy fatty acids described herein were prepared in conjunction with other research, and their syntheses will be described elsewhere. Each hydroxylated fatty acid, natural and synthetic, was employed as its methyl ester (>98% GC-pure) and had spectral characteristics (IR, ^{1}H NMR, ^{13}C NMR, and MS) consistant with its structure. (*R*)- and (*S*)-α-NEI that was 98% pure by label was purchased from Aldrich.

Synthesis of diastereomeric carbamate derivatives

The general procedure was to place 100 μl each of the (*R*)- or (*S*)-α-NEI and the unsaturated hydroxy fatty acid methyl ester in 1 ml of toluene. This was heated at 90–95°C under nitrogen for 1 h. The mixture was concentrated on a flash evaporator and then placed on top of a column of 60–200-mesh silica gel (1 g) in a disposable pipet. Portions of 10 ml of hexane–chloroform mixtures were used to chromatograph the crude product, and the elution was monitored by TLC. Unreacted isocyanate eluted first; the carbamates eluted with 20–30% chloroform. For example, in this manner was obtained the adduct of racemic methyl 9-hydroxy-(*Z*)-(12)-octadecenoate a colorless oil that solidified on standing: IR 3460, 3010, 1740, 1715 cm^{-1}, ^{1}H NMR δ 7.4-8.2 (m, 7H, naphthyl H), 5.65 (m, 1H, NHC*H*CH$_3$), 5.4 (m, 2H, RCH=CHR'), 5.1 (m, 1H, HCO), 3.65 (*R,R*) and 3.66 (*R,S*) (2s, 3H, CH_3O_2C–), 2.30 (m, 2H, $CH_2C=O$), 2.03 (m, 2H, $CH_2C=C$), 1.63 (d, J = 6.2 Hz, *ca.* 3H, CH_3CH), 1.5 (m, *ca.* 2H, $CH_2CH_2C=O$), 1.2 [CH_5 envelope (env.)], 0.85 [broad triplet (bt), 3H, CH_3CH_2] ppm; MS *m/e* (relative abundance) 509 [M]$^+$ (0.07), 294 (0.65), 215 (0.71), 214 (0.30), 200 (0.68), 182 (0.29), 155 (1.00). HPLC data are presented in Table I. The other carbamate derivatives gave analogous data.

RESULTS AND DISCUSSION

Racemic methyl isoricinoleate (**1**, Fig. 1), was synthesized by us in connection with another project [8], and was converted to a mixture of diastereomeric carbamates by reaction with (*S*)-α-NEI.

TABLE I

CHROMATOGRAPHIC DATA FOR α-NAPHTHYLETHYLCARBAMATES[a]

Alcohol	k' values	α	^{1}H NMR shifts (ppm) for $-CO_2CH_3$		
			HPLC-1[b]	HPLC-2[b]	$\Delta\delta(2-1)$
1	5.07, 5.95	1.17	3.654(*R*,R**)	3.665(*R*,S**)[c]	0.011
2	6.54, 7.80	1.19	3.639(*R*,R**)	3.650(*R*,S**)[d]	0.011
3	3.73, 4.85	1.30	3.665(*R*,R**)	3.660(*R*,S**)[c]	−0.005
4	5.10, 5.76	1.13	3.656(*R*,S**)	3.623(*R*,R**)[d]	−0.034
5	4.73, 5.08	1.07	3.637(*R*,S**)	3.625(*R*,R**)[d]	−0.012

[a] Silica gel analytical column using hexane–ethyl acetate–tetrahydrofuran (95:5:1). Stereochemical designators are for relative configuration. Note that the designator for the alcohol component of 1 and 2 is opposite from that of 3–5. k' = Capacity factor; α = separaton factor.

[b] HPLC-1 and -2 refer to elution order.

[c] Stereochemistry known (natural product).

[d] Stereochemistry inferred from relative ^{1}H NMR shifts of $-CO_2CH_3$ signals.

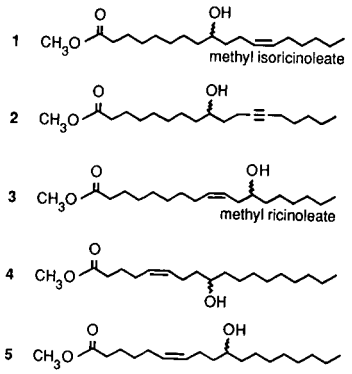

Fig. 1. Structures of alcohols the α-NEI derivatives of which are discussed. The racemic structures are indicated.

These were cleanly separated by a silica gel HPLC column (Fig. 2). The elution order of the diastereomers (Table I) was determined using a sample of isoricinoleic acid of known configuration that we had obtained by isolation from seeds of *Holarrhena antidysenterica* [7]. A synthetic precursor to the racemic acid, the corresponding acetylenic structure **2**, similarly provided chromatographically separated diastereomers. The elution order for **2** was judged to be the same as for **1** since the ^{1}H NMR singlets for $-CO_2CH_3$ of the diastereomers bore the same relationship for **2** as for **1**, namely the methyl singlet was shifted upfield by 0.01 ppm in the earlier eluting diastereomer in both cases.

D-Methyl ricinoleate (**3**) a commercially available natural product with (*R*)-configuration was converted to the analogous derivatives using each enantiomer of α-NEI. Again chromatographic separation was excellent (Fig. 3) though the shift difference for the $-CO_2CH_3$ was much smaller. For both ricinoleate and isoricinoleate structures the *R*R** diastereomer (the asterisk denotes relative configuration of the two asymmetric centers of the derivative) elutes first. We also derivatized samples of methyl 9-hydroxy-(*Z*)-5-octadecenoate (**4**) and methyl 10-hydroxy-(*Z*)-6-octadecenoate (**5**). These compounds (racemic) were available from related work and are bishomoallylic alcohols like methyl isoricinoleate. The relevant diastereomers were again resolved by silica gel HPLC (Table I).

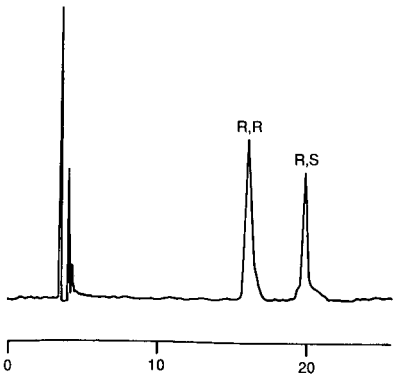

Fig. 2. Chromatogram of carbamates obtained from *rac.*-methyl isoricinoleate (**1**) and (*S*)-α-NEI using silica gel, 1.0 ml/min, hexane–ethyl acetate–tetrahydrofuran (95:5:1).

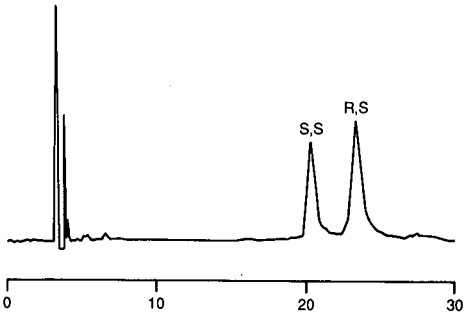

Fig. 3. Chromatogram of carbamates obtained from D-methyl ricinoleate, (*R*)-**3** and (*R*)- and (*S*)-α-NEI using silica gel, 1.0 ml/min, hexane–ethyl acetate–tetrahydrofuran (95:5:1).

The principal solution conformation of diastereomeric carbamates of type **6** (Fig. 4) is such as to place the substituents R_1 and R_2 of the chiral alcohol on either side of a central plane defined by the carbamate structure and its attached asymmetric centers [9]. In **6A** R_1 will on average experience more of the diamagnetic anisotropy associated with the large 1-naphthyl group and conversely for **6B** in which R_2 is placed in that situation. Although the $-OCH_3$ is remote from the aryl ring (9 bonds from the asymmetric carbon of methyl isoricinoleate, for example), shift differences of 0.01–0.04 ppm were observed for these singlets. Similar shift differences of remotely situated protons in diastereomeric

Fig. 4. Principal solution confirmation of simple diastereomeric carbamates [9]; Np = 1-Naphthyl.

amides have been noted and used to make configurational assignments [10]. For compounds **1** and **3**, assignments of configuration of the alcohol components by ^1H NMR was not necessary since the (configurationally pure) natural products were available and could be derivatized directly for HPLC comparison. However, we noted that such an assignment was indeed consistent with that predicted from the ^1H NMR spectra of the derivatives.

The shift differences for **3**, **4** and **5** were determined in C^2HCL_3 solutions of mixtures of the diastereomers biased by appropriate HPLC collections to allow the signal assignment to be related to elution pattern. Assignment of stereochemistry based on ^1H NMR of a single diastereomer would be doubtful because of the small shift differences. Nevertheless, since the major solution conformation of such compounds would not be expected to deviate from that of secondary alcohols not bearing a terminal carbomethoxy group (Fig. 4), we were able to make assignment of stereostructure using NMR having both diastereomers on hand. For an unknown hydroxy fatty acid, therefore, one would prepare the carbamates from each of the enantiomeric CDAs and determine configuration by ^1H NMR. The configurational purity, however, could be determined better by HPLC.

No simple relationship seems to exist for the observed elution orders and the structures of the major solution conformers. The elution orders are reversed from that of, for example, methyl isoricinoleate adducts when the unsaturation is inserted between the carbamate and carbomethoxy groups as in **4** and **5**. This probably is a reflection of the multiplicity of adsorption sites available in these compounds; both the ester and carbamate groups can become associated with the stationary phase. Nevertheless, judging from these observations, one may expect to separate and characterize the α-naphthylethylcarbamates of both homo- and bis-homoallylic hydroxy fatty acids.

ACKNOWLEDGEMENTS

We thank Dr. R. Benedict of the Eastern Regional Research Center and Dr. Robert Kleiman of the National Center for Agricultural Utilization Research for generous samples of D-methyl isoricinoleate and seeds of *Holarrhena antidysenterica* (Apocynaceae).

REFERENCES

1 R. W. Souter, in *Chromatographic Separation of Stereoisomers*, CRC Press, Boca Raton, FL, 3rd Printing 1987, Ch. 2 and 3.
2 P. A. Cornelis, O. S. Van, M. Vente and J. F. G. Vliegenhart, *Biochim. Biophys. Acta*, 574 (1979) 103.
3 T. Oritani and K. Yamashita, *Agric. Biol. Chem.*, 44 (1980) 2407.
4 K. Mori and H. Akao, *Tetrahedron Lett.*, (1978) 4127.
5 J. W. Hagemann and J. A. Rothfus, *J. Am. Oil Chem. Soc.*, 68 (1991) 139.
6 C. R. Smith, Jr., in F. D. Gunstone (Editor), *Topics in Lipid Chemistry*, Vol. 1, Logo Press, London, 1970, pp. 320–323.
7 R. G. Powell, R. Kleiman, and C. R. Smith, Jr., *Lipids*, 4 (1969) 450.
8 D. Schwartz *et al.*, in preparation.
9 W. H. Pirkle and J. R. Hauske, *J. Org. Chem.*, 42 (1977) 1839.
10 P. E. Sonnet, J. A. Gazzillo, R. L. Dudley and R. T. Boswell, *Chem. Phys. Lipids*, 54 (1990) 205.

Journal of Chromatography, 586 (1991) 259–263
Elsevier Science Publishers B.V., Amsterdam

CHROM. 23 608

Chromatographic separation of mixed peptides from amino acids in biological digests with volatile buffers

Ian P. Armstead and John R. Ling*

Department of Biochemistry, The University College of Wales, Aberystwyth SY23 3DD, Wales (UK)

(First received April 2nd, 1991; revised manuscript received June 26th, 1991)

ABSTRACT

Two chromatographic methods, capable of separating mixed peptides from contaminating amino acids in biological digests, are described. Both methods involve separation on copper–Chelex resin, but each uses a different set of elution buffers. When separation method 1 was applied to a commercially available proteolytic digest of casein, the free amino acid content was reduced from 26.0% to 0.5%. With an enzymic digest of ^{14}C-labelled proteins derived from plant biomass, separation method 2 decreased the contaminating free amino acids from 20.3% to 1.9%. Since the separated peptides are eluted with volatile buffers, they are suitable as substrates for biological experiments.

INTRODUCTION

More and more research is being conducted into the metabolism of peptides across a wide range of biological systems. Such experimentation, especially that of a biochemical or nutritional nature, often requires procedures for the separation of complex mixtures of peptides either from their precursors, or from their catabolic products namely, amino acids. Several such chromatographic procedures exist, but they all possess disadvantages. Some, such as high-performance liquid chromatography (HPLC) [1], require elaborate and expensive laboratory equipment and are typically used to separate a limited number of peptides, often only one [2]. Similarly, flash chromatography, though relatively cheap [3], is mostly used to purify single peptides and indeed its ability to resolve complex mixtures of similar compounds has been questioned [4]. Most earlier separation procedures were based on the chelating properties of copper–Sephadex or copper–Chelex. Some of these concentrated on the separation of the amino acid fraction [5] and while others were capable of separating mixed peptides, the latter were always eluted in solutions and conditions, such as sodium tetraborate and at pH 11, that were quite unsuitable for use in biological experiments [5–7].

The aim of the present work was to prepare purified fractions of mixed peptides from protein digests using volatile solvents. The two methods reported here involve separations on columns of copper–Chelex resin, but each uses a different set of elution buffers. These methods were developed to separate peptidyl fractions from a commercially available proteolytic digest of casein (separation method 1) and also from an enzymic digest of ^{14}C-labelled proteins derived from plant biomass (separation method 2). Since the separated peptides are eluted with volatile buffers, they are suitable for subsequent biological applications, such as those of Cooper and Ling [8].

EXPERIMENTAL

Sources of peptides and amino acids

Two sources of mixed peptides and amino acids were used. One was a commercially available pancreatic digest of casein (Tryptone; Oxoid, London). The other was a ^{14}C-labelled mixture prepared by extracting water-soluble proteins from barley (*Hor-*

0021-9673/91/$03.50

deum vulgare cv. Kym or Gerbel) grown in a $^{14}CO_2$ atmosphere and digesting them with proteolytic enzymes based on the method of Cooper and Ling [8].

Preparation of copper–Chelex resin

Chelex 100 resin (50–100 mesh, sodium form; Bio-Rad, Richmond, CA, USA) was first washed with 1 *M* hydrochloric acid and then added to 0.16 *M* cupric sulphate solution; the mixture was adjusted to pH 2.5 with 5 *M* sodium hydroxide and stirred for 16 h. For use with the casein digest (separation method 1), the resultant copper–Chelex resin was washed with distilled water until the supernatant was colourless and then it was adjusted to pH 9.5 with 20 *M* ammonia solution. For the separation of the ^{14}C-labelled mixture (separation method 2), the copper–Chelex resin was washed with 0.1 *M* acetic acid until the eluent was colourless.

Separation of mixed peptides from amino acids

For method 1, a column of copper–Chelex resin (190 mm × 25 mm I.D.) was packed and washed with 100 ml 1 m*M* ammonia solution. Samples (50 mg of casein digest dissolved in 2.5 ml distilled water) were loaded onto the column, which was eluted sequentially with 100 ml 1 m*M* and 200 ml 5 *M* ammonia solution; the eluate was collected in 10.4-ml fractions. In method 2, a column of copper–Chelex resin (125 mm × 25 mm I.D.) was first washed with 100 ml 0.1 *M* acetic acid before samples (10 mg ^{14}C-labelled enzymic digest dissolved in 2 ml 0.1 *M* acetic acid) were loaded. The column was then developed with 240 ml 0.1 *M* acetic acid, 80 ml distilled water (to prevent the formation of ammonium acetate) and 480 ml 1 *M* ammonia solution; eluate fractions of 8.0 ml were collected. The elution flow-rate for both methods was approximately 60 ml/h.

Methods of analysis

The absorbances of eluate fractions from method 1 were measured at 280 nm. The radioactivity contents of fractions eluted from method 2 were measured with a liquid scintillant (Ecoscint; National Diagnostics, Manville, NJ, USA) and a scintillation counter (Model SL 30; Intertechnique SA, Plaisir, France) fitted with an external-standard channel-ratio facility to correct for quenching. Column effluent fractions that corresponded to a peak of either absorbance or radioactivity were pooled.

To remove any residual copper, each of the pooled groups was evaporated to dryness under reduced pressure at 37°C in a rotary evaporator, dissolved in 5 ml distilled water, loaded onto a column (60 mm × 7.5 mm I.D.) of Chelex 100 resin and eluted with five bed volumes of 0.01 *M* ammonia solution; the latter was removed from each pooled group by rotary evaporation.

Volumes of each pooled group were deproteinised with ice-cold picric acid [9]. Additional volumes derived from method 2 were acid-hydrolysed by refluxing in 6 *M* hydrochloric acid for 22 h [10]. The amino acid contents of both deproteinised and acid-hydrolysed samples were determined by cation-exchange chromatography and ninhydrin detection using a Locarte (London, UK) Model 5 analyser fitted with a Roseate data management system (Drew Scientific, London, UK). If asparagine or glutamine were present they would have been assayed as aspartic and glutamic acids respectively. Tryptophan concentrations were not measured in any of the samples. The peptide contents of the casein digest samples were estimated by the method of Lowry *et al.* [11]; the assay was calibrated with a standard solution of Tryptone. Peptidyl concentrations in the ^{14}C-labelled samples were calculated as the acid-hydrolysed values (total amino acids) minus those of the deproteinised, unhydrolysed supernatants (free amino acids).

RESULTS

The concentrations of free amino acids detected in the enzymic digest of casein before and after elution from a copper–Chelex column are shown in Table I. The proportion of free amino acids in the digest was calculated to be 26.0% (w/w), composed of these fifteen amino acids with especially high concentrations of free leucine and lysine. The relatively low concentration of tyrosine could not be accurately measured because it co-eluted with large peptidyl peaks.

The elution profile of the casein digest from a copper–Chelex column using separation method 1 is shown in Fig. 1. The first peak eluted (fractions 3–9) was found to contain 29.0 mg peptidyl material with only 0.14 mg free amino acid contamination, mainly in the form of glutamic acid (Table I). Table I also shows that the second peak (fractions 15–26)

TABLE I

FREE AMINO ACID CONTENTS BEFORE AND AFTER COPPER-CHELEX CHROMATOGRAPHY

Free amino acids of a commercially available enzymic digest of casein (mg per 50 mg sample loaded) and in elution fractions using separation method 1 and of an enzymic digest of ^{14}C-labelled proteins (mg per 10 mg sample loaded) and in elution fractions using separation method 2 as described in Experimental. – = Detection limit less than 0.005 mg amino acid. * = not determined because of co-elution with peptides, see Results.

Amino acid	Method 1			Method 2		
	Casein digest	Fractions 3–9	Fractions 15–26	^{14}C-labelled mixture	Fractions 6–21	Fractions 54–65
Asp	–	–	–	0.35	0.30	–
Thr	0.37	–	0.12	0.13	0.12	–
Ser	0.50	–	0.15	0.20	0.18	–
Glu	0.20	0.07	0.01	0.32	0.28	–
Pro	–	–	–	0.07	0.04	–
Gly	0.07	–	0.05	0.54	0.48	0.01
Ala	0.24	–	0.16	0.27	0.25	–
Cys	0.13	–	0.01	–	–	–
Val	0.70	–	0.45	–	–	–
Met	0.75	0.02	0.33	–	–	–
Ile	0.62	0.02	0.28	–	–	–
Leu	2.81	0.03	1.55	0.08	–	–
Tyr	*	–	0.08	*	–	*
Phe	0.96	–	0.47	*	–	*
His	0.31	–	0.19	–	–	–
Lys	3.51	–	1.64	0.06	–	0.06
Arg	1.82	–	0.03	–	–	–

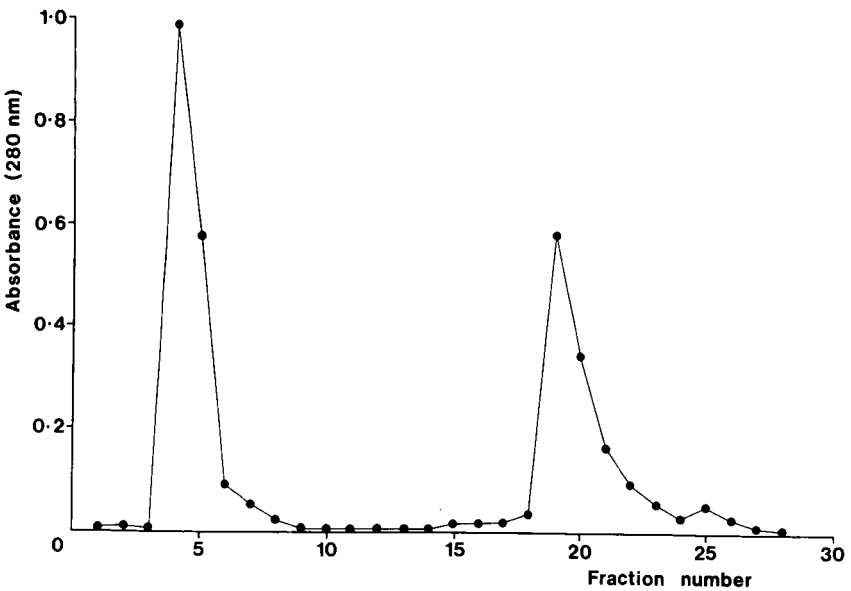

Fig. 1. Elution profile from a copper–Chelex resin column of an enzymic digest of casein (sample size, 50 mg dissolved in 2.5 ml water) eluted according to separation method 1.

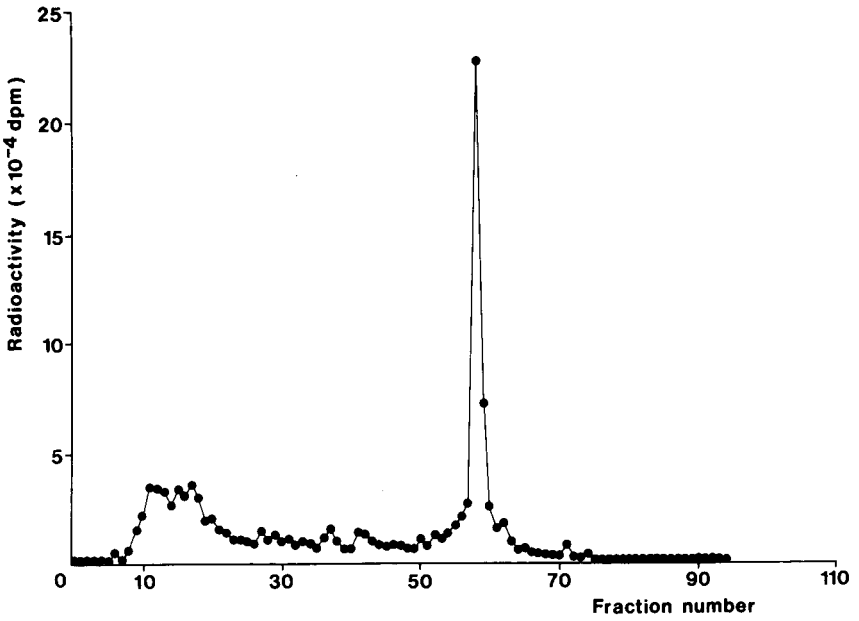

Fig. 2. Elution profile from a copper–Chelex resin column of an enzymic digest of ^{14}C-labelled proteins (sample size, 10 mg dissolved in 2 ml 0.1 *M* acetic acid and containing $1.19 \cdot 10^6$ dpm) eluted according to separation method 2.

contained a large amount (5.52 mg) of free amino acids together with 9.2 mg mixed peptides.

The free amino acid composition of the ^{14}C-labelled mixture is shown in Table I; the eleven amino acids that were detected accounted for 28.1% (w/w) of the sample. Values for free tyrosine and phenylalanine are not included because they co-eluted with a number of peptides which interfered with their accurate estimation, nevertheless their concentrations appeared to be negligible.

The elution pattern of radioactivity of the ^{14}C-labelled mixture of amino acids and peptides from a copper–Chelex column using separation method 2 is shown in Fig. 2. Analysis of the first peak (fractions 6–21) showed that it contained 1.65 mg free amino acids and 0.9 mg peptides, whereas the second peak (fractions 54–65) contained 3.6 mg peptides, but only 0.07 mg amino acids.

DISCUSSION

The two separation methods, based on copper–Chelex chromatography described here, have been successfully used to prepare fractions of mixed peptides by removing the majority of contaminating free amino acids from biological samples containing the two species. Free amino acid contamination has been reduced from 26.0% to 0.5% in an enzymic digest of casein using separation method 1 and from 20.3% to 1.9% in a mixture of ^{14}C-labelled peptides and amino acids derived from an enzymic digest of plant proteins using method 2.

The difference in effectiveness of the two separation methods apparently depends upon the predominant amino acids contaminating the peptides. When a standard solution of amino acids (AA-S-18; Sigma, Poole, UK) was subjected to separation by method 1, aspartic and glutamic acids were eluted in fractions 4–9, whereas the other amino acids appeared in fractions 15–26. Furthermore, when a sample of casein digest was eluted under the conditions of method 2, separations were most unsatisfactory; the first peak was found to contain 4.17 mg free amino acids and 9.8 mg peptides, while the second peak contained 3.22 mg free amino acids, composed mostly of free phenylalanine, histidine and lysine, with 29.8 mg peptide material.

Method 1 therefore seems to be more efficient at removing the basic amino acids, whereas method 2 is more efficient when acidic amino acids are pres-

ent. Since the casein digest contained comparatively low concentrations of free glutamic acid and no free aspartic acid, method 1 is the appropriate choice for this mixture. On the other hand, the ^{14}C-labelled mixture contained relatively large concentrations of these acidic amino acids and low concentrations of the basic amino acids, so separation method 2 is the more suitable procedure.

Comparisons of the mechanistically similar copper–Sephadex separation method of Rothenbühler *et al.* [7] with the copper–Chelex procedure described here as method 2, showed the former to be far less effective; using the ^{14}C-labelled mixture, the peptide fraction eluted from the copper–Sephadex column was still contaminated by as much as 20% free amino acids. And in addition, the problem of the removal of tetraborate remained. Furthermore, the volatile eluent, ammonia solution, used in method 2 could not be used to elute copper–Sephadex columns as the copper ions would be removed and precipitated at such a high pH.

Using methods 1 and 2, recoveries of the original peptidyl material were 78% for the casein digest and 45% for the ^{14}C-labelled mixture. Incomplete recoveries of peptides appear to be typical of many chromatographic procedures; for example, Rothenbühler *et al.* [7], using their copper–Sephadex method, stated that "the recovery for most peptides is higher than 80%" and a similar value has been reported for an HPLC method [12]. The poor recovery of peptides from the ^{14}C-labelled mixture separated by method 2 was investigated in an additional trial. When fractions 22–53 were collected, combined and re-eluted through the copper–Chelex column, the distribution of radioactivity altered so that when the re-eluted fractions 54–65 were combined with the original 54–65 fractions, a recovery of 76% peptidyl material was obtained. Thus improved yields of ^{14}C-labelled purified mixed peptides may be obtained, if required, by this procedural addendum.

A major advantage of these reported methods is that they require only simple, cheap laboratory equipment, as opposed to HPLC procedures. Furthermore, since the peptidyl fractions are eluted with acetic acid, water or ammonia solutions, which are easily removed by evaporation under reduced pressure, they may be used as substrates in subsequent biological experiments [8]. These procedures thus overcome the problems of elution with non-volatile buffers, such as sodium tetraborate, in previously reported copper–Chelex [6] and copper–Sephadex [5,7] methods. These particular advantages may also apply to procedures using flash chromatography, but as yet no comparable methods have been published using such a system and doubts have been expressed concerning its potential to resolve such complex mixtures [4]. Finally, in addition to their usefulness in purifying preparative amounts of peptidyl substrates, the copper–Chelex methods reported here may be of benefit in pre-processing crude samples prior to HPLC analysis.

ACKNOWLEDGEMENT

The authors wish to acknowledge the financial support of the Agricultural and Food Research Council, UK.

REFERENCES

1 R. C. Judd, *Methods Enzymol.*, 182 (1990) 613.
2 P. Arjomaa and M. Hallman, *Anal. Biochem.*, 171 (1988) 207.
3 W. C. Still, M. Kahn and A. Mitra, *J. Org. Chem.*, 43 (1978) 2923.
4 I. Chappell and P. E. Baines, *BioTechniques*, 10 (1991) 236.
5 S. Fazakerley and D. R. Best, *Anal. Biochem.*, 12 (1965) 290.
6 N. R. M. Buist and D. O'Brien, *J. Chromatogr.*, 29 (1967) 398.
7 E. Rothenbühler, R. Waibel and J. Solms, *Anal. Biochem.*, 97 (1979) 367.
8 P. B. Cooper and J. R. Ling, *Proc. Nutr. Soc.*, 44 (1985) 144.
9 H. A. Masson and J. R. Ling, *J. Appl. Bacteriol.*, 60 (1986) 341.
10 J. R. Ling and P. J. Buttery, *Brit. J. Nutr.*, 39 (1978) 165.
11 O. H. Lowry, N. J. Rosebrough, A. L. Farr and R. J. Randall, *J. Biol. Chem.*, 193 (1951) 265.
12 T. Sasagawa, L. H. Ericsson, D. C. Teller, K. Titani and K. A. Walsh, *J. Chromatogr.*, 307 (1984) 29.

Journal of Chromatography, 586 (1991) 265–270
Elsevier Science Publishers B.V., Amsterdam

CHROM. 23 600

Preparative separation and analysis of the enantiomers of [^{3}H]Abbott-69992, an HIV anti-infective nucleoside, by ligand-exchange high-performance liquid chromatography

Samuel B. Thomas* and Bruce W. Surber

Drug Metabolism Department, Abbott Laboratories, 1 Abbott Park Road, Abbott Park, IL 60064-3500 (USA)

(First received March 20th, 1991; revised manuscript received June 27th, 1991)

ABSTRACT

Several chiral stationary phases (CSPs) were examined to separate the enantiomers of A-69992, a chiral HIV anti-infective nucleoside. The only CSP found to be effective was Nucleosil Chiral-1, a ligand-exchange CSP, which was used to prepare microgram amounts of the enantiomers of high optical purity. This appears to be the first separation of the enantiomers of a nucleoside by chiral high-performance liquid chromatography.

INTRODUCTION

Structure–activity relationship studies have shown that the enantiomers of A-69992, an HIV anti-infective nucleoside consisting of a guanine nucleus attached to a pseudo-sugar (Fig. 1), have different antiviral activities. In order to carry out receptor-binding studies, the radiolabelled enantiomers of A-69992 of high optical purity were required. Owing, in part, to the lability of the tritium label at position 8 of the guanine residue [1,2], chiral synthesis of the pure enantiomers was deemed impractical and we sought a chromatographic method of resolving the labeled racemic mixture. A thorough search of the literature on chiral chromatography failed to reveal any examples of nucleoside separations. Thus, a screening of the chiral stationary phases (CSPs) in hand ensued. This paper describes the results of that screening and the optical resolution of [^{3}H]A-69992.

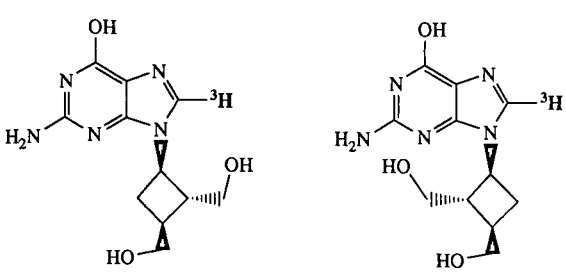

Fig. 1. The enantiomers of [^{3}H]A-69992: [^{3}H]A-75179 (**1**) and [^{3}H]A-75962 (**2**).

EXPERIMENTAL

Chemicals

Copper(II) acetate monohydrate [$Cu(OAc)_2$], triethylamine [$(C_2H_5)_3N$], glacial acetic acid (HOAc), acetonitrile (CH_3CN), methylene chloride (CH_2Cl_2), methanol (CH_3OH), ammonia (NH_3) solution, ammonium acetate (NH_4OAc), monobasic potassium phosphate (KH_2PO_4) and ethanol (C_2H_5OH) were purchased commercially and used without purification. All solvents except the ethanol were of high-performance liquid chromatographic (HPLC) grade. [^{3}H]A-69992 and A-75179 and A-75962 reference materials were synthesized at Abbott Labs.

0021-9673/91/$03.50

Analytical high-performance liquid chromatography

The chromatographic mobile phase was delivered by a Perkin-Elmer Model 250 binary pump. Samples were injected using a Rheodyne Model 7125 syringe-loading sample injector with a 200-μl loop. Peaks were detected with an Applied Biosystems Model 783A UV programmable detector set at 254 nm connected in series with a Flo-One Beta Model CR radioactivity detector (Radiomatic). Chromatograms were obtained by a Mini Micro (Korea) computer and a Spectra-Physics Model SP4270 integrator. A FlAtron CH-30 column heater controlled by a TC50 controller was used for the high-temperature experiments (Table I). Analysis of optical purity was performed using a Nucleosil Chiral-1 column (250 × 4.0 mm I.D.) (Machery-Nagel, Germany). The following columns did not achieve enantiomeric resolution (see Table I): Cyclobond I (250 × 4.6 mm I.D.) (Advanced Separation Technologies, Whippany, NJ, USA), Resolvosil

TABLE I

EFFECT OF CSP, MOBILE PHASE CONCENTRATION, FLOW-RATE AND TEMPERATURE ON THE RESOLUTION AND ENANTIOSELECTIVITY OF [^{3}H]A-69992

CSP	Mobile phase	Flow-rate (ml/min)	t_1[a] (min)	t_2[a] (min)	R_s[b]	α[c]
Nucleosil Chiral-1 (250 × 4.0 mm I.D.)	1 m*M* $Cu(OAc)_2$ (pH 5.75)–CH_3CN (95:5)	1.0	9.37	10.47	0.69	1.14
	0.5 m*M* $Cu(OAc)_2$ (pH 5.75)–CH_3CN (95:5)	1.0	9.72	10.90	0.80	1.22
		0.5	19.40	21.80	0.80	1.26
	0.25 m*M* $Cu(OAc)_2$ (pH 5.75)–CH_3CN (95:5)	1.0	15.55	17.55	0.67	1.17
	0.5 m*M* $Cu(OAc)_2$ (pH 5.75)–CH_3CN (95:5) at 45°C	1.0	6.10	6.36	0.60	1.17
		0.5	12.21	12.78	0.60	1.16
	0.5 m*M* $Cu(OAc)_2$ (pH 5.75)–CH_3CN (95:5) at 38°C	0.5	15.01	16.25	0.68	1.18
Cyclobond I B-cyclodextrin (250 × 4.6 mm I.D.)	50 m*M* KH_2PO_4 (pH 6.8)	1.0	5.82	5.82		
Resolvosil BSA-7 (150 × 4.0 mm I.D.)	0.1 *M* KH_2PO_4 (pH 6.8)	1.0	1.99	1.99		
YMC A-KO3 (250 × 4.6 mm I.D.)	CH_3CN–C_2H_5OH (25:75)	1.0	9.60	9.60		
Cellulose triacetate (250 × 10 mm I.D.)	100% C_2H_5OH	1.0	7.20	7.20		

[a] t_1 and t_2 refer to the retention times of [^{3}H]A75179 (**1**) and [^{3}H]A75962 (**2**), respectively.
[b] R_s is the resolution factor.
[c] α is the enantioselectivity factor.

BSA-7 (150 × 4.0 mm I.D.) (Machery-Nagel), YMC A-KO3 (*R*)-(+)-naphthylethylamine (250 × 4.6 mm I.D.) (YMC, Morris Plains, NJ, USA) and cellulose triacetate (250 × 10 mm I.D.) (Merck, Darmstadt, Germany).

Radiochemical purity determination was performed using a Whatman Partisil 5 ODS 3 column (250 × 4.6 mm I.D.) (Whatman, Clifton, NJ, USA).

The mobile phase used for the optical purity determination consisted of CH_3CN (5%) and $Cu(OAc)_2$ (0.5 m*M*) with the pH adjusted to 5.75 with HOAc (95%). The flow-rate was set at 1.0 ml/min. The mobile phase used for the radiochemical purity determination consisted of 88% NH_4OAc (0.45 *M*) plus $(C_2H_5)_3N$ (0.1%) with the pH adjusted to 4.8 with HOAc, and 12% CH_3OH. The flow-rate was set at 1.3 ml/min.

Preparative high-performance liquid chromatography

Separations were carried out using a Waters Delta Prep 3000, a Rheodyne Model 7000L syringe-loading injector with a 5-ml loop and a Waters Model 484 variable-wavelength absorbance detector operated at 254 nm. The chromatograms were obtained using a Waters Model 745B integrator. The chiral semi-preparative HPLC column used was a Nucleosil Chiral-1 (250 × 10 mm I.D.) (Machery-Nagel) made by chemically bonding L-hydroxyproline Cu^{2+} complexes to Nucleosil 120 silica.

The mobile phase consisted of 5% CH_3CN and 95% $Cu(OAc)_2$ (0.25 m*M*) with the pH adjusted to 5.95 with HOAc, and filtered through a 0.45-μm nylon filter. The flow-rate was set at 5.0 ml/min and the column back-pressure ranged from 950 to 1000 p.s.i. The points at which fractions were collected are shown in Fig. 4. Four fractions were collected in the first pass (group A, Table II) and three fractions in the second pass (group B: rechromatography of fraction 4A, Table II).

For sample preparation, the labeled racemic mixture was dissolved in water and diluted with mobile phase to give a concentration of *ca.* 20 μg/ml (1.0-ml injection).

Isolation of pure enantiomers

Fractions 1A containing purified [^{3}H]A-75179 were evaporated to dryness under reduced pressure. The residue was dissolved in the mobile phase and applied to a column of Merck silica gel (60–230 mesh) dry-packed in a 5-ml glass serological pipette. A filtered mobile phase consisting of CH_2Cl_2–CH_3OH–NH_3 solution (60:40:1) was used to elute the product, which was then evaporated to dryness and the residue dissolved in water. A portion was tested for the presence of copper by adding 6 *M* NH_3 solution. Fractions 3B containing purified [^{3}H]A-75962 were treated in an identical fashion.

RESULTS AND DISCUSSION

Of the several CSPs tried, the enantiomers of A-69992 were resolved only on a Nucleosil Chiral-1 column. The stationary phase consists of L-hydroxyproline chemically bonded to silica gel and complexed with copper. The mobile phase contains Cu^{2+} to prevent the loss of copper ion from the stationary phase. Suitably functionalized analytes compete for complexation sites and separations are based on the formation of an enantioselective ternary complex between hydroxyproline (fixed ligand),

TABLE II

CHROMATOGRAPHIC DATA FROM PREPARATIVE RESOLUTION OF [^{3}H]A-69992

[^{3}H]A-75179 is designated as **1** and [^{3}H]A-75962 is designated as **2**. Percentages given are optical purities; see text for a discussion.

Step	Fraction 1	Fraction 2	Fraction 3	Fraction 4
(A) Chromatography of racemic [^{3}H]A-69992	~98% (**1**)	90% (**1**) 10% (**2**)	15% (**1**) 85% (**2**)	9% (**1**) 91% (**2**)
Activity per fraction (μCi)	13	12	19	17
(B) Rechromatography of fraction 4A	97% (**1**) 3% (**2**)	6% (**1**) 94% (**2**)	3% (**1**) 97% (**2**)	
Activity per fraction (μCi)	2	6	5	

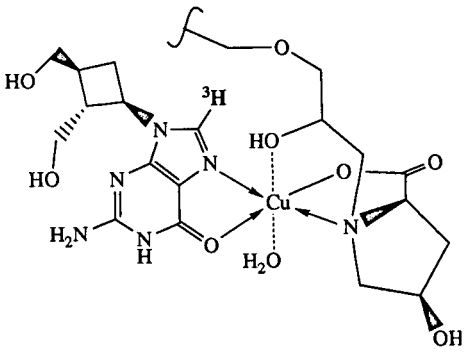

Fig. 2. Possible structure of the mixed complex between L-hydroxyproline, copper and [^{3}H]A-75179.

copper and the analyte (mobile ligand). The difference in stabilities between complexes with the D- and L-forms of the analyte leads to the separation of the enantiomers [3]. Ligand-exchange chromatography for the separation of enantiomers evolved as a result of pioneering work by Davankov *et al.* [4,5]. This method has been shown to be effective for the optical resolution of amino acids, amino acid derivatives and hydroxy acids [6–12]. Here, we report the use of ligand-exchange HPLC for the resolution of a chiral nucleoside.

It is unclear which functional groups of A-69992 are involved in chelation, but it seems likely that the guanine nucleus is participating as nucleoside copper complexes are well known [13]. Fig. 2 shows a possible structure of the mixed complex between L-hydroxyproline (bound to silica gel), copper and [^{3}H]A-75179. This structure is modeled after ligand-exchange complexes proposed for the resolution of amino acids [3,5,12]. The rationale for the structure in Fig. 2 stems from studies which show that guanine (and adenine) bind with copper at N-7 when N-9 is blocked [13] and from the fact that this portion of the nucleoside is structurally similar to α-amino acids which are thought to bind copper at the amino and carboxyl groups as shown for the L-hydroxyproline portion of the complex [3–12].

A chromatogram of the separation is shown in Fig. 3. [^{3}H]A-75179 was eluted first at 14.7 min, a

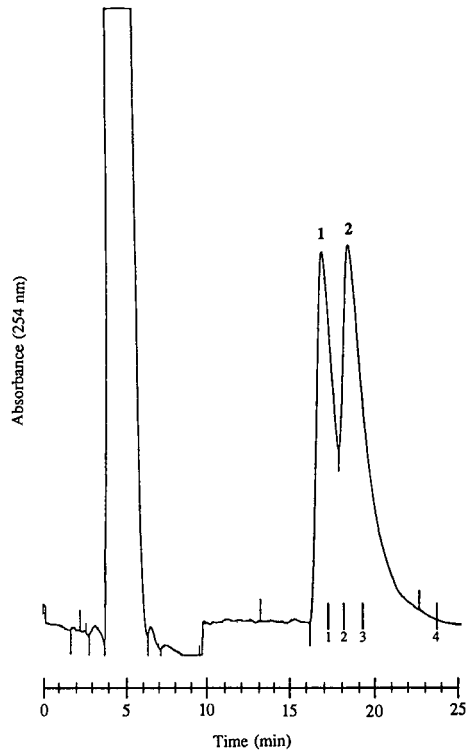

Fig. 3. Enantiomeric separation and resolution of [^{3}H]A-69992 on a Nucleosil Chiral-1 column (250 × 10 mm I.D.) showing cut-off points for fraction collection during preparative runs. The mobile phase consisted of 5% CH_3CN and 95% $Cu(OAc)_2$ (0.25 m*M*) with the pH adjusted to 5.95 with HOAc. The flow-rate was set at 5.0 ml/min.

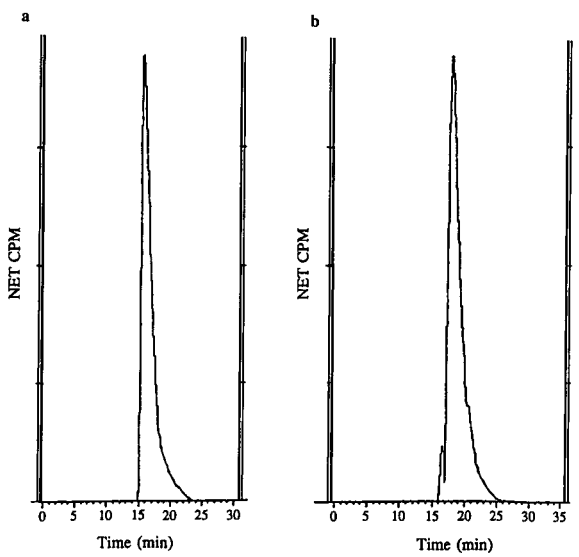

Fig. 4. Optical purity determination of (a) [^{3}H]A-75179 (**1**, *ca.* 98%), (b) [^{3}H]A-75962 (**2**, *ca.* 96%) on a Nucleosil Chiral-1 column (250 × 4.0 mm I.D.). The mobile phase consisted of 2% CH_3CN and 98% $Cu(OAc)_2$ (0.50 m*M*) with the pH adjusted to 5.75 with HOAc. The flow-rate was set at 1.0 ml/min.

retention time identical with that of authentic A-75179 standard, and was followed by [^{3}H]A-75962 at 16.1 min. A number of different solvent combinations, loads and concentrations were examined during the analytical method development (Table I); however, the results could not be reproduced when done on a semi-preparative scale. This required a mobile phase consisting of 0.25 m*M* $Cu(OAc)_2$ (pH 5.95)–CH_3CN (95:5) for the separation (α = 1.15; R_s = 0.83). It should be noted that increasing the temperature of the column to 45°C, as suggested by the manufacturer, did not improve the separation. In order to obtain research amounts of [^{3}H]A-69992 enantiomers, eight 1-ml injections (75 μCi total) of radiochemically pure racemic drug were performed and four fractions were collected for each injection (Fig. 3). The optical purities as determined by rechromatography are listed in row A of Table II. Fraction 1A was essentially pure [^{3}H]A-75179, as shown in the chromatogram in Fig. 4a. Fraction 4A was further purified by a second round of chromatography (four 1-ml injections). As detailed in row B of Table II, fraction 3B contained *ca.* 96% of [^{3}H]A-75962, as shown in Fig. 5b. The stated optical purities are only estimates owing to peak tailing and the low resolution factor. When pure unlabeled A-75179 was spiked with 2% of the other enantiomer, a shoulder was detectable (Fig. 5); however, these materials were not certified 100% enantiomerically pure so an accurate optical purity could not be determined.

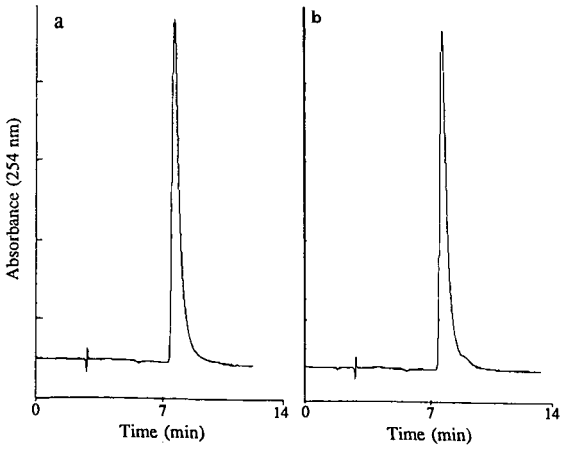

Fig. 5. HPLC of (a) A-75179 reference material and (b) A-75179 containing *ca.* 2% of A-75962.

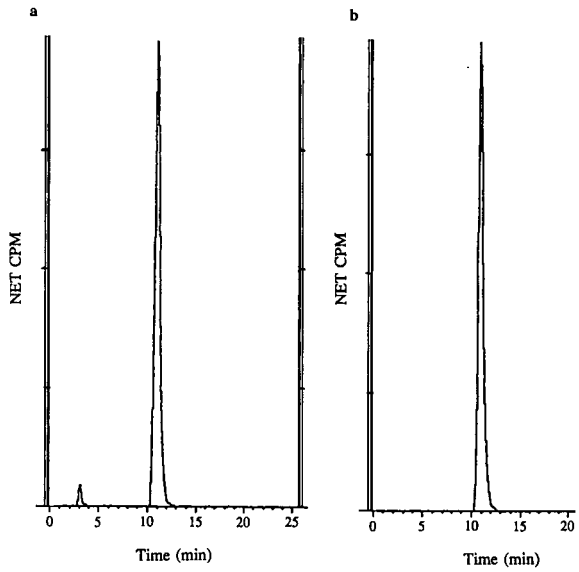

Fig. 6. Radiochemical purity determination of (a) [^{3}H]A-75179 (**1**, >97%) and (b) [^{3}H]A-75962 (**2**, >99%) on a Whatman Partisil 5 ODS 3 column (250 × 4.6 mm I.D.). The mobile phase consisted of 88% NH_4OAc (0.45 *M*) plus $(C_2H_5)_3N$ (0.1%) with the pH adjusted to 4.8 with HOAc and 12% CH_3OH. The flow-rate was set at 1.3 ml/min.

The copper salts in fractions 1A and 3B were efficiently removed by using a gravity silica column, forming a blue band at the top of the column. A 7-μCi amount of the [^{3}H]A-75179 and 2.6 μCi of the [^{3}H]A-75962 were recovered. Samples were isolated *in vacuo* and each sample residue was dissolved in water. A portion of each was tested for the presence of copper salts by the addition of excess of 6 *M* NH_3 solution (USP XXII). The radiochemical purities were >97% and >99% for [^{3}H]A-75179 and [^{3}H]A-75962, respectively (Fig. 6).

In conclusion, the preparative procedure described above allows the isolation of microgram amounts of the enantiomers of [^{3}H]A-69992 in high purity but poor yield. This appears to be the first use of ligand–exchange HPLC for the resolution of enantiomeric nucleosides. Although attention was directed at maximization of the yield of the [^{3}H]A-75179, the yield of the [^{3}H]A-75962 could have been increased by rechromatography of mixed fractions 2A, 3A and 2B, but this was not done because the capacity factor decreased with repeated injections. Additionally, a chiral column consisting of the analogous D-hydroxyproline CSP (currently not

commercially available) would be expected to elute [^{3}H]A-75962 first, potentially increasing the yield of [^{3}H]A-75962.

ACKNOWLEDGEMENTS

The authors thank Mr. Gary Rotert for the synthesis of the radiolabeled material and Ms. Karen Wegrzyn for assistance with the manuscript.

REFERENCES

1 E. A. Evans, H. C. Sheppard and J. C. Turner, *J. Labelled Compd. Radiopharm.*, 6 (1970) 77.
2 R. S. Feldberg and L. M. Reppucci, *J. Chromatogr.*, 410 (1987) 226.
3 A. C. Mehta, *J. Chromatogr.*, 426 (1988) 1.
4 V. A. Davankov, S. V. Rogozlin, A. V. Senechkin and T. P. Sachkova, *J. Chromatogr.*, 82 (1973) 359.
5 V. A. Davankov, *Adv. Chromatogr.*, 18 (1980) 139.
6 G. Gubitz and W. Jellenz, *J. Chromatogr.*, 203 (1981) 377.
7 G. Jeanneret-Gris, C. Sorrensen, H. Su and J. Porret, *Chromatographia*, 28 (1989) 337.
8 M. Gimpel and K. Unger, *Chromatographia*, 16 (1982) 117.
9 R. Dappen, H. Arm and V. R. Meyer, *J. Chromatogr.*, 373 (1986) 1.
10 D. R. Taylor, *Lab. Pract.*, (1986) 45.
11 Y. Yuki, K. Saigo, H. Kimoto, K. Tachibana and M. Masegawa, *J. Chromatogr.*, 400 (1987) 65.
12 W. H. Pirkle and T. C. Pochapsk, *Chem. Rev.*, 89 (1989) 347.
13 M. Sundaralingam and J. A. Carrabine, *J. Mol. Biol.*, 61 (1971) 287.

Journal of Chromatography, 586 (1991) 271–276
Elsevier Science Publishers B.V., Amsterdam

CHROM. 23 597

Peak distortion in the column liquid chromatographic determination of omeprazole dissolved in borax buffer☆

Torbjörn Arvidsson*,☆☆ and Elisabeth Collijn

Analytical Control, Astra Pharmaceutical Production AB, S-151 85 Södertälje (Sweden)

Anna-Maria Tivert and Lena Rosén

Department of Analytical Chemistry, Astra Hässle AB, S-431 83 Mölndal (Sweden)

(First received February 5th, 1991; revised manuscript received June 26th, 1991)

ABSTRACT

Injection of a sample containing omeprazole dissolved in borax buffer (pH 9.2) into a reversed-phase liquid chromatographic system consisting of a mixture of acetonitrile and phosphate buffer (pH 7.6) as the mobile phase and a C_{18} surface-modified silica as the solid phase resulted under special conditions in split peaks of omeprazole. The degree of peak split and the retention time of omeprazole varied with the concentration of borax in the sample solution and the ionic strength of the mobile phase buffer as well as with the column used. Borax is eluted from the column in a broad zone starting from the void volume of the column. The retention is probably due to the presence of polyborate ions. The size of the zone varies with the concentration of borax in the sample injected. In the borax zone the pH is increased compared with the pH of the mobile phase, and when omeprazole (a weak acid) is co-eluting in the borax zone its retention is affected. In the front part and in the back part of the borax zone, pH gradients are formed, and these gradients can induce the peak splitting. When the dissolving medium is changed to a phosphate buffer or an ammonium buffer at pH 9 no peak distortion of omeprazole is observed.

INTRODUCTION

Omeprazole is a substituted benzimidazole which selectively inhibits the proton pump in the gastric mucosa [1]. In solution omeprazole degrades rapidly at low pH values [2]. Therefore, during analysis omeprazole is preferably dissolved under alkaline conditions. Omeprazole can be dissolved in a borax buffer of pH 9.2 and assayed by reversed-phase chromatography with a C_{18} modified silica as the solid phase and with a phosphate buffer–acetonitrile mixture as eluent. However, in some cases, injection of such a sample into the liquid chromatographic system results in a deformed or even split peak of omeprazole.

Peak deformation is a commonly occurring phenomenon in column liquid chromatography. Sample overloading often results in peak tailing. For hydrophobic amines severe peak tailing is obtained even at low sample concentrations, which can be explained as being due to a heterogeneous column surface [3], an effect often named 'the silanol effect' [4]. Most peak distortion phenomena can be related to disturbances in the column equilibrium. In ion-pairing systems split, broadened and compressed peaks of the analyte have all been observed. These occur when the sample injected has a different concentration of the ion-pairing reagent compared with the mobile phase, or contains a second non-detectable hydrophobic ion. The phenomena have been explained as being due to co-elution of the analyte

☆ Presented at the *13th Symposium on Column Liquid Chromatography 1989, Stockholm, June 25, 1989.*

☆☆ Present address: Astra Pain Control, S-151 85 Södertälje, Sweden.

0021-9673/91/$03.50

in a non-detectable zone induced by the ion-pairing reagent [5,6]. Also, in a simple chromatographic system containing buffer and acetonitrile as eluent, similar effects have been obtained when a hydrophobic non-detectable ion is injected and co-eluted with the analyte [7].

Deformed peaks have also been reported when applying samples with the ability to form strong complexes between the analyte and an agent in the sample solution in cases when the analyte and the complexing agent have different retentions [8]. The strong drug–protein binding between naproxen and albumin results in a deformed peak of naproxen [8]. Adduct formation between tannins and methanol in the sample solution results in deformed peaks of the tannins [9].

Peak splitting has also been observed in chromatography of proteins when the protein occurs in both native and denaturated forms. Two separate peaks are obtained [10].

In the present study deformed peaks of omeprazole in borax buffer were observed. The degree of peak distortion varied from column to column and with the concentration of borax in the sample solution. This study attempts to explain this phenomenon.

EXPERIMENTAL

Chemicals

Omeprazole was obtained from Hässle (Mölndal, Sweden). Sodium tetraborate ($Na_2B_4O_7 \cdot 10H_2O$, borax) was obtained from Merck (Darmstadt, Germany). Acetonitrile was of high-performance liquid chromatography (HPLC) grade and was obtained from Merck or from Rathburn (Walkerburn, UK). All other chemicals were of analytical grade.

Equipment

The pump was a LKB 2150 (LKB, Bromma, Sweden) or an SP 8700 (Spectra Physics, San José, CA, USA). The injector was a WISP 710B, (Waters Assoc, Milford, MA USA) or an SP 8780XR (Spectra Physics). The UV detector was a Spectraflow 783 (Kratos, Ramsey, NJ, USA). UV spectra were obtained with a 1000S diode-array detector (Applied Biosystems, Ramsey, NJ, USA). The integrator was an SP 4270 (Spectra Physics).

The columns were 150 × 4.6 mm I.D. Nucleosil C_{18}, 5 μm (Macherey-Nagel, Duren, Germany) or 100 × 5 mm I.D. Novapak C_{18}, 4 μm, Radial PAK (Waters Assoc.) fixed in a Waters RCM 8 × 10 cartridge holder.

A micro combined pH-electrode with needle membrane (Ingold, Urdert, Switzerland) was used to measure the pH of the column elutate.

Procedures

Stock solutions of omeprazole were prepared by dissolving 5 mg of omeprazole in 5 ml of ethanol followed by dilution to 25 ml with 0.01 *M* borax solution. Sample solutions were obtained by diluting the stock solution with aqueous borax solutions.

The phosphate buffers were prepared by mixing different volumes of 1 *M* phosphoric acid, 1 *M* sodium dihydrogenphosphate, 0.5 *M* disodium hydrogenphosphate and 0.25 *M* trisodium phosphate, which were diluted with water to obtain the specified pH and ionic strength. The eluents were prepared by mixing volumes of buffer and acetonitrile in the specified ratios.

A 10-to 20-μl aliquot of the sample was injected into the column with a flow-rate of 1.0 ml/min. Detection of omeprazole was made at 280 nm and of borax at 190 nm. The conditional pH (pH*) of the column eluate was measured in 0.5-ml fractions.

Computer calculations

Calculation of polyborate equilibria was made with a personal computer using the programs INPUT and SED obtained from the Department of Inorganic Chemistry, KTH (Stockholm, Sweden). The programs are based on the well known programs HALTAFALL [11] and SOLGASWATER [12].

RESULTS AND DISCUSSION

Chromatography of omeprazole

Omeprazole (Fig. 1) is an ampholyte with pK_a of about 4 (pyridinium) and 8.8 (benzimidazole). It is rapidly degraded in acidic solutions but has an acceptable stability at higher pH. The half-life of omeprazole in a solution of pH 6.5 is about 18 h and at pH 11 about 300 days [2]. It is therefore suitable to have sample solutions at high pH during the chromatographic analysis and to perform the chromato-

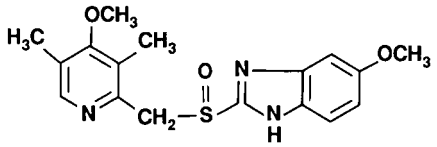

Fig. 1. Chemical structure of omeprazole.

graphy with a mobile phase of a pH as high as possible.

A phosphate buffer of pH 7.5 with an ionic strength (μ) of 0.025 was chosen as mobile phase buffer. Because of the risk of degradation of the silica-based column, a higher pH was avoided. The acetonitrile concentration varied between 25 and 40% depending on the column used. The retention of omeprazole is sensitive to changes in pH above 7.5, which is demonstrated in Table I, which shows the effect of using phosphate buffers of various pH as the mobile phase with acetonitrile. This is obviously due to the protolysis of the molecule, which should be noticeable in this pH range.

To avoid degradation, omeprazole was dissolved in a sodium tetraborate solution of pH 9.2. This means that the solvent of the sample differs widely from that of the mobile phase.

A distorted peak of omeprazole was found on some columns (Fig. 2, upper chromatograms). Different batches of columns from the same brand gave different results. When the distortion occurred the omeprazole peak was usually split into two peaks, one large peak eluting before a smaller second peak (Fig. 2A, I). The degree of peak split increased with increasing borax concentration in the sample solution (Fig. 2A and B).

The distortion was found to be due to the borax buffer since, when omeprazole was dissolved in other types of buffers (ammonium or phosphate) with the same pH as the borax buffer or in the eluent, a normal peak shape of omeprazole was obtained, *i.e.* similar to the peak shown in Fig. 2B, I.

TABLE I

INFLUENCE OF THE MOBILE PHASE pH ON THE RETENTION OF OMEPRAZOLE

Eluent: acetonitrile–phosphate buffer (μ=0.025) (40:60, v/v)
Column: Nucleosil C_{18}

Mobile phase pH	k' omeprazole
6.5	2.0
7.5	2.0
8.5	1.1

Retention of borax buffer

To study the influence of borax buffer in the sample solution, samples of omeprazole with different concentration of borax buffer were injected. Omeprazole was detected by UV at 280 nm, whereas borax was detected by UV at 190 nm. The results from three different columns (Fig. 2) show that the borax buffer was retained as a wide zone. The shape of the zone varied drastically from column to column, and the width of the zone increased with the borax concentration (columns A and B).

Retention of omeprazole in borax zone

The retention of omeprazole decreases with increasing borax concentration in the sample solution. This is illustrated by using column C (Fig. 2C) where omeprazole is eluted within the borax zone and the peak is not split, *i.e.* omeprazole has a lower retention in the borax zone than in the bulk mobile phase.

In columns A and B (Fig. 2A and B) the retention of omeprazole also decreased with increasing borax concentration in the sample solution, but peak split occurred. A small peak containing omeprazole with the same retention as if omeprazole were dissolved in the bulk mobile phase occurs. The retention of the rest of omeprazole, the split part, decreases with increasing borax concentration. In column B (Fig. 2B, III), omeprazole is even split into three peaks. In the lower chromatogram in Fig. 2A (III) when the injected sample contained 0.050 *M* borax, the first eluting peak of omeprazole was compressed, which seems to be because of the elution of omeprazole in a gradient.

In column C (Fig. 2C) omeprazole is not split. This may be because omeprazole is eluted within the borax zone and no steep gradient of the borax zone is present.

pH in the borax zone

The results above clearly show that the retention of omeprazole is affected by the borax buffer. The retention of omeprazole is dependent on the mobile phase pH (Table I). Therefore, experiments were

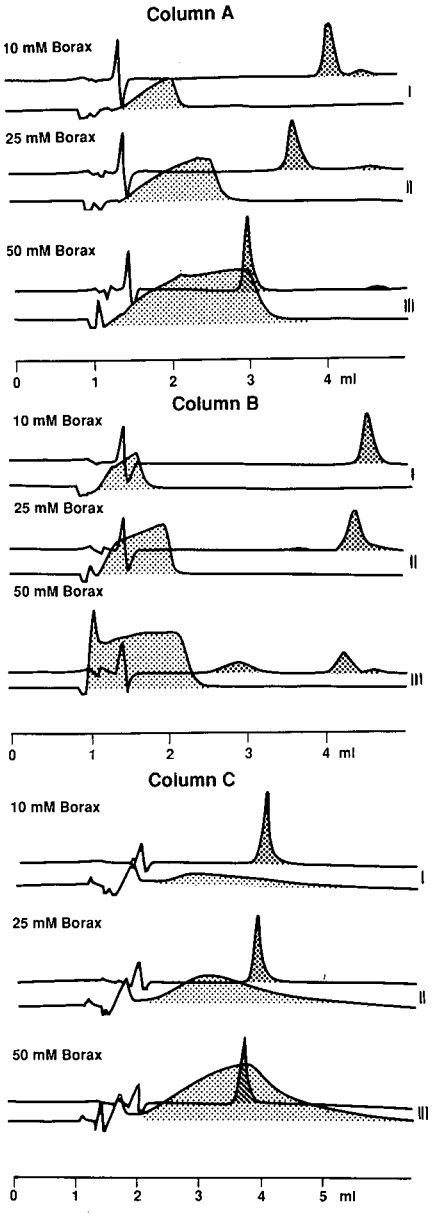

Fig. 2. Retention of omeprazole and borax in borax buffer. Samples: 1 μM omeprazole-containing borax and borax. Upper (I) 10 mM borax, middle (II) 25 mM borax, lower (III) 50 mM borax. Detection: omeprazole (darker shaded peak) UV at 280 nm, borax (lighter shaded peak) UV at 190 nm. Columns: A and B Novapak C_{18}, C Nucleosil C_{18}. Eluent: acetonitrile–phosphate buffer pH 7.6 ($\mu = 0.025$): A and B 30:70 (v/v); C 40:60 (v/v).

performed to determine the pH of the eluate. Fractions of the eluate (0.5 ml) were collected and the conditional pH (pH*) was determined with a microelectrode. The results after injection of a 0.1 M borax solution showed (Fig. 3) that the pH* was increased by about 0.5 units in the borax zone compared with the pH* in the bulk mobile phase and that pH gradients were formed in the front and back parts of the borax zone. Changing the mobile phase pH by 0.5 units drastically influences the retention of omeprazole (Table I). The peak-split phenomenon may be explained by the pH difference between the sample solution and the mobile phase. The plug created by injection of borax gives pH gradients in the front and back parts of the zone. When omeprazole is retained in the steep back gradient of the borax zone the back part of the omeprazole zone has a lower retention compared with the front part, whereas in the front gradient the situation is reversed, *i.e.* the back part of the omeprazole zone has a higher retention than the front part.

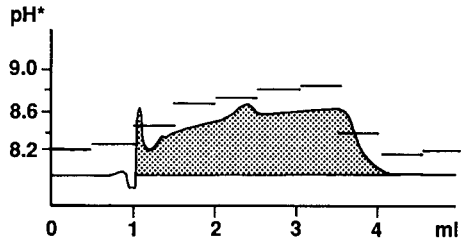

Fig. 3. pH of eluate after borax buffer injection. Sample: 10 μl of 100 mM borax. Detection: UV at 190 nm (shaded peak). pH* of 0.5 ml fractions are indicated by horizontal bars. Column: Novapak C_{18} (RCM). Eluent: acetonitrile–phosphate buffer pH 7.5 ($\mu = 0.025$) (30:70, v/v)

Therefore, around the point where the gradients meet the omeprazole molecules will struggle in different directions, *i.e.* they will have different migration rates depending on the gradient in which they are eluted, and in that way induce peak splitting.

At high borax concentrations (Fig. 2B, III) the borax zone seems to create several pH gradients and omeprazole is split into three peaks.

Identity of omeprazole

The identity of omeprazole in the split peaks was examined using a photo diode-array detector, and agreement between the spectra from the two peaks was obtained (Fig. 4).

Borax buffer

When dissolving borax in water, boric acid and

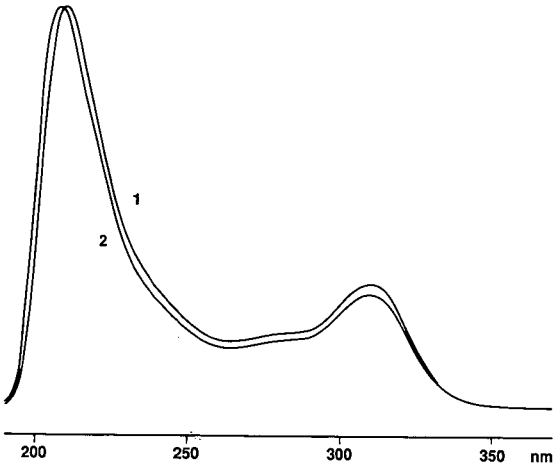

Fig. 4. Photodiode-array UV spectra from split omeprazole peaks. Normalized absorbances from peak maximum. Chromatogram similar to Fig. 2 (column A, I). 1 = Large peak; 2 = small peak.

borate ions are formed. The pK_a value is about 9.2. However, according to Ingri [13], at higher concentrations of borate, polyborate ion complexes can be formed. Stability constants for the different borate polyions were determined [13]. The distribution of boron between different ions was calculated from the stability constants given by Ingri [13] for three different borax concentrations and is presented in Fig. 5. The figure shows that the fraction of polyions increases with increasing borate concentration. It also shows that polyions occur at pH between 6 and 11, *i.e.* at the pH used in the mobile phase for the omeprazole assay polyions certainly exist. When injecting borax buffer into a chromatographic system consisting of a mobile phase of acetonitrile–phosphate buffer, pH 3.0, or a similar phase with pH 11.0, only one peak eluting with the front was observed. This indicates that both boric acid and the borate ion are eluted unretained. The retention of borax seems to be affected by the polyanions.

The column equilibrium is obviously attributed to the distribution between the different polyions, which varies with the borax concentration (see Fig. 5), *i.e.* with the dilution of the injected zone during chromatographic elution. Since the polyborates are retained and boric acid as well as borate are unretained, the retention mechanism will be very complex.

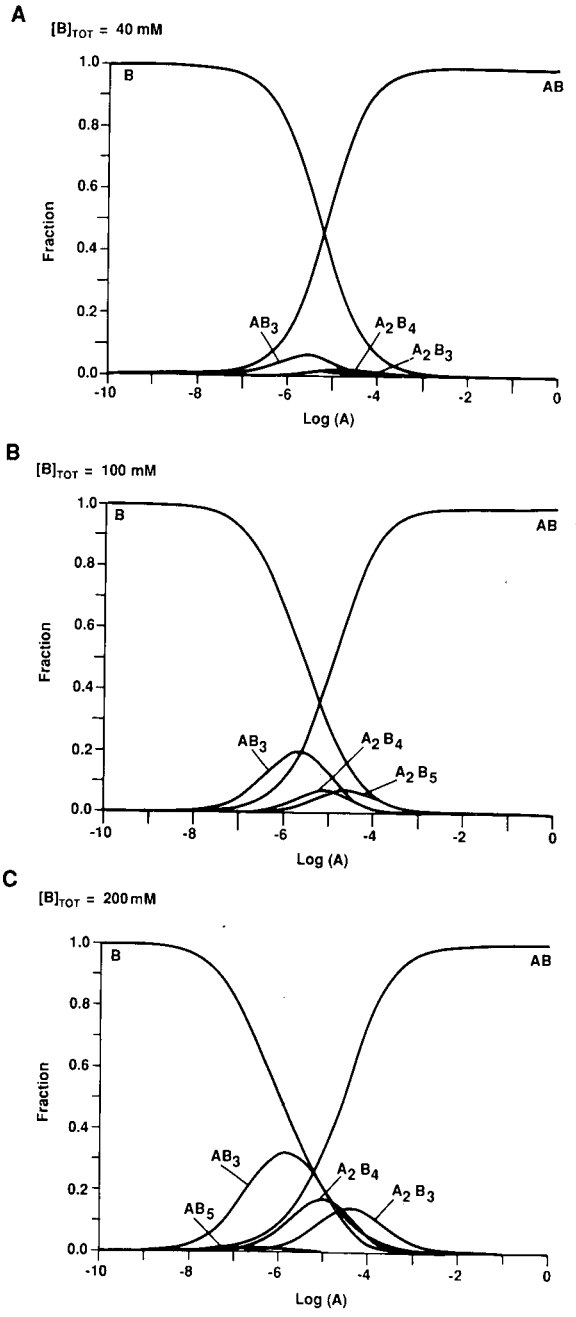

Fig. 5. Distribution of boron between different ions in borax solution: (A) 10 m*M* borax; (B) 25 m*M* borax; (C) 50 m*M* borax. Calculated by computer programs with stability constants according to Ingri [13]. A = $[OH^-]$, B = $[B(OH)_3]$ and $\beta_{pq} = [A_pB_q][A]^{-p}[B]^{-q}$. $\log \beta_1 = 5.2$, $\log \beta_{13} = 7.3$, $\log \beta_{24} = 13.5$, $\log \beta_{23} = 12.0$ and $\log \beta_{15} = 7.4$.

Effects of the ionic strength in the mobile phase

In the study so far the mobile phase buffer ionic strength was 0.025. The buffer capacity of the mobile phase may be too low to neutralize the sample zone containing borax efficiently. If the mobile phase ionic strength is increased, the pH of the borax zone may decrease, the pH gradients will be reduced and the influence of the polyborates will become negligible as their concentration approaches zero (see Fig. 5). The results (Fig. 6) show that the peak distortion of omeprazole decreases with increasing ionic strength. The peak split disappeared when using an ionic strength of 0.1 in the eluent. The retention of omeprazole as well as the size of the borax zone decreases with increasing ionic strength. The effect is possibly due to the fact that the pH in the zone decreases, thus counteracting the formation of the polyborate ions.

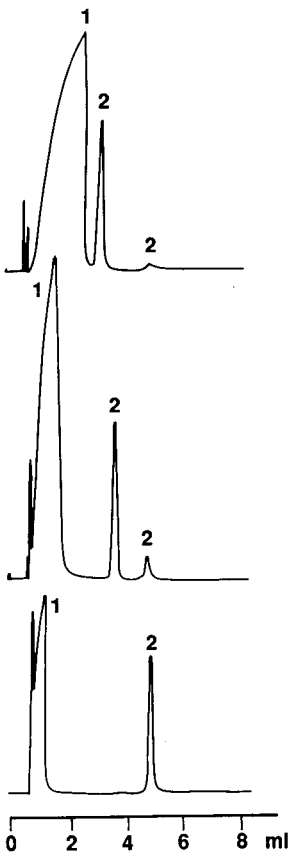

Fig. 6. Effect of mobile phase pH ionic strength on peak split of omeprazole. Sample: 1 μM omeprazole in 50 mM borax. Detection: UV at 190 nm. Peaks: 1 = Borax; 2 = Omeprazole. Eluent: acetonitrile–phosphate buffer pH 7.6 (30:70, v/v). Ionic strength of buffers: upper chromatogram, 0.025; middle chromatogram, 0.05; lower chromatogram, 0.10. Column: Novapak C_{18} (RCM).

CONCLUSIONS

Sample solutions containing borax buffer may give peak disturbances of the analyte. The effect occurs predominantly when the pH of the mobile phase is 6–8. The reason for the disturbance was found to be the presence of polyborate ions, which were retained as a broad zone. In this zone the pH was increased compared with the bulk mobile phase and pH gradients were created. Disturbance occurred when the analyte was present in the pH gradient and its retention was affected by a change of the pH. It was possible to decrease the disturbances by increasing the ionic strength of the mobile phase. If the sample was dissolved in other types of buffer, *e.g.* phosphate or ammonium, no peak distortion of omeprazole was observed.

REFERENCES

1 B. Wallmark, P. Lorentzon and H. Larsson, *Scand. J. Gastroenterol.*, 20 (Suppl. 108) (1985) 37.
2 Å. Pilbrant and C. Cederberg, *Scand. J. Gastroetenrol.*, 20 (Suppl. 108) (1985) 113.
3 A. Sokolowski and K.-G. Wahlund, *J. Chromatogr.*, 189 (1980) 299.
4 M. A. Stadalius, J. S. Berus and L. R. Snyder, *LC · GC*, 6 (1988) 494.
5 L. B. Nilsson and D. Westerlund, *Anal. Chem.*, 57 (1985) 1835.
6 T. Arvidsson, *J. Chromatogr.*, 407 (1987) 59.
7 T. Fornstedt, D. Westerlund and A. Sokolowski, *J. Chromatogr.*, 535 (1990) 93.
8 K.-G. Wahlund and T. Arvidsson, *J. Chromatogr.*, 282 (1983) 527.
9 T. Hatano, T. Yoshida and T. Okuda, *J. Chromatogr.*, 435 (1988) 285.
10 S. A. Cohen, K. P. Benedik, S. Dong, Y. Tapuhi and B. L. Karger, *Anal. Chem.*, 56 (1984) 217.
11 N. Ingri, W. Kakolowicz, L. G. Sillén and B. Warnqvist, *Talanta*, 14 (1967) 1261.
12 G. Eriksson, *Anal. Chim. Acta*, 112 (1979) 375.
13 N. Ingri, *Sv. Kem. Tidskr.*, 75 (1963) 199.

Journal of Chromatography, 586 (1991) 277–281
Elsevier Science Publishers B.V., Amsterdam

CHROM. 23 601

Secondary equilibrium size-exclusion chromatography of ions with polymeric mobile phase additives

Tetsuo Okada

Faculty of Liberal Arts, Shizuoka University, Shizuoka 422 (Japan)

(First received April 5th, 1991; revised manuscript received June 27th, 1991)

ABSTRACT

Polymeric ligands play an important role in the secondary equilibrium size-exclusion chromatography of small molecules. Polyethylene glycol and polybrene were employed in mobile phases to separate inorganic cations and anions, respectively. Addition of polymeric ligands to the mobile phases permits the elution order to be altered, the partition coefficients of solutes in the polymer phase to be determined and the analysis time to be reduced.

INTRODUCTION

Secondary equilibria in liquid chromatography allow one to modify the selectivity, to enhance the separation efficiency and to determine equilibrium constants in solution [1–11]. Chromatographic stationary phases are essentially developed for the separation of particular target solutes, *e.g.*, ion-exchange chromatography is for the separation of ions and size-exclusion chromatography is for polymers. However, secondary equilibria make it possible to separate analytes other than the essential solutes of the stationary phase. The author previously reported "micelle exclusion chromatography", wherein a size-exclusion chromatographic (SEC) stationary phase was employed for the separation of simple small ions in combination with micellar mobile phases [6–8]. Correspondingly, mobile phases containing polymeric additives were used for the SEC separation of simple ions in this work. It is known that stationary phases for SEC retain simple ions principally by electrostatic interaction between an ion and residual ionic groups in the stationary phase [12–14]. The selectivity obtained in the SEC separation of ions is therefore identical with that in ion-exchange chromatography in the absence of secondary equilibria, *e.g.*, the selectivity between inorganic anions is basically explained by the "Hofmeister series" [15]. Secondary equilibria, partitioning to the polymer phase or complexation with the polymer in mobile phases permit the selectivity to be altered.

Polymerized agents are excluded in terms of their effective sizes by the stationary phase, whereas small ions can penetrate into the inner part of the stationary phase, and probably interact with the stationary phase. If an ionic analyte interacts with a polymeric agent in mobile phases, the elution volume is reduced according to the partitioning to the polymer phase. A completely reversed elution order is expected if analytes interact weakly with the stationary phase.

EXPERIMENTAL

The chromatographic system consisted of a Tosoh Model CCPM or CCPD computer-controlled pump, a Tosoh CO-8000 column oven set at 25°C, a JASCO Model 875-UV UV–visible detector, a JASCO Model 830-RI refractive index (RI) detector and a Rheodyne injection valve equipped with a 100-μl sample loop. The elution of cations was monitored with RI detection and that of anions with UV detection Separation columns were Asahipak

0021-9673/91/$03.50

GS-300H and GS-320H [250 × 7.6 mm I.D. packed with poly(vinyl alcohol) gel, particle size 9 μm]. These stationary phases have different degrees of saponification and therefore show different hydrophobicities.

Methanol of analytical-reagent grade was distilled and stored over molecular sieves. Distilled methanol was redistilled daily before experiments. Distilled, deionized water was used throughout. Other reagents were of analytical-reagent grade and used as received.

Partial volumes of polymers ($\bar{v}$) were determined by measuring the density of the solution; $\bar{v}$ (PEG) and $\bar{v}$ (polybrene)

$$([-(CH_2)_6-\overset{+}{N}(CH_3)_2-(CH_2)_3-\overset{+}{N}(CH_3)_2-]_n\ [2Br^-]_n)$$

were determined as 0.8 and 0.7 ml/g, respectively.

RESULTS AND DISCUSSION

Retention model

In the present studies, the following equilibria are involved in the retention of an analyte (A):

$$A + P \rightleftharpoons AP \quad (1)$$

$$A + S \rightleftharpoons AS \quad (2)$$

where P and S refer to binding sites in a polymer and in the stationary phase, respectively. Because of difficulty in defining equilibrium constants (see below), partition coefficients for these above equilibria were used instead; K_s and K_p represent the partition coefficients of an analyte to the stationary phase and to the polymer phase, respectively. Partitioning of a polymer or a polymer–ion complex was not observed, and therefore was not taken into account in deriving the following equations.

In SEC, the retention volume of an analyte (V_r) can be described by the distribution coefficient (K_d), the volume of the external solvent (V_e) and the volume of the inner solvent, V_i:

$$V_r = V_e + K_d V_i \quad (3)$$

V_e and V_i are not constant for the stationary phase, but are changed by the effective size of the polymer employed in the mobile phase. Substitution of partition coefficients in eqn. 3 yields

$$1/K_d = V_i(1 + K_p\bar{v}C_p)/(V_i + V_sK_s) \quad (4)$$

According to eqn. 4, $1/K_d$ *vs.* C_p plots are linear, and permit the calculation of partition coefficients. This equation is analogous to that derived for micellar chromatography [5–8].

Polyethylene glycol as polymeric reagent for the separation of Ba^{2+} and alkali metal cations

Polyethylene glycol (PEG) is known to be capable of forming complexes with some hard metal ions such as alkali and alkaline earth metal ions [16–18]. The chemistry of this complexation has attracted fundamental and practical interest. The retention behaviours of alkali metal cations and Ba^{2+} were investigated here by adding PEG to methanolic mobile phases. Fig. 1 shows the changes in the retention with the concentration (C_p) of PEG 20 000 (the number following PEG represents the average molecular weight). Ba^{2+} is most strongly retained on GS-320H in the absence of PEG by electrostatic interactions; the elution order of other cations, $Li^+ < Na^+ < K^+ < Rb^+ < Cs^+$, correlates with that in cation exchange. However, retention of cations capable of forming stable complexes with PEG decreases on addition of PEG to the mobile phase, but the retention of Na^+ and Li^+ is little changed. Although Na^+ and Li^+ are known to form PEG complexes in solution or the solid state, the complexation was too weak to be detected in the present experiments. The elution order of Ba^{2+} and Na^+ or Li^+ is thus altered by adding PEG to the mobile phase.

Fig. 2 shows the plots based on eqn. 2 for determining K_p values for Ba^{2+}. Regardless of the molecular weight of PEG, linear plots are obtained. Partition coefficients and V_e values for PEG are summarized in Table I. The K_p values vary with the molecular weight of PEG. A Ba^{2+}–PEG complex is extracted into organic solvents as an ion pair with a lipophilic anion, and precipitates its phosphomolybdate, phosphotungstate or tetraiodobismutate salt. Such studies permitted the estimation of the stoichiometry of Ba^{2+}–PEG complexes; usually 1:10–12 [Ba^{2+}: oxyethylene (EO) units] are thought to be possible molar ratios [18]. If complexation by a particular binding site consisting of ten successive EO units does not affect complexation by the adjacent binding sites, the binding constant of eqn. 1 for Ba^{2+} can be determined. However, such values calculated from results depicted in Figs. 1 and 2 are

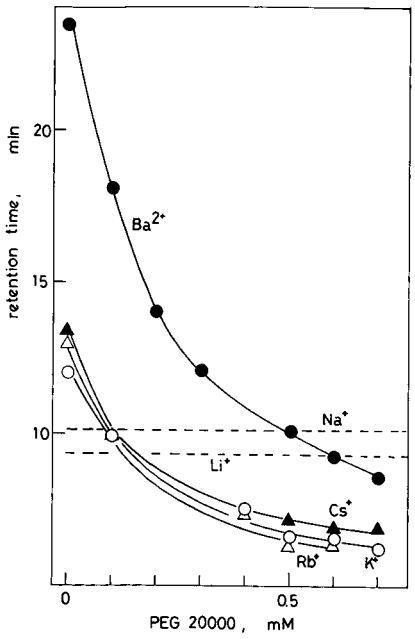

Fig. 1. Change in retention of cations with PEG 20 000 concentration in methanolic mobile phase. Mobile phase contains 0.1 *M* NH_4Cl. Stationary phase, GS-320H.

too small in comparison with literature values. The binding constant for Ba^{2+}–PEG 20 000 is, for example, estimated to be *ca.* 60 in this work, whereas that for Ba^{2+}–pentaethylene glycol was reported to be 200.

The complex formation ability of PEG is enhanced with increasing number of EO units; there is

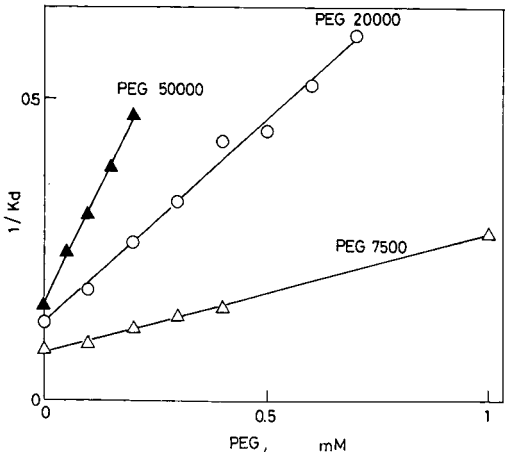

Fig. 2. $1/K_d$ *vs.* C_p plots for Ba^{2+} based on eqn. 2. Mobile phase contains 0.1 *M* NH_4Cl. Stationary phase, GS-320H.

TABLE I

PARTITION COEFFICIENTS (K_p) OF Ba^{2+} AND ALKALI METAL CATIONS TO PEG POLYMER PHASES

Polymer	Elution volume, V_e (ml)	K_p			
		Ba^{2+}	K^+	Rb^+	Cs^+
PEG 2000	6.43	980			
PEG 7500	5.27	440			
PEG 20 000	4.43	340	400	400	220
PEG 50 000	3.93	230			

a linear relationship between the molecular weight and the complex formation constant when the molecular weight is lower than 1000 [19,20]. It was reported previously that this enhancement of complex formation ability is caused by a statistical effect for relatively long PEG chains [20]. These results indicate that PEG of higher molecular weight shows a higher complex formation ability, which does not correlate with the present results. However, in the present experiments, we detected not only 1:1 complex formation but also multiple complex formation. Complex formation must affect the subsequent complexation of the adjacent binding sites. Kraus and Rogers [21] reported that the retention of PEG in SEC was changed by adding a salt to the mobile phase, and this effect was caused by the conformational change of PEG induced by the complex formation. The conformational changes and repulsion from metal cations trapped in PEG lead to unfavourable conditions for consecutive complexation. Highly multiple complex formation therefore becomes more difficult. In the present instance, the binding constant calculated from the corresponding partition coefficient is the mean value of consecutive complexation constants, and is smaller than the formation constant of a 1:1 complex.

Fig. 3 shows a chromatogram of some metal ions with PEG 20 000 as a mobile phase modifier. Although the separation efficiency is not high because of the narrow elution range, the elution order is unique. An advantage of the present method is thus not the efficiency but the unique selectivity.

Separation of anions

Despite much effort, common complexing agents for anions, comparable to crown ethers, cryptand,

Fig. 3. Separation of alkali metal cations and Ba^{2+} with secondary equilibrium SEC with methanol containing 0.75 m*M* PEG 2000. Stationary phase, GS-320H. Detection, RI ($8 \cdot 10^{-5}$ f.s.). Peaks: 1 = K^+; 2 = Cs^+; 3 = Ba^{2+}; 4 = Li^+; 5 = Na^+.

cycrodextrins, etc., have not been found. Electrostatic interaction should therefore be employed to separate anions by secondary equilibrium SEC with a polymeric mobile phase additive. A cationic polymer (polybrene) wss selected for this purpose. As it was difficult to determine the partition coefficients precisely because of the weak retention ability of the stationary phase, the stationary phase (GS-310H) pre-equilibrated with a hexadecyltrimethylammonium (HTA) bromide solution (8 m*M* in 50% methanol) was used. Partition coefficients obtained in 0.05 *M* sodium chloride solution are listed in Table II. K_p values for NO_2^- and IO_3^- could not be determined because of their weak affinity to polybrene.

TABLE II

PARTITION COEFFICIENTS (K_p) OF INORGANIC ANIONS TO POLYBRENE POLYMER PHASE AND COMPARISON WITH PARTITION COEFFICIENTS (K_m) TO HTA CHLORIDE MICELLAR PHASE

Partition coefficients were determined in 0.05 NaCl.

Anion	K_p	K_m[a]
NO_2^-	—[b]	74.3
NO_3^-	240	189
I^-	660	850

[a] From ref. 8.
[b] Not determined.

TABLE III

EFFECTIVE REDUCTION OF RETENTION TIMES WITH POLYMER MOBILE PHASE ADDITIVES IN ION-INTERACTION CHROMATOGRAPHY

Mobile phase composition	Retention times calculated			
	IO_3^-	NO_2^-	NO_3^-	I^-
69 m*M* NaCl	7.0	8.3	10.8	20.0
0.51 g/l polybrene with 50 m*M* NaCl	7.0	8.5	11.4	20.0
0.11 *M* NaCl	6.9	6.8	9.9	15.0
2.1 g/l polybrene with 50 m*M* NaCl	7.0	8.5	10.5	15.0

Soldi *et al.* [22] reported that cationic polyelectrolytes behaved like cationic micelles with respect to counter-ion binding, counter-ion-exchange selectivity, etc., and concluded that this type of polyelectrolyte could be a micelle-mimetic system. The author previously determined partition coefficients of inorganic anions to HTA chloride micelles under various ionic strength conditions. In 0.05 *M* sodium chloride solution, the partition coefficients of NO_2^-, NO_3^- and I^- to HTA chloride micelles were determined as 74.3, 189 and 850, respectively [8]. These values in general correlate with the partition coefficients to polybrene as shown in Table II.

In anion-exchange chromatography, elution of analytes is usually accelerated or retarded only by changing the salt concentration in the mobile phase. In such cases, there is a linear relationship between log k' and the logarithm of salt concentration. This means that a high salt concentration reduces the retention time of all analytes; this often causes poor resolution between analytes that are eluted rapidly. In Table III, retention times obtained, when mobile phases capable of eluting I^- at 15 and 20 min were used are given. A high salt concentration causes co-elution of NO_2^- and IO_3^-, whereas a high polymer concentration does not result in a poor separtion between these anions.

CONCLUSIONS

Polymeric mobile phases in secondary equilibrium SEC of ions are effective for modification of the

chromatographic selectivity, reduction of the total analysis time, the separation of small analytes on a size-exclusion column even when the stationary phase is intrinsically unable to retain the analytes and the evaluation of the partition behaviours of analytes to polymer phases. Polymeric additives thus provide versatility for SEC.

ACKNOWLEDGEMENT

The author thanks Asahi Chemical for generous gifts of separation columns.

REFERENCES

1 M. T. W. Hearn, *Ion-Pair Chromatography*, Marcel Dekker, New York, 1985.
2 D. W. Armstrong, F. Nome and L. A. Spino, *J. Am. Chem. Soc.*, 108 (1986) 1418.
3 T. Nakagawa, A. Shibukawa and T. Uno, *J. Chromatogr.*, 239 (1982) 685.
4 G. J. Sevenich and J. S. Fritz, *Anal. Chem.*, 55 (1983) 12.
5 D. W. Armstrong, *Sep. Purif. Methods*, 14 (1985) 213.
6 T. Okada, *Anal. Chem.*, 62 (1988) 1511.
7 T. Okada, *Anal. Chem.*, 62 (1988) 2116.
8 T. Okada, *J. Chromatogr.*, 538 (1991) 341.
9 J. P. Foley and W. E. May, *Anal. Chem.*, 59 (1987) 102.
10 B. L. Karger and J. N. LePage, in C. Horváth (Editor), *High Performance Liquid Chromatography: Advances and Perspectives*, Vol. 1, Academic Press, New York, 1980, p. 113.
11 W. R. Melander and Cs. Horváth, in Cs. Horváth (Editor), *High Performance Liquid Chromatography: Advances and Perspectives*, Vol. 2, Academic Press, New York, 1980, p. 113.
12 M. Shibukawa and N. Ohta, in P. L. Dubin (Editor), *Aqueous Size-Exclusion Chromatography*, Elsevier, Amsterdam, 1988, Ch. 4; and references cited therein.
13 T. G. Tji, H. J. Krips, W. J. Gelsema and C. L. de Ligny, *J. Chromatogr.*, 504 (1990) 403.
14 N. V. B. Marsden, *J. Chromatogr.*, 319 (1985) 247.
15 M. Nakagaki, in *Hyomen Jotai to Colloid Jotai*, Tokyo Kagaku Dojin, Tokyo, 1968, Ch. 1.
16 B. L. Haymore, J. D. Lamb, R. M. Izatt and J. J. Christensen, *Inorg. Chem.*, 21 (1982) 1598.
17 F. Vögtle and E. Weber, *Angew. Chem., Int. Ed. Engl.*, 18 (1979) 753.
18 J. Cross, in J. Cross (Editor), *Nonionic Surfactant—Chemical Analysis*, Marcel Dekker, New York, 1987, Ch. 2; and references cited therein.
19 J. W. Gokel, D. M. Goli and R. A. Schultz, *J. Org. Chem.*, 48 (1983) 2837.
20 T. Okada, *Macromolecules*, 23 (1990) 4216.
21 S. Kraus, L. B. Rogers, *J. Chromatogr.*, 257 (1983) 237.
22 V. Soldi, N. de M. Erismann, F. H. Quina, *J. Am. Chem. Soc.*, 110 (1988) 5137.

Journal of Chromatography, 586 (1991) 283–289
Elsevier Science Publishers B.V., Amsterdam

CHROM. 23 651

Membrane-based sample preparation device for the pretreatment of acidic samples prior to cation analysis by ion chromatography☆

Peter E. Jackson*,☆☆ and William R. Jones

Waters Chromatography Division of Millipore, 34 Maple Street, Milford, MA 01757 (USA)

(First received May 21st, 1991; revised manuscript received July 16th, 1991)

ABSTRACT

A hollow-fiber, membrane-based sample preparation device was investigated for the pretreatment of acidic samples prior to (separate) mono- and divalent cation analysis by ion chromatography. A device consisting of aminated DuPont Nafion fiber immersed in a counter-ion donating solution of either tetrabutylammonium hydroxide (for monovalent cations) or tetrabutylammonium borate (for divalent cations) can effectively neutralize samples with a pH as low as 1. No contaminants are added to the sample using this approach and quantitative recoveries are obtained for standard solutions of alkali metal and alkaline earth cations after passage through the device.

INTRODUCTION

The analysis of alkali metal and alkaline earth cations by ion chromatography (IC) is becoming accepted as an alternative to the more traditional atomic absorption and emission techniques [1,2]. The determination usually involves an ion-exchange separation followed by conductimetric detection. The eluents used for cation-exchange chromatography are typically mineral acids in the 1–10 m*M* range for monovalent cations [3] and amines at pH 4–6 for divalent cations [4]. Both of these separations are adversely affected in a number of ways by the injection of very acidic samples; shifts in analyte retention times occur due to the acidic sample acting as an internal eluent, the resulting large void peak may mask early eluting cations and the high ionic strength of the sample may result in poor peak shape due to column overloading. Dilution of the sample may not always be appropriate, especially if the analytes are present in the original sample at very low levels and direct addition of base to the sample is not generally permitted due to the contamination from the co-cation. A commonly used sample pretreatment method is to pass the sample through an anion-exchanger in the hydroxide form [5], however, this approach requires a relatively large sample volume and each portion of resin may only be used once per sample before regeneration and cleaning.

It has been demonstrated that hollow-fiber ion-exchange membranes offer advantages over resin-based ion-exchangers for sample pretreatment, especially for ease of use with small sample volumes [6]. In some applications they may also give better recoveries and less ionic contamination [7,8]. In this paper we discuss the use of a re-usable hydroxide form, anion-exchange, hollow-fiber device for the neutralization of acidic samples prior to mono- and divalent cation analysis by IC.

☆ Presented in part at the *1990 Pittsburg Conference and Exposition, New York, March 5–9, 1990.*

☆☆ Present address: Waters Chromatography Division of Millipore, Private Bag 18, Lane Cove, N.S.W. 2066, Australia.

0021-9673/91/$03.50

EXPERIMENTAL

Instrumentation

The liquid chromatograph consisted of a Waters Chromatography Division of Millipore (Milford, MA, USA) Model 510 pump, U6K injector, Model 430 conductivity detector and either a Waters 745 integrator or 840 data station. The analytical column used was a Waters IC-Pak Cation (50 × 4.6 mm I.D.) polystyrene-based cation exchanger. The eluent used for monovalent cation analysis was 2 m*M* nitric acid (Ultrex) operated at a flow-rate of 1.2 ml/min. The eluent used for divalent cation analysis was 0.5 m*M* ethylenediamine adjusted to pH 6.0 with nitric acid (Ultrex), also operated at a flow-rate of 1.2 ml/min. An IC-Pak Cation Guard Column (50 × 4.6 mm I.D.) was placed between the pump and injector for monovalent cation analysis. The eluents were prepared daily, filtered and degassed with a Waters solvent clarification kit.

Reagents

Water purified (18 MΩ) using a Millipore Milli-Q water purification system (Bedford, MA, USA) was used for all solutions. Ethylenediamine and boric acid were obtained from Sigma (St. Louis, MO, USA), Ultrex nitric acid and tetrabutylammonium hydroxide (30%) were obtained from J. T. Baker (Phillipsburg, NJ, USA), as were the analytical grade chloride salts used for the preparation of all the cation standards.

Hollow-fiber sample pretreatment device

The strong anion-exchange hollow-fiber (0.87 mm O.D. × 0.5 mm I.D.) was made from Nafion perfluorosulfonate fiber obtained from Permapure Products Inc. (Toms River, NJ, USA). The sample pretreatment device was a 150 cm length of this fiber immersed in the counter-ion donating (CID) solution which was housed in an 80-ml plastic sample storage bottle, similar to the experimental device previously described by Jones and Jandik [7]. A female plastic Luer-Lok fitting was attached at one end of the fiber to enable sample to be passed through the fiber with a disposable Luer-Tip syringe. The fiber was rinsed with 10 ml of Milli-Q water prior to each sample application.

RESULTS AND DISCUSSION

Selection of CID solution for monovalent cation analysis

For an anion-exchange fiber device to neutralize acidic samples, hydroxide ions in the CID solution are exchanged for anions in the sample (forming water in the sample) and ideally, no cations should cross the membrane. It has previously been demonstrated that the greater the molecular weight of the CID co-cation, the less leakage of the forbidden ions (cations in this case) through the membrane occurs [9]. For this reason, tetrabutylammonium hydroxide (TBAOH) was initially chosen as the CID solution as the relatively large, positive tetrabutylammonium ion would not be expected to penetrate the anion-exc hange membrane. The anion-exchange fiber was immersed in the CID solution (60 ml of 25 m*M* TBAOH) and initially rinsed with 20 ml of Milli-Q water. A standard monovalent cation mix (2.5 ml of a solution containing 1 ppm lithium, 5 ppm sodium, 10 ppm ammonium and 10 ppm potassium) was then passed through the fiber at approximately 1 ml/min with a disposable Luer-Tip syringe. The 2.5 ml of effluent from the device was collected in succesive 0.5 ml fractions and the monovalent cations in the fractions were quantitated using a nitric acid eluent and an IC-Pak C column with conductivity detection. Recoveries for the cations were calculated relative to the influent and are shown in Table I.

The results from Table I indicate that essentially

TABLE I

MONOVALENT CATION RECOVERIES OF SUCCESSIVE 0.5-ml FRACTIONS OF A FOUR-CATION MIX PASSED THROUGH THE HOLLOW-FIBER SAMPLE PRETREATMENT DEVICE WITH 60 ml OF 25 m*M* TETRABUTYLAMMONIUM HYDROXIDE AS THE CID SOLUTION

Fraction (ml)	Cation recovery (%)			
	Li	Na	NH_4	K
0.5	45.5	51.7	41.3	37.4
1.0	97.1	102.2	94.1	89.9
1.5	103.1	104.9	97.5	99.5
2.0	102.4	104.2	95.4	105.6
2.5	103.5	106.9	96.8	103.6

quantitative recoveries were attained within 1 ml of sample being passed through the hollow-fiber sample preparation device and that once the interstitial volume of the fiber had been flushed with sample, consistent recoveries were obtained for the cations in subsequent 0.5-ml fractions. The capacity of the hollow-fiber device to neutralize an acidic sample solution was then measured using a breakthrough technique. A 150 cm length of aminated Nafion fiber was placed in 60 ml of 25 m*M* TBAOH as the CID solution. Nitric acid (10 m*M*) was pumped through the fiber at 1.0 ml/min and 0.5-ml effluent fractions were collected every 2 min. The pH of the fractions was measured using a glass pH electrode and a breakthrough curve was plotted as % removal of acid *versus* volume of acid passed through the fiber. Defining effective ion-exchange capacity as 50% breakthrough gave a capacity of 0.137 mequiv. for the device, or expressed simply, the device could neutralize 13.7 ml of 10 m*M* nitric acid before 50% breakthrough was achieved. Unfortunately, this capacity was too low considering that the sample preparation device was intended to be used for the pretreatment of multiple samples. A number of fiber lengths, solution volumes and concentrations were investigated and it was found that a device prepared using a 150 cm length of animated Nafion fiber and 30 ml of 100 m*M* TBAOH as the CID solution provided reasonable capacity. The breakthrough curve was measured as described previously and to reach 50% breakthrough required 220 ml of 10 m*M* nitric acid, which corresponded to a capacity of 2.2 mequiv. for the device. Also, the shape of ion-exchange breakthrough curve was sigmoidal with this CID solution, as would be expected for a strong ion exchanger [10], which was not the case when the CID solution was 25 m*M* TBAOH.

The recoveries of the four cations through a device prepared using the aminated Nafion fiber and 30 ml of 100 m*M* TBAOH as the CID solution were then measured as described previously. The same monovalent cation standard (12 ml) was passed through the device with the first 2 ml being discarded to waste. The remaining 10 ml was collected in 1-ml fractions and the concentrations of the four cations in the fractions were determined using the conditions described previously. The average recovery for each of the four cations in the ten fractions was determined to be 98.8% for lithium, 103.2% for sodium, 94.6% for ammonium and 97.5% for potassium. The recovery for the ammonium ion was slightly low as it appeared that a small percentage was converted (or neutralized) to form ammonia in the fiber at a TBAOH concentration of 100 mM. Fig. 1 shows chromatograms of the monovalent cation standard before (a) and after (b) passage through the optimized hollow-fiber, sample preparation device. No breakthrough of the tetrabutylammonium through the fiber was evident in any of the chromatograms.

Selection of CID solution for divalent cation analysis

The optimized hollow-fiber, sample preparation device was then used to test the recoveries for a

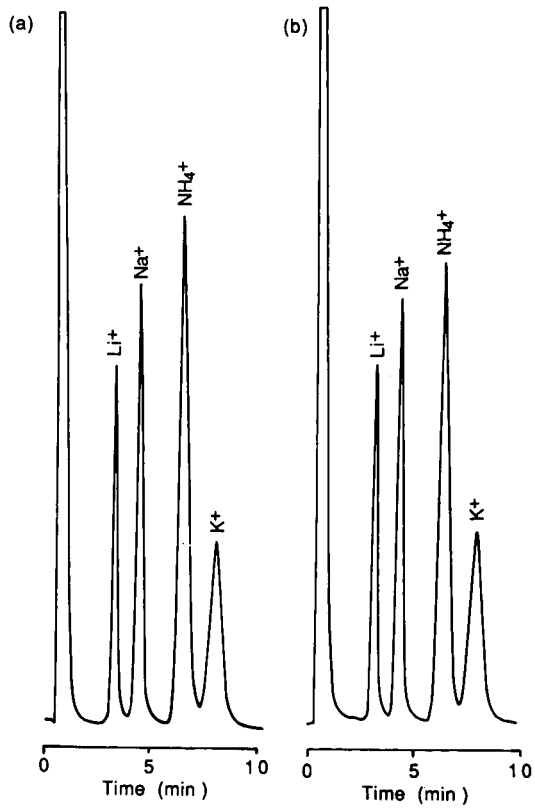

Fig. 1. Chromatogram of monovalent cation standard before (a) and after (b) being passed through an aminated fiber, hydroxide-based sample preparation device. Conditions: column, Waters IC-Pak Cation; eluent, 2.0 m*M* nitric acid; flow-rate, 1.2 ml/min; injection volume, 20 μl; detection, conductivity. Solutes: lithium (1 ppm), sodium (5 ppm), ammonium (10 ppm) and potassium (10 ppm).

mixture of divalent cations using the same procedure as for the monovalent cations. A divalent cation standard (2.5 ml of a solution containing 10 ppm magnesium, 20 ppm calcium, 30 ppm strontium and 80 ppm barium) was passed through the fiber immersed in a CID solution of 100 m*M* TBAOH at approximately 1 ml/min. The 2.5 ml of effluent was collected in successive 0.5-ml fractions and the divalent cations in the fractions were quantitated using an eluent of 0.5 m*M* ethylenediamine at pH 6.0 with an IC-Pak C column and conductivity detection. Recoveries for the cations were calculated relative to the influent and are shown in Table II. The recoveries for calcium, strontium and barium were essentially quantitative after 1 ml of the standard had been passed through the device, however poor recovery was obtained for magnesium. It appeared that magnesium was being precipitated as its hydroxide inside the fiber, hence the poor recovery.

It was evident that hydroxide was not appropriate for the CID solution due to the poor recovery obtained for magnesium. Sodium tetraborate was then investigated for use as the CID solution, however the sodium cation penetrated the anion-exchange fiber quite readily, resulting in a relatively large void peak which interfered with the quantitation of the magnesium peak. While the magnesium could not be accurately quantitated under these conditions the peak area was approximately quantitative. As the tetrabutylammonium cation did not appear to penetrate the fiber, it appeared that tetrabutylammonium borate would be an appropriate CID solution for the sample preparation device when being used for divalent cation analysis. A solution of tetrabutylammonium borate was prepared by the neutralization of 100 m*M* TBAOH with 100 m*M* boric acid to pH 10.7. The recoveries for the divalent cation standard after passage through the fiber immersed in a CID solution of 100 m*M* tetrabutylammonium borate were then measured for ten successive 1-ml fractions as described previously. The average recovery for each of the cations in the ten fractions was determined to be 95.0% for magnesium, 95.2% for calcium, 100.2% for strontium and 97.8% for barium. Fig. 2 shows

TABLE II

DIVALENT CATION RECOVERIES OF SUCCESSIVE 0.5-ml FRACTIONS OF A FOUR-CATION MIX PASSED THROUGH THE HOLLOW-FIBER SAMPLE PRETREATMENT DEVICE WITH 30 ml OF 100 m*M* TETRABUTYLAMMONIUM HYDROXIDE AS THE CID SOLUTION

Fraction (ml)	Cation recovery (%)			
	Mg	Ca	Sr	Ba
0.5	4.3	93.7	94.5	95.2
1.0	14.3	92.6	91.7	92.5
1.5	28.6	96.3	95.7	99.9
2.0	27.1	98.3	98.5	95.2
2.5	12.9	95.4	97.2	94.8

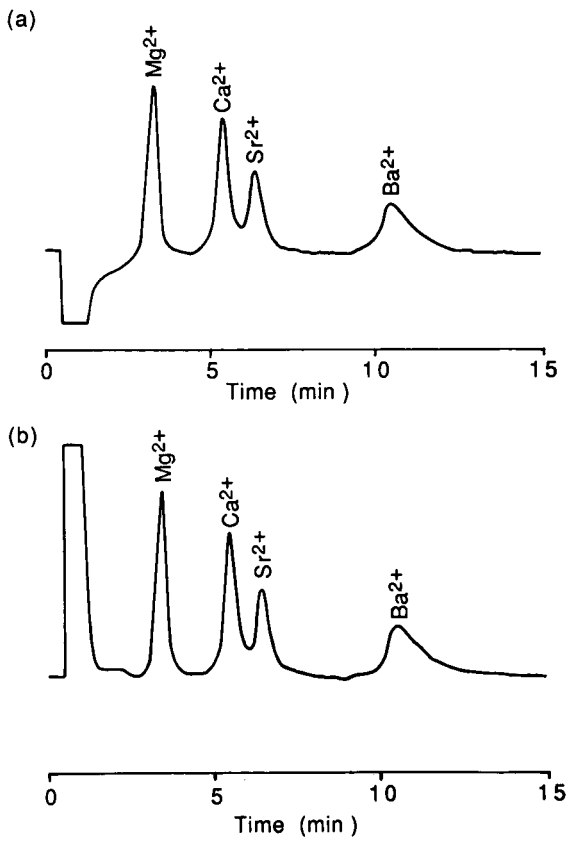

Fig. 2. Chromatogram of divalent cation standard before (a) and after (b) being passed through an aminated fiber, borate-based sample preparation device. Conditions: column, Waters IC-Pak Cation; eluent, 0.5 m*M* ethylenediamine adjusted to pH 6.0 with nitric acid; flow-rate, 1.2 ml/min; injection volume, 50 μl; detection conductivity. Solutes: magnesium (10 ppm), calcium (20 ppm), strontium (30 ppm) and barium (80 ppm).

chromatograms of the 10–80 ppm divalent cation standard before (a) and after (b) passage through the hollow-fiber, sample preparation device using tetrabutylammonium borate as the CID solution.

The capacity of the tetrabutylammonium borate hollow-fiber device to neutralize an acidic sample solution was then measured as described previously. The aminated Nafion was placed in 30 ml of a 100 m*M* tetrabutylammonium borate CID solution. Nitric acid was passed through the fiber, effluent fractions were collected and the pH of the fractions was measured using a glass pH electrode. The 50% breakthrough point required only 130 ml of 10 m*M* nitric acid in this instance, which corresponded to a capacity of 1.3 mequiv. for the device. This was significantly lower than the 50% breakthrough point for the corresponding sample preparation device which used 100 m*M* TBAOH as the CID solution. This lower capacity occurred as a result of the breakthrough curve for the borate device being less steep than was the case for the hydroxide-based device. This was to be expected as borate, being a weaker base than hydroxide, should give a less steep titration (or breakthrough) curve.

Application of hydroxide and borate-based devices for sample pretreatment

The application of a hydroxide-based, hollow-fiber device for the neutralization of acidic samples prior to monovalent cation analysis was then investigated. The device was prepared as previously using aminated Nafion fiber and 30 ml of 100 m*M* TBAOH as the CID solution. A monovalent cation standard (2 ml) containing 0.5 ppm lithium, 2.5 ppm sodium, 5 ppm ammonium and 5 ppm potassium made up in 50 m*M* nitric acid was passed through the device with the last 0.5 ml being retained for injection into the liquid chromatograph. Fig. 3 shows the chromatograms obtained (using a nitric acid eluent and an IC-Pak C column with conductivity detection) of the acidic standard before (a) and after (b) passage through the hydroxide-based sample preparation device. Fig. 3a clearly illustrates the deleterious effect of acidic samples on the chromatography of the monovalent cations as both lithium and sodium are eluted near the large void peak and all the cations exhibit poor peak shape due to column overloading. Fig. 3b shows that there was a dramatic improvement in the chromatography

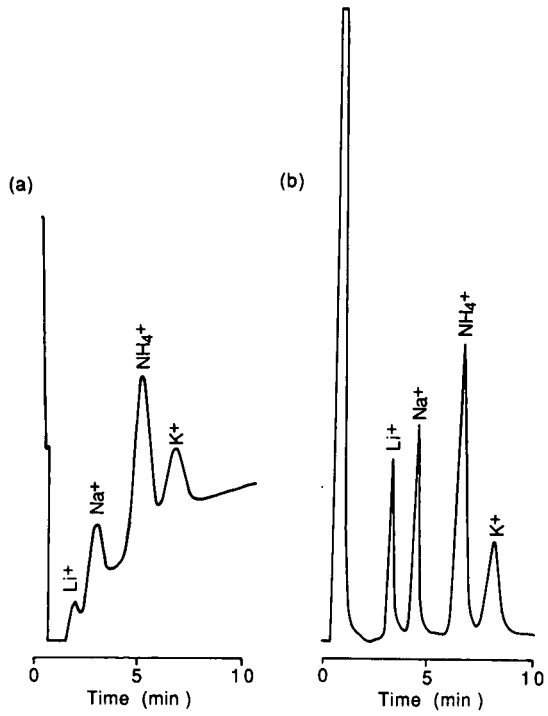

Fig. 3. Chromatogram of acidic monovalent cation standard before (a) and after (b) being passed through an aminated fiber, hydroxide-based sample preparation device. Solutes: lithium (0.5 ppm), sodium (2.5 ppm), ammonium (5 ppm) and potassium (5 ppm) in 50 m*M* nitric acid. Other conditions as in Fig. 1.

after the acidic standard was passed through the hydroxide-based sample preparation device. The pH of the acidic cation solution changed from 1.23 to 3.69 after being passed through the device; samples as concentrated as 100 m*M* acid could be treated before any significant disturbance of the chromatography was evident. A 2-ml sample of an acid copper plating bath, diluted 1:50, was then passed through the same device with the last 0.5 ml being retained for injection. Fig. 4 shows the chromatograms of the diluted acid bath before (a) and after (b) passage through the device. The hollow-fiber device enabled quantitation of the low levels of monovalent cations (0.87 ppm sodium, 0.26 ppm ammonium and 0.19 ppm potassium) in a sample which otherwise could not have been analyzed using the chromatographic conditions employed.

A borate-based, hollow-fiber device was then used for the treatment of acidic samples prior to divalent cation analysis. A divalent cation standard

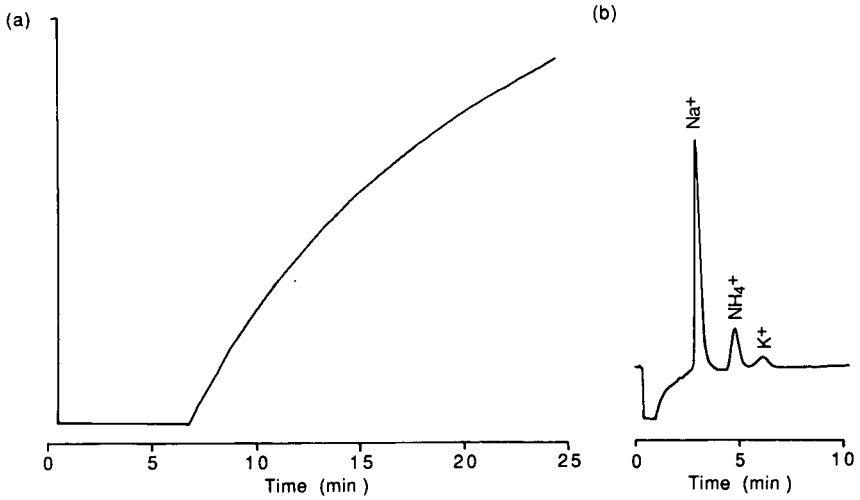

Fig. 4. Chromatogram of a diluted acid copper plating bath before (a) and after (b) being passed through an aminated fiber, hydroxide-based sample preparation device. Conditions as for Fig. 1 except: sample, acid copper plating bath diluted 1:50. Solutes: sodium (0.87 ppm), ammonium (0.26 ppm) and potassium (0.19 ppm).

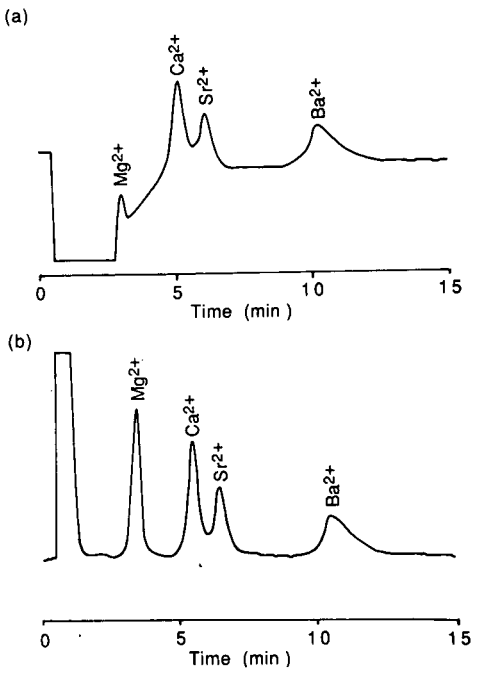

Fig. 5. Chromatogram of acidic divalent cation standard before (a) and after (b) being passed through an aminated fiber, borate-based sample preparation device. Solutes: magnesium (10 ppm), calcium (20 ppm), strontium (30 ppm) and barium (80 ppm) in 25 m*M* nitric acid. Other conditions as in Fig. 2.

of 10 ppm magnesium, 20 ppm calcium, 30 ppm strontium and 80 ppm barium acidified with 25 m*M* nitric acid was passed through the device (30 ml of 100 m*M* tetrabutylammonium borate as the CID solution) and 0.5 ml was retained for injection into the liquid chromatograph. Fig. 5 shows the chromatograms obtained (using an eluent of 0.5 m*M* ethylenediamine at pH 6.0 with an IC-Pak C column and conductivity detection) of the acidic standard before (a) and after (b) passage through the borate-based device. Again, there was a dramatic improvement in the chromatography after the acidic standard was passed through the hollow-fiber sample preparation device. The maximum acid concentration which could be tolerated with the borate-based device was approximately 40 m*M*. as the divalent cation analysis method was more affected by low pH samples than was the monovalent cation analysis approach. The borate-based device was also effective for neutralizing acidic monovalent cation solutions, however the capacity (and efficiency) of the device was not as high as a hydroxide-based device with a CID solution of equivalent concentration. The borate-based device was applied to the clean-up of a calcium salt lipid active drug. The drug formulation was only soluble in a solution of 30% tetrahydrofuran acidified to pH 4 with nitric acid. Fig. 6 shows the chromatograms of the drug formulation

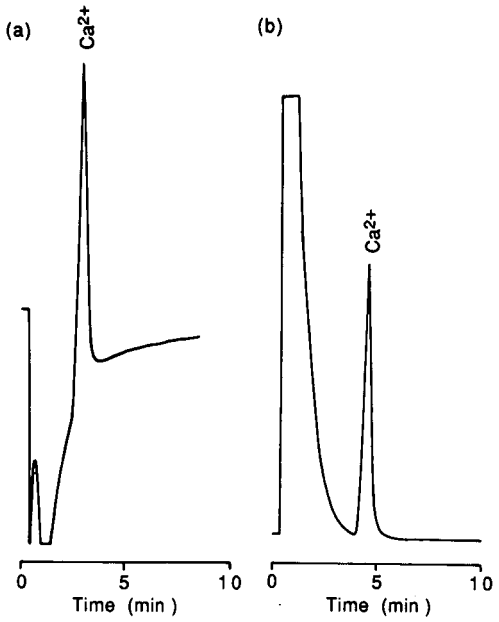

Fig. 6. Chromatogram of a calcium salt lipid active drug formulation before (a) and after (b) being passed through an aminated fiber, borate-based sample preparation device. Sample: dilution 1:100 in 30% tetrahydrofuran acidified to pH 4 with nitric acid. Solute: calcium (21.4 ppm). Other conditions as in Fig. 2.

solution before (a) and after (b) passage through the borate-based device. With the untreated sample, the calcium peak suffers interference from the large baseline disturbance at the void, making quantitation difficult. After passage through the sample preparation device, accurate quantitation was obtained for calcium, which was well resolved from the void peak.

CONCLUSIONS

The neutralization of acidic samples prior to the IC analysis of mono- and divalent cations can be accomplished using a sample pretreatment device consisting of 150 cm of aminated Nafion fiber immersed in a CID solution of either TBAOH or tetrabutylammonium borate. Minimal sample volumes are required (approximately 1 ml) for use with the hollow-fiber based device, no contaminants are added to the sample and quantitative recoveries are obtained for monovalent cations using a CID solution of tetrabutylammonium hydroxide (or borate), while quantitative recoveries are obtained for divalent cations using a CID solution of tetrabutylammonium borate. The device(s) can be prepared to have an ion-exchange capacity as high as 2 mequiv. which enables them to be used for the treatment of many samples with only a deionized water rinsed required between successive sample applications. Regenerated of an exhausted device can be achieved simply by replacing the CID solution and this sample pretreatment approach allows the IC determination of trace levels of mono- and divalent cations in samples with a pH as low as 1.

ACKNOWLEDGEMENT

The authors wish to thank Jack Kurtzman of Permapure Products Inc. (Toms River, NJ, USA) for the gift of the aminated Nafion fiber.

REFERENCES

1 P. R. Haddad and P. E. Jackson, *Ion Chromatography: Principles and Applications*, (*Journal of Chromatography Library*, Vol. 46), Elsevier, Amsterdam, 1990.
2 O. A. Shpigun and Yu. A. Zolotov, *Ion Chromatography in Water Analysis*, Ellis Horwood, Chichester, 1988.
3 R. C. L. Foley and P. R. Haddad, *J. Chromatogr.*, 366 (1986) 13.
4 P. R. Haddad and R. C. Foley, *Anal. Chem.*, 61 (1989) 1435.
5 *Ion Chromatography Laboratory Report No. 258*, Waters Chromatography Division of Millipore, Milford, MA, 1988.
6 J. A. Cox, E. Dabek-Zlotorzynska, R. Saari and N. Tanaka, *Analyst (London)*, 113 (1988) 1401.
7 W. R. Jones and P. Jandik, *J. Chromatogr. Sci.*, 27 (1989) 449.
8 P. E. Jackson and W. R. Jones, *J. Chromatogr.*, 538 (1991) 497.
9 Y. Hanaoka, T. Murayama, S. Muramoto, T. Matsuura and A. Nanba, *J. Chromatogr.*, 239 (1982) 537.
10 P. E. Jackson and P. R. Haddad, *J. Chromatogr.*, 389 (1987) 65.

Journal of Chromatography, 586 (1991) 291–295
Elsevier Science Publishers B.V., Amsterdam

CHROM. 23 581

Separation of some platinum(II) complexes by ionic strength gradient on a solvent-generated ion-exchange sorbent

M. Macka*, J. Borák and F. Kiss

Lachema, Research Institute of Fine Chemicals, Karásek 28, 62133 Brno (Czechoslovakia)

(First received April 8th, 1991; revised manuscript received June 17th, 1991)

ABSTRACT

The compatibility of ionic strength gradient with solvent-generated ion-exchange chromatography on an octadecylsilica sorbent was proven for a mobile phase containing octanesulphonate. Only a slight baseline shift was observed during the gradient of the phosphate buffer, even at 210 nm. An equilibration time of 3 min between the runs was sufficient to obtain retention times with a reproducibility better than 1%. The compounds separated were cisplatin, carboplatin and related neutral and cationic platinum(II) complexes, including transplatin and the aquation products of cisplatin.

INTRODUCTION

Several platinum(II) complexes have been used extensively in cancer treatment [1]. Mainly neutral or positively charged complexes exist in aqueous solutions of cisplatin [*cis*-diamminedichloroplatinum(II), CDDP] and carboplatin [*cis*-diammine-1,1-cyclobutanedicarboxylateplatinum(II), Pt-CBDCA] (Fig. 1), the aquation products of cisplatin [2–5], *trans*-diamminedichloroplatinum(II) [6] and triamminechloroplatinum(II) and tetraammineplatinum(II) complexes [6].

Cisplatin and the related platinum complexes have been separated chromatographically on reversed-phase sorbents dynamically modified with cationic surfactants [7]. However, positively charged molecules have generally negligible retentions under these conditions. The current methods for the separation of CDDP and its cationic aquation products or other cationic platinum(II) complexes use an octadecylsilica sorbent dynamically modified with an anionic surfactant [7–10]. Isocratic elution is most often used. Nevertheless, for the analysis of complicated mixtures gradient techniques should give a better separation and/or shorter analysis time [11].

The use of a gradient of organic modifier concentration has been reported [9,12,13]. As the distribution coefficients of surfactants depend strongly on the organic modifier concentration, a change in surfactant concentration in the stationary phase caused by the gradient results. Consequently poor reproducibility [13] and long equilibration times after each run [9] can occur. For this reason, the application of an ionic strength gradient should be more convenient, especially in separation systems where the ion-exchange mechanism dominates.

In ion-exchange chromatography (IEC) on classical ion exchangers, the use of an ionic strength gradient is essential [11]. The application of an ionic strength gradient (at constant concentrations of organic modifier and surfactant) to solvent-generated IEC is not so common. De Waal *et al.* [9] used a mixed gradient of increasing organic modifier concentration and increasing ionic strength. When using the related separation principle of ion-exclusion chromatography on octadecylsilica dynamically modified with sodium dodecyl sulphate, a

0021-9673/91/$03.50

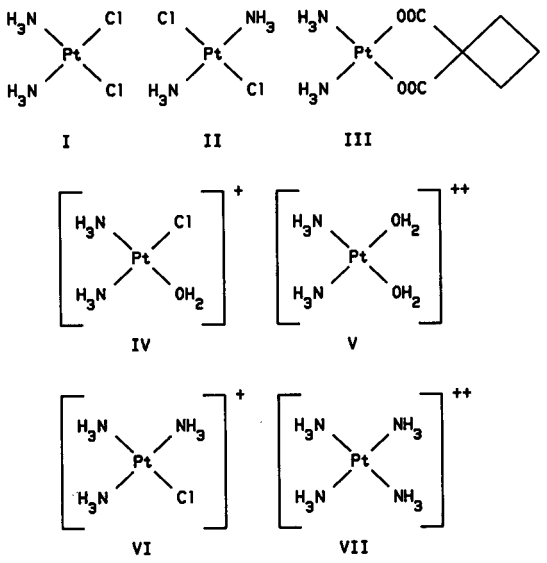

Fig. 1. Structures of platinum(II) complexes. I = *cis*-diamminedichloroplatinum(II) (cisplatin, CDDP); II = *trans*-diamminedichloroplatinum(II) (transplatin, TDDP); III = *cis*-diammine-1,1-cyclobutanedicarboxylateplatinum(II) (carboplatin, Pt-CBDCA); IV = *cis*-diammineaquachloroplatinum(II); V = *cis*-diamminediaquaplatinum(II); VI = triamminechloroplatinum(II); and VII = tetraammineplatinum(II).

sample-induced internal gradient of decreasing ionic strength has been applied [14].

This paper reports the separation of platinum(II) complexes applying an ionic strength gradient on an octadecyl column dynamically coated with octanesulphonate dissolved in the mobile phase. The convenience of the gradient technique is shown.

EXPERIMENTAL

Materials

Sodium octanesulphonate and sodium dihydrogenphosphate were of analytical-reagent grade (E. Merck).

Cisplatin and carboplatin were synthesized in the Research Institute of Pure Chemicals (Lachema). They were characterized according to USP XXII and the assay show them to be more than 99.5% pure by high-performance liquid chromatography (HPLC).

The *trans*-diamminedichloroplatinum(II) complex was prepared according to Chernyaev *et al.* [6]. It contained less than 0.1% CDDP and the assay was more than 99% pure (HPLC, internal normalization 210 nm).

The *cis*-diamminediaquaplatinum(II) complex was prepared according to Dhara [4]. To a CDDP solution (concentration 1 mg/ml), silver nitrate was added at a molar ratio of CDDP to Ag of 1:2.2. The mixture was shaken and allowed to stand overnight. After centrifugation the supernatant was acidified with nitric acid to pH 2 and stored in a dark bottle. The chromatogram showed one major peak (in addition to nitrate), an unknown peak (9%), and less than 1% CDDP and *cis*-diammineaquachloroplatinum(II).

The *cis*-diammineaquachloroplatinum(II) complex was prepared by modifying the above procedure so that silver nitrate was added to CDDP in molar ratio of only 1:1.1. The chromatogram showed (in addition nitrate) one major peak of 11% *cis*-diamminediaquaplatinum(II) and 16% CDDP.

Triamminechloroplatinum(II) was prepared by partial ammonolysis of CDDP (concentration 1 mg/ml) at 90°C. Small portions of 0.2 *M* aqueous ammonia were used so that pH did not exceed 7.5. The reaction was stopped when the amount of side-product formed, tetraammineplatinum(II), was about the same as that of the unreacted CDDP. The assay of triamminechloroplatinum(II) was approximately 40% pure (HPLC, internal normalization 210 nm); the remainder was CDDP and tetraammineplatinum(II).

Tetraammineplatinum(II) was prepared according to Chernyaev *et al.* [6]. The assay was more than 99% pure (HPLC, internal normalization 210 nm).

The HPLC method described here was used to characterize the reference samples of platinum complexes II and IV–VII.

Apparatus and chromatographic conditions

The system used was a Hewlett-Packard 1090 chromatograph consisting of an HP1040 diode-array detector and a DR5 binary pumping system. The samples were injected by a Rheodyne 7125 manual injection valve equipped with a 10-μl sample loop. For system control and data evaluation an HP-79994A workstation based on an HP-310 computer was used.

A stainless-steel column (4 × 250 mm) packed with Silasorb SPH C_{18}, $d(p)$ = 7.5 μm (Lachema) was used. The column temperature was 30°C.

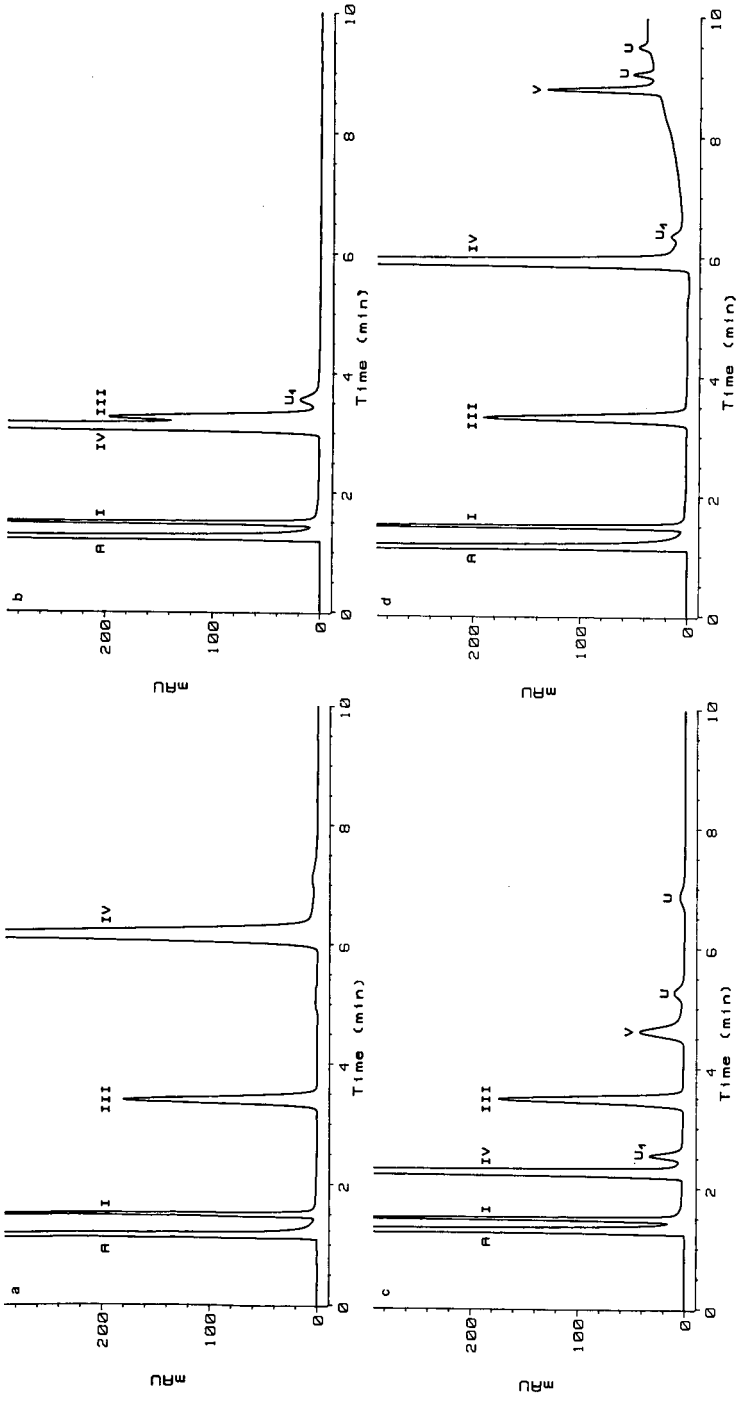

Fig. 2. Separation of Pt-CBDCA (III), CDDP (I) and its aquation products (IV, V). Isocratic analysis with a mobile phase containing (a) 10% B, (b) 30% B, (c) 50% B, (d) gradient analysis of standard mixture and (e) a real sample. Peak identification: A = anions; U, U_1 = unknown; for others, see Fig. 1. For other experimental conditions, see text.

The following mobile phases were used. Eluent A was sodium octanesulphonate (2 mM) and eluent B sodium octanesulphonate (2 mM), dihydrogen phosphate (0.5 M). The analyses were run under isocratic conditions (90% A and 10% B, pH 4.53) or with the following gradient: 10% B for t = 0 to t = 4 min, 10–100% B from t = 4 to t = 8 min, 100% B from t = 8 to t = 9 min, 100–10% B from t = 9 to t = 9.1 min.

The stationary phase was generated by pumping the mobile phase until the retention times were constant (about 4 h). The flow-rate was 1.5 ml/min, resulting in a column inlet pressure of about $9 \cdot 10^6$ Pa.

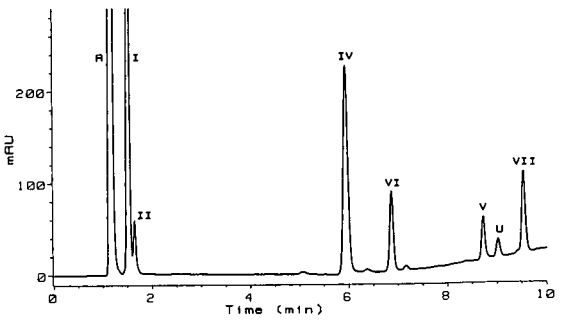

Fig. 3. Separation of a mixture of various amminechloroplatinum(II) complexes (I, II, VI and VII) and aquation products of CDDP (IV and V). Peak identification: A = anions; U = unknown; for others, see Fig. 1. For other experimental conditions, see text.

RESULTS AND DISCUSSION

The chromatograms for the isocratic separations of model mixtures of I, III, IV and V (Fig. 2) document the strong influence of ionic strength on the retention times of the charged complexes IV and V; complex V is not eluted within 10 min using a mobile phase containing less than 30% B. The retention of the uncharged complexes I and III remain almost unchanged. The standard mixture is baseline-resolved under isocratic conditions with a mobile phase containing 50% B (Fig. 2c). However, some real samples, e.g., the reaction mixture obtained by the reaction of CDDP and cyclobutanedicarboxylic acid, gave rise to unknown peaks interfering with complex IV. Gradient analysis allowed these interfering peaks from real samples to be separated (Fig. 2e). Another example in Fig. 3 shows the gradient separation of various amminechloroplatinum(II) complexes and the aquation products of CDDP.

It is important to determine whether there are changes in the surfactant sorption–desorption process caused by the ionic strength gradient which would shift the retention times in the next run or produce baseline disturbances when using photometric detection. Even at 210 nm only a slight baseline shift caused by the gradient was observed during the run. An equilibration time of 5 min between runs is sufficient to condition the system. The reproducibility of retention times for all the peaks detected was better than 1% during a single day.

An equilibration time of less than 3 min gave shorter and irreproducible retention times for the positively charged complexes. The required equilibration time can be related to washing out the higher concentration of the phosphate from the column rather than to changing the octanesulphonate concentration in the stationary phase, as the latter would require a much longer time. To estimate the extent of the change of the octanesulphonate stationary phase concentration as a result of the higher phosphate content in the mobile phase, a further experiment was carried out. The mobile phase, consisting of 100% B, was pumped for 2 h through the column, then the composition was switched to 10% B and after 5 min standard solutions of Pt-CBDCA, CDDP and its aquation products were injected. Only small changes in the retention times [maximum +5% for *cis*-diammineaquachloroplatinum(II) complex] resulted. Therefore it can be concluded that the change in the octanesulphonate stationary phase concentration with increasing phosphate concentration is not significant for the application of the ionic strength gradient.

This method was successfully applied to the analyses of samples related to technology development and to the analyses of drugs, including stability studies.

ACKNOWLEDGEMENTS

We thank Dr. K. Šlais, Dr. J. Chmelík and Dr. M. Holík for valuable discussions and critical reviews of

this work and Mrs. A. Doubravová and Mrs. M. Weisslampelová for assistance.

REFERENCES

1 M. Nicolini (Editor), *Platinum and Other Metal Coordination Compounds in Cancer Chemotherapy, Proceedings of the XVth ISPCC '87, Padua*, Martinus Nijhoff, Boston, 1988.
2 A. F. Le Roy, *Cancer Treat. Rep.*, 63 (1979) 231.
3 A. A. Hincal, D. F. Long and A. J. Repta, *J. Parent. Drug Assoc.*, 33 (1977) 107.
4 S. C. Dhara, *Indian J. Chem.*, 8 (1970) 193.
5 R. F. Greene, D. C. Chatterji, P. K. Hiranaka and J. F. Gallelli, *Am. J. Hosp. Pharm.*, 36 (1979) 38.
6 I. I. Chernyaev, A. V. Babaeva, V. A. Golovnya, O. E. Zvyagintsev, L. A. Nazarova and I. A. Fedorov (Editors), *Sintez Kompleksnykh Soedinenii Metallov Platinovoi Gruppy (Spravochnik)*, Izd. Nauka, Moscow, 1964.
7 G. M. Riley, L. A. Sternson, A. J. Repta and S. A. Slyter, *Anal. Biochem.*, 130 (1983) 203, and references cited therein.
8 P. J. Parsons, P. F. Morrison and A. F. Le Roy, *J. Chromatogr.*, 385 (1987) 323.
9 W. A. J. de Waal, F. J. M. J. Maessen and J. C. Kraak, *J. Chromatogr.*, 407 (1987) 253.
10 G. S. Baldew, K. J. Volkers and J. J. M. de Goeij, *J. Chromatogr.*, 491 (1989) 163.
11 P. Jandera and J. Churáček, *Gradient Elution in Column Liquid Chromatography*, Elsevier, Amsterdam, 1985, pp. 21 and 157.
12 N. D. Brown, R. B. Sweet, J. A. Kintzios, H. D. Cox and B. P. Doctor, *J. Chromatogr.*, 164 (1979) 35.
13 L. E. Vera-Avila, M. Cande and R. Rosset, *Analusis*, 10 (1982) 36.
14 K. Šlais, *J. Chromatogr.*, 469 (1989) 223.

Journal of Chromatography, 586 (1991) 297–301
Elsevier Science Publishers B.V., Amsterdam

CHROM. 23 618

Prediction of retention in gas–liquid chromatography using the UNIFAC group contribution method

III. Recent developments in UNIFAC

Gareth J. Price

School of Chemistry, University of Bath, Claverton Down, Bath BA2 7AY (UK)

(Received April 12th, 1991)

ABSTRACT

Previous publications have described the application of the UNIFAC group contribution method to the prediction of retention in chromatographic systems via their thermodynamic properties but concluded that the basic method was of limited, if any, use for this purpose. This paper describes results from some recent developments in UNIFAC including modifications to the equations and newly calculated parameter sets applied to the retention of a range of solvents in squalane, dinonyl phthalate, N-methylpyrollidone, poly (isobutylene) and poly(ethylene oxide) stationary phases.

The best results obtained predicted the specific retention volumes to about 10%, although this model could only be applied to a few systems; predictions for a wide range of polar and non-polar systems in the phases could be correlated to approximately 20–25%. While this level of accuracy is sufficient to allow prediction of elution orders in some systems, none of the modifications to UNIFAC in current use are suitable for widespread application to chromatographic systems.

INTRODUCTION

The selection of an appropriate stationary phase for a particular analysis is an ever present problem for the chromatographer and a number of strategies such as the use of retention indices [1] or "window diagrams" [2] have been developed. Previous papers [3,4] in this series have explored the use of UNIFAC for this purpose. This is a "group contribution" method [5,6] which takes the components of a solution, splits them into a number of functional groups and sums their properties to arrive at the overall solution activity, from which activity coefficients, γ_1, can be calculated. Comparisons of the infinite dilution activity coefficient, γ_1^∞, with chromatographic data can then be made in terms of the measured specific retention volumes, V_g^0, of the solutes in the stationary phases using the well known relationship [7],

$$\gamma_1^\infty = 273.15\ R/V_g^0\ P_1^0\ M_2 \quad (1)$$

where R is the gas constant, M_2 is the molecular weight of the stationary phase liquid, P_1^0 is the saturated vapour pressure of the solute at the column temperature and V_g^0 is the retention volume of the solute per gram of stationary phase fully corrected to standard temperature and pressure. However, when considering polymeric stationary phases as are commonly used in current gas–liquid chromatography (GLC), this definition is often complicated by lack of an accurate value for M_2. Thus, the activity coefficients, Ω_1^∞, are usually defined on a weight fraction rather than mole fraction concentration basis [8]. Thus,

$$\Omega_1^\infty = 273.15\ R/V_g^0\ P_1^0\ M_1 \quad (2)$$

where M_1 is now the molecular weight of the volatile solute.

0021-9673/91/$03.50

The UNIFAC method was developed by Fredenslund and co-workers [5,6] to allow the prediction of phase equilibria and other thermodynamic properties of solution in liquid mixtures and has been fully described in the previous papers [3,4]. The basic technique assumes two contributions to the thermodynamic activity in solution. The combinatorial (or entropic) part, a_1^C, accounting for differences in size and shape between the molecules in solution and a second, residual (or enthalpic) contribution to the activity, a_1^R, accounting for energetic interactions in solution. These two contributions were found to be adequate for small molecules solutions but, when working with polymer solutions, an extra contribution, a_1^{FV}, to the solvent activity arising from the well known free volume differences between polymers and solvents must be considered as shown by Oishi and Prausnitz [9]. The overall activity of the volatile solute in the solution is thus given by:

$$\ln a_1 = \ln a_1^C + \ln a_1^R + \ln a_1^{FV} \quad (3)$$

Roth and Novak [10] applied the original UNIFAC method to a number of systems and concluded that "... (it) can be used merely to give a rough estimation of relative retentions". We have applied both the original and free volume modified versions to a number of stationary phases such as squalane, dinonyl phthalate and similar compounds [3] and found that, in most cases, although the absolute values of V_g^0 were not accurately predicted, the correct order of elution was obtained although very wide discrepancies were found with polar stationary phases such as N-methylpyrollidone. Similar results were found [4] with polymer stationary phases including "OV" silicones and Carbowax. It was thus concluded that, in its current state of development, UNIFAC was of limited, if any, use to the chromatographer.

In this paper, results using some of the more recent developments to the UNIFAC method to estimate V_g^0 are described to determine whether they will allow retention to be predicted with greater accuracy and hence assist with the selection of appropriate systems for analyses where little or no experimental data is available. To test the range of applicability of the methods (if any), calculations were performed for five representative stationary phases covering a range of properties. Three were low-molecular-weight phases: squalane (SQ, non-polar), dinonyl phthalate (DNP, moderately polar) and N-methylpyrollidone (NMP, polar). Two polymeric phases, polyisobutylene (PIB, non-polar) and polyethylene oxide (PEO, polar) were also used. The experimental results were taken from the same sources as used previously [3,4] and were chosen from high-quality thermodynamic measurements made by GLC. As many solutes as possible were used, these having been described in our earlier papers [3,4]. From a chromatography point of view, studies of polydimethyl siloxane, the base material of the widely used OV series would have been useful but there are a very limited number of UNIFAC parameters available for silicones so that they were not considered here.

RESULTS AND DISCUSSION

Since a value of zero concentration cannot be used in the UNIFAC equations, a solute weight fraction of $1 \cdot 10^{-6}$ was used to simulate infinite dilution, the usual situation pertaining to analytical gas chromatography. The use of lower concentrations was found to have negligible effect on the results. The UNIFAC activity of the solute was calculated using the appropriate equations as outlined above in a BASIC program written for the IBM-PC and converted to an activity coefficient by dividing by the mole or weight fraction as appropriate to the system. Values of the specific retention volume were then calculated from eqns. 1 or 2 using physical property data from literature sources [11–13].

Values have been calculated for each of the modifications considered using both the original treatment and with the free volume correction proposed for polymer solutions. These will be designated "uni" and "uni-fv", respectively. The deviation of the predictions from the experimental results was calculated according to

$$\Delta V_g^0(\%) = 100 \{[V_g^0(\text{UNIFAC}) - V_g^0(\text{Expt.})]/ V_g^0(\text{Expt.})\} \quad (4)$$

Modifications to UNIFAC

The combinatorial factor. One of the main features of UNIFAC is that it assigns a zero interaction parameter between groups of similar chemical nature, *e.g.*, methyl and methylene. This results in no contribution to the activity coefficient, and hence retention volume, from residual or energetic factors.

Thus in hydrocarbon mixtures, the activity coefficient is composed solely of combinatorial terms together with, for UNIFAC-FV, a free volume term. Since even in such mixtures, *e.g.*, hexane–squalane, V_g^0 is not predicted well by the basic methods, we first tried some of the suggested modifications to the equation for the combinatorial activity, a_1^C, given in the original treatment by

$$\ln a_1^C = \ln \phi_1 + \phi_2 + (z\, M_1 q_1/2)[\ln (\theta_1/\phi_1) - 1 - (\phi_1/\theta_1)] \quad (5)$$

where M_1 is the solvent molecular weight, z is a "lattice coordination number", conventionally set to 10 to conform with recent practice [6,9] and ϕ_1 and θ_1 are the UNIFAC segment and surface area fractions, respectively, given for a weight fraction of solvent W_1 by:

$$\phi_1 = W_1\, r_1 \Big/ \sum_i W_i\, r_i; \quad \theta_1 = W_1\, q_1 \Big/ \sum_i W_i\, q_i \quad (6)$$

the molecular parameters r_i and q_i are found by summing the volume and surface parameters for each group which are listed in the literature [6], having been calculated from Van der Waals properties as given by Bondi [12].

By optimizing activity coefficients for a large number of alkane and alcohol systems, Thomas and Eckert [14] suggested an empirical alteration to eqns. 5 and 6 where

$$\phi_1' = W_1\, r_1^{3/4} \Big/ \sum_i W_i\, r_i^{3/4} \quad (6a)$$

and

$$\ln a_1^C = \ln \phi_1' + (1 - \phi_1') + (z\, M_1 q_1/2)[\ln (\theta_1/\phi_1) - 1 - (\phi_1/\theta_1)] \quad (5a)$$

Other workers [6] have suggested that a 2/3 power term gives better results than the 3/4 power term. As a third altenative, particularly for the polymeric stationary phases, we have also calculated V_g^0 using a Flory–Huggins (F–H) [15,16] type combinatorial term as used in polymer solution thermodynamics,

$$\ln a_1^C = \ln \varphi_1 + (1 - V_2^0/V_1^0)\, \varphi_2 \quad (6b)$$

where φ is the volume fraction of a species and V^0 its molar volume.

To compare these expressions, V_g^0 values were calculated for each solute-stationary phase system and the average absolute deviation for each phase is shown in Table I.

The final row of Table I shows the average percentage deviation for each of the modifications tested for all of the V_g^0 values calculated for each phase (58 systems in total). It can be seen that the free-volume corrected results give the best overall results except in the case of NMP, but none of these has a significant advantage over the original UNIFAC treatment. The individual results have not been included here for the sake of brevity, but even in the hydrocarbon mixtures there was no dramatic improvement in the results.

The energetic factor. Clearly then, modification of the combinatorial terms alone using the existing set of interaction parameters is insufficient to give a better prediction of chromatographic behaviour. The parameters were calculated by minimising the deviation of UNIFAC derived activity coefficients from the corresponding experimental values from a large number of vapour–liquid equilibrium systems over a range of concentrations. More recently, several tables of results derived exclusively from experimental data at infinite dilution have been compiled so that it seemed a potentially useful approach to investigate these. Two such parameter tables have been used here. However, it must be stressed that, as yet, these values are only available for a restricted range of systems so that any conclusions must, of necessity, be narrow.

Bastos *et al.* [17] used 11 500 results for vapour–liquid equilibria at infinite dilution covering 40

TABLE I

PERCENTAGE DEVIATION OF UNIFAC V_g^0 VALUES FROM EXPERIMENTAL FOR MODIFICATIONS TO THE COMBINATORIAL TERMS

See text for explanation of column headings.

	Original		$r^{3/4}$		$r^{2/3}$		F–H	
	uni	uni-fv	uni	uni-fv	uni	uni-fv	uni	uni-fv
SQ	17.8	14.4	19.5	18.4	20.2	19.0	29.9	19.5
DNP	19.9	8.7	22.6	11.5	27.0	16.1	35.3	12.9
NMP	41.1	55.0	38.4	53.0	35.4	50.7	92.3	52.9
PIB	99.9	16.3	90.6	15.8	83.4	15.2	61.8	22.5
PEO	32.1	14.0	33.2	22.5	35.9	27.6	22.2	32.7
All	40.4	18.7	34.4	19.2	58.5	23.2	44.6	25.3

groups to calculate values which allowed them to correlate most of the data with an average error of 20%. The original UNIFAC and UNIFAC-FV equations were used with these new parameters and the results are shown in Table II.

It can be seen by comparing values from Table II with those for the original UNIFAC model in Table I that this data set does not significantly improve the predictive value of the method. The "uni" results give a somewhat worse fit to the experimental data. While the free-volume corrected values are slightly closer to experiment using these interaction parameters, the improvements are not significant in terms of using the method to prodict chromatographic behaviour. In particular, the new interaction parameter for "CH_2O" as in PEO seems to be unsuitable for use with polymers.

The final modification to the UNIFAC method used here is to employ the set of parameters derived by Weidlich and Gmehling [18]. These workers changed the original UNIFAC model by incorporating a $r_i^{3/4}$ term into the expression for the combinatorial term as described above in addition to deriving a new set of interaction parameters that they claimed greatly improved prediction of infinite dilution activity coefficients and enthalpies of mixing. Rather than a single parameter to describe interactions between groups, three new constants for each group were calculated to take account of temperature, T, dependence,

$$\Psi_{ij} = \exp - (a_{ij}/T + b_{ij} + c_{ij}T)$$

where Ψ represents the UNIFAC interaction energy of group i with group j and a_{ij}, b_{ij} and c_{ij} are the tabulated interaction parameters. With this model, the average error in predicted γ_1^∞ for a wide range of small molecule systems was reduced from 21.1% to 5.3%.

Unfortunately, a number of groups needed for the systems studied here, *e.g.*, the ester group in DNP were not included in the new parameter table so that only a limited range of results could be obtained and these are shown in Table III. For each of SQ and PIB phases, values were calculated for nine solvents and the average deviation from experiment calculated.

As can be seen, this model does give somewhat improved predictions for the systems considered and gives the best fit to experimental results of all the models examined here. However, the best predictions give errors that are of the order of 10% and perhaps it is worth stressing that SQ is a somewhat "ideal" phase in which the best results would be expected. More detailed consideration awaits further development of the parameter sets.

Further discussion

The results presented here have only considered deviations from experimental results. Our previous work [3,4] has shown that, in general, the order of elution of a series of compounds can be reasonably well predicted using UNIFAC. The closest predictions show differences of around 10% from experimental and this is sufficient to lead to reversal of predicted elution order for compounds of different chemical nature and hence to limited application to chromatography.

The reasons for the deviation of the predictions of the UNIFAC models from experimental results can be ascribed to a number of sources. Firstly, any group contribution method must, by its nature, be approximate since it assumes that all functional groups will behave in the same manner irrespective of the molecule in which it occurs and that there are no proximity effects. Clearly, with more groups included, a larger number of environments could be

TABLE II

PERCENTAGE DEVIATION OF UNIFAC V_g^0 VALUES FROM EXPERIMENTAL FOR MODIFICATIONS TO THE UNIFAC INTERACTION PARAMETERS

	uni	uni-fv
SQ	20.5	11.7
DNP	22.1	7.4
NMP	41.1	35.1
PIB	94.6	14.6
PEO	108.2	53.3

TABLE III

PERCENTAGE DEVIATION OF UNIFAC V_g^0 VALUES FROM EXPERIMENTAL FOR METHOD OF WEIDLICH AND GMEHLING [18]

	uni	uni-fv
SQ	10.6	9.4
PIB	74.9	14.3

described but this would lead to an increasing number of parameters needed, reducing the flexibility of the technique.

The application of UNIFAC to chromatographic systems modifies two of the basic situations for which it was developed. The current application requires infinite dilution of solvent while the combinatorial expression and, with the exception of those of Bastos *et al.*, the interaction parameters are derived from results at finite concentrations. An alternative expression to eqns. 5 and 5a may be more appropriate at infinite dilution. However, even when used with interaction parameters derived solely from data measured at infinite dilution, UNIFAC does not yield satisfactory predictions of solution behaviour.

The largest source of error lies in the use of parameters derived using small molecule solutions for polymers. In solutions of low-molecular-weight components, all of the functional groups will be relatively accessible to each other so that it is valid to sum interactions over all groups in solution. However, it is well known that polymer chains can adopt a range of conformations so that a solvent molecule may not be able to interact with all polymer segments. Other reasons for the inability of UNIFAC to describe polymer solutions have been suggested [19–21]. While squalane and dinonyl phthalate are not polymers, they are relatively large molecules so that the same arguments may apply, albeit to a lesser extent. NMP is a much more polar molecule than the others considered and the large deviations found with this system are clearly indicative of the inability of UNIFAC to accurately deal with highly polar interactions which, due to specific interactions, can greatly influence a_1^C as well as a_1^R.

Clearly then, as it stands UNIFAC is unable to predict the retention behaviour of chromatographic systems with sufficient accuracy to justify its widespread use. Future developments that may change this would include the derivation of a parameter set exclusively from polymer systems. Although relatively few have been studied in detail, sufficient studies have been published to allow a preliminary test of this approach. To be useful, we estimate that UNIFAC, or a derivative of the approach, would have to predict V_g^0 to within 5% for a wide range of solvents. If this can be achieved, it would be a relatively straightforward extension to the computer program to calculate the amount of stationary phase or length of capillary column necessary to perform the separation assuming a reasonable efficiency. This seems some way in the future.

REFERENCES

1 W. McReynolds, *J. Chromatogr.*, 8 (1970) 685.
2 R. J. Laub and J. H. Purnell, *Anal. Chem.*, 48 (1976) 799.
3 G. J. Price and M. R. Dent, *J. Chromatogr.*, 483 (1989) 1.
4 G. J. Price and M. R. Dent, *J. Chromatogr.*, 585 (1991) 83.
5 A. Fredenslund, R. L. Jones and J. M. Prausnitz, *AIChE J.*, 21 (1975) 1086.
6 A. Fredenslund, J. Gmehling and P. Rasmussen, *Vapour–Liquid Equilibria using UNIFAC*, Elsevier, Amsterdam, 1977.
7 J. R. Conder and C. L. Young, *Physicochemical Measurement by Gas Chromatography*, Wiley, Chichester, 1977.
8 D. Patterson, Y. Tewari, H. P. Schreiber and J. E. Guillet, *Macromolecules*, 4 (1971) 356.
9 T. Oishi and J. M. Prausnitz, *Ind. Eng. Chem. Process Des. Dev.*, 17 (1978) 333.
10 M. Roth and K. Novak, *J. Chromatogr.*, 258 (1983) 23.
11 *Selected Values of the Properties of Hydrocarbons*, T.R.C. Data Project, Texas A&M University, College Station, TX, 1967.
12 A. Bondi, *Physical Properties of Molecular Crystals, Liquids and Glasses*, Wiley, New York, 1968.
13 S. Ohe, *Computer Aided Data Book of Vapour Pressures*, Data Publ. Co., Tokyo, 1976.
14 E. R. Thomas and C. A. Eckert, *Ind. Eng. Chem. Process Des. Dev.*, 23 (1984) 194.
15 P. J. Flory, *J. Chem. Phys.*, 9 (1941) 660.
16 M. L. Huggins, *J. Am. Chem. Soc.*, 64 (1942) 1712.
17 J. C. Bastos, M. E. Soares and A. G. Medina, *Ind. Eng. Chem. Res.*, 27 (1988) 1269.
18 U. Weidlich and J. Gmehling, *Ind. Eng. Chem. Res.*, 26 (1986) 1372.
19 A. Bekker, D. E. Knox and S. E. Sund, *J. Solution Chem.*, 16 (1987) 435.
20 G. J. Price and M. R. Dent, *Polymer*, 31 (1990) 1745.
21 L. A. Belfiore, A. A. Patwardhan and T. G. Lenz, *Ind. Eng. Chem. Res.*, 27 (1988) 284.

Journal of Chromatography, 586 (1991) 303–307
Elsevier Science Publishers B.V., Amsterdam

CHROM. 23 607

Activity coefficients at infinite dilution determined by gas–liquid chromatography

Organic solvents in Apiezon L

Aurelio Vega and José Coca*

Department of Chemical Engineering, University of Oviedo, 33071 Oviedo (Spain)

(First received November 22nd, 1990; revised manuscript received July 3rd, 1991)

ABSTRACT

Activity coefficients at infinite dilution were determined by gas–liquid chromatography for a variety of solutes using Apiezon L as the solvent (liquid phase). Two temperature ranges (60–90 and 150–190°C) were used depending on the boiling points of the solutes. Solubility parameters were determined from retention data for Apiezon L at 90 and 150°C using regular solution theory and Flory–Huggins interaction parameters.

INTRODUCTION

Activity coefficients at infinite dilution are important for the prediction of vapour–liquid equilibria, the selection of solvents in extractive distillation, the determination of solvent–solute interaction parameters and many other applications in chemical processes. Gas–liquid chromatography (GLC) has been used extensively to obtain these coefficients [1]. A limitation of the GLC technique is that the liquid phase (solvent) must have a low volatility. When a volatile solvent is used, a major problem is the entrainment of the stationary phase from the column. This problem can be overcome, at least to some extent, by non-steady-state [2] and reversed-flow [3] techniques. Another method is to use a combination of GLC and liquid–liquid chromatography (LLC) retention data, using a high-molecular-weight compound as the liquid phase in both instances [4].

Unlike the GLC method, only ratios of the activity coefficients of a solute at infinite dilution in the mobile and stationary phases can be obtained by LLC. To obtain solute activity coefficients in the volatile mobile phase it is necessary to use independent methods (*e.g.*, GLC) to determine the corresponding activity coefficient in the other phase.

In this work the activity coefficients for several solutes, such as aliphatic and aromatic hydrocarbons, alcohols, cresols, toluidines and picolines at infinite dilution were determined using Apiezon L as the solvent (stationary phase) in GLC. Measurements were made in two temperature ranges, 60–90 and 150–190°C, and the results are discussed with respect to regular solution theory.

These coefficients allow the determination of activity coefficients at infinite dilution in volatile solvents (such as acetonitrile or methanol) from LLC measurements [5].

THEORY

The specific retention volumes, V_g°, were determined by the following equation [6]:

$$V_g^\circ = (t_R - t_d)\left(\frac{273.15F}{T_0 w_s}\right)\left(\frac{p_0 - p_w}{p_0}\right)j \qquad (1)$$

0021-9673/91/$03.50

where t_R is the retention time, t_d the dead time, F the carrier gas flow-rate, T_0 the flow meter temperature, w_s the mass of the stationary phase, p_0 the outlet column pressure, p_i the inlet column pressure, p_w the vapour pressure of water at the flow meter temperature and j the James–Martin factor defined as:

$$j = \frac{3}{2}\left[\frac{(p_i/p_0)^2 - 1}{(p_i/p_0)^3 - 1}\right] \quad (2)$$

The activity coefficients at infinite dilution, γ_2^∞, were determined from the specific retention volume V_g° [7] by the equation:

$$\ln \gamma_2^\infty = \ln\left(\frac{273.15R}{V_g^\circ M_1 p_2^\circ}\right) - \frac{P}{RT}(2B_{12} - V_2^\circ) - \frac{p_2^\circ}{RT}(B_{22} - V_2^\circ) \quad (3)$$

where M_1 is the molecular weight of the liquid phase, p_2° the saturated vapour pressure of the pure solute, P the average column pressure, V_2° the molar volume of the pure solute, B_{12} the second virial coefficient of interaction between the solute and the carrier gas, R the gas constant, T the column temperature and B_{22} the second virial coefficient of the solute at temperature T.

At moderate pressures using helium as the carrier gas, B_{12} can be safely neglected and V_2° is also negligibly small compared with B_{22} [7]. Thus eqn. 3 can be approximated by:

$$\ln \gamma_2^\infty = \ln\left(\frac{273.15R}{V_g^\circ M_1 p_2^\circ}\right) - \frac{p_2^\circ B_{22}}{RT} \quad (4)$$

Solute vapour pressures were obtained from literature data [8] for the following solutes: *n*-propanol, isopropanol, butanol, benzene, toluene, heptane, *o*-, *m*- and *p*-cresols and *o*- and *m*-toluidines. The Antoine equation was used at pressures up to 1500 mmHg and the Harlacher–Braun equation [9] for higher vapour pressures, following suggestions given by Reid *et al.* [10]. B_{22} was estimated from the Beattie–Bridgeman correlation [11]:

$$B_{22}/V_c = 0.461 - 1.158(T_c/T) - 0.503(T_c/T)^3 \quad (5)$$

where V_c and T_c are the critical volume and the critical temperature of the solute, respectively.

The activity coefficient is commonly expressed as the contribution of two effects: the thermal contribution, γ_{th}^∞, resulting from molecular interactions of the compounds, and the athermal contribution, γ_{at}^∞, associated with the difference in size between the solute and solvent molecules:

$$\ln \gamma_2^\infty = \ln \gamma_{th}^\infty + \ln \gamma_{at}^\infty \quad (6)$$

The interaction parameter, χ^∞, is, according to the Flory–Huggins theory, related to $\ln \gamma_2^\infty$ by subtracting the Flory–Huggins size correction [12,13]:

$$\chi^\infty = \ln \gamma_2^\infty - \ln(1/r) - (1 - 1/r) \quad (7)$$

where r is approximated as the molar volume ratio of solvent to solute.

The size correction is usually taken as the value of $\ln \gamma_{at}^\infty$. The interaction parameter redefined as a "residual" free energy [14] involves the enthalpy and entropy effects:

$$\chi^\infty = \chi_H^\infty + \chi_S^\infty \quad (8)$$

and from the regular solution theory:

$$\chi_H^\infty = (V_2^\circ/RT)(\delta_1 - \delta_2)^2 \quad (9)$$

Substituting eqn. 9 into eqn. 8 and rearranging leads to:

$$\left(\frac{\delta_2^2}{RT} - \frac{\chi^\infty}{V_2^\circ}\right) = \left(\frac{2\delta_1}{RT}\right)\delta_2 - \left(\frac{\delta_1^2}{RT} + \frac{\chi_S^\infty}{V_2^\circ}\right) \quad (10)$$

A plot of the left-hand side of eqn. 10 *versus* the solute solubility parameter, δ_2, should yield a straight line from which the liquid phase solubility parameter, δ_1, can be obtained [14,15].

The molar excess thermodynamic properties of the solution are given by the equation:

$$\Delta G_e^\infty = RT \ln \gamma_2^\infty = \Delta H_e^\infty - T\Delta S_e^\infty \quad (11)$$

EXPERIMENTAL

Measurements were carried out with a Hewlett-Packard 5750 G gas chromatograph equipped with a thermal conductivity detector. A glass chromatographic column, 2.4 m × 0.25 in., was packed with Apiezon L (Hewlett-Packard) as the stationary phase, supported on Chromosorb P-AW (80–100 mesh); the liquid loading was 25.3% by mass. The column packing was prepared by dissolving a weighed amount of Apiezon L in trichloromethane and adding to the solution a known amount of the solid support. The slurry was gently dried in a rotary

evaporator with nitrogen flowing above the drying stationary phase. The percentage loading of the stationary phase on the packing material was determined gravimetrically.

Samples of 0.1 μl were injected after 8 h of thermal equilibration. The elution peaks were only slightly asymmetric, which is a good indication of infinite dilution conditions [16]. Furthermore, the stationary phase is not polar and a high liquid phase loading on a highly inert support was used. It can therefore be assumed that the experimental data are reasonably unaffected by adsorption phenomena. The results reported here are the average of at least three experimental determinations.

The solutes were supplied by Romil Chemicals (UK), Fluka (Switzerland) and Ega-Chemie (Germany), and were selected because they show a variety of functional groups and some of them are important coal by-products.

The molecular mass of the Apiezon L stationary phase, 1160, was determined using a Knauer osmometer.

RESULTS

Values of specific retention volumes, V_g°, and the activity coefficients are listed in Tables I and II for the various solutes with Apiezon L as the liquid phase.

TABLE I

SOLUTE-SPECIFIC RETENTION VOLUMES AND ACTIVITY COEFFICIENTS IN APIEZON L

Solute	60°C		70°C		80°C		90°C	
	V_g° (ml/g)	γ_2^∞	V_g° (ml/g)	γ_2^∞	V_g° (ml/g)	γ_2^∞	V_g° (ml/g)	γ_2^∞
Ethanol	12.7	3.45	10.0	2.75	7.9	2.34	6.7	1.90
n-Propanol	33.9	3.07	25.8	2.48	20.4	1.99	15.8	1.67
Isopropanol	18.9	2.87	14.6	2.29	11.8	1.85	9.6	1.53
Butanol	86.2	2.78	64.7	2.29	48.2	1.89	37.1	1.60
Benzene	134.8	0.28	101.1	0.27	75.6	0.27	57.7	0.26
Toluene	348.4	0.31	243.5	0.30	173.1	0.30	125.8	0.30
n-Pentane	26.6	0.36	20.4	0.36	16.1	0.35	12.9	0.34
n-Hexane	68.2	0.39	50.6	0.38	37.9	0.38	29.0	0.37
n-Heptane	171.9	0.42	122.2	0.41	87.6	0.40	65.0	0.39

TABLE II

SOLUTE-SPECIFIC RETENTION VOLUMES AND ACTIVITY COEFFICIENTS IN APIEZON L

Solute	150°C		160°C		170°C		180°C		190°C	
	V_g° (ml/g)	γ_2^∞	V_g° (ml/g)	γ_2^∞	V_g° (ml/g)	γ_2^∞	V_g° (ml/g)	γ_2^∞	V_g° (ml/g)	γ_2^∞
o-Xylene	58.1	0.30	46.6	0.29	37.4	0.29	30.4	0.29	25.0	0.28
m-Xylene	49.8	0.31	40.3	0.30	32.5	0.30	26.5	0.30	21.8	0.30
p-Xylene	49.5	0.30	40.1	0.30	32.3	0.30	26.4	0.30	21.7	0.30
o-Cresol	98.8	0.68	77.6	0.63	60.3	0.59	48.2	0.55	38.7	0.52
m-Cresol	107.2	0.87	84.2	0.80	67.3	0.73	53.1	0.68	42.8	0.63
p-Cresol	104.9	0.95	83.0	0.85	64.4	0.78	51.2	0.71	40.6	0.67
o-Toluidine	135.1	0.61	104.5	0.59	85.4	0.53	65.4	0.51	52.0	0.48
m-Toluidine	134.3	0.71	104.0	0.68	84.9	0.61	64.9	0.59	51.4	0.55
γ-Picoline	42.0	0.42	34.3	0.41	28.6	0.39	23.0	0.38	19.3	0.37

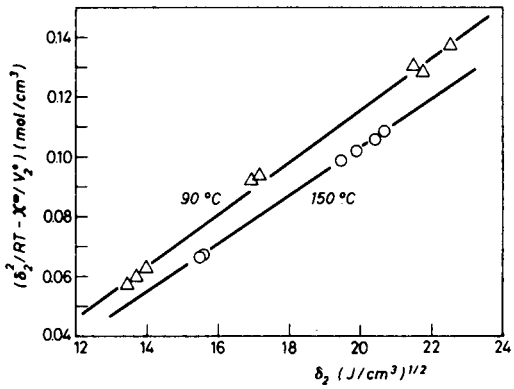

Fig. 1. Evaluation of the solubility parameters at 90 and 150°C for the solutes in Table I.

Two temperature ranges were selected based on the boiling point of the solutes. For the high-boiling-point compounds the temperature range 150–190°C was selected to obtain reasonable retention times; the retention times would have been too high in the range 60–90°C and would have been difficult to measure with the accuracy needed for thermodynamic calculations.

All the aliphatic and aromatic compounds used, with the exception of the aliphatic alcohols, showed very low activity coefficients ($\gamma_2^\infty < 1$), indicating the good solvation of these solutes in Apiezon L. The aliphatic alcohols have high γ_2^∞ values ($\gamma_2^\infty > 1$), which result from repulsive interaction due to the high polarity of the alcohols. This is also reflected by the high excess enthalpies, ΔH_e^∞, in Apiezon L (in the range 18.4–20.9 kJ/mol) compared with the values for aliphatic hydrocarbons (in the range 2.1–2.4 kJ/mol).

Fig. 1 shows the plot of the terms in eqn. 10 for the evaluation of the solubility parameters at 90 and 150°C. The values of the estimated solubility parameters for Apiezon L are 13.3 $(J/cm^3)^{1/2}$ at 90°C and 14.1 $(J/cm^3)^{1/2}$ at 150°C. Some workers [14,15] have reported similar results using different solvents.

SYMBOLS

B_{12} second virial coefficient of interaction between the solute and carrier gas (cm^3/mol)
B_{22} second virial coefficient for the pure solute (cm^3/mol)
F carrier gas flow-rate (cm^3/min)
ΔG_e^∞ excess partial molar Gibbs free energy at infinite dilution of the solute (J/mol)
ΔH_e^∞ excess partial molar enthalpy at infinite dilution of the solute (J/mol)
j James–Martin factor
M_1 molecular weight of stationary phase (g/mol)
p_i inlet column pressure (atm)
p_o outlet column pressure (atm)
p_w vapour pressure of water at the flow meter temperature (atm)
p_2° vapour pressure of the pure solute (atm)
P average column pressure (atm)
R gas constant (82.05 cm^3 atm/mol K in eqns. 3 and 4; 8.3144 J/mol K in eqns. 9–11)
r molar volume ratio of solvent to solute (V_1°/V_2°)
ΔS_e^∞ excess partial molar entropy at infinite dilution of the solute (J/mol K)
t_R retention time (min)
t_d dead time (min)
T column temperature (K)
T_c critical temperature of the solute (K)
T_0 flow meter temperature (K)
V_c critical volume of the solute (cm^3/mol)
V_g° specific retention volume (cm^3/g)
V_1° molar volume of the stationary phase (cm^3/mol)
V_2° molar volume of the solute (cm^3/mol)
w_s mass of stationary phase (g)

Greek letters

γ_2^∞ activity coefficient at infinite dilution of the solute
γ_{at}^∞ athermal contribution to the activity coefficient at infinite dilution of the solute
γ_{th}^∞ thermal contribution to the activity coefficient at infinite dilution
χ^∞ interaction parameter at infinite dilution
χ_H^∞ enthalpic contribution to the interaction parameter
χ_S^∞ entropic contribution to the interaction parameter
δ_1 solubility parameter of the solvent (stationary phase) $[(J/cm^3)^{1/2}]$
δ_2 solubility parameter of the solute $[(J/cm^3)^{1/2}]$

REFERENCES

1 J. R. Conder and C. L. Young, *Physicochemical Measurement by Gas Chromatography*, Wiley, New York, 1979.
2 A. J. Belfer and D. C. Locke, *Anal. Chem.*, 56 (1984) 2485.
3 N. A. Katsanos, G. Karaiskakis and P. J. Agathonos, *J. Chromatogr.*, 349 (1986) 369.
4 D. Locke, *J. Chromatogr.*, 35 (1968) 24.
5 A. Vega and J. Coca, *J. Liq. Chromatogr.*, 13 (1990) 789.
6 D. H. Desty and W. T. Swanton, *J. Phys. Chem.*, 65 (1961) 766.
7 D. H. Desty, A. Goldup, G. R. Luckhust and W. T. Swanton, *Gas Chromatography*, Butterworths, London, 1962, p. 67.
8 R. H. Perry and C. H. Chilton, *Chemical Engineering Handbook*, McGraw-Hill, New York, 6th ed., 1984.
9 E. A. Harlacher and W. G. Braun, *Ind. Eng. Chem. Process Des. Dev.*, 9 (1970) 479.
10 R. C. Reid, J. M. Prausnitz and T. K. Sherwood, *The Properties of Gases and Liquids*, McGraw-Hill, New York, 1977.
11 P. Alessi, I. Kikic, A. Papo and G. Torriano, *J. Chem. Eng. Data*, 23 (1978) 29.
12 P. J. Flory, *J. Chem. Phys.*, 10 (1942) 51.
13 M. L. Huggins, *Ann. N.Y. Acad. Sci.*, 43 (1942) 1.
14 G. DiPaola-Baranyi and J. E. Guillet, *Macromolecules*, 11 (1978) 228.
15 G. J. Price and J. E. Guillet, *J. Solution Chem.*, 16 (1987) 606.
16 J. R. Conder, *J. Chromatogr.*, 39 (1969) 373.

Journal of Chromatography, 586 (1991) 309–313
Elsevier Science Publishers B.V., Amsterdam

CHROM. 23 639

Measurements using gas chromatography with coelution and dual-isotope atomic emission detection

Lawrence C. Thomas*

Department of Chemistry, Seattle University, Seattle, WA 98122 (USA)

Terry L. Ramus

Western Analytical Research Laboratories, Dow Chemical Company, Pittsburg, CA 94565 (USA)

(Received May 13th, 1991)

ABSTRACT

Dual-isotope measurements by gas chromatography (GC)–atomic emission detection (AED) may enhance results for quantitative analyses. Adding a known amount of an isotopically labelled form of target analytes in each sample can compensate for irreproducibilities or uncertainties associated with sample pretreatments and sample loading. Similarly, fluctuations in AED temperatures, flows and interferants can be compensated via the added labelled forms if each target analyte and its isotopically labelled form coelute. Under these conditions they are subject to identical excitation environments and are measured from the same viewed volumes. Consequently, improved quantitative results may be attained by coelution in GC–AED methods which mimic isotope dilution.

INTRODUCTION

Atomic emission detection (AED) for gas chromatography (GC) is a powerful instrumental method which has become increasingly popular in recent years [1,2]. Multielement measurements may be made with GC–AED, providing high selectivities for a wide range of isotopes, typically spanning wide dynamic ranges with excellent sensitivities. GC–AED is usually accomplished passing eluates directly into a plasma region, typically into a microwave-induced plasma. Thus, the temporal selectivity of GC separations is supplemented by the spectral resolution of AED. Quantitative AED analyses can yield elemental concentrations for selected eluates and thereby it may be feasible to attain elemental composition and sometimes molecular formulae via GC–AED [3].

Methods using added isotopically labeled substances can be very powerful for quantitative measurements and comparisons [4–8]. Use of two or more radioactive isotopes is not uncommon and exploits the great selectivities and sensitivities of radioactivity measurements. However, potential health hazards and regulations make alternatives to use of radiolabeled materials attractive. Consequently, isotope selective methods which use non-radioactive substances, *e.g.*, mass spectrometry (MS) or atomic emission, are attractive options to radiometric procedures if appropriate isotope selectivities with sufficient corresponding sensitivities can be attained.

Dual-isotope methods with MS of equilibrated mixtures of target analytes with appropriate isotopically labeled compounds have been used for many years for accurate analyses [9]. Approaches which mimic isotope dilution and use GC–MS have gained general acceptance for use in important environmental analyses [10]. For those procedures an isotopically labeled form of each target analyte is added to samples before pretreatment and the two forms of each analyte thereby undergo essentially

0021-9673/91/$03.50

identical effects during sample preparation. Subsamples are then analyzed by GC–MS using accepted procedures, with each analyte and its isotopically labeled form being measured via their respective characteristic m/z values. However, the good selectivity and sensitivity of GC–MS is sometimes not sufficient to allow for reliable measurements via those approaches, partly due to variations in ionization efficiencies in the MS source, perhaps from variable source pressures or coeluting interferants: Ensuring coelution of both forms of each analyte can partially remedy effects of varying ionization efficiencies [8], even those caused by interferants or variable source pressures.

GC–AED is also compatible with dual-isotope techniques which mimic isotope dilution, partly because AED can concurrently measure two or more isotopes of elements from both the target analyte and its isotopically labeled form. Consequently, dual-isotope methods with GC–AED may compensate for variations in pretreatments and measurements, and ensuring coelution of both isotopic forms of target eluates can reduce variations in relative sensitivities for the two forms during the GC–AED measurements, as discussed below.

THEORY

If differently labeled forms, *e.g.*, h *vs.* d, of an analyte a elute into a microwave plasma and are atomized and excited in a thermally equilibrated region, then the observed characteristic radiant power emitted, P_E, will be related to the total number of eluate atoms, n_{ah} and n_{ad} (in atoms cm^{-3}), in the observed viewed volume, V, for form d is

$$P_{Ed} = A_{jid}(h\nu_{jid})V_d n_{jd} = A_{jid}(h\nu_{jid})V_d n_{ad} g_{jd} e^{-E_{jd}/kT}[Z(T)]^{-1} \quad (1)$$

where A_{ji} is the probability of excited state j undergoing deexcitation to state i, $(h\nu_{ji})$ is the energy of the emitted photon from the j to i transition, g_j and E_j are the statistical weight and energy for state j, $Z(T)$ is the partition function for the species, k is the Boltzmann's constant and T is the absolute temperature [11].

If both isotopic forms of the target analyte elute, then their respective radiant powers can be combined into a ratio for their corresponding j to i transition:

$$\frac{P_{Eh}}{P_{Ed}} = \frac{A_{jih}(h\nu_{jih})V_h n_{ah} g_{jh} e^{-E_h/kT}[Z(T)]^{-1}}{A_{jid}(h\nu_{jid})V_d n_{ad} g_{jd} e^{-E_d/kT}[Z(T)]^{-1}} \quad (2)$$

which, if both forms exist at the same temperature, simplifies to

$$P_{Eh}/P_{Ed} = (B_h n_{ah})(B_d n_{ad})^{-1} = (B_h B_d^{-1})(n_{ah}/n_{ad}) \quad (3)$$

where B_h and B_d are constants. Thus, their relative emission intensities from the viewed volumes would be directly proportional to the number of eluate atoms passing through the viewed volume at the time of observation.

The net measured signal for each power, $E_{measured} = E_{total} - E_{dark} - E_{background}$, will be related to the emission intensities through encoding transforms $E_m = E_{measured} = G(P_E)$, and they may be integrated over the duration of elution [11]. If the transforms are directly proportional to emission intensities, *e.g.*, $E_m = KP_E$ with K = a constant, then the relative integrated measured signals may be directly related to the respective integrated atom concentrations:

$$\frac{\int_{R-bw}^{R+bw} E_{mh}dt}{\int_{R-bw}^{R+bw} E_{md}dt} = \frac{\int K_h P_{Eh}dt}{\int K_d P_{Ed}dt} = \frac{\int K_h B_h n_{ah}dt}{\int K_d B_d n_{ad}dt} = K_h K_d^{-1} B_h B_d^{-1} \frac{\int n_{ah}dt}{\int n_{ad}dt} \quad (4)$$

where R is the analytes' retention time, w is the corresponding peak width, b is a constant, and t is time.

If mass flow patterns are constant or reproduced, then the ratio of integrated net signals should be directly proportional to the integrated concentrations of the eluates leaving the column, and thereby to the sample concentrations. Of course, non-equilibrium thermal conditions, irreproducible mass flows through viewed volumes and variable emission signal sensitivities could cause deviations from the direct relation between relative integrated net signals and relative sample analyte concentrations.

Coelution of the two forms of each analyte can force flow patterns, temperatures, etc., to be identical for the two forms even if potential interferants are present, because they would exist in the same

environment concurrently. Therefore, coelution may appreciably enhance the direct proportionality between relative concentrations and integrated areas, and thereby improve results for GC–AED analyses.

The direct proportionality between relative integrated responses, *e.g.*, chromatogram areas, and relative concentrations indicates compatibility with dual-isotope internal standard chromatography methods, for which each added internal standard is chemically identical but isotopically different than its corresponding target analyte. Moreover, the use of isotopically labeled forms of each target analyte as internal standards may also allow for: (a) possible quantitative measurements or comparisons of selected analytes without necessarily identifying each analyte [5,6], (b) for special comparisons to be made between reaction products in dual-isotope experiments [6] and (c) for effects of impurities or isotope effects to be assessed in dual-isotope reaction experiments [7].

EXPERIMENTAL

Reagents

Anthracene and decadeuteroanthracene were purchased from Aldrich, both at >99% purity. All solvents were Mallinkrodt ChromAR grade, and helium carrier gas was >99.9999% pure.

Apparatus

A Hewlett-Packard Model 5921A atomic emission detector interfaced to a Hewlett-Packard Model 5890 Series II gas chromatograph with a Model 7673 autosampler was used, controlled and monitored by a Hewlett-Packard Model 9000 computer via ChemStation software written especially for the Model 5921A GC–AED system. Emission intensities at 656.302 nm and 656.039 nm were monitored for hydrogen and deuterium, respectively. A DB-1 column, 25 m × 0.2 mm I.D. with 0.17-μm stationary phase thickness was used for all separations described herein.

Procedures

The on-column injection port was used with 1.0 μl volumes of sample for each separation and measurement. The injector was maintained at 150°C during injection, held at 150°C for 1 min then increased to 250°C at 100°C min^{-1}, maintained at 250°C for 5 min and then decreased to 200°C for the rest of each elution. Eluates were separated via a temperature program: isothermal at 150°C for 5 min and then increased at 20°C min^{-1} to 250°C. The temperature program resulted in moderate separation of the nonanthracene eluates but yielded coelution of the isotopic forms of the anthracene target analyte.

Separate solutions of natural isotopic abundance anthracene and decadeuterated anthracene were made at 0.002 *M* in methanol, *i.e.*, nearly saturated at 25°C, for these investigations. Test solutions were made by mixing and diluting the 0.002 *M* solutions, yielding solutions spanning 10^{-5} to $2 \cdot 10^{-3}$ *M* and varying in relative concentrations, $C_{anthracene}/C_{decadeuteroanthracene}$, between $5.6 \cdot 10^{-3}$ and $1.8 \cdot 10^{2}$. Triplicate replications for these solutions were analyzed by GC–AED via the temperature program described above.

RESULTS AND DISCUSSION

Moderate resolution separations via the temperature program essentially coeluted anthracene with [$^2H_{10}$]anthracene (see Fig. 1). Unfortunately, spectral resolution between deuterium and hydrogen was not complete, allowing interference into the hydrogen measurement with the presence of deuterium; thus, deuterium-caused interferences were subtracted from hydrogen results to calculate the net measured responses due to hydrogen. However, no interferences due to hydrogen were observed for deuterium even at $C_{hydrogen}/C_{deuterium}$ ratios of 180:1 and for deuterium concentrations diminishing below the limit of detection, $1.7 \cdot 10^{-11}$ mol [$^2H_{10}$]-anthracene, *i.e.*, $1.8 \cdot 10^{-10}$ mol deuterium, by the GC–AED system.

Sensitivities for both anthracene via hydrogen emission and for [$^2H_{10}$]anthracene via deuterium emission varied somewhat with concentration, as shown by curvature and slope $\neq 1.0$ in the log–log relations of their calibration plots, as expected when several orders of magnitude in concentrations are spanned (see Fig. 2). The sensitivity uncertainties were typically about ±20% relative standard deviation (R.S.D.) ($n = 3$) and may result, in part, from variations in effective plasma temperatures or variable flow patterns which fluctuate from run to run.

Relative sensitivities for the two coeluted forms, however, varied directly with their relative con-

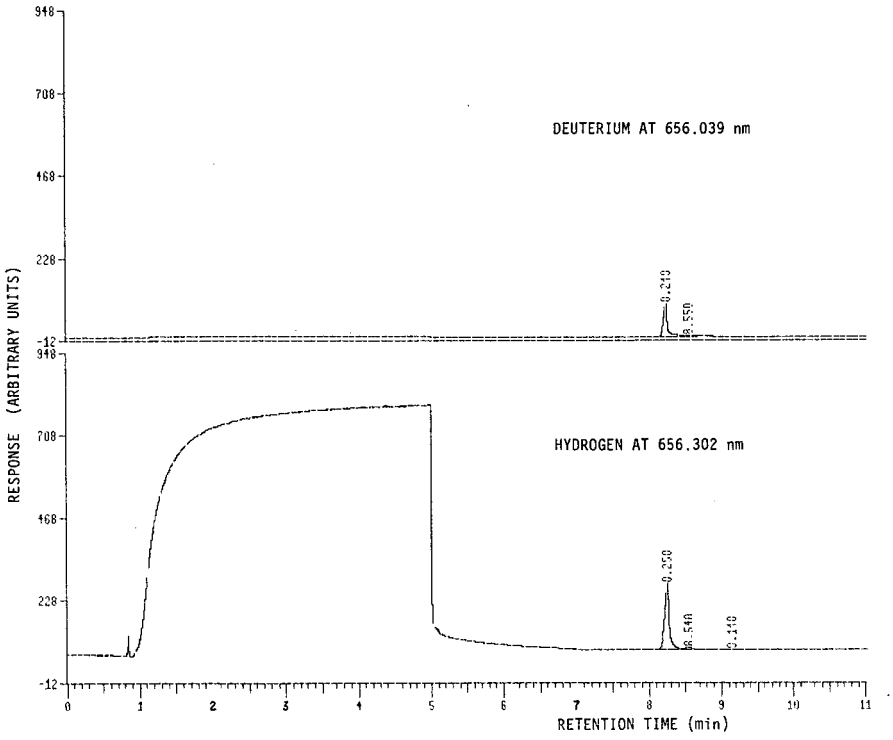

Fig. 1. GC–AED chromatograms for coelution of $3.9 \cdot 10^{-8}$ g anthracene and $3.4 \cdot 10^{-7}$ g [$^2H_{10}$]anthracene, *i.e.*, $2.2 \cdot 10^{-9}$ g hydrogen and $3.6 \cdot 10^{-8}$ g deuterium.

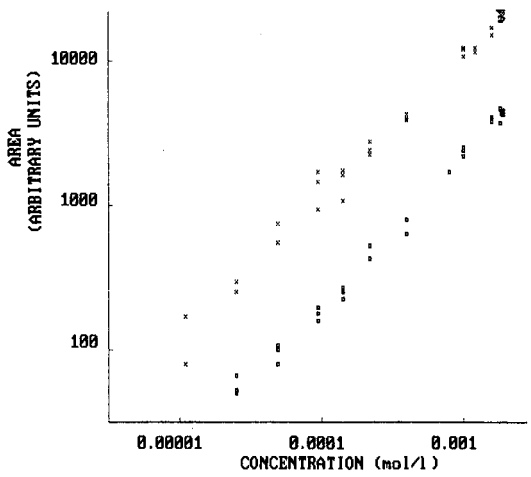

Fig. 2. Calibration plots for GC–AED measurements of anthracene (×) and [$^2H_{10}$]anthracene (□), using 1-μl injections of solutions varying in concentrations between limits of reliable measurement of about 10^{-5} mol l^{-1} to the limit of solubility of $2 \cdot 10^{-3}$ mol l^{-1}.

centrations, spanning a linear dynamic range of nearly four orders of magnitude from $C_{\text{anthracene}}/C_{\text{decadeuteroanthracene}}$ ratios of $5.6 \cdot 10^{-3}$ to $8 \cdot 10^{1}$ (see Fig. 3). Moreover, precisions for the relative sensitivities were excellent, typically varying between $\pm 3\%$ and $\pm 12\%$ R.S.D. ($n = 3$), becoming worse near the limits of detection, as expected.

Consequently, GC–AED measurements of coeluted deuterated and normal hydrogenated anthracene is compatible with dual-isotope procedures which mimic isotope dilution. By adding a small-but-reliably-measured amount of deuterated anthracene to samples containing normal anthracene one may expect the deuterated form to work as a reliable internal and recovery standard, as well as compensating for variable excitation conditions, making more accurate and precise determinations feasible. The direct proportionality between relative sensitivities and relative concentrations is an important condition for valid use of internal standard methods

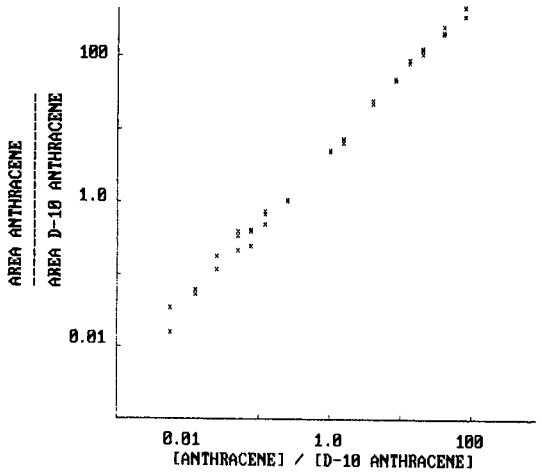

Fig. 3. Relative response *vs.* relative concentration relations for GC–AED measurements of anthracene and [$^2H_{10}$]anthracene (D-10 anthracene), using 1-μl injections of solutions varying in relative concentrations, $C_{anthracene}/C_{decadeuteroanthracene}$, between 80:1 and $5.6 \cdot 10^{-3}$:1.

for quantitative analyses with chromatography; coelution with dual-isotope internal standard procedures can be especially reliable for such determinations.

In general, GC–AED systems should be compatible with a variety of dual-isotope procedures in addition to those which mimic isotope dilution, perhaps with other compatible isotope pairs. For example, dual-isotope GC–AED methods may be useful for measurements or comparisons of reaction product concentrations [5,6] and for assessing effects of impurities or isotope effects upon reaction product formations [7]. Moreover, coelution of the isotopically different forms of target analytes may substantially compensate for variations in flows through the viewed volume and for variations in excited-state populations resulting from fluctuations in plasma conditions from run-to-run or within runs, thereby potentially improving GC–AED measurement accuracy and precisions which may be evident in higher-resolution GC separations.

ACKNOWLEDGEMENTS

We thank Dow Chemical Company for use of facilities and other support of this work, and we thank the National Institutes of Health for their support of earlier related work via grant 1R15 GM36273-01A1 which stimulated basic developments investigated herein.

REFERENCES

1 P. N. Kelibar, H. Ibrahim and D. J. Gerth, *Anal. Chem.*, 62 (1990) 184R.
2 R. E. Clement, F. I. Onuska, G. A. Eiceman and H. H. Hill, Jr., *Anal. Chem.*, 62 (1990) 415R.
3 D. B. Hooker and J. DeZwaan, *Anal. Chem.*, 61 (1989) 2207.
4 T. R. Roberts, *Radiochromatography*, Elsevier, Amsterdam, 1978.
5 L. C. Thomas and T. L. Ramus, *Anal. Chim. Acta*, 154 (1983) 143.
6 L. C. Thomas and C. L. Wood, *J. Chromatogr.*, 522 (1990) 117.
7 L. C. Thomas and T. L. Ramus, *Anal. Lett.*, 17 (1984) 2001.
8 L. C. Thomas and W. Weichmann, *J. Chromatogr.*, 587 (1991) 255.
9 A. V. Grosse, S. G. Hindin and A. D. Kirshenbaum, *Anal. Chem.*, 21 (1949) 386.
10 *Methods 1624 and 1625, Revs. C*, US Environmental Protection Agency, Washington, DC, 1988.
11 J. D. Ingle and S. R. Crouch, *Spectrochemical Analysis*, Prentice-Hall, Englewood Cliffs, NJ, 1988.

Journal of Chromatography, 586 (1991) 315–322
Elsevier Science Publishers B.V., Amsterdam

CHROM. 23 604

Trapping system for trace organic volatiles

Tomáš Jursík, Karel Stránský* and Karel Ubik

Institute of Organic Chemistry and Biochemistry, Czechoslovak Academy of Sciences, Flemingovo nám. 2, 166 10 Prague 6 (Czechoslovakia)

(First received March 27th, 1991; revised manuscript received July 4th, 1991)

ABSTRACT

A technique is described for the collection and concentration of volatile compounds produced by plants, insects, animals and other materials. The method is a modification of the continuous-flow system based on absorption of volatiles in a low amount of solvent at low temperature. The advantages and disadvantages of the technique used are described in detail.

INTRODUCTION

So far several different techniques have been used for the trapping and concentration of volatile substances: (1) cold trapping and cryogenic trapping (*e.g.* ref. 1–3); (2) trapping on a solid sorbent (*e.g.* refs. 4–7); (3) trapping in a liquid stationary phase coated on a solid support [8–13] and (4) chromatography evaporation of a solvent in a capillary tube [11,14,15]. A short survey of preconcentration methods in capillary gas chromatography has been published by Roeraade [16] and an excellent review concerning headspace–gas chromatographic (GC) analysis of medicinal and aromatic plants and flowers has been published recently by Bicchi and Joulain [17]. So far trapping on a solid sorbent is still the most widespread technique, the properties and use of which have been reviewed by Golub and Weatherston [1], Núñez *et al.* [18] and Günther *et al.* [19].

For an analysis by means of GC, gas chromatography–mass spectrometry (GC–MS), gas chromatography–Fourier transform infrared spectroscopy (GC-FT-IR) or gas chromatography–electroantennography (GC-EAG) it is indispensable to release the volatile compounds from the sorbent. Basically, there are two methods of doing this.

(a) The substances may be washed out with a solvent (if a small amount of solvent is used a quantitative washing out may not be achieved, while when larger amounts of solvent used the eluate must be concentrated, which may lead to quantitative changes in the proportion of the most volatile components.

(b) Volatile substances may be desorbed by heating the sorbent for several minutes, which is usually followed by cryofocusing at the beginning of the chromatographic capillary column, where the substances may not be retained quantitatively [20].

For a thermal desorption of the volatiles, microwave radiation has also been used successfully, but this method has limitations with respect to the choice of sorbent [21,22]. In addition to this, decomposition of substances may take place on the large surface of the sorbent. Thus, desorption of volatiles both from solid sorbents and from the liquid stationary phase requires the use of further equipment [23,24].

The device described in this paper is a modification of the continuous-flow system [25,26], in which absorption of volatiles into a solvent at low temperature is used instead of adsorption [27]. The device works off-line, *i.e.* it is independent of the gas chromatograph. The method was tested by trapping and concentration of volatile substances from natural and artificial sources.

0021-9673/91/$03.50

EXPERIMENTAL

The trapping system

For all experiments described in this paper a tempered desorption vessel of a 30-ml internal volume was used. A U-tube containing 50 μl of solvent had an I.D. of 3 mm at its narrower part and 8 mm at the broader part, which is the section for the trapping of the condensed water. The inner surface of all glass parts of the device was silanized [28] with a solution of dimethyldichlorosilane in toluene (20%, v/v, for 20 min). Air or nitrogen was used as the carrier gas. The carrier gas was purified by means of cartridges packed with silica gel, charcoal (both extracted and activated) and a 5-Å molecular sieve (activated) before entering the desorption vessel. The gas flow-rate was checked with a rotameter and measured using a bubble flow meter. For the cooling of the U-tube with the solvent a mixture of ethanol and dry ice (−78°C) was used. A schematic diagram of the whole arrangement is shown in Fig. 1, and a detailed view of the main part of the desorption device and the location of the sample is shown in Fig. 2.

After each experiment condensed water and a trapping solvent were withdrawn (separately) from the U-tube with a Hamilton syringe and divided into several portions and stored in sealed glass tube (1 mm I.D.) in a freezer.

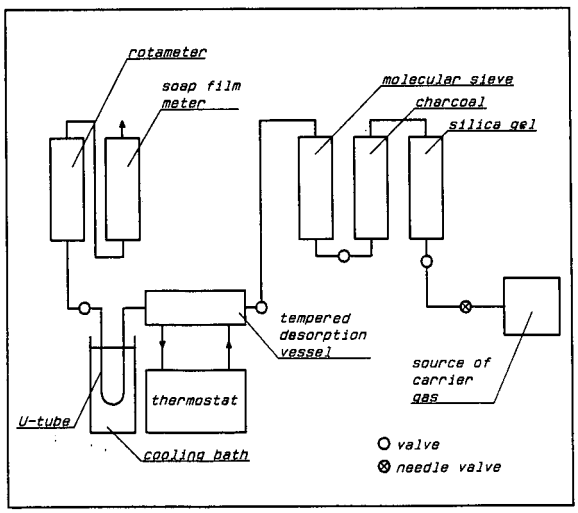

Fig. 1. Schematic diagram of the trapping system.

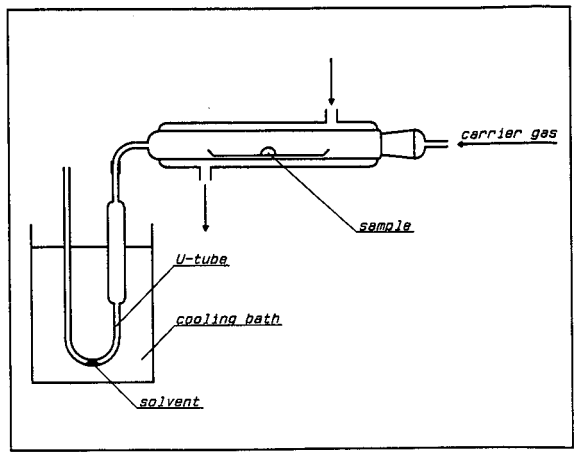

Fig. 2. Detail of the trapping system showing the desorption vessel and U-tube (not to scale).

Testing the device by means of n-alkanes

Fifteen *n*-alkanes (C_8–C_{22}, Applied Science Labs., USA) in equal weight proportions were dissolved in *n*-hexane (10%, w/v) and 5 μl were injected with a Hamilton syringe through a septum directly into the small boat in the desorption vessel. Three equal U-tubes (4 mm I.D.), connected in series, were always used for trapping the volatiles. Each of them contained 150 μl of an absorption solvent. The experiments were carried out: (a) with temperatures in the desorption vessel of 30, 60 and 90°C, (b) at flow-rate of 10, 20 and 30 ml/min and (c) for 1, 2 and 4 h. The retention times (in minutes) of *n*-alkanes (for GC conditions see the Experimental section) were as follows: 14.13 (C_8), 22.30 (C_9), 30.81 (C_{10}), 39.06 (C_{11}), 46.88 (C_{12}), 54.24 (C_{13}), 61.18 (C_{14}), 67.70 (C_{15}), 73.89 (C_{16}) and 79.75 (C_{17}).

Solvents and gases

Prepurified and distilled methanol (99.999%) or *n*-hexane (puriss., p.a., Fluka, Buchs, Switzerland) was used as the absorbing solvent. An air generator (Chrompack) was used as a source of air as carrier gas, while nitrogen was used from a cylinder.

Gas chromatography

An HP 5890A gas chromatograph with flame ionization detector and split–splitless injector was used: injector temperature 200°C; detector temper-

ature, 250°C; oven temperature, 35°C (5 min), then 2°C/min up to 165°C; carrier gas, hydrogen (70 kPa); column flow-rate, 2.0 ml/min; flow velocity, 49.7 cm/s (at 35°C), split ratio, 1:29; injections, always 2 μl; fused-silica capillary column, 30 m × 0.25 mm I.D. with DB-1; film thickness, 1 μm. An HP 3393A integrator was used.

Gas chromatography–mass spectrometry

A combined HP 5890A gas chromatograph and ZAB-EQ mass spectrometer (VG Analytical, UK) using electron-impact ionization at 70 eV was used. The chromatography conditions were the same as for GC experiments.

RESULTS AND DISCUSSION

The efficiency of the device was tested with a mixture of fifteen *n*-alkanes (C_8–C_{22}). The influence of temperature of the desorption vessel, flow-rate of the carrier gas and time of desorption was determined. The tests showed that approximately 97% of desorbed alkanes were trapped in the first U-tube, while the rest (3%) were trapped in the second one. The third U tube contained only trace amounts of alkanes in some cases. Fig. 3 represents the influence of desorption temperature on the percentage of substances trapped (the injected amount was equal to 100%, time of desorption 2 h and flow-rate 10 ml/min). The effect of temperature is most distinct up to 60°C; a further increase in temperature no longer causes a substantial increase in desorbed material. The effect of temperature is less distinct at desorption of lower hydrocarbons (up to *n*-C_{13}). The influence of the time of desorption or the flow-rate is much weaker than that of temperature. *n*-Heptadecane was the highest hydrocarbon which could still be trapped under any conditions. The resulting quantity was most probably affected by the way in which a 10% solution of fifteen hydrocarbons was injected into the desorption vessel. The hexane solution (5 μl) occupied only a limited area on the glass surface of the small boat. In contrast to

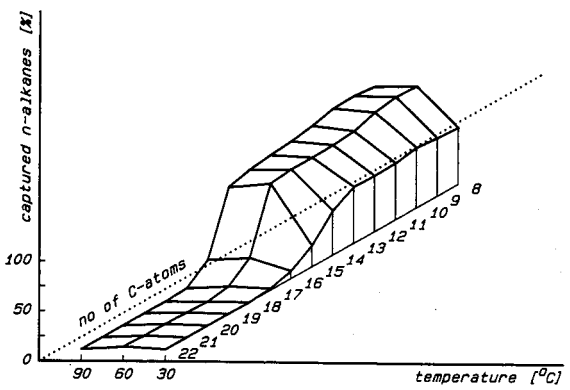

Fig. 3. Distribution of *n*-alkanes trapped at different temperatures in the desorption vessel (time of trapping 2 h, air flow-rate 10 ml/min).

TABLE I

TRAPPING CONDITIONS

Material	Quantity	Temperature of desorption vessel (°C)	Length of trapping (h)	Carrier gas (ml/min)
Coffee beans (Prague mixture type, roast and ground)	0.9 g	90	2	Air, 15
Bark of spruce (*Picea pungens* Engelm. cv. *Argentea*)	1.6 g	50	3	Air, 15
Black pepper (ground)	1.3 g	40	2	Air, 15
Shield bug [*Graphosoma lineatum* (L.1758)]	30 adults	30	2	Air, 15
Polyvinyl chloride (PVC flooring material)	10.5 g (30 cm^2)	50	5	Air, 15
Beer (Sládek 11° lager type)	18 ml	30[a]	2	Nitrogen, 25

[a] A desorption vessel was used for preheating of carrier gas only, the sample of beer was placed in a stripping tube.

this, volatile substances from natural material are evaporated from a much larger surface.

Since the effect of the trapping in the first U-tube was 97%, we always used a single U-tube in further experiments. For a practical testing of our device we concentrated volatile substances from randomly selected samples. The conditions for their analysis are given in Table I. Since a detailed qualitative analysis of the sample was not the main purpose of this study, we identified, by means of GC–MS, only some main components from several samples.

Practically every natural organic material contains a larger or smaller amount of water. As a rule this water causes difficulties during the capturing of the volatiles (*e.g.* ref. 29 and 30). When the device described is used, allmost all of the water condenses and freezes in the wider part of the U-tube, *i.e.* before it can reach the absorption solvent. We found that attention must also be paid to the analysis of water trapped in this manner. Some authors have warned against the presence of water in a sample analysed by capillary gas chromatography (CGC) because this water may change the properties of the chromatographic column [31] or even change retention times [32–34]. In contrast to this, a number of authors currently use aqueous solutions for analyses by CGC [35–37] as well, and they even determine water quantitatively using a thermal conductivity detector (see ref. 38). Under our chromatographic conditions we observed no differences in the retention of substances from aqueous and non-aqueous samples.

During the analysis of our samples we observed several different cases: in the case of coffee beans (roast and ground) the aqueous solution contained approximately six times more volatile substances (by weight) and approximately twice as many compounds as the methanolic solution (Fig. 4). The analysis of volatile substances from the bark of the spruce *Picea pungens* Engelm. cv. *Argentea* represented the other extreme. Volatile substances were captured only in methanol (Fig. 5). In the case of black pepper (ground) only some compounds out of the wide spectrum of volatile substances were present in water (Fig. 6). However, in many cases the water contained approximately the same spectrum of substances as methanol, but in lower concentrations.

Our equipment may also be used for concentration of volatile substances produced by insects and

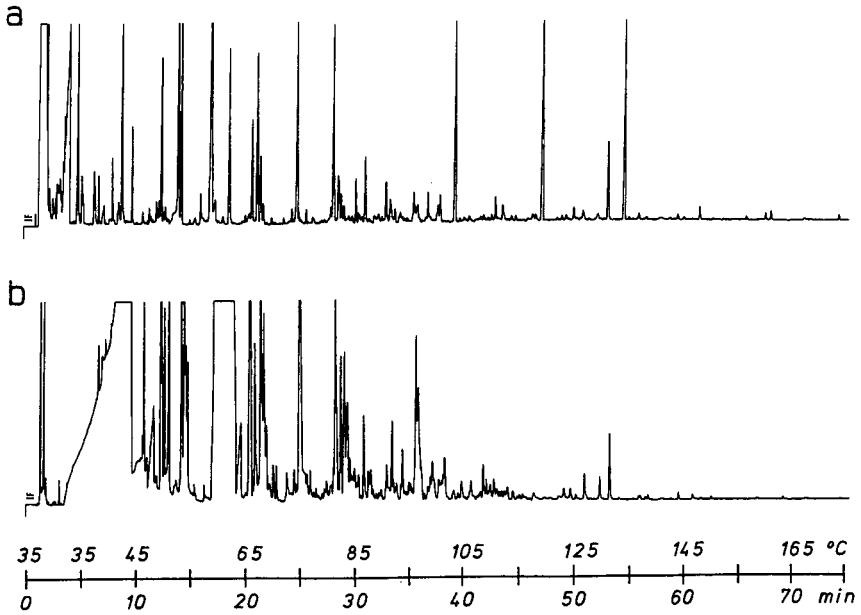

Fig. 4. Gas chromatogram of volatiles from coffee beans (Prague mixture type, roast and ground); (a) methanolic solution, (b) condensed water (for conditions see Experimental section).

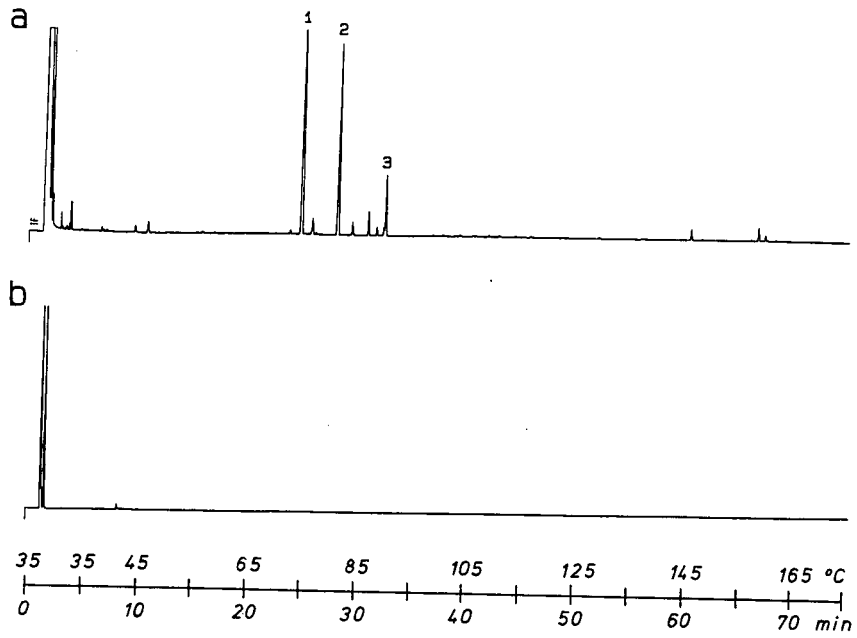

Fig. 5. Gas chromatogram of volatiles from the bark of spruce *Picea pungens* Engelm. cv. *Argentea*: (a) methanolic solution, (b) condensed water. Peaks: 1 = α-pinene; 2 = β-pinene; 3 = limonene.

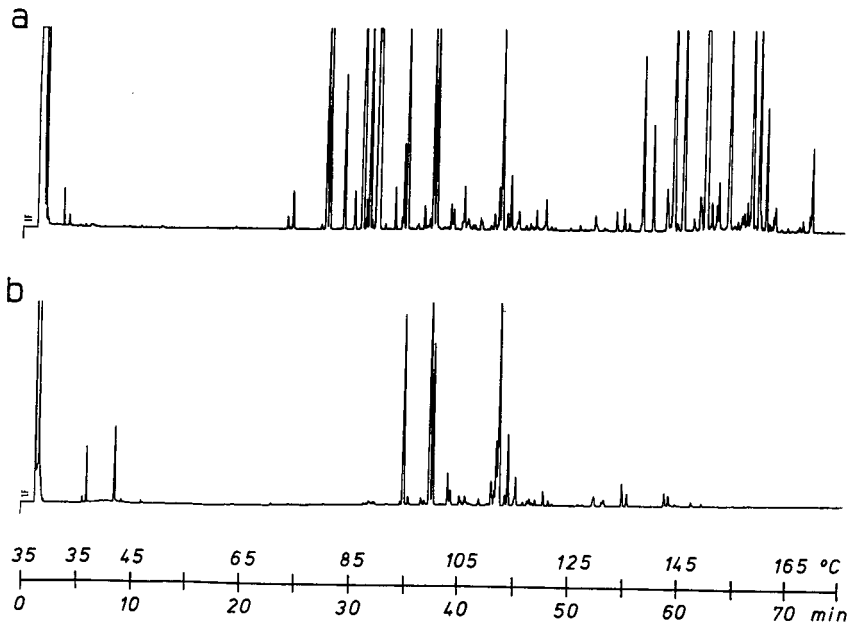

Fig. 6. Gas chromatogram of volatiles from black pepper (ground): (a) methanolic solution, (b) condensed water.

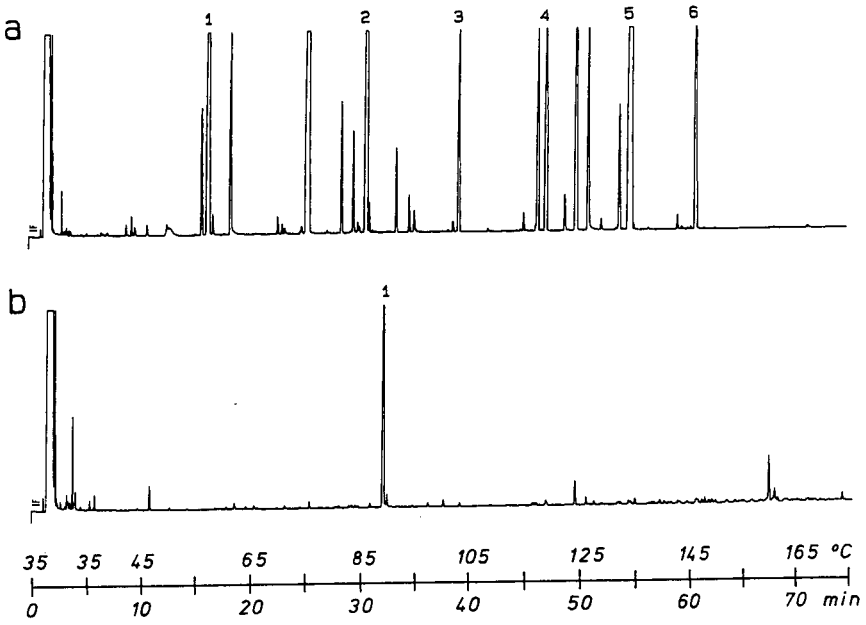

Fig. 7. Gas chromatogram of volatiles. (a) Chromatogram produced by the shield bug *Graphosoma lineatum* (L. 1758); methanolic solution. Peaks: 1 = 2-hexenal; 2 = 2-hexen-1-ol acetate; 3 = n-$C_{11}H_{24}$; 4 = n-$C_{12}H_{26}$; 5 = n-$C_{13}H_{28}$; 6 = 2-decen-1-ol acetate. (b) Chromatogram from PVC flooring; methanolic solution. Peak: 1 = 2-ethyl-1-hexanol.

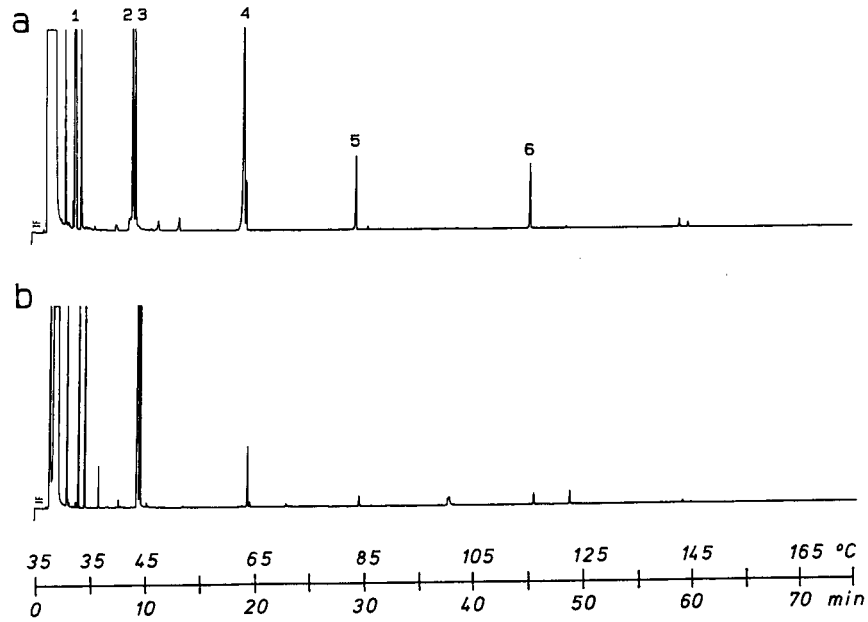

Fig. 8. Gas chromatogram of volatiles from beer (Sládek 11°, lager type): (a) methanolic solution, (b) condensed water. Peaks: 1 = 2-methyl-1-propanol; 2 = 3-methyl-1-butanol; 3 = 2-methyl-1-butanol; 4 = 3-methyl-1-butanol acetate; 5 = ethyl hexanoate; 6 = ethyl octanoate.

animals. As an example we present the analysis of compounds produced by the shield bug *Graphosoma lineatum* (L. 1758) (Fig. 7a).

An example of the concentration of compounds evaporated from floor covering on the basis of polyvinyl chloride (PVC) is shown in Fig. 7b.

The device described was also used for trapping of substances absorbed in liquids (stripping). A test tube containing the liquid was attached to the tempered vessel used to temper the carrier gas, and this was blown through a tube provided with a frit. As expected, a considerable amount of water was also trapped in the U-tube. The water contained practically the same compounds as methanol (Fig. 8).

In view of the fact that the trapping and the concentration of volatile substances was carried out using amounts in the microgram range, we considered it necessary to silanize the inner surface of the glass parts of the device and so minimize the losses caused by adsorption on the surface.

The disadvantages and advantages of the device described above are given in Table II.

TABLE II

DISADVANTAGES AND ADVANTAGES OF THE DEVICE

Disadvantages

1. The device is not suitable for ultramicroanalysis.
2. The selection of solvents is limited (methanol, ethanol, carbon disulfide, *n*-pentane, *n*-hexane, 2,2,4-trimethylpentane); m.p. must be lower than −80°C. Methanol proved to be best because (a) it is obtainable in a very pure state (up to 99.999%); (b) it gives a narrow signal at the beginning of the chromatogram; (c) it miscible with water; and (d) it is stable.

Advantages

1. A concentrated solution of volatiles is obtainable in one operation without any losses.
2. There is no need for desorption equipment and/or to carry out cryofocusing.
3. The amount of sample from one experiment is sufficient for several GC analyses, GC–MS, GC–FT-IR, GC–EAG and biological testing.
4. It is possible to obtain accurate retention times for identification by means of retention indices [39–41] due to split injection technique.
5. Easy quantification of experiments.
6. The device is very versatile in terms of (a) the size of the U-tube; (b) the size and shape of the desorption vessel (from 5 ml to 20 l, special shape for living objects); (c) different desorption temperatures (20–90°C), carrier gas flow-rate (for a U-tube of 3 mm I.D. about 15 ml/min) and length of time of collection; (d) different carrier gases (nitrogen, helium, argon, air) can be used; (e) it is useful for concentration of volatiles from liquid samples (stripping).

ACKNOWLEDGEMENT

The author (K.S.) wishes to thank Professor C. Bicchi (Dipartimento di Scienza e Tecnologia del Farmaco, Università Degli Studi di Torino, Turin, Italy) for very valuable discussion on this theme.

REFERENCES

1 M. A. Golub and I. Weatherston, in H. E. Hummel and T. A. Miller (Editors), *Techniques in Pheromone Research*, Springer, New York, Berlin, Heidelberg, Tokyo, 1984, Ch. 10, p. 223.
2 D. Joulain, in E.-J. Brunke (Editor), *Progress in Essential Oil Research, Proceedings of the International Symposium on Essential Oils, Holzminden/Neuhaus, Sept. 18–21, 1985*, Walter de Gruyter, Berlin, New York, 1986, p. 57.
3 D. Joulain, *Flavour Fragrance J.*, 2 (1985) 149.
4 L. K. Gaston, in H. E. Hummel and T. A. Miller (Editors), *Techniques in Pheromone Research*, Springer, New York, Berlin, Heidelberg, Tokyo, 1984, Ch. 9, p. 217.
5 A.-K. Borg-Karlson, G. Bergström and I. Groth, *Chem. Scr.*, 25 (1985) 283.
6 B. V. Burger, Z. M. Munro and J. H. Visser, *J. High Resolut. Chromatogr., Chromatogr. Commun.*, 11 (1988) 496.
7 J. F. Horwood, *Aust. J. Dairy Technol.*, November (1989) 91.
8 C. Bicchi, A. D'Amato, F. David and P. Sandra, *Flavour Fragrance J.*, 2 (1987) 49.
9 C. Bicchi, A. D'Amato, F. David and P. Sandra, *Flavour Fragrance J.*, 3 (1988) 143.
10 C. Bicchi, A. D'Amato, F. David and P. Sandra, *J. High Resolut. Chromatogr.*, 12 (1989) 316.
11 J. Roeraade and S. Blomberg, *J. High Resolut. Chromatogr.*, 12 (1989) 138.
12 M. Le Roux, H. J. J. van Vuuren, L. M. T. Dicks and M. A. Loos, *System. Appl. Microbiol.*, 11 (1989) 176.
13 S. Blomberg and J. Roeraade, *J. High Resolut. Chromatogr.*, 13 (1990) 509.
14 J. Roeraade and S. Blomberg, *Chromatographia*, 17 (1983) 387.
15 S. Blomberg and J. Roeraade, in P. Sandra, G. Redant, F. David and M. Leuridan (Editors), *Proceedings of the 10th International Symposium on Capillary Chromatography, Riva del Garda, Italy, May 22–25, 1989*, Hüthig, Heidelberg, Basle, New York, 1989, p. 390; *J. High Resolut. Chromatogr.*, 12 (1989) 294.
16 J. Roeraade, in P. Sandra, G. Redant, F. David and M. Leuridan (Editors), *Proceedings of the 10th International Symposium on Capillary Chromatography, Riva del Garda, Italy, May 22–25, 1989*, Hüthig, Heidelberg, Basle, New York, 1989, p. 289.
17 C. Bicchi and D. Joulain, *Flavour Fragrance J.*, 5 (1990) 131.

18 A. J. Núñez, L. F. Gonzáles and J. Janák, *J. Chromatogr.*, 300 (1984) 127.
19 W. Günther, J. Wohland, M. Lux and F. Schlegelmilch, in E.-J. Brunke (Editor), *Progress in Essential Oil Research, Proceedings of an International Symposium on Essential Oils, Holzminden/Neuhaus, September 18–21, 1985*, Walter de Gruyter, Berlin, New York, 1986, p. 637.
20 J. W. Graydon and K. Grob, *J. Chromatogr.*, 254 (1983) 265.
21 H.-J. Neu, W. Merz and H. Panzel, *J. High Resolut. Chromatogr., Chromatogr. Commun.*, 5 (1982) 382.
22 J. Rektorik, in P. Sandra (Editor), *Sample Introduction in Capillary Gas Chromatography*, Vol. 1, Hüthig, Heidelberg, Basle, New York, 1985, Ch. 11, p. 217.
23 *The Supelco Reporter*, 7 (2) (1988) 1; 7 (5) (1988) 1; 8 (6) (1989) 1; 9 (1) (1990) 9.
24 W. R. Betz, S. A. Hazard and E. M. Yearick, *Int. Labmate*, 14 (1990) 41.
25 K. Ubik, in *F. E. C. S. Third International Conference on Chemistry and Biotechnology of Biologicaly Active Natural Products, Sofia, Sept. 16–21, 1985*, The Publishing House of the Bulgarian Academy of Sciences, p. 205.
26 K. Ubik, in P. Drašar (Editor), *Handbook of Organic Laboratory*, Institute of Organic Chemistry and Biochemistry of the Czechoslovak Academy of Sciences, Prague, 1986, p. 35.
27 T. Jursík, K. Stránský and K. Ubik, in I. Hrdý (Editor), *Proceedings of a Conference on Insect Chemistry and Ecology, Tábor, Aug. 12–18, 1990*, Academia, Prague, and SPB Academic Publishing, The Hague, 1991, p. 327.
28 Applied Science Laboratories, State College, PA, *Catalog No. 18*, 1975, p. 17.
29 J. W. Cochran and J. M. Henson, *J. High Resolut. Chromatogr. Chromatogr. Commun.*, 11 (1988) 869.
30 Y. Ghoos, M. Hiele, P. Rutgeerts and G. Vantrappen, *J. High Resolut. Chromatogr.*, 12 (1989) 739.
31 K. Grob, in P. Sandra, G. Redant, F. David and M. Leuridan (Editors), *Proceedings of the 10th International Symposium on Capillary Chromatography, Riva del Garda, Italy, May 22–25, 1989*, Hüthig, Heidelberg, Basle, New York, 1989, p. 465.
32 W. F. Burns, D. Tingey and R. C. Evans, *J. High Resolut. Chromatogr. Chromatogr. Commun.*, 5 (1982) 504.
33 K. Grob and A. Habich, *J. High Resolut. Chromatogr. Chromatogr. Commun.*, 6 (1983) 34.
34 K. Grob, Jr. and B. Schilling, *J. Chromatogr.*, 260 (1983) 265.
35 J. Buyten, J. van Dalen, P. Musche and J. Peene, in P. Sandra, G. Redant, F. David and M. Leuridan (Editors), *Proceedings of the 10th International Symposium on Capillary Chromatography, Riva del Garda, Italy, May 22–25, 1989*, Hüthig, Heidelberg, Basle, New York, 1989, p. 225.
36 D. V. McCalley, *J. High Resolut. Chromatogr.*, 12 (1989) 465.
37 *The Packed Column Alternative—Megabore*, J&W Scientific, Folsom, CA, 1987, p. 8; J&W Capillaries, Erba Science, Vienna, 1990, p. 24.
38 H. C. H. Yeo and T. Shibamoto, *J. Food Sci.*, 55 (1990) 1175.
39 L. S. Ettre, *Anal. Chem.*, 36 (1964) 31A.
40 J. F. Sprouse and A. Varano, *Int. Lab.*, 1984 (11/12) 54.
41 L. Blomberg, *Adv. Chromatogr.*, 26 (1987) 229.

Journal of Chromatography, 586 (1991) 323–328
Elsevier Science Publishers B.V., Amsterdam

CHROM. 23 596

Origin and control of multi-peak formation in the analysis of trimethylsilyl derivatives of flavanone aglycones by capillary column gas chromatography

Colin S. Creaser*, Mohammed R. Koupai-Abyazani and G. Richard Stephenson

School of Chemical Sciences, University of East Anglia, Norwich NR4 7TJ (UK)

(First received January 22nd, 1991; revised manuscript received June 26th, 1991)

ABSTRACT

Trimethylsilyl derivatives of flavanone aglycones give double peaks in their gas chromatograms. The origin of these peaks, from an isomerization between the flavanones and their corresponding chalcones, has been examined using gas chromatography–mass spectrometry and UV spectrophotometry. The effects of derivatization temperature, time and capillary column injection technique on the rate of the interconversion have been defined.

INTRODUCTION

Flavanones (**I**) are one of the most common groups of flavonoid aglycones, and have been extensively studied by natural product chemists [1–6]. Unlike other flavonoids, *e.g.*, flavones, isoflavones and flavonols, which are fully unsaturated, flavanones contain a partially reduced heterocyclic C-ring. For this reason, the ether linkage of the C-ring of flavanones is more labile than the corresponding bond in fully unsaturated flavonoids, an effect that gives rise to the different chemical properties commonly observed in the flavanone group of natural products. In this paper we examine consequences of these reactivity differences on the behaviour of the flavanones during derivatization and analysis by gas chromatography (GC).

GC is a successful technique for the analysis of most flavonoid compounds, but complications have been encountered with flavanone substrates. Packed-column GC has been used for the separation of a variety of flavonoid derivatives [7–14] and for their identification in several plants [15–17] and fruits [18,19]. Trimethylsilyl (TMS) derivatives of the flavonoid aglycones (flavones, isoflavones and flavonols) generally show a single peak in GC analysis, whereas flavanones exhibit multiple peaks [8,10]. Furuya [9] suggested that the flavanones may undergo dehydration after B-ring cleavage or other chemical changes on the column leading to multiple peak formation. Narasimhachari and Von Rudloff [7] proposed that these peaks arise from the isomerization between the flavanones (**I**) and the corresponding chalcones (**II**) during GC analysis as a result of the high temperature necessary for chromatography. Their assignment was based on the isolation of the eluted compounds and a comparison of their UV spectra with those of standard materials.

We have recently reported a successful capillary column GC separation of methyl and TMS derivatives of flavonoid aglycones [20]. In this study, it was observed that the conversion of the TMS derivatives of the flavanone aglycones into the corresponding chalcones occurs both in the derivatization mixture (prior to injection) and in the injection port during GC analysis. Hence the ratio of peaks due to the TMS derivatives of the flavanone and chalcone varied with both derivatization and GC conditions. We report here a systematic investigation of the effect of the derivatization time,

0021-9673/91/$03.50

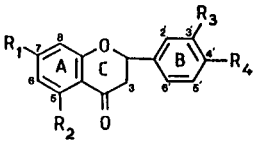

(I)

Ia: R_1, R_2, R_3, R_4 = H
Ib: R_1, R_2, R_4 = OH; R_3 = H
Ic: R_1, R_2, R_3 = OH; R_4 = OCH_3
Id: R_1, R_2, R_3, R_4 = OH

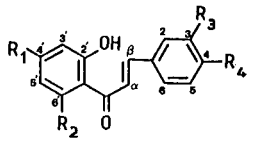

(II)

IIa: R_1, R_2, R_3, R_4 = H
IIb: R_1, R_2, R_4 = OH; R_3 = H
IIc: R_1, R_2, R_3 = OH; R_4 = OCH_3
IId: R_1, R_2, R_3, R_4 = OH

temperature and capillary column injection technique on the rate of the flavanone–chalcone interconversion, using GC, combined GC–mass spectrometry (GC–MS) and UV spectrophotometry.

EXPERIMENTAL

All the flavanones and 2′-hydroxychalcone were gifts from the AFRC Institute of Plant Science Research and John Innes Institute (Norwich, UK). Naringenin, hesperetin and eriodictyol chalcones were purchased from A-Apin Chemicals. These compounds were used without further purification. Pyridine (silylation grade) was obtained from Pierce. 1,1,1,3,3,3-Hexamethyldisilazane, 98% (HMDS), trimethylchlorosilane (TMCS) and methanol, 99.9% (spectrophotometric grade), were purchased from Aldrich.

Derivatization

GC and GC–MS. A 1–2-mg amount of each flavanone or chalcone was dissolved in 0.1 ml of anhydrous pyridine in a screw-capped vial and 0.1 ml of HMDS and 0.05 ml of TMCS were added. The mixture was shaken vigorously for 1 min and allowed to stand at room temperature for 30 min (mild conditions) or heated at 60°C overnight (vigorous conditions). After centrifugation, 0.5–2 μl of the solution was used for injection into the gas chromatograph.

UV spectrophotometry. A 1-mg amount of each flavanone or chalcone was dissolved in 0.4 ml of pyridine in a screw-capped vial and 0.4 ml of HMDS and 0.2 ml of TMCS were added. The mixture was shaken vigorously for 1 min and allowed to stand at room temperature for 30 min. The supernatant solution was separated by centrifugation. An aliquot of 0.05 ml was removed and the remaining solution was heated at 60°C overnight. Aliquots (0.05 ml) were removed from the sample after 2, 4, 6, 8, 10 and 24 h at 60°C. The solvent and excess of reagents in each aliquot were evaporated in a stream of dry nitrogen. The residue was dried *in vacuo* and the dry residue was dissolved in 5 ml methanol for UV spectrophotometry.

Gas chromatographic analysis

GC analysis was carried out on a Phillips PU 4400 series gas chromatograph equipped with a flame ionization detector. The output from the detector was recorded using a Phillips Analytical Chromate PC data system or a chart recorder. A 50 m × 0.25 mm I.D. RSL 200 BP capillary column (0.2 μm film thickness) (Alltech) was maintained isothermally at 280 or 250°C (for flavanone and 2′-hydroxychalcone, respectively) for GC separation. The linear velocity of the oxygen-free nitrogen carrier gas was 17.5 cm s^{-1} (97 kPa) and the split flow-rate was set to 30 ml min^{-1}. GC–MS was carried out on a Varian 3400 gas chromatograph directly interfaced to a Finnigan MAT ion trap mass spectrometer (ITMS) operated via a Walters International Baby AT/PC. A 30 m × 0.24 mm I.D. DB-5 capillary column (0.25 μm film thickness) (J & W Scientific) was used for analysis at an isothermal temperature of 280 or 250°C (for flavanone and 2′-hydroxychalcone, respectively). The injector and transfer line temperatures were maintained at 300 and 275°C, respectively. The carrier gas was helium (83 kPa) and the split flow-rate was set at 30 ml min^{-1}. The conditions for MS were electron impact ionization under automatic gain control at a trap temperature of 150°C. UV spectra were recorded on a Pye Unicam SP8-500 UV–VIS spectrophotometer or a Hitachi 557 double-wavelength, double-beam spectrophotometer. The following conditions were applied: cell path length, 1 cm; scan range, 500–240 nm; scan speed, 120 nm min^{-1} (20 nm cm^{-1}); and slit width, 2 nm.

RESULTS AND DISCUSSION

In our initial investigation of the derivatization and capillary GC analysis of flavonoid aglycones [20], the gas chromatograms obtained for TMS

derivatives of flavones, isoflavones and flavonols generally showed a single peak under mild derivatization conditions. However, TMS derivatives of flavanones (naringenin, **Ib**, hesperetin, **Ic**, and eriodictyol, **Id**) produced double peaks, a small peak followed by a major one, under these conditions. Growth of the minor peak at the expense of the major peak occurred when the derivatization mixture was stored at room temperature for several days. This observation differs from earlier reports [8,10] which suggested that the high temperature necessary for GC analysis alone accounted for the formation of multiple peaks in the chromatogram. Heating the derivatization mixture at 60°C showed that the rate of the interconversion of the two peaks increases significantly at this temperature, such that the reaction was complete within 24 h compared with several days at room temperature. The rate of the conversion is faster for the TMS derivative of hesperetin (**Ic**) than for the TMS derivatives of eriodictyol (**Id**) and naringenin (**Ib**). Hence, after heating overnight at 60°C, chromatograms obtained for the TMS derivatives of hesperetin (**Ic**) and eriodictyol (**Id**) contained a single peak at the retention time of the original minor peak. In contrast, for the derivatization of naringenin (**Ib**) two peaks, a major peak followed by a small one, were still present at this stage, and further prolonged heating was needed in order to simplify the chromatogram to a single peak.

In GC–MS experiments on the TMS derivatives of the flavanones, the expected double peaks were present in the total ion current traces. The mass spectra associated with the two peaks showed that for all the flavanones, the second peak corresponded to the derivatized flavanone, whereas the first peak gave a simple spectrum containing a strong ion (base peak) 72 dalton above the main peak in the mass spectrum of the silylated flavanone. This second component arises from ring opening and further TMS derivatization of the C-ring, *i.e.*, the formation of the corresponding derivatized chalcone in the presence of excess of silylating reagents. For example, in the mass spectrum of the TMS derivative of eriodictyol, **Id**, the derivatized chalcone [eriodictyol chalcone (**IId**), first peak] is identified by a strong ion at *m/z* 633 (100%) and the TMS derivative of eriodictyol, **Id**, (second peak) by an ion at *m/z* 561 (100%). The base peak in each spectrum arises from loss of a methyl group [21]. Fig. 1 shows the GC–MS total ion current traces for the TMS derivative of eriodictyol under the mild derivatization conditions (i) and after almost complete conversion to the chalcone (ii), and the corresponding mass spectra of the derivatized chalcone (Fig. 1a) and flavanone (Fig. 1b).

In order to confirm that the flavanones are converted into the corresponding chalcones, derivatization experiments (under both mild and vigorous

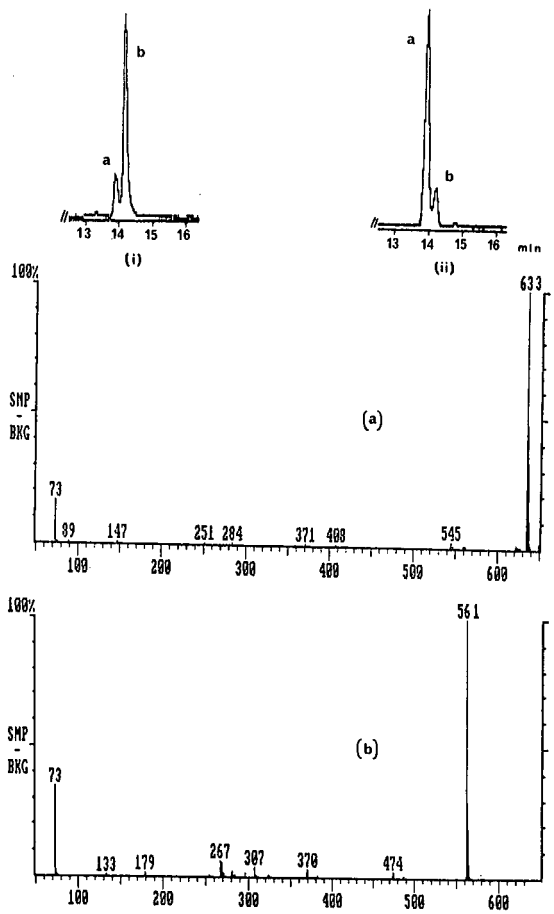

Fig. 1. GC–MS total ion current traces after the TMS derivatization of eriodictyol under (i) mild derivatization conditions and (ii) after almost complete conversion to the chalcone, and the corresponding mass spectra of the derivatized (b) flavanone and (a) chalcone. GC–MS conditions: column, bonded-phase DB-5 fused-silica capillary (30 m × 0.24 mm I.D.; 0.25 μm film thickness); column temperature, 280°C isothermal; linear velocity of helium carrier gas, 25 cm s^{-1}; transfer line temperature, 275°C; electron impact ionization under automatic gain control at a trap temperature of 150°C.

conditions) were carried out using the naringenin, hesperetin and eriodictyol chalcones, (**IIb**, **IIc** and **IId**) as starting materials. The gas chromatograms of the TMS derivatives of the chalcones obtained under the mild derivatizing condition also showed double peaks where the first peak was considerably stronger than the corresponding peak observed when the starting material was a flavanone. In this instance, heating the sample also caused the growth of the first peak at the expense of the second, as observed for flavanones. Injection of a mixture of each TMS derivative of flavanone and its corresponding chalcone in HMDS–TMCS silylating reagent showed two peaks in the gas chromatogram, confirming that the double peaks in the TMS derivatization of the flavanones have the same retention times as the corresponding peaks for the TMS derivatization of the chalcones.

Confirmation of the interconversion of flavanones and their corresponding chalcones under the derivatization conditions was sought by UV spectrophotometry. The absorbance maximum for flavanones occurs in the range 270–295 nm whereas the absorbance maximum for the chalcones is usually in the range 340–390 nm [4]. Changes in the UV spectra of TMS derivatives of naringenin (**Ib**), hesperetin (**Ic**) and eriodictyol (**Id**) as a function of time at 60°C revealed a decrease in absorbance for the flavanone and an increase in absorbance for the corresponding chalcone. Fig. 2 shows the UV spectra for the conversion of TMS derivative of hesperetin into the corresponding chalcone with time in the derivatization mixture at 60°C. These results are consistent with the data obtained from the GC analysis, demonstrating that the conversion of flavanones into the chalcones does not arise solely because of high temperature used in GC. The calculated pseudo-first-order rate constants for the TMS derivatization of naringenin, hesperetin and eriodictyol are $2.8 \cdot 10^5$; $3.1 \cdot 10^5$ and $3.7 \cdot 10^5$ s^{-1}, respectively.

The effect of different capillary column injection techniques (split, splitless and cold on-column injection) was studied using the trimethylsilylation reaction of eriodictyol (**Id**) as a model system to determine the behaviour of the flavanone aglycones. Because of differences in the injector residence times in the split and splitless techniques, kinetic experiments were carried out under the following conditions: split mode, splitless mode, splitless mode (with glass-wool in the injection port) and cold on-column injection.

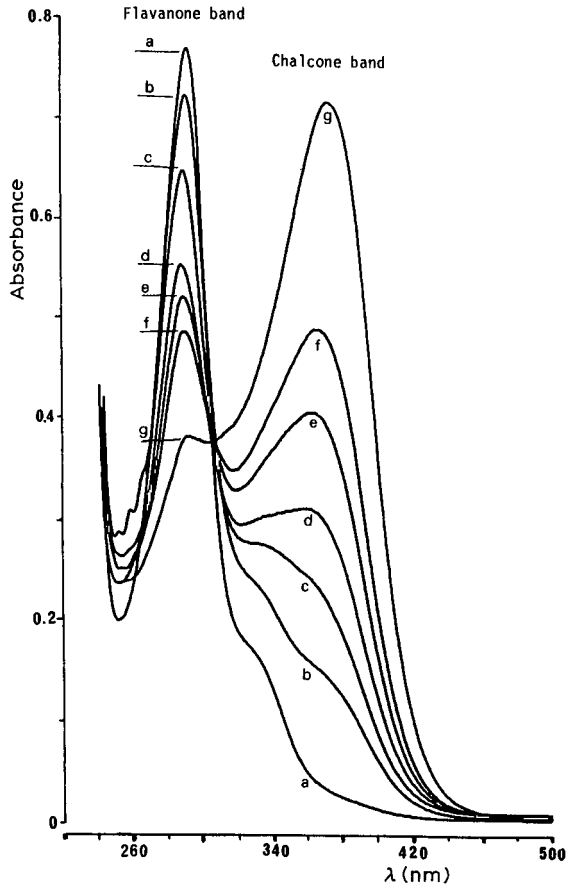

Fig. 2. UV spectra for the conversion of the TMS derivative of hesperetin into the corresponding chalcone in the derivatization mixture at 60°C with time. Spectra (a)–(g) show the increase in absorbance for chalcone and the decrease in absorbance for flavanone after (a) 0, (b) 2, (c) 4, (d) 6, (e) 8, (f) 10 and (g) 24 h.

The results for a series of injections during the TMS derivatization of eriodictyol (**Id**), at various times after addition of the derivatization reagents at 60°C, showed that the rate of the conversion of the TMS derivatives of the flavanones into the corresponding chalcones follows the order splitless mode (with glass-wool) > splitless mode > split mode > cold on-column injection. Injections under splitless (with glass-wool) conditions could cause the reaction to proceed rapidly because of two factors: the longer residence time (*ca.* 30 s) in the hot injection port and the presence of the large surface area of the

glass-wool. Even without the use of glass-wool packing, under splitless conditions the conversion rate is faster than in the split mode because of the longer injector residence time. The rate of the conversion is slowest in cold on-column injection, as expected from the behaviour of the flavanones in HMDS–TCMS solution.

In contrast to the behaviour of naringenin, hesperetin and eriodictyol, the parent compound, flavanone (**Ia**), and its corresponding chalcone (2′-hydroxychalcone, **IIa**), exhibited different gas chromatograms. An injection of the flavanone (**Ia**) in silylating reagents (mild conditions) produced a single peak in the gas chromatogram. Heating the sample overnight at 60°C did not cause any of the rapid changes in the height of the peak observed for other flavanones, producing only a small additional peak at higher retention time. When the sample was stored at room temperature for 3 weeks, the growth of the small peak and the appearance of a new peak at a longer retention time was observed. In the same way, the gas chromatogram of the TMS derivative of the corresponding chalcone (2′-hydroxychalcone, **IIa**) also showed a single peak under mild derivatization conditions. A small secondary peak appeared at lower retention time following vigorous conditions for derivatization. This peak became larger as the sample was left at room temperature for 3 weeks. The second and third eluting peak obtained from flavanone, with silylating reagents, have retention times identical with those of the two peaks observed for the TMS derivative of 2′-hydroxychalcone in their gas chromatograms. GC–MS studies of these compounds showed that the mass spectra of these two peaks in the gas chromatogram of the TMS derivative of 2′-hydroxychalcone are similar, both showing ions at m/z 296 ($M^{+\cdot}$), and 281 (base peaks, $[M - 15]^+$). The presence of two GC peaks with similar mass spectra for the TMS derivative of 2′-hydroxychalcone may be attributed to *cis*- and *trans*-isomerization of the open C-ring in the derivatized chalcone. This isomerization was not observed for naringenin, hesperetin and eriodictyol chalcones because of steric hindrance arising from the presence of bulky TMS groups on the B-ring, which disfavour the formation of the *cis*-isomer. The mass spectrum of the first-eluting peak in the gas chromatograms of flavanone (silylating conditions) showed an ion at m/z 224 corresponding to flava-

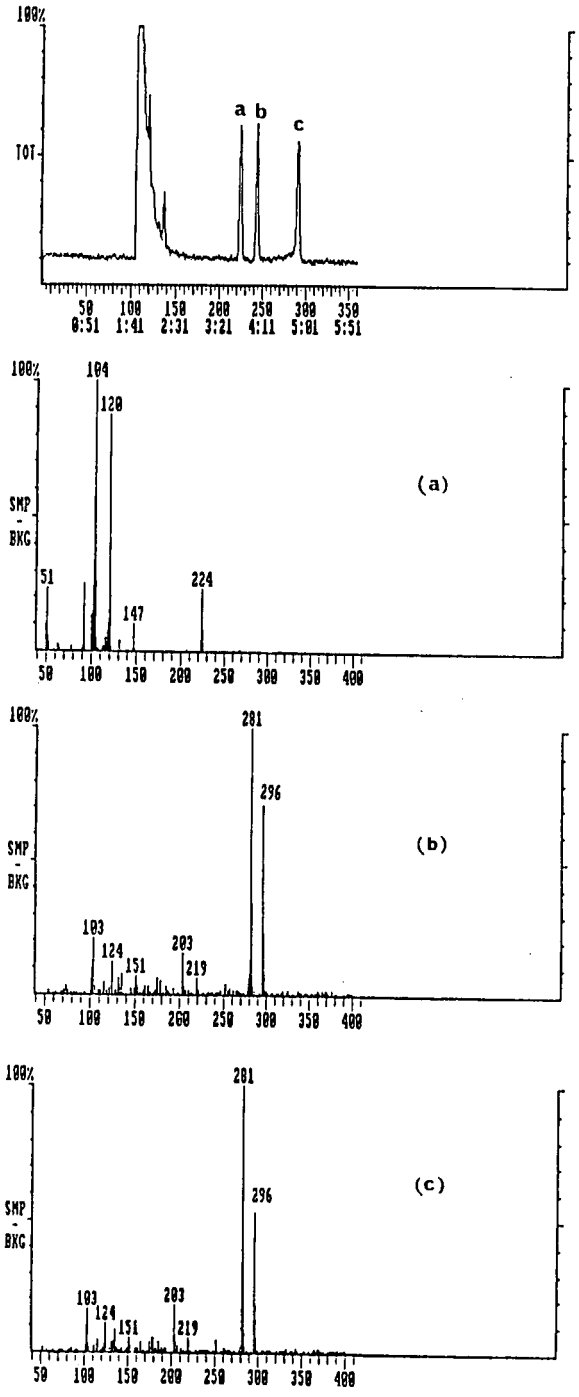

Fig 3. GC–MS total ion current trace of the TMS derivatization products of flavanone and the corresponding mass spectra of (a) the flavanone and (b and c) the derivatized *cis*- and *trans*-chalcone isomers. GC–MS conditions: column temperature, 250°C isothermal; other conditions as in Fig. 1. Time in min:s (top chromatogram); mass units (spectra a, b and c).

none, but the second- and third-eluting peaks exhibited mass spectra that were comparable to that for the TMS derivative of 2′-hydroxychalcone. The identical retention time in both instances and the similarity of the mass spectra of the last two peaks in the gas chromatogram obtained from flavanone and those of the TMS derivative of 2′-hydroxychalcone suggest that the flavanone is slowly converted into the TMS derivative of corresponding chalcone (2′-hydroxychalcone) under the silylating conditions used. Fig. 3 shows the GC–MS total ion current trace of the parent compound, flavanone (after vigorous derivatization conditions and 3 weeks at room temperature), and the corresponding mass spectra of the flavanone (Fig. 3a) and derivatized *cis*- and *trans*-chalcone isomers (Fig. 3b and c).

Interconversion of TMS derivatives of flavanones and the corresponding chalcones is observed in both the derivatization mixture (prior to injection) and during GC because of the high temperature necessary for analysis. The derivatization temperature, time and capillary column injection technique all have an influence on the rate of the interconversion. This phenomenon is very slow for the parent compound, flavanone, and gives rise to two characteristic peaks for chalcone under the conditions reported here, whereas for the TMS derivatives of other flavanones investigated, the conversion rate is faster and only one peak is observed for the corresponding chalcone. The observations in this study provide a basis for the optimization of the derivatization procedure for the identification of these compounds by capillary column GC, especially in complex biological systems.

ACKNOWLEDGEMENTS

We thank Professor A. W. B. Johnston (School of Biological Sciences, University of East Anglia) and Dr. J. L. Firmin (AFRC Institute of Plant Science Research and John Innes Institute) for the gift of some flavanone and chalcone compounds. G.R.S. thanks the Royal Society for a 1983 University Research Fellowship.

REFERENCES

1 T. J. Mabry, K. R. Markham and M. B. Thomas, *The Systematic Identification of Flavonoids*, Springer, Berlin, 1970, Ch. 6, p. 165.
2 C. Van De Sande, J. W. Serum and M. Vandewalle, *Org. Mass Spectrom.*, 6 (1972) 1333.
3 B. A. Bohm, in J. B. Harborne, T. J. Mabry and H. Mabry (Editors), *The Flavonoids*, Chapman & Hall, London, 1975, Ch. 11, p. 560.
4 T. J. Mabry and A. Ulubelen, in G. R. Waller and O. C. Dermer (Editors), *Biochemical Application of Mass Spectrometry*, Wiley, New York, 1980, Ch. 35, p. 1138.
5 B. A. Bohm, in J. B. Harborne and T. J. Mabry (Editors), *The Flavonoids, Advances in Research*, Chapman & Hall, New York, 1982, Ch. 6, p. 349.
6 B. A. Bohm, in J. B. Harborne (Editor), *The Flavonoids, Advances in Research Since 1980*, Chapman & Hall, London, 1988, Ch. 9, p. 348.
7 N. Narasimhachari and E. Von Rudloff, *Can. J. Chem.*, 40 (1962) 1123.
8 E. Von Rudloff, *J. Gas Chromatogr.*, 2 (1964) 89.
9 T. Furuya, *J. Chromatogr.*, 19 (1965) 607.
10 E. S. Keith and J. J. Powers, *J. Food Sci.*, 31 (1966) 971.
11 C. G. Nordström and T. Kroneld, *Acta Chem. Scand.*, 26 (1972) 2237.
12 T. Katagi, A. Horii, Y. Oomura, H. Miyakawa, T. Kyu, Y. Ikeda and K. Isoi, *J. Chromatogr.*, 79 (1973) 45.
13 K. Van de Casteele, H. De Pooter and C. F. Van Sumere, *J. Chromatogr.*, 121 (1976) 49.
14 M. Vanhaelen and R. Vanhaelen-Fastré, *J. Chromatogr.*, 187 (1980) 255.
15 P. D. Collier and R. Mallows, *J. Chromatogr.*, 57 (1971) 29.
16 R. W. Hemingway and W. E. Hillis, *J. Chromatogr.*, 43 (1969) 250.
17 A. R. Pierce, H. N. Graham, S. Glassner, H. Madlin and J. G. Gonzalez, *Anal. Chem.*, 41, 2 (1969) 298.
18 D. E. Coffin and J. E. Dupont, *J. Assoc. Off. Anal. Chem.*, 54, 5 (1971) 1211.
19 M. B. Duggan, *J. Assoc. Off. Anal. Chem.*, 52 (1969) 1038.
20 C. S. Creaser, M. R. Koupai-Abyazani and G. R. Stephenson, *J. Chromatogr.*, 478 (1989) 415.
21 C. S. Creaser, M. R. Koupai-Abyazani and G. R. Stephenson, *Org. Mass Spectrom.*, 26 (1991) 157.

Journal of Chromatography, 586 (1991) 329–340
Elsevier Science Publishers B.V., Amsterdam

CHROM. 23 598

Evaluation of gas chromatographic columns for the determination of methylmercury in aqueous head space extracts from biological samples

Patrick Lansens*

Analytische Scheikunde, Vrije Universiteit Brussel, Pleinlaan 2, 1050 Brussels (Belgium)

Carmela Casais Laiño

Universidad de Santiago de Compostela, Departemento de Quimica Analitica, 15706 Santiago de Compostela (Spain)

Carine Meuleman and Willy Baeyens

Analytische Scheikunde, Vrije Universiteit Brussel, Pleinlaan 2, 1050 Brussels (Belgium)

(First received March 7th, 1991; revised manuscript received July 2nd, 1991)

ABSTRACT

Several gas chromatographic columns were evaluated for the determination of methylmercury in aqueous solution. The goal of the study was to further decrease the detection limit of the recently developed method of head space gas chromatography with microwave-induced plasma detection (HS-GC–MIP) for the determination of methylmercury in biological samples. The columns were first evaluated using gas chromatography with electron-capture detection (ECD). At the same time, the column efficiencies for the determination of ethyl- and phenylmercury were also studied. Of the packed columns the stationary phase used previously in HS-GC–MIP, AT-1000, yielded the best results. Better results were obtained with two wide-bore thick-film fused-silica open tubular (FSOT) columns, one of which was suitable for aqueous injections (Superox-FA) and the other for benzene or toluene (RSL-300). With these FSOT columns, absolute detection limits at the sub-picogram level were reached. A new HS-GC–MIP system was then constructed, which was adapted for the use of FSOT columns. As more sensitive measurements were obtained with a Superox-FA FSOT column than with an AT-1000 packed column using the GC–ECD system in the first part of this study, the FSOT column was evaluated in this HS-GC–MIP system for the determination of methylmercury in real tissue samples. It was demonstrated that the use of an FSOT column gives only a small decrease in the detection limit compared with a packed column; reconditioning of the FSOT column is, however, a disadvantage in routine measurements.

INTRODUCTION

Methylmercury (MeHg) is one of the most dangerous pollutants in the environment. It is highly toxic and is often found concentrated at the end of the food web. Fish especially tend to concentrate mercury in their tissues and analyses have shown that most of the mercury accumulated in their tissues is in the form of MeHg [1–5], despite the lack of obvious significant MeHg inputs to natural aquatic systems. The MeHg concentrations in natural waters and sediments are very low (pg kg^{-1}) [2,6]. Compared with this, the MeHg content in fish is usually in the range of micrograms per kilogram [2,6]. Concentration factors of 10^5–10^7 are commonly observed [6–9]. Most of the MeHg taken up by fish from the aquatic environment is accumulated in edible tissues [6]. MeHg uptake by fish is therefore the main route from the aquatic environment to humans. This has led to a

0021-9673/91/$03.50

considerable effort in the development of reliable, precise and sensitive analytical methods specific for the determination of this compound in fish and other aquatic organisms.

The most widely used analysis technique is gas chromatography with electron capture detection (GC–ECD) or microwave-induced plasma detection (GC–MIP) [1,10–18]. MIP has the advantage that it can be used as mercury-specific detection. In this method, usually referred to as the Westöo method, elaborate and time-consuming extractions have to be carried out prior to injection of the sample onto the GC column. One of the major problems in the determination is that organic mercury halides exhibit poor GC properties.

Most of the reported chromatography methods have used packed columns [10,12–16,19]. A variety of stationary phases has been recommended, but many of these columns have exhibited one or more of the following disadvantages [19]: (a) poor and often variable response to methyl- and ethylmercury chloride (MeHgCl and EtHgCl) because of apparent interactions with the column or their decomposition on it; (b) moderate to very severe tailing; and (c) poor column efficiency that can then lead to problems with interferences. Hence time-consuming and laborious column conditioning procedures are necessary [19]. The beneficial effects of the treatment are only temporary, as the presence of high-molecular-weight compounds in the sample often leads to degradation of the "column performance" [19].

Only a few methods have been reported in which capillary columns have been used [20–25]. Cappon and Toribara [26] and Olsen *et al.* [17] were the first to use wide-bore thick-film fused-silica open tubular (FSOT) columns (0.53 mm I.D., 1.2 μm film thickness) and they obtained very good results. However, they only used standard solutions in the evaluation. Wide-bore thick-film columns have the advantages that they accept large injections without the use of a splitter, are compatible with higher flow-rates and do not need a make up gas to be added after the column.

Petersen [27] evaluated FSOT columns with different internal diameters and film thicknesses coated with CP-Sil 8. These experiments suggested that it is important to use capillary columns with a thick film. This may be because the thick film reduces the contact between the volatilized mercury compound and a fused-silica column which is not entirely deactivated. Even with thick-film columns there was still a problem of high standard deviations on the results. Petersen [27] also tested several other capillary columns but most of these did not give any response for MeHgCl. The compound disappeared in the GC system if it was not primed with a mercury compound before analysis.

Lee and Mowrer [28] used a wide-bore thick-film FSOT column coated with OV 1701. Their chromatograms show a high number of peaks (sometimes interfering) and each sample analysis required about 30 min to elute all the peaks that could interfere with a subsequent injection.

A fast, accurate, precise and sensitive method for the determination of MeHg in biological samples has been developed at this laboratory [18,29,30]. In this method, the MeHg is cleaved from the biological tissue by sulphuric acid and by the addition of iodoacetic acid converted to the iodide form. These reaction steps take place in a closed head space vial. The MeHg iodide is then injected into the head space of a gas chromatograph and detected by MIP. This method has several advantages over the widely used Westöo method. By using direct headspace sampling (HS), the problem of "column performance" degradation is solved. Indeed, high-boiling compounds which often poison the stationary GC phase are no longer introduced into the column as occurs in direct injection chromatography. Another major advantage of this sampling procedure is its simplicity; all the reaction steps take place in the head space vial and the laborious isolation of the MeHg by multiple extraction with benzene or toluene is no longer required. The HS-GC–MIP method has a detection limit of 0.4 $\mu g\ l^{-1}$ or 20 $ng\ g^{-1}$ for MeHg in biological tissues.

Head space analysis above an aqueous solution provides a considerable enrichment of MeHg in the vapour phase compared with the analysis above a benzene solution [18]. Therefore aqueous solutions will give a more sensitive determination, but a water-resistant chromatographic column must be used. Very few stationary phases are suitable for aqueous injections; only Talmi [15] has mentioned the use of a column packing suitable for aqueous solutions. He used a 1% free fatty acid phase (FFAP) liquid phase on graphitized carbon beads.

In the HS-GC–MIP method [29–31], AT-1000 was used as the stationary phase. This stationary phase is well suited to aqueous injections. The water is completely eluted from the column within 30 s and quantitative peaks are obtained for the MeHgX (X = Cl, Br, I) eluted thereafter. No special column conditioning procedures are required. The column efficiency, however, is very low (200–250 plates per meter for MeHgCl).

In this work, the efficiencies of several columns (packed and capillary) were studied for the determination of MeHgCl in aqueous solution. The objective of this work was to further decrease the detection limit of this HS-GC–MIP method.

The columns were first evaluated by injecting aqueous MeHgCl standard solutions. At the same time, the column properties for the determination of EtHgCl and phenylmercury chloride (PhHgCl) were studied. An electron-capture detector was used for this study as its non-specificity, a disadvantage compared with the MIP detector when analysing real samples, does not play a role when only organomercury standard solutions are injected into the gas chromatograph.

A new HS-GC–MIP system was then constructed, which was adapted for the use of capillary columns. More sensitive measurements were obtained using a GC–ECD system with a Superox-FA FSOT column than with the AT-1000-packed column, so the FSOT column was evaluated in this HS-GC–MIP system for the determination of MeHg in real tissue samples.

EXPERIMENTAL

GC–ECD study

All the columns were evaluated on an HP 5730A gas chromatograph with an electron-capture detector (^{63}Ni radioactive source). Standard solutions were injected with Hamilton microliter syringes into the injector at 200°C. A glass liner was placed in this injector to avoid possible interactions of the organomercury compounds with the hot metal surface. For the same reason, glass was used for the packed columns. The detector temperature was 300°C. Argon was used as the carrier gas.

The columns evaluated are listed in Table I. The AT-1000 column was also tested in this system so that the results obtained with the other columns could be compared with those obtained with the stationary phase used earlier in the HS-GC–MIP system. Chromosorb 101 to 108 of the Chromosorb Century Series (Alltech Assoc.) were chosen because they are known to be hydrophobic. They are porous, polyaromatic, cross-linked resins with a uniform rigid structure of a distinct pore size. They do not have to be coated before use (this is in fact gas–solid chromatography). Two FSOT columns were tested: Superox-FA and RSL-300 (both from Alltech Assoc.). These are wide-bore thick-film columns.

TABLE I

COLUMNS TESTED USING THE GC–ECD SYSTEM

Column	Type and chemical name	Dimensions [length (m) × I.D. (mm)]
10% AT-1000 on Chromosorb W AW	Packed, polyethylene glycol ester	2 × 2
Chromosorb 101	Packed, styrene-divinylbenzene	2 × 2
Chromosorb 102	Packed, styrene-divinylbenzene	2 × 2
Chromosorb 103	Packed, cross-linked polystyrene	2 × 2
Chromosorb 104	Packed, acrylonitrile-divinylbenzene	2 × 2
Chromosorb 105	Packed, polyaromatic	2 × 2
Chromosorb 106	Packed, cross-linked polystyrene	2 × 2
Chromosorb 107	Packed, cross-linked acrylic ester	2 × 2
Chromosorb 108	Packed, cross-linked acrylic ester	2 × 2
Superox-FA	FSOT, polyethylene glycol ester	10 × 0.53
RSL-300	FSOT, polyphenylmethylsiloxane	10 × 0.53 (both 1.2 μm film)

The RSL-300 column is not suitable for aqueous injections, but this column was evaluated to compare the results with those obtained with the water-resistant Superox-FA column. It was chosen because it has a similar stationary phase to the DB-5 column used very successfully by Olsen *et al.* [17].

HS-GC–MIP study

The HS-GC–MIP system for the determination of MeHg using the AT-1000-packed column and the head space extraction method used to determine MeHg in biological samples have been described previously [29–31]. A typical chromatogram obtained with this system is given in Fig. 1.

The HS-GC–MIP system used here consists of four commercially available components: an HS-6 semi-automated head space sampler (Perkin-Elmer), an Intersmat 120 gas chromatograph, a heated four-way valve for solvent ventilation (Valco GC-T) and an MPD 850 microwave plasma instrument (Applied Chromatography Systems). The HS-6 semi-automated head space sampler is mounted on the Intersmat gas chromatograph. The HS-6 sampler was first modified so that the sample com-

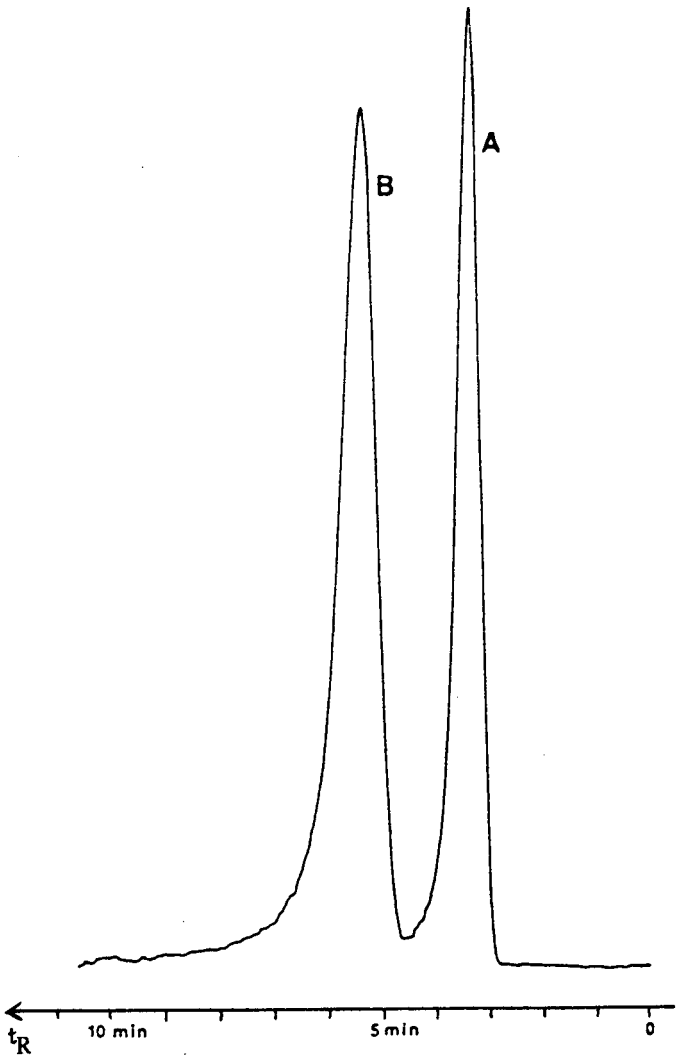

Fig. 1. Chromatogram obtained with the HS-GC–MIP system using an AT-1000-packed column. Peaks: A = MeHgCl; B = EtHgCl.

pounds make contact only with a PTFE surface [32].

The GC analyses were carried out with a 15 m × 0.53 mm I.D. (1.2 μm film thickness) FSOT column coated with Superox-FA (Alltech Assoc.). The outlet of the column is connected to the heated four-way valve. This valve is used when it is necessary for the column effluent to by-pass the plasma during the elution of the solvent peak. The four-way valve also allows a continuous argon flow to the plasma tube at all times. A second length of fused-silica capillary column (about 75 cm long, 0.53 mm I.D., no coating, deactivated) is used to connect the valve outlet to the plasma tube. Outside the GC oven, this second piece of column is enclosed in a 5 mm I.D. insulated copper tube that is heated to the maximum column temperature with a heating tape. The argon plasma is sustained in a 1 mm I.D. quartz tube. As on the packed column system, this tube is centered in a quarter-wave Evenson-type cavity (Electro Medical Supplies, Model 214L). The cavity is connected to the microwave generator via a 50-Ω coaxial cable. The plasma tube is aligned before the entrance split of the spectrometer.

The MPD 850 incorporates a 0.75 m Rowland spectrometer with six phototubes and associated slits above which are mounted a control unit, an amplifier and power supply unit and a microwave generator. A reciprocal linear UV dispersion of 0.695 nm mm^{-1} is achieved using a 960 groove mm^{-1} holographic grating fitted into a Paschen-Runge mounting.

Reagents

GC–ECD study. All chemicals were of analytical-reagent grade. Analytical standard solutions of MeHgCl, EtHgCl and PhHgCl (all from Merck) with a concentration of 10 ng μl^{-1} were prepared daily from a stock solution of 200 ng μl^{-1}. For PhHg benzene solutions were used because of the very low solubility of that compound in water. Generally, 1.0 μl of working standard was injected onto the packed columns and 0.2 μl onto the FSOT columns.

HS-GC–MIP study. Iodoacetic acid was of analytical-reagent grade and the sulphuric acid of Suprapur quality (Merck). The standard MeHgCl solutions in the range 0–100 ng ml^{-1} were prepared daily from a stock solution of 10 μg ml^{-1}, which was stored in a refrigerator [33].

All solutions were prepared in distilled, deionized water obtained with a Milli-Q apparatus (Millipore).

RESULTS AND DISCUSSION

GC–ECD study

For each column, the optimum GC conditions (optimum oven temperature and carrier gas flow-rate) were determined first. The analysis time, resolution, reproducibility (relative standard deviation on the MeHg peak heights obtained in six replicate measurements) and detection limit were also evaluated.

With the AT-1000 column, sharp peaks were observed not only for MeHgCl but also for EtHgCl. The height equivalent to a theoretical plate (HETP) was considerably lower here (for MeHgCl, HETP = 0.36 cm, for EtHgCl, HETP = 0.28 cm) than with the HS-GC–MIP system (for MeHgCl, HETP = 0.77 cm, for EtHgCl, HETP = 0.38 cm). This is possibly due to dilution taking place at the interface of this GC–MIP system between the outlet of the column and the quartz capillary plasma tube. Olsen *et al.* [17] avoided this problem by using a piece of their working column incorporated inside a heated nickel tube at the temperature of the GC oven, between the GC outlet and the plasma tube. As with the HS-GC–MIP system, no PhHg peak was observed.

Of the eight Chromosorb column packings tested, Chromosorb 101 gave the best results for the determination of MeHgCl and EtHgCl (Table II). The HETP was even lower than the plate height obtained with AT-1000. The sensitivity for MeHgCl was, however, fourteen times lower with the Chromosorb 101 column. In addition, when injecting MeHgCl and EtHgCl two small by-peaks were observed. When only MeHgCl was injected, one much smaller by-peak was observed. These results suggest an interaction between the mercury compounds and the stationary phase. Of the other Chromosorbs, 103, 106, 107 and 108 yielded a high number of theoretical plates but the sensitivity was much lower than with AT-1000 and a gradual decrease of the peak height with successive injections was observed due to interactions between the solvent (water), the mercury compounds and the stationary phase. After a certain time of reconditioning, the maximum peak height obtained for the first injection was again reached. In all instances the solvent (water) probably changed the polarity of the stationary phase.

TABLE II

GC SEPARATION EFFICIENCIES OBTAINED WITH THE GC CONDITIONS OF TABLE III

Column	MeHgCl HETP (cm)	MeHgCl relative sensitivity[a]	EtHgCl HETP (cm)	MeHgCl–EtHgCl resolution	PhHgCl HETP (cm)	PhHgCl relative sensitivity[b]
AT-1000	0.36	1	0.28	3.41	n.d.[c]	–
Chromosorb 101	0.19	14	0.16	6.55	n.d.	–
Chromosorb 102	1.00	45	1.00	0	0.61	19
Chromosorb 103	0.25	40	0.26	5.28	0.83	27
Chromosorb 104	n.d.	–	n.d.	–	n.d.	–
Chromosorb 105	2.22	25	2.67	0	n.d.	–
Chromosorb 106	0.56	60	0.36	0	0.50	56
Chromosorb 107	0.15	75	n.d.	–	0.11	49
Chromosorb 108	0.71	190	0.16	0	n.d.	–
Superox-FA	3.79	0.23	3.60	2.30	3.01	0.93
RSL-300	2.18	0.23	1.28	5.23	2.07	0.32

[a] Relative sensitivity: height of the MeHg peak obtained on the AT-1000 column divided by the MeHg peak height obtained on the tested column.

[b] MeHg peak height obtained on the AT-1000 column divided by the PhHg peak height obtained on the tested column.

[c] n.d. = not detectable.

PhHg peaks could only be observed on Chromosorb 102, 103, 106 and 107. Good peak shapes and reproducibility were obtained especially with Chromosorb 102, but the sensitivity was nineteen times lower than the MeHgCl peak on AT-1000 and interactions of the solvent with the stationary phase were also observed. In the Chromosorb series the best stationary phase for MeHgCl and EtHgCl was non-polar (Chromosorb 101) and for PhHgCl it was weakly polar (Chromosorb 102). For MeHgCl and EtHgCl, the AT-1000 column showed a much higher sensitivity.

Better results were obtained with the two FSOT columns. The best efficiency with these columns would be obtained in the capillary mode (2–4 ml min^{-1}) and using hydrogen as the carrier gas. Unfortunately, the operating parameters used (they are summarized and compared with the AT-1000 column conditions in Table III) are not optimum, as with the HS-GC–MIP system argon has to be used

TABLE III

GC CONDITIONS USED WITH THE GC–ECD SYSTEM

Column	Temperature	Carrier flow-rate (ml min^{-1})	Solvent
AT-1000	Isothermal: 150°C (MeHgCl, EtHgCl)	100	Water
Chromosorb 101–108	Isothermal: 155°C (MeHgCl, EtHgCl)	20	Water
	155°C (PhHgCl)		Benzene
Superox-FA	Isothermal: 150°C (MeHgCl, EtHgCl)	25	Water
	150°C (PhMeCl)		Benzene
RSL-300	Isothermal: 100°C (MeHgCl, EtHgCl)	25	Benzene
	150°C (PhHgCl)		Benzene
	Programme: 90°C, 16°C min^{-1} to 180°C (separation of all three components)		Benzene

(hydrogen cannot be used because it is unsuitable as a plasma support gas for the MIP). In addition, to benefit the advantage of adding no make up gas after the column (in fact the "capillary mode" is not used) requires much higher flow-rates than optimum.

With the Superox-FA column sharp and fairly symmetrical peaks were observed for the three mercury compounds (Fig. 2). The sensitivity was much higher than with the AT-1000 column (peak heights about four times higher, detection limit about six times lower) and PhHg also eluted from the column. It was not possible to obtain baseline separation between the PhHg and MeHg peak on the Superox-FA column, even with temperature programming. In contrast, this was possible on the RSL-300 column. This column gave the best results: increased baseline stability, sharp peaks (Fig. 3), low retention times, lower detection limits (Table IV) and excellent baseline resolution for the three selected organomercury chlorides. With temperature programming, more than 2000 plates were obtained for EtHg and PhHg (Fig. 4). A disadvantage for our purposes (working with aqueous mercury solutions in an HS sampler) is that aqueous solutions cannot be used.

Each of the two FSOT columns has advantages and disadvantages when used in the HS-GC–MIP system. The RSL-300 column allows the determination of the three mercury compounds but leads to a serious loss in sensitivity at the level of the HS sampler as water cannot be used with this column. With the Superox-FA column water can be used as the solvent, providing a vapour phase enrichment in the head space vial compared with a benzene solution, but the analysis then suffers from an incomplete separation of MeHgCl and PhHgCl. However, the presence of PhHg is very rare in most environmental samples.

HS-GC–MIP study

The only column that might give an improvement in sensitivity for the determination of MeHg with the HS-GC–MIP system using the AT-1000 column is the Superox-FA column. However, it is very likely that a smaller volume of sample will be injected into the head space of the FSOT column than into the packed column. Band broadening will also occur more easily with an open tubular column, therefore there can be a loss in sensitivity. Head space sampling into open tubular columns is more critical than into packed columns due to the low flow resistance of the former. Also, lower inlet pressures are generally applied to open tubular columns. The sample volume injected depends on this pressure and the flow resistance of the column. For reproducible sampling it is essential that the column head pressure is higher than the vapour pressure in the sample vial, otherwise phenomena such as double peaking and broad peaks with excessive tailing may occur. Moreover, the lower detection limit attained with the FSOT column in the GC–ECD system was partly due to an increased baseline stability. With another type of detector this effect can be totally different.

The MPD-850 detector was first evaluated and compared with the detector used in the packed column system, the Perkin-Elmer AAS-403 [29–31]. The only correct way for comparison is to use the same head space and gas chromatography system coupled to each of the detectors. The Perkin-Elmer AAS-403 detector coupled to the packed-column system was already evaluated. The AAS detector in this system was therefore replaced by the MPD-850. The HS-GC system was maintained at the normal optimum working conditions. It was shown that the best detection limit that could be attained using the MPD-850 detector was twice as high as the detection limit attained when using the AAS-403. The MeHg signal was almost three times higher with the MPD-850, but unfortunately the noise level was approximately six times higher.

Finally, the Superox-FA FSOT column was tested on the HS-GC–MIP system. Before sharp, symmetrical and reproducible peaks could be obtained for the lower MeHg concentrations (0–100 $\mu g\ l^{-1}$, the normal range for the working standards used with standard additions) it was necessary to "activate" the Superox-FA column by injecting a large concentration of MeHgCl several times (10 mg l^{-1}). It was necessary to repeat this activation every 5–10 days, depending on the number of analyses performed.

A stable plasma could be obtained at all the carrier gas flow-rates evaluated (15–35 ml min^{-1}). It was not therefore necessary to add a make up gas. The MeHg signal was almost doubled when the internal diameter of the plasma tube was reduced from 2 mm (that used on the packed column system)

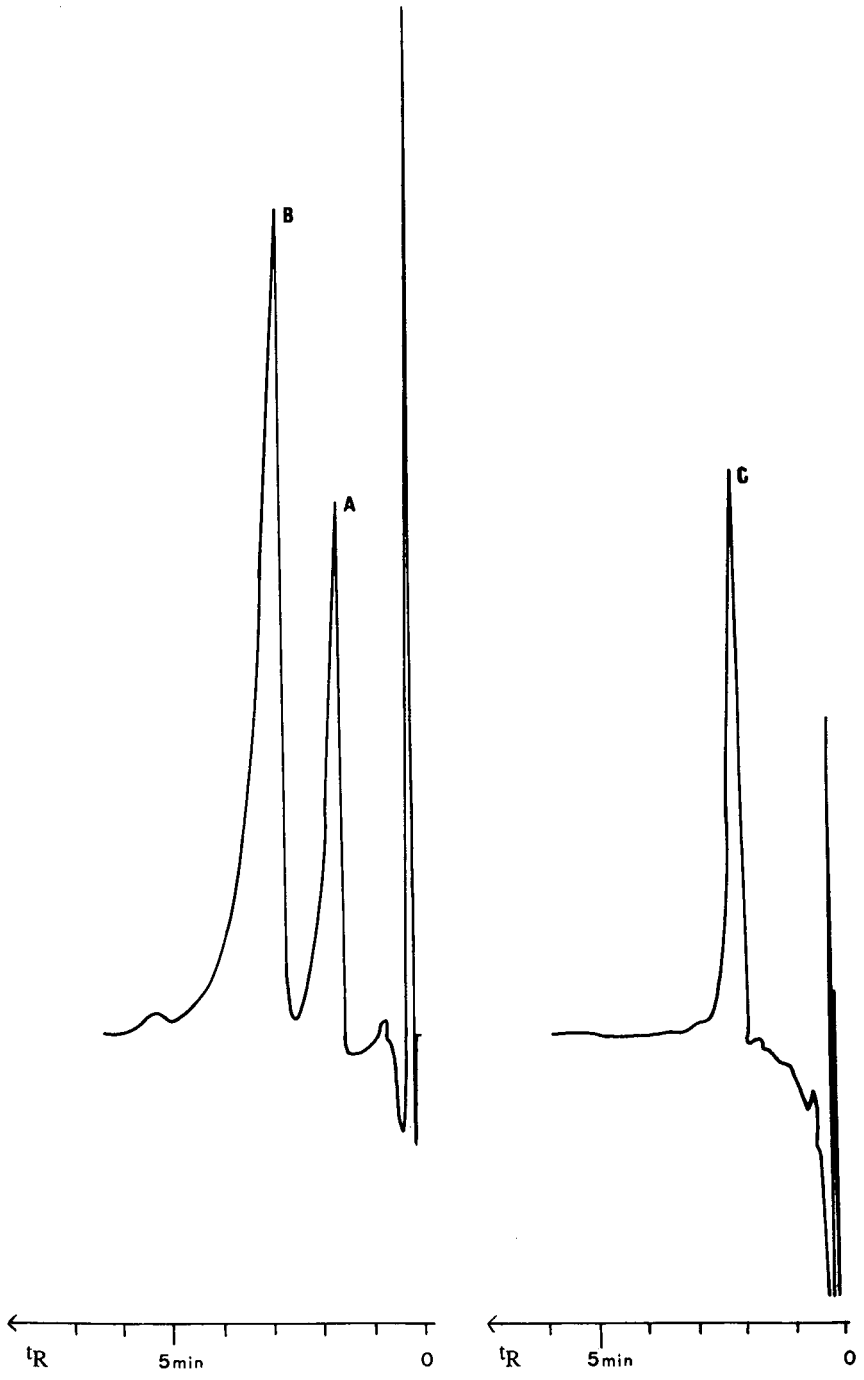

Fig. 2. Chromatograms (isothermal) obtained with the GC–ECD system using a Superox-FA FSOT column. Peaks: A = MeHgCl; B = EtHgCl; C = PhHgCl.

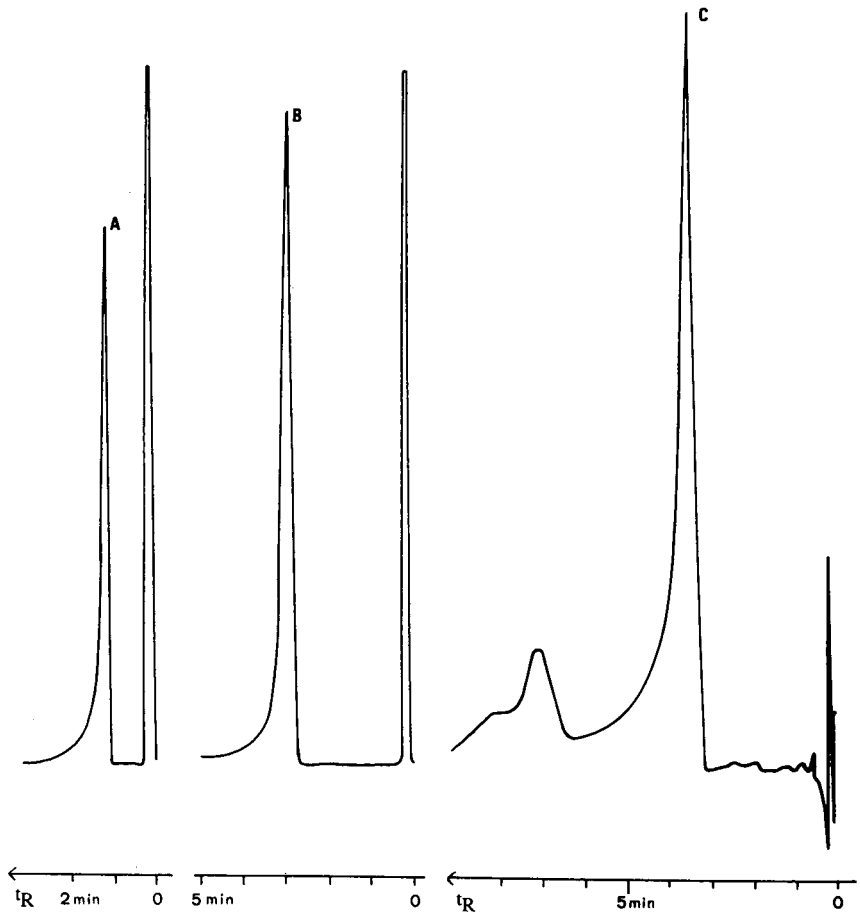

Fig. 3. Chromatograms (isothermal) obtained with the GC–ECD system using an RSL-300 FSOT column. Peaks: A = MeHgCl; B = EtHgCl; C = PhHgCl.

to 1 mm, whereas the noise level remained constant. It was also revealed that an adequate heating of the interface tube from the column to the plasma tube is essential to avoid tailing of the peaks. Cold spots in the interface have to be avoided, otherwise condensation will occur.

TABLE IV

ABSOLUTE DETECTION LIMITS (GC–ECD SYSTEM)

Defined as the signal level corresponding to twice the standard deviation of the background signal.

Column	MeHgCl (pg)	EtHgCl (pg)	PhHgCl (pg)
AT-1000	4.1	4.1	–
Superox-FA	0.7	0.5	3.1
RSL-300	0.4	0.3	0.5

The HETP attained was very high (6.8 cm). The retention time was very short (1 min) and was close to the time necessary for the column effluent to by-pass the plasma (30 s), the time necessary for complete elution of the solvent peak. A typical chromatogram (at 170°C and 30 ml min^{-1}, the optimum conditions) is shown in Fig. 5. Compared with the MeHg peak obtained with the packed column system (Fig. 1) a narrower peak showing less tailing is obtained.

When the pure solvent (water) was injected after the injection of a standard solution, a small memory peak was observed. As a modified head space

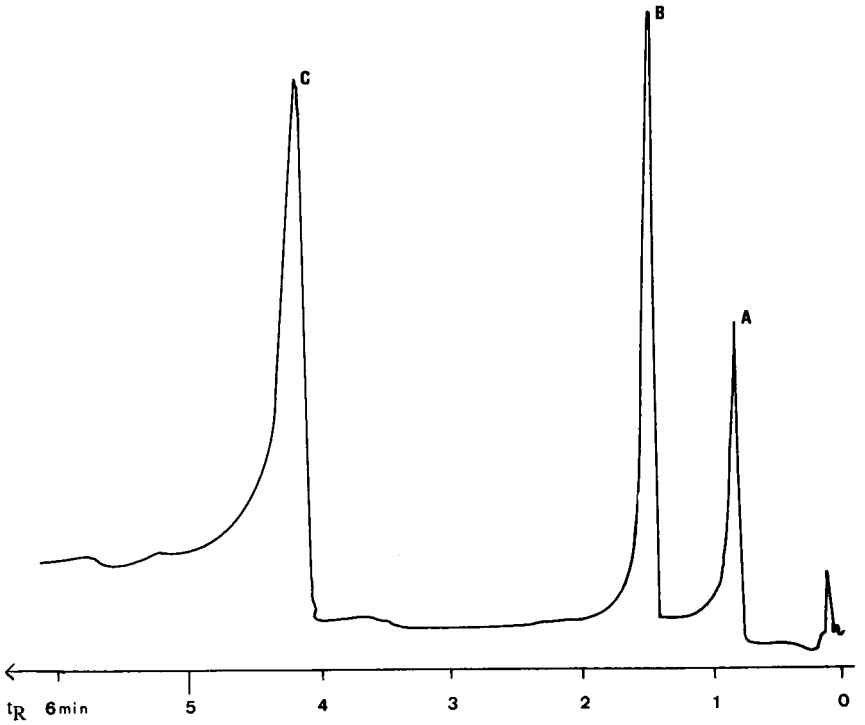

Fig. 4. Chromatogram (temperature programming) obtained with the GC–ECD system using an RSL-300 FSOT column. Peaks: A = MeHgCl; B = EtHgCl; C = PhHgCl.

sampler was used it seems that head space sampling into the FSOT column is more critical to avoid memory peaks than head space sampling into the packed column. This memory effect was dependent on the concentration of the standard: the memory peak was higher for a standard with a higher concentration. Despite this small memory effect, the reproducibility for the measurement of MeHgCl standard solutions on the capillary HS-GC–MIP system was very good. The relative standard deviation of the peak heights of six replicate measurements was typically 4%, which is slightly higher than that typically obtained with the packed column system (3%). The correlation coefficient of the linear regression for the calibration graph was 0.999 (seven concentrations, each concentration injected three times to give a total of 21 injections). The detection limit, expressed as the signal level corresponding to twice the standard deviation of the background signal, was 0.5 $\mu g\ l^{-1}$. The detection limit obtained with the packed column system using the MPD-850 was 0.8 $\mu g\ l^{-1}$, or 1.6 times higher. If the AAS-403 was used as the detector in the capillary system, it was possible to obtain a detection limit of about 0.25 $\mu g\ l^{-1}$.

In a final step, a real sample was analysed using the capillary column system. The mussel sample (*mytilus edulis*), was obtained from the Community Bureau of Reference for an intercomparison exercise on the determination of MeHg in biological tissues. Ten other laboratories also analysed this sample. It was analysed in this laboratory with both systems, the packed column and capillary HS-GC–MIP systems. Fig. 6 shows the calibration graph obtained with the capillary system using the standard additions method [29,30]. As can be seen, a correction for the memory effect is very important. Without correction, a value of $0.189 \pm 0.005\ \mu g\ g^{-1}$ MeHgCl (result $\pm$ S.D.) is found for MeHg in mussel tissue. With correction (the signal is the sum of the major MeHg peak and the small memory peak), a value of $0.170 \pm 0.011\ \mu g\ g^{-1}$ MeHgCl is found. Fig. 7 compares this result with that obtained with the packed column system and those obtained

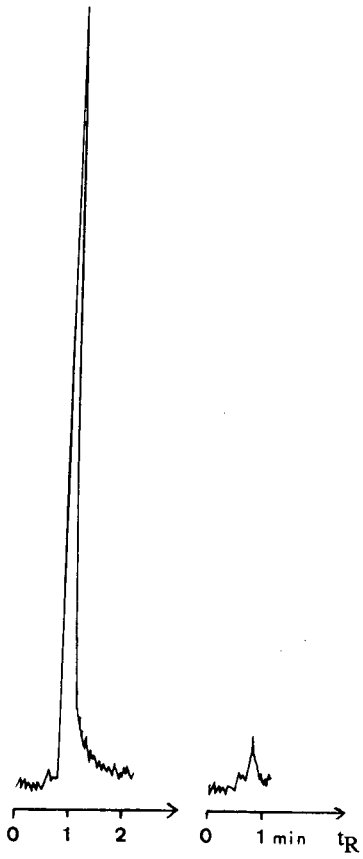

Fig. 5. Chromatogram (isothermal) obtained with the new HS-GC–MIP system using a Superox-FA FSOT column. The small peak is a typical memory peak obtained for this MeHg peak.

by the other laboratories participating in the intercalibration exercise.

In conclusion, the capillary column system yields only a limited success in terms of attaining a better sensitivity. With the Superox-FA column, a factor of 1.6 in the detection limit can be gained, compared with a packed column, but a factor 6 was obtained with a capillary column and the GC–ECD system. It should be noted that this factor 6 was partly due to an increased baseline stability for the capillary column. With the MIP detector, the difference in noise level for both columns was minimal.

It is also clear from this study that it is impossible to compare only the packed and the capillary columns when using the HS-GC–MIP system. The HS-GC and the GC–MIP interfaces have to be

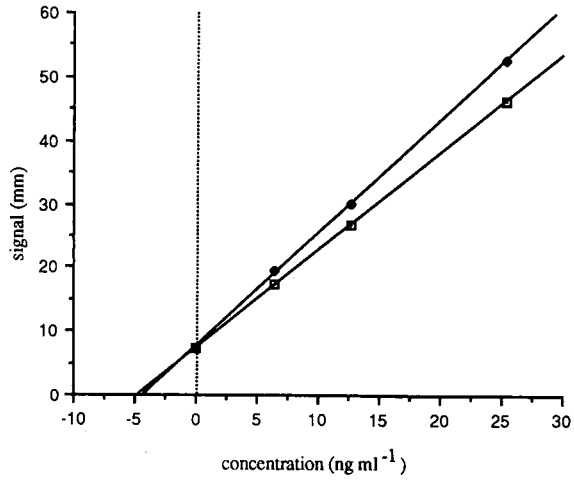

Fig. 6. Calibration graph obtained for the mussel sample using the HS-GC–MIP system with Superox-FA FSOT column. (⊡) Without correction for the memory effect; (◆) with correction. (⊡) $y = 7.28 + 1.53x, r^2 = 1.000$; (◆) $y = 7.60 + 1.78x, r^2 = 1.000$.

optimized for each specific column (*e.g.* the amount of sample which can be injected onto the capillary column is smaller than onto the packed column; the internal diameter of the interface tube from the capillary column to the plasma tube is smaller than with a packed column and the plasma tube itself has

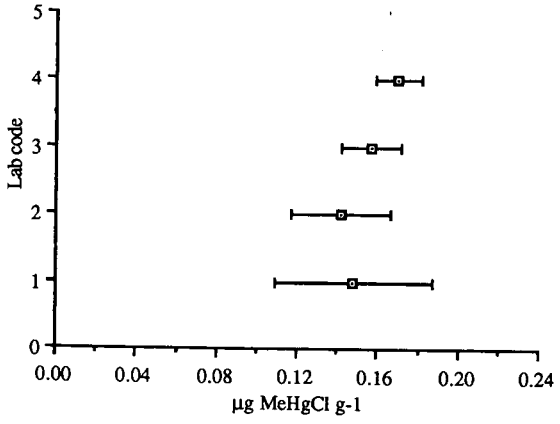

Fig. 7. Intercomparison of the results found for the mussel sample. Lab code 1, mean of all individual values ±S.D. reported by the ten different laboratories participating in the intercalibration exercise; lab code 2, mean of mean values ±S.D. reported by the same labs; lab code 3, result ±S.D. found by this laboratory using packed HS-GC–MIP; lab code 4, result ±S.D. found by this laboratory using capillary HS-GC–MIP.

a smaller internal diameter), so that more than the column parameters differ for the two systems.

The capillary column has some important disadvantages compared with the packed column: the capillary column has to be activated regularly and there is a limited memory effect. As packed columns are also cheaper and more easy to handle than capillary columns, it seems obvious to continue working with a packed column.

REFERENCES

1 Y. Thibaud and J. Noel, *Evaluation des Teneurs en Mercure, Methylmercure et Selenium dans les Poissons et Coquillages des Cotes Françaises de la Méditerranée, Rapport Définitif*, Ifremer, Nantes, 1989.
2 N. Bloom, *Can. J. Fish. Aquat. Sci.*, 46 (1989) 1131.
3 K. May, M. Stoeppler and K. Reisinger, *Toxicol. Environ. Chem.*, 13 (1987) 153.
4 S. P. Raj, *J. Environ. Biol.*, 8 (1987) 151.
5 A. M. Scheuhammer, *Environ. Pollut.*, 46 (1987) 263.
6 K. Reisinger, M. Stoeppler and H. W. Nürnberg, *Fresenius Z. Anal. Chem.*, 316 (1983) 612.
7 J. Yamamoto, Y. Kaneda and Y. Hikasa, *Int. J. Environ. Anal. Chem.*, 16 (1983) 1.
8 N. S. Bloom, C. J. Watras and J. P. Hurley, in *Proceedings of an International Conference on Mercury as an Environmental Pollutant, Gävle, Sweden, June 1990, Wat. Air Soil Pollut.*, (1991) in press.
9 N. S. Bloom and S. W. Effler, in *Proceedings of an International Conference on Mercury as an Environmental Pollutant, Gävle, Sweden, June 1990, Wat. Air Soil Pollut.*, (1991) in press.
10 M. Dermelj, M. Horvat, A. R. Byrne and P. Stegnar, *Chemosphere*, 16 (1987) 877.
11 M. Horvat, T. Zvonaric, P. Stegnar and A. R. Byrne, *3rd International Conference on Environmental Contamination, Venice, 1988.*
12 S. C. Hight and M. T. Corcoran, *J. Assoc. Off. Anal. Chem.*, 70 (1987) 24.
13 M. Horvat, K. May, M. Stoeppler and A. R. Byrne, *Appl. Organomet. Chem.*, 2 (1988) 515.
14 M. Horvat, A. R. Byrne and K. May, *Talanta*, 37 (1990) 207.
15 Y. Talmi, *Anal. Chim. Acta*, 74 (1975) 107.
16 K. Chiba, K. Yoshida, K. Tanabe, H. Haraguchi and K. Fuwa, *Anal. Chem.*, 55 (1983) 450.
17 K. B. Olsen, D. S. Sklarew and J. C. Evans, *Spectrochim. Acta, Part B*, 40 (1985) 357.
18 G. Decadt, W. Baeyens, D. Bradley and L. Goeyens, *Anal. Chem.*, 57 (1985) 2788.
19 J. E. O'Reilly, *J. Chromatogr.*, 238 (1982) 433.
20 A. G. F. Brooks, E. Bailey and R. T. Snowden, *J. Chromatogr.*, 374 (1986) 289.
21 R. Dumarey, R. Dams and P. Sandra, *J. High Resolut. Chromatogr. Chromatogr. Commun.*, 5 (1982) 687.
22 S. P. Wasik and F. P. Schwartz, *J. Chromatogr. Sci.*, 18 (1980) 660.
23 B. D. Quimby, M. F. Delaney, P. C. Uden and R. M. Barnes, *Anal. Chem.*, 52 (1980) 259.
24 T. Hanie, S. Coulombe, M. Moison and J. Hubert, *Dev. At. Plasma Spectrochem. Anal. Proc. Int. Winter Conf. 1980*, (1981) 337.
25 S. A. Estes, P. C. Uden and R. M. Barnes, *Anal. Chem.*, 54 (1982) 2402.
26 C. J. Cappon and T. Y. Toribara, *LC · GC*, 4 (1986) 1010.
27 J. H. Petersen, *Report: Evaluation of CP Sil 8 Stationary Phase in Gas Chromatographic Determinations of Methylmercury*, Levnedsmiddelstyrelsen, Søborg.
28 Y. H. Lee and J. Mowrer, *Anal. Chim. Acta*, 221 (1989) 259.
29 P. Lansens and W. Baeyens, *Anal. Chim. Acta*, 228 (1990) 93.
30 P. Lansens, M. Leermakers and W. Baeyens, in *Proceedings of an International Conference on Mercury as an Environmental Pollutant, Gävle, Sweden, June 1990, Wat. Air Soil Pollut.*, (1991) in press.
31 P. Lansens, C. Meuleman, M. Leermakers and W. Baeyens, *Anal. Chim. Acta*, 234 (1990) 417.
32 P. Lansens and W. Baeyens, *J. High Resolut. Chromatogr.*, 12 (1989) 132.
33 P. Lansens, C. Meuleman and W. Baeyens, *Anal. Chim. Acta*, 229 (1990) 281.

Journal of Chromatography, 586 (1991) 341–346
Elsevier Science Publishers B.V., Amsterdam

CHROM. 23 656

Predicting partition coefficients in polyethylene glycol–potassium phosphate aqueous two-phase systems

Mark A. Eiteman*,☆ and John L. Gainer

Center for Bioprocess and Product Development, Department of Chemical Engineering, University of Virginia, Charlottesville, VA 22903-2442 (USA)

(First received April 25th, 1991; revised manuscript received July 23rd, 1991)

ABSTRACT

Partition coefficients in polyethylene glycol–potassium phosphate aqueous two-phase systems are predicted using a previously developed mathematical model. The model is based on a simplification of equations which arise from an osmotic pressure virial expansion and relates the partition coefficient to the concentration difference between phases of one of the phase-forming components and to the solute hydrophobicity. The predicted partition coefficients are compared to experimental values for several different solutes in this phase system over the range of pH of 5.5 to 9.2. The predictions are generally good for uncharged solutes, but show disagreement with experimental values for charged solutes.

INTRODUCTION

An aqueous two-phase system may occur when two mutually incompatible components, such as polyethylene glycol (PEG) and dextran, or PEG and certain salts, are dissolved together in water. Two liquid phases form, with each of the incompatible components tending to enrich one or the other phase. A solute added to such a system partitions between the phases, and its partition coefficient, K, is defined as the solute concentration in the upper phase divided by the solute concentration in the lower phase. Numerous studies have focussed on the general prediction of partition coefficients in aqueous two-phase systems. For example, the partition coefficient is thought to depend on solute hydrophobicity [1,2], molecular weight [3], temperature [4], pH [5–7], solute charge [8], and the presence of additional salts [9–12]. Since such two-phase systems are composed primarily of water, they provide a gentle environment for the fractionation of biomaterials [4,13–15], and a detailed review of the use of two-phase systems for the recovery of proteins has recently been published by Huddleston and Lyddiatt [16].

Several models and correlations have been developed to predict partition coefficients in aqueous two-phase systems. Diamond and Hsu [17,18] simplified the lattice model of Flory [19] and Huggins [20] to correlate the partitioning of peptides and proteins. Baskir *et al.* [21] modified a spherical lattice model to predict the distribution of particulates between two polymer–polymer phases. Kang and Sandler [22,23] extended the UNIQUAC equation to predict the binodal phase diagram, while King *et al.* [24] combined a term for electrostatic effects with the osmotic pressure virial expansion to predict protein partitioning. Cabezas *et al.* [25] proposed a model derived from the Hill solution theory, and Forciniti and Hall [26] have used statistical mechanical models for predicting phase diagrams and partition coefficients of proteins. All of these approaches have provided insights into polymer solution behavior and partitioning, but many are of limited use

☆ Present address: Department of Biological and Agricultural Engineering, Driftmier Engineering Center, University of Georgia, Athens, GA 30602, USA.

0021-9673/91/$03.50

because of the difficulty in predicting the pertinent parameters. However, one result has been that, to a good approximation, the logarithm of a solute's partition coefficient is proportional to the concentration difference between the phases of one of the phase-forming components (Δw_2):

$$\ln K = k\Delta w_2. \quad (1)$$

Obviously, if a suitable expression is found for the proportionality constant, then eqn. 1 can be very convenient and useful for predicting partition coefficients. Although no insight is gained into the actual molecular mechanisms of phase formation and solute partitioning, eqn. 1, nevertheless, permits *a priori* predictions of partition coefficients in aqueous two-phase systems.

For several years, Zaslavsky and co-workers [27–30] have studied the effect that the number of methylene groups on the solute molecule has on its partition coefficient. In all systems studied, they found that a linear relationship exists between the logarithm of the partition coefficient and the number of methylene groups on the aliphatic chain of the solute. Moreover, the hydrophobic properties of aqueous two-phase systems were quantified by a Δg^{CH2} value [31], which has been defined as the free energy for a methylene group transfer between the phases. The introduction of such a hydrophobicity scale permits comparison of different phase systems.

One method to describe solute hydrophobicity in terms which are independent of the two-phase system has recently been advanced by Eiteman and Gainer [32]. Consistent with observations of Zaslavsky and co-workers [27–30], the logarithm of the partition coefficient of a solute in an aqueous two-phase system has been shown to be linearly related to the solute hydrophobicity (as measured by its log P value [33,34]). Since a value for log P for a solute may be calculated using a group contribution method [35], this approach allows an *a priori* estimation of partition coefficients. Specifically, the partition coefficient may be correlated by:

$$\ln K = D\Delta w_2 \log(P/P_0), \quad (2)$$

where D has been termed the discrimination factor and log P_0 the intrinsic hydrophobicity of the phase system.The value of the intrinsic hydrophobicity marks the boundary on the hydrophobicity scale above which solutes will partition into the upper phase and below which solutes will partition into the lower phase. Both of these parameters should be constant for any given two-phase system. Their values for a particular phase system (constant Δw_2) may be readily determined by partitioning a series of normal alcohols. The partition coefficients will be related to the hydrophobicity of the solutes:

$$\ln K = B + m \log P \quad (3)$$

If the value of Δw_2 is also measured for the specific system of interest, the D and log P_0 may be calculated directly by comparing eqns. 2 and 3:

$$D = \Delta w_2/m \quad (4)$$

$$\log P_0 = -B/m \quad (5)$$

The model (eqn. 2) has previously been applied to the prediction of partition coefficients in the PEG–$MgSO_4$ system, at a single pH [32]. The same model should apply for simple compounds in other systems, such as a system which spans several units of pH. In this study the PEG–potassium phosphate system, without additional buffering, was selected to examine the applicability of eqn. 2.

MATERIALS AND METHODS

PEG molecular weight 8000, potassium phosphate monobasic (KH_2PO_4) and potassium phosphate dibasic (K_2HPO_4) were each purchased from Sigma, St. Louis, USA. Stock solutions of 1.00 M monobasic and dibasic salts were each prepared with distilled deionized water. Ten phase systems covering a range of pH values (but each of 1.00 M phosphate ion concentration) were prepared by combining proportions of the monobasic and dibasic stock solutions. The proportion of the monobasic salt solution used varied between 0 and 90%. An amount of 2.00 g PEG was added to each of the 10 ml 1.00 M phosphate solutions. For pH, density, PEG concentration measurements, and partitioning experiments the capped solutions were equilibrated at 25°C (±0.05°C) in a constant temperature bath (Brinkmann Instruments) for about one week.

Amounts of 10–50 mg of various solutes were

added to each of the separate systems. After equilibration, the phases were then carefully separated with glass Pasteur pipets. Gas or liquid chromatography, as appropriate, was employed to determine the solute concentration in each phase. The partition coefficients for small molecules were found to be independent of solute concentration for the range of dilute solutions prepared. The two-phase systems used for the determination of pH were placed in capped tubes under nitrogen, and the analysis performed on the lower of separated phases at 23°C using an Orion Sureflow pH electrode and a Corning general purpose combination electrode. A 10-ml pycnometer was used to measure density (ρ) at 25°C. The concentration of PEG was found by freeze-drying each phase, then extracting PEG from the residue with warm acetone.

The gas chromatographic (GC) column selected was a 6 ft. × 2 mm I.D. glass column packed with Chromosorb 101 (80/100) from Alltech, Deerfield, USA. The instrument itself was a Hewlett-Packard 5890A fitted with a flame ionization detector. The operating temperatures, carrier gas (helium) flow-rate and pressure were adjusted depending upon the particular solute analyzed. The high-performance liquid chromatographic (HPLC) system comprised a Whatman 5-μm Partisphere C_8 column, Waters pumps Model 510, with a Gilson Model 231 sample injector, a Waters UV detector (Model 481), and Hewlett-Packard 3392A integrator. The standard error of the mean from the analyses did not exceed 6%.

RESULTS AND DISCUSSION

Ten different two-phase systems, each containing 1.00 *M* phosphate ion concentration, were prepared over the pH range of 5.5 to 9.2, and Table I lists their properties. The effect of pH on the PEG concentration difference between the phases is shown in Fig. 1. The value of the PEG concentration difference is greatest at the highest values of pH. Since eqn. 1 suggests that the logarithm of the partition coefficient is proportional to the PEG concentration difference, one might anticipate that any hydrophobic solute will exhibit the greatest partition coefficient at high pH values. (Conversely, a hydrophilic solute will partition more into the lower phase the higher the pH.)

Initially, a series of normal alcohols (from ethanol to hexanol) was studied, and the partition coefficients are shown in Fig. 2 as a function of pH. The partition coefficients for each alcohol were lowest at acidic pH values. This observation should not be attributed to any change in the solute with pH, but rather to a change in the phase system itself since the PEG concentration difference between the phases (Δw_2) is greatest at the highest pH values. Furthermore, the more hydrophobic the alcohol, the greater its partition coefficient. Therefore, the partitioning behavior observed qualitatively agrees with eqn. 2.

The parameters D and log P_0 may be calculated from the data shown in Fig. 2. These two parameters will have different values for each solution.

TABLE I

SUMMARY OF THE PEG–1.00 *M* POTASSIUM PHOSPHATE AQUEOUS TWO-PHASE SYSTEM AT 25°C.

pH$^-$ denotes lower phase pH, while ρ' and ρ'' denote upper and lower phase densities, respectively.

% Dibasic (1.00 *M*)	PEG (wt.%)	K (wt.%)	PO_4^{3-} (wt.%)	pH″	ρ' (g/ml)	ρ'' (g/ml)	Δw_2
100	0.150	0.0586	0.0712	9.17	1.0839	1.1773	0.64
90	0.150	0.0559	0.0714	7.88	1.0827	1.1736	0.60
80	0.151	0.0531	0.0717	7.44	1.0819	1.1699	0.53
70	0.151	0.0504	0.0720	7.17	1.0813	1.1660	0.52
60	0.152	0.0476	0.0722	6.90	1.0809	1.1622	0.48
50	0.153	0.0447	0.0724	6.63	1.0810	1.1587	0.46
40	0.153	0.0419	0.0727	6.39	1.0814	1.1540	0.44
30	0.154	0.0390	0.0730	6.13	1.0825	1.1499	0.40
20	0.154	0.0362	0.0732	5.83	1.0848	1.1454	0.35
10	0.155	0.0333	0.0735	5.52	1.0889	1.1400	0.30

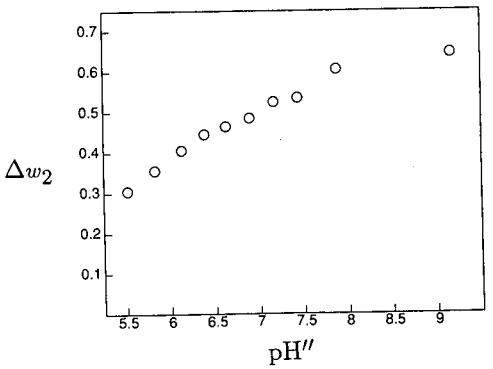

Fig. 1. PEG concentration difference between the phases (Δw_2) *versus* the lower phase pH in the PEG–1.00 *M* potassium phosphate aqueous two-phase system at 25°C.

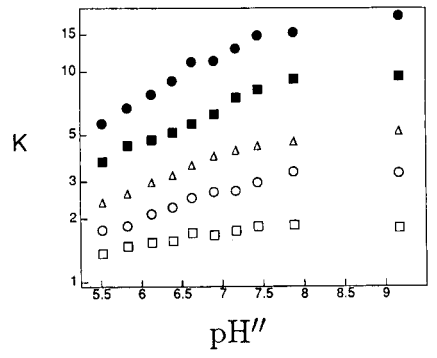

Fig. 2. Measured partition coefficients (K) of normal alcohols *versus* the lower phase pH in the PEG–1.00 *M* potassium phosphate aqueuos two-phase system at 25°C. ● = Hexanol; ■ = pentanol; △ = butanol; ○ = propanol; □ = ethanol.

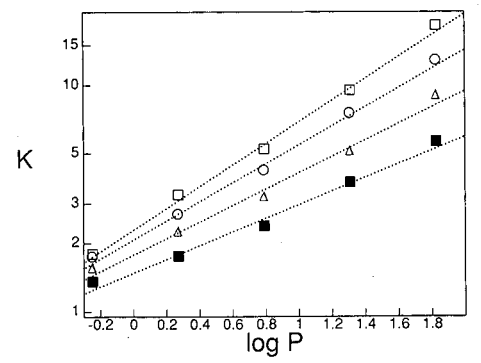

Fig. 3. Measured partition coefficients (K) of normal alcohols *versus* their hydrophobicity (log P) as calculated by the method of Rekker and DeKort [35]. Dotted lines show least squares fit of data to eqn. 3 (numeric values of constants shown in Table II). Lower phase pH: □ = 9.17; ○ = 7.17; △ = 6.39; ■ = 5.52.

The parameters are determined using eqn. 3 by plotting the logarithm of the observed partition coefficient *versus* the calculated hydrophobicity. Fig. 3 shows such plots for four of the solutions, while Table II lists the calculated values of the slope (m), intercept (B) and correlation coefficient (R) for all of the systems studied. In general, the slopes and intercepts (of eqn. 3) are larger the higher the pH. The values of these slopes and intercepts may be used in eqn. 4 and 5, along with the measured concentration differences to calculate the discrimination factor and intrinsic hydrophobicity for each phase system. Fig. 4 shows the values for the paramaters D and log P_0 for each solution. The value of each parameter generally decreases with increasing pH, so that the phosphate system having the lowest pH is the most intrinsically hydrophobic.

With these calculated values for the discrimination factor and intrinsic hydrophobicity, as well as the measured concentration difference, eqn. 2 may be used to predict partition coefficients for other solutes. Fig. 5 shows the predicted and observed partition coefficients for three organic solutes in the PEG–potassium phosphate aqueous two-phase system. The partition coefficients for methyl pentanone and butanediol are very well predicted by the model, while the predicted partition coefficients for phenylpropanol are consistently about 15% below the observed values.

TABLE II

CALCULATED SLOPES (m), INTERCEPTS (B) AND CORRELATION COEFFICIENTS (R) OF PARTITION COEFFICIENTS OF NORMAL ALCOHOLS IN THE PEG–1.00 *M* POTASSIUM PHOSPHATE AQUEOUS TWO-PHASE SYSTEM AT 25°C

Data was fit to the Eqn. 3.

pH″	Slope (m)	Intercept (B)	R
9.17	1.0978	0.8351	0.999
7.88	1.0081	0.8484	0.996
7.44	0.9987	0.7905	0.997
7.17	0.9636	0.7341	0.998
6.90	0.8973	0.6985	0.998
6.63	0.8790	0.6652	0.991
6.39	0.8320	0.5804	0.995
6.13	0.7809	0.5396	0.995
5.83	0.7501	0.4615	0.991
5.52	0.6909	0.3957	0.994

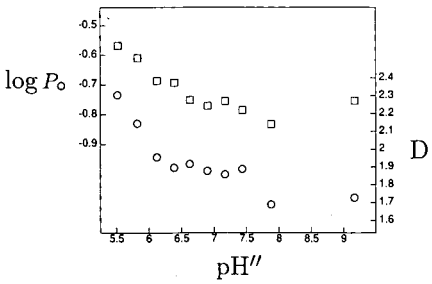

Fig. 4. Intrinsic hydrophobicity (log P_0) and discrimination factor (D) in the PEG–1.00 M potassium phosphate aqueous two-phase system at 25°C. □ = Intrinsic hydrophobicity; ○ = discrimination factor.

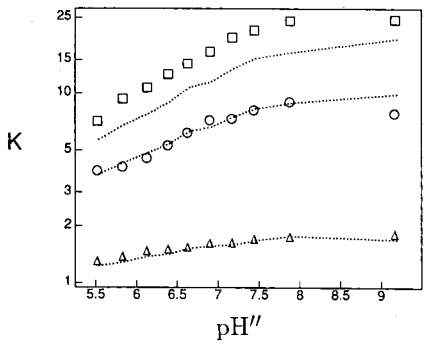

Fig. 5. Predicted (dotted curves) and observed partition coefficients *versus* the pH of the lower phase in the PEG–1.00 M potassium phosphate aqueous two-phase system at 25°C. Hydrophobicities calculated by the method of Rekker and DeKort [35]. □ = Phenylpropanol (log P = 1.93); ○ = 4-methyl 5-pentanone (log P = 1.32); △ = 2,3-butanediol (log P = −0.286).

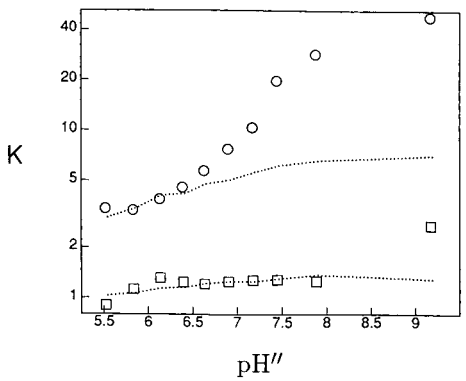

Fig. 6. Predicted (dotted curves) and observed partition coefficients *versus* the pH of the lower phase in the PEG–1.00 M potassium phosphate aqueous two-phase system at 25°C. Hydrophobicities calculated by partition in PEG–magnesium sulfate system [32,36]. ○ = Tyrosine-phenylalanine (log P = 1.01); □ = tyrosine (log P = −0.539).

The solutes shown in Fig. 5 are all uncharged, while Fig. 6 shows the application of the model to two charged compounds, tyrosine and the peptide tyrosine-phenylalanine. The model predicts the partitioning behavior of tyrosine at low pH; however, at the highest pH the observed partition coefficient is twice as high as the prediction. Since these partition coefficients are close to one and a relatively small change may be difficult to detect, a more hydrophobic peptide was selected. As Fig. 6 shows, the partition coefficients of tyrosine-phenylalanine are predicted well by the model only at low pH, which are solutions in which the peptide will be uncharged. When the pH increases and the peptide becomes increasingly negatively charged, the observed partition coefficients increasingly exceed the model predictions. Although limited, these results suggest that in the PEG–phosphate system, a negatively charged solute will tend to have a greater partition coefficient at a particular pH than it would have if it were uncharged at that same pH. An additional term appears to be necessary in the model to account for these charge effects.

CONCLUSIONS

Partition coefficients of uncharged solutes have been successfully predicted in PEG–potassium phosphate aqueous two-phase systems over the pH range of 5.5–9.2. However, partitioning results with charged solutes indicate that, in this phase system, the observed partition coefficients become greater than predicted when solutes become more negatively charged.

REFERENCES

1 V. P. Shanbhag and C.-G. Axelsson, *Eur. J. Biochem.*, 60 (1975) 17.
2 M. A. Eiteman and J. L. Gainer, *Biotechnol. Prog.*, 6 (1990) 479.
3 P.-Å. Albertsson, A. Cajarville, D. E. Brooks and F. Tjerneld, *Biochim. Biophys. Acta*, 926 (1987) 87.
4 P.-Å. Albertsson, *Partition of Cell Particles and Macromolecules*, Wiley, New York, 1986.
5 P.-Å. Albertsson, S. Sasakawa and H. Walter, *Nature (London)*, 228 (1970) 1329.
6 H. Walter, S. Sasakawa and P.-Å. Albertsson, *Biochemistry*, 11 (1972) 3880.
7 C. L. DeLigny and W. J. Gelsema, *Sep. Sci. Techno.*, 17 (1982) 375.

8 C. M. Ballard, J. P. Dickinson and J. J. Smith, *Biochim. Biophys. Acta*, 582 (1979) 89.
9 G. Johansson, *Biochim. Biophys. Acta*, 221 (1970) 387.
10 G. Johansson, *Acta Chem. Scand.*, B28 (1974) 873.
11 S. Bamberger, G. V. F. Seaman, J. A. Brown and D. E. Brooks, *J. Colloid Interface Sci.*, 99 (1984) 187.
12 B. Yu. Zaslavsky, L. M. Miheeva, G. Z. Gasanova and A. U. Mahmudov, *J. Chromatogr.*, 392 (1987) 95.
13 H. Hustedt, K. H. Kroner, U. Menge and M.-R. Kula, *Trends Biotechnol.*, 3 (1985) 1.
14 H. Walter, D. E. Brooks and D. Fisher, *Partitioning in Aqueous Two-Phase Systems*, Academic Press, 1985.
15 B. Mattiasson and R. Kaul, *ACS Symp. Ser.*, 314 (1986) 78.
16 J. G. Huddleston and A. Lyddiatt, *Appl. Biochem. Biotechnol.*, 26 (1991) 249.
17 A. D. Diamond and J. T. Hsu, *Biotechnol. Bioeng.*, 34 (1989) 1000.
18 A. D. Diamond and J. T. Hsu, *J. Chromatogr.*, 513 (1990) 137.
19 P. J. Flory, *J. Chem. Phys.*, 10 (1942) 51.
20 M. L. Huggins, *J. Phys. Chem.*, 46 (1942) 151.
21 J. N. Baskir, T. A. Hatton and U. W. Suter, *Macromolecules*, 20 (1987) 1300.
22 C. H. Kang and S. I. Sandler, *Fluid Phase Equil.*, 38 (1987) 245.
23 C. H. Kang and S. I. Sandler, *Biotechnol. Bioeng.*, 32 (1988) 1158.
24 R. S. King, H. W. Blanch and J. M. Prausnitz, *AIChE J.*, 34 (1988) 1585.
25 H. Cabezas, J. D. Evans and D. C. Szlag, *Fluid Phase Equil.*, 53 (1989) 453.
26 D. Forciniti and C. K. Hall, *ACS Symp. Ser.*, 419 (1990) 53.
27 B. Yu. Zaslavsky, L. M. Miheeva and S. V. Rogozhin, *J. Chromatogr.*, 212 (1981) 13.
28 B. Yu. Zaslavsky, N. M. Mestechkina, L. M. Miheeva and S. V. Rogozhin, *J. Chromatogr.*, 240 (1982) 21.
29 B. Yu. Zaslavsky, A. A. Masimov, A. A. Gasanov and S. V. Rogozhin, *J. Chromatogr.*, 294 (1984) 261.
30 B. Yu. Zaslavsky, L. M. Miheeva, G. Z. Gasanova and A. U. Mahmudov, *J. Chromatogr.*, 403 (1987) 123.
31 S. S. Davis, T. Higuchi and J. H. Rytting, *J. Pharm. Pharmacol.*, 24 (1972) 30P.
32 M. A. Eiteman and J. L. Gainer, *Biosepar.*, 2 (1991) 31.
33 A. J. Leo, C. Hansch and D. Elkins, *Chem. Rev.*, 71 (1971) 525.
34 A. J. Leo, *J. Pharm. Sci.*, 76 (1987) 166.
35 R. F. Rekker and H. M. DeKort, *Eur. J. Med. Chem.-Chim.*, 14 (1979) 479.
36 M.A. Eiteman, *Ph.D. Dissertation*, University of Virginia, Charlottesville, USA (1991).

Journal of Chromatography, 586 (1991) 347–350
Elsevier Science Publishers B.V., Amsterdam

CHROM. 23 666

Short Communication

Derivatization of saturated long-chain fatty acids with phenacyl bromide in non-ionic micelles

Ilana Zamir

Department of Inorganic and Analytical Chemistry, Hebrew University, 91904 Jerusalem (Israel)

(First received April 18th, 1991; revised manuscript received July 23rd, 1991)

ABSTRACT

The derivatization of saturated long-chain fatty acids (LCFA) with a UV chromophore, 1,4-dibromoacetophenone, using non-ionic micelles to facilitate the reaction is described. Synperonic NP-12 was used as a non-ionic surfactant and tetrakis(decyl)ammonium bromide as an ion-pair agent. The reaction was carried out in the dark at 60°C for 20 min. After adding 1 ml of chloroform to the reaction mixture and centrifugation for 30 s, the mixture was ready for high-performance liquid chromatographic analysis on an RP-18 column. The derivatization rate constant for LCFA was found to be in the range $6 \cdot 10^{-4}$–$9 \cdot 10^{-4}$ s^{-1}. The use of micelles overcomes solubility difficulties with highly lipophilic compounds such as LCFA and provides a simple derivatization procedure.

INTRODUCTION

Lipophilic compounds such as fatty acids lack a chromophore or a fluorophore that permits their detection and they therefore require derivatization steps prior to their high-performance liquid chromatographic (HPLC) analysis. Most often these derivatization reactions are carried out in aprotic solvents. Micellar solutions have been used to enhance the reactions by extractive separation similarly to liquid–liquid extraction [1]. Among the compounds that have been made to react in such solutions are amino acids [2], fatty acids [3] and others [4].

Recently, Van der Horst and co-workers [5,6] reported the advantages of micellar systems in the derivatization of carboxylic acids with fluorphore reagents such as 4-bromomethyl-7-methoxycoumarin and 9-bromomethylacridine [7]. The theory and practice of micellar phase-transfer catalysis (MPTC) have been discussed extensively (*e.g.*, [8]).

Derivatization in an aqueous micellar system, without the need for isolation of the analyte prior to the derivatization reaction, is likely to result in good yields and to be less time consuming. In addition, the use of MPTC permits the derivatization of long-chain fatty acids (LCFA) directly in aqueous solutions. The aim of this study was to apply the recently developed micellar-aided derivatization technique to the analysis of LCFA.

The procedure used is based on that of Van der Horst *et al.* [8,9], which has been extended to allow the determination of LCFA with the use of a common UV label bromophenacyl bromide, which has not been used before in MPTC. The micellar system consisted of an aqueous solution containing Synperonic NP-12 as a non-ionic surfactant. A non-ionic surfactant was chosen to allow for better interactions with, and therefore better solvation of, the hydrophobic LCFA [10]. Tetrakis(decyl)ammonium bromide (TDeABr) was used as an ion-pair

agent and 1,4-dibromoacetophenone (bromophenacyl bromide) (Br-Ph-Br) [11] as derivatizing reagent.

EXPERIMENTAL

Chemicals

Synperonic NP-12 non-ionic surfactant [a polyoxyethylene(12) nonylphenyl ether], was a gift from Professor Nissim Garti (Casali Institute of Applied Chemistry, Jerusalem, Israel). TDeABr was purchased from Fluka (Buchs, Switzerland) and Br-Ph-Br from Sigma (St. Louis, MO, USA).

Standard fatty acids (C16:0, C18:0, C20:0, C22:0, C24:0, C25:0, C26:0, C27;0 and C28:0) were purchased from Fluka. HPLC-grade chloroform, methanol and acetone were obtained from BioLab (Jerusalem, Israel) and were filtered through an RC-55 membrane filter from Tamar (Jerusalem, Israel). Silica gel (63–100 μm) was purchased from Woelm (Eshwege, Germany).

Solutions

Synperonic NP-12 surfactant was prepared at a concentration of 0.025 *M* in 0.01 *M* phosphate buffer (pH 7.0) (the critical micelle concentration is about 0.1 m*M* in phosphate buffer). A 0.006 *M* solution of the ion-pair reagent, TDeABr, was prepared in 0.01 *M* phosphate buffer (pH 7.0). Fatty acid stock solutions were prepared by dissolving 5 mg of each acid in 100 ml of chloroform. A Br-Ph-Br stock solution was prepared daily by dissolving 0.525 g in 25 ml of acetone; it was stored in the dark at 4°C.

Derivatization reaction

To dried fatty acids mixtures (which were evaporated under nitrogen) the following solutions were added: 300 μl of Br-Ph-Br, 560 μl of Synperonic NP-12 and 140 μl of TDeABr. The mixture reacted, protected from light, by refluxing at 60°C for 20 min while stirring.

The fatty acid esters in the reaction mixture were initially extracted using one of three techniques: (1) purification by filtration through a silica gel column (protected from light) and extraction with chloroform; (2) direct extraction with chloroform and absorption of the aqueous phase with anhydrous sodium sulphate, followed by filtration; (3) extraction with chloroform and separation by centrifugation. The third method was the easiest and gave the best yield, and was therefore adopted. Chloroform (1 ml) was added to the reaction mixture while stirring. Centrifugation for 30 s resulted in two separate phases. The lower chloroform phase was injected into the HPLC system directly without any further treatment.

HPLC system

The analyses were made on a Spectra-Physics (Santa Clara, CA, USA) Model 8700 liquid chromatograph equipped with 20-μl loop injector and a Model D-2000 Chromato Integrator (Merck, Darmstadt, Germany).

Separations of the fatty acid esters were done on an RP-18 reversed-phase column (LiChrosorb cartridge, 12.5 cm × 0.4 cm I.D.) protected by a 2.5 cm × 0.4 cm I.D. guard column (Merck). Both columns were packed with 5-μm particles.

All organic solvents were filtered through Type RC-55 0.45-μm membrane filters (Tamar). The mobile phase was methanol at a flow-rate of 1.5 ml/min. The analytical column was kept in a water-bath at 16°C. Detection of the fatty acid esters was performed with a Spectra-Physics UV detector operated at 254 nm.

RESULTS AND DISCUSSION

As the analysis of fatty acids is hindered by the lack of a chromophore or a fluorophore, derivatization is necessary. Most of the derivatization procedures require first the preparation of fatty acid salts, followed by extraction into an organic phase with a phase-transfer catalyst such as an 18-crown-6-ether [11,12]. The derivatization reaction takes place in the organic phase and is difficult to combine with reversed-phase (RP) HPLC. In the micellar system, "pseudo-phases" exist and the combination with RP-HPLC is easier. In addition, as the aqueous micellar solution is buffered at pH 7, the fatty acids are converted into their salts, which aids in the derivatization reaction. Therefore, the derivatization procedure is simple and requires minimum volumes of reagent and solvents. The derivatization scheme used is a modification of the method described by Van der Horst *et al.* [8] for other substances and allows the satisfactory separation of LCFA by HPLC.

Reaction conditions

Several experimental conditions were examined to find the optimum for preparing the derivatives. Derivatization of LCFA was done with excess of Br-Ph-Br at 60°C. The reaction time was varied from 5 to 70 min and it was found that 20 min represent a suitable compromise between reaction time and completion of reaction.

Fig. 1 shows a three-dimensional surface diagram of LCFA reaction rates. Chromatographic peak areas are plotted *versus* reaction time and *versus* chain length of the acid. Each crossing point on the surface represents one set of experimental conditions. Fig. 1 shows an initial increase in the reaction completion (larger peak areas) with increasing reaction time. After 40 min the reaction reaches a plateau.

Using the approach of van der Horst *et al.* [7] and of Schmid and Sapunov [13], the data in Fig. 1 allow the calculation of the derivatization reaction rate constants of the fatty acids. Table I gives these constants for all the acids studied, and they vary between $6 \cdot 10^{-4}$ and $9 \cdot 10^{-4}$ s^{-1}. As expected [8], the k_{obs} values for LCFA from C16:0 to C28:0 were found to be in the same range, and the general trend seems to be a slight decrease with increasing chain length.

Influence of the surfactant

We examined the effect of the non-ionic surfactant concentration (0.025, 0.05, 0.1 and 0.125 *M*) on the derivatization reaction. It was found that the best yield of the derivative was obtained with a 0.025 *M* surfactant concentration.

Extraction was necessary prior to injection for HPLC analysis in order to obtain a homogeneous solution, avoid blocking of the RP-18 column and obtain reproducible results. Separation by centrifugation was found to be adequate for this purpose.

Chromatographic separations of LCFA

The HPLC separation of LCFA derivatives from C16:0 to C28:0 in 24 min is shown in Fig. 2. Limits of detection for the nine fatty acids, as calculated at a signal-to-noise ratio of 3, are given in Table I. As only 1/40th of the reaction mixture was injected into the HPLC system, the detection limits could be lowered by dissolving the dried reaction mixture in a smaller volume of chloroform.

Reproducibility and linearity

Reproducibility of the method was evaluated using standard fatty acids at a certain concentration (30 μg of each) in four replicates. The data are given in Table I. The reproducibility ranges between 4.5 and 9% (relative error).

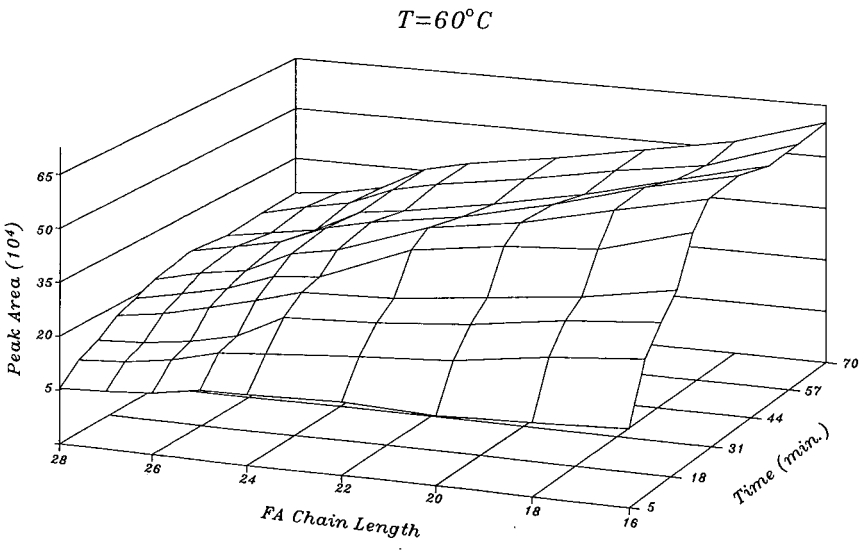

Fig. 1. Three-dimensional surface diagram of LCFA reaction rates.

TABLE I

DERIVATIZATION RATE CONSTANTS AND DATA ON REPRODUCIBILITY AND DETECTION LIMITS OF LCFA PHENACYL ESTERS IN MICELLAR PHASE-TRANSFER CATALYSIS

Fatty acid	Rate constant, k_{obs} (10^{-3} s^{-1})	Reproducibility (%)[a]	Detection limit (nmol)
C16:0	0.963	9.0	0.293
C18:0	0.836	8.6	0.282
C20:0	0.760	8.5	0.321
C22:0	0.778	6.9	0.368
C24:0	0.825	4.5	0.544
C25:0	0.788	8.9	0.589
C26:0	0.783	6.8	0.631
C27:0	0.800	7.7	0.646
C28:0	0.644	6.2	0.649

[a] Relative error for four identical samples injected into the HPLC system five times.

Calibration graphs in the range 2.5–30 μg (*ca.* 5.9–117 nmol) of LCFA showed a correlation coefficient above 0.99.

CONCLUSIONS

The method described offers a solution for the solubility problems of LCFA in aqueous media. Using a non-ionic surfactant, Synperonic NP-12, and a cationic ion-pair agent, TDeABr, derivatization was carried out with a UV reagent, 1,4-dibromoacetophenone, without the need for multi-step purification procedures of the analyte prior to HPLC analysis.

The use of MPTC allows the derivatization of LCFA in only one step. Hence, it can be applied to automated analyses of plasma, as discussed recently by Van der Horst *et al.* [14]. The use of MPTC may be of great interest for the determination LCFA which are present in the plasma of patients with genetic diseases.

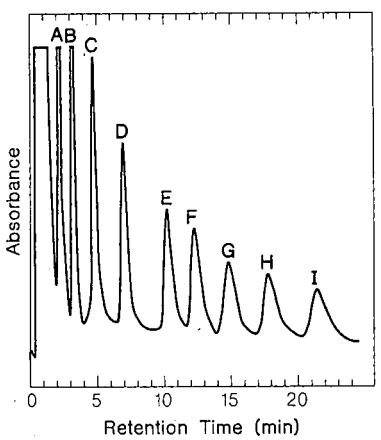

Fig. 2. Chromatogram of LCFA phenacyl esters. (A) C16:0; (B) C18:0; (C) C20:0; (D) C22:0; (E) C24:0; (F) C25:0; (G) C26:0; (H) C27:0; (I) C28:0.

ACKNOWLEDGEMENTS

The author thanks Professor E. Grushka for his guidance and encouragement. She also thanks Professor N. Garti (Casali Institute of Applied Chemistry, Jerusalem, Israel) for the gift of Synperonic NP-12 surfactant, Dr. M. Dodu (Computation Centre of the Hebrew University) for drawing the three-dimensional diagram in Fig. 1 and Mr. G. E. Drachsler for drawing Fig. 2.

REFERENCES

1 U. Tonellato, *J. Chem. Soc., Perkin Trans. 2*, (1977) 822.
2 J. Sherma, B. P. Sleckman and D. W. Armstrong, *J. Liq. Chromatogr.*, 6 (1983) 95.
3 P. Becher, in M. J. Schick (Editor), *Nonionic Surfactants*, Marcel Dekker, New York, 1967, Ch. 22.
4 K. A. Connors and M. P. Wong, *J. Pharm. Sci.*, 68 (1978) 1470.
5 F. A. L. van der Horst, M. H. Post and J. J. M. Holthuis, *J. Chromatogr.*, 456 (1988) 201.
6 F. A. L. van der Horst, G. G. Eikelboom and J. J. M. Holthuis, *J. Chromatogr.*, 456 (1988) 191.
7 F. A. L. van der Horst, M. H. Post, J. J. M. Holthuis and U. A. Th. Brinkman, *Chromatographia*, 28 (1989) 267.
8 F. A. L. van der Horst, J. M. Reijn, M. H. Post, A. Bult, J. J. M. Holthuis and U. A. Th. Brinkman, *J. Chromatogr.*, 507 (1990) 351.
9 F. A. L. van der Horst and J. J. M. Holthuis, *J. Chromatogr.*, 426 (1988) 267.
10 M. J. Schick (Editor), *Nonionic Surfactants: Physical Chemistry*, Marcel Dekker, New York, 1987.
11 D. Durst, M. Milano, E. I. Kikta, S. A. Connelly and E. Grushka, *Anal. Chem.*, 47 (1976) 1797.
12 R. F. Borch, *Anal. Chem.*, 47 (1975) 2437.
13 R. Schmid and V. N. Sapunov (Editors), *Non-Formal Kinetics* (*Monographs in Modern Chemistry*, Vol. 14), Verlag Chemie, Weinheim, 1982, Ch. 8.
14 F. A. L. van der Horst, J. J. M. Holthuis and U. A. Th. Brinkman, *J. Chromatogr.*, 500 (1990) 443.

Journal of Chromatography, 586 (1991) 351–355
Elsevier Science Publishers B.V., Amsterdam

CHROM. 23 697

Short Communication

Direct separation of nadolol enantiomers on a Pirkle-type chiral stationary phase

A. M. Dyas* and M. L. Robinson

Bristol-Myers Squibb Pharmaceuticals, Moreton, Merseyside L46 1QW (UK)

A. F. Fell

Pharmaceutical Chemistry, School of Pharmacy, University of Bradford, Bradford, West Yorkshire BD7 1DP (UK)

(First received May 27th, 1991; revised manuscript received August 20th, 1991)

ABSTRACT

The enantiomers of the β-adrenergic blocking drug nadolol may be separated on a chiral stationary phase following conversion to their 1-naphthylurea derivatives by reaction with the achiral reagent 1-naphthylisocyanate. A mixture of *n*-hexane, propan-2-ol and acetonitrile is used to elute the enantiomers from a column comprising (*R*)-N-(3,5-dinitrobenzoyl)-L-leucine covalently bound to 5-μm aminopropylsilica. Nadolol is a *cis*-diol structure which has three stereogenic centres, however the two diol carbons are held in a fixed configuration and it therefore has only four optical isomers. These are resolved in under 30 mn using the procedure described herein, which is therefore suitable for use in the quality control context.

INTRODUCTION

The chromatographic separation of drug enantiomers has assumed greater importance with the realisation that pharmacologically significant differences exist between stereoisomers. The increased emphasis on research into enantiospecific drug action has been accompanied by increased activity in the field of chromatographic chiral separations. This has resulted in an upsurge in published methods for such separations and the development of an almost bewildering array of chromatographic chiral stationary phases (CSPs). The β-adrenergic blocking agents have received particular attention as they are a pharmacologically important class of drugs and consequently have been used as models in the development of a great many chiral separations systems. Nadolol is a distinctive β-blocker in that although it has three stereogenic centres it is a *cis*-diol and has only four optical isomers. Only one direct separation of all four has been reported by Lee *et al.* [1] who investigated the separation of nadolol using supercritical fluid chromatography under sub-critical conditions with carbon dioxide as an eluent and were unable to resolve more than three peaks when using Chiralcel-type or the Pirkle-type stationary phases. However, they obtained full resolution of all four optical isomers using an α_1-acid glycoprotein column. As part of a wide-ranging programme examining the critical parameters that determine chiral separation on Pirkle-type phases a method has been successfully developed for the direct separation of all four optical isomers of nadolol on an (*R*)-N-(3,5-dinitrobenzoyl)-L-leu-

0021-9673/91/$03.50

cine CSP following achiral derivatisation of the analyte with 1-naphthylisocyanate.

EXPERIMENTAL

Reagents and chemicals

Bristol-Myers Squibb (Princeton, NJ, USA) standard reference samples of racemic nadolol, nadolol racemate A [(*RS*)–(*SR*)], nadolol racemate B [(*RR*)–(*SS*)], (*RS*)-nadolol, (*SR*)-nadolol and (*SS*)-nadolol were used. 1-Naphthylisocyanate (99%) and 2-ethoxy-1-ethoxycarbonyl-1,2-dihydroquinoline (EEDQ; 97%) were obtained from Aldrich (Poole, UK) whilst the chromatographic solvents (*n*-hexane, propan-2-ol, ethanol and acetonitrile) were obtained from BDH (Liverpool, UK) and were analytical-reagent grade.

Chromatographic conditions

An eluent consisting of *n*-hexane–ethanol–acetonitrile (45:5:1, v/v/v) was mixed, degassed by helium sparging and pumped at 2 ml/min using a Constametric I pump (LDC-Milton Roy, Riviera Beach FL, USA), fitted with a Rheodyne 7037 pressure relief valve (Rheodyne, Cotati, CA, USA). A Rheodyne 7420 valve was used to apply 20-μl samples to the column, which contained (*R*)-N-(3,5-dinitrobenzoyl)-L-leucine covalently bound to aminopropylsilica. The absorbance of the eluent at 239 nm was monitored with a Shimadzu SPD-6A UV detector (Shimadzu, Duisburg, Germany) set at 0.16 a.u.f.s. All chromatograms were collected using both a Perkin-Elmer PE56 chart recorder (Perkin-Elmer, Norwalk, CT, USA) and the Beckman CALS PeakPro laboratory data system (Beckman Instruments, Fullerton, CA, USA).

Two separate columns were employed in the study. The first was a 250 mm × 4.6 mm I.D. commercially available column containing 5-μm packing (CHI-1-LEU, Hichrom, Reading, UK). The second column was prepared in the laboratory by passing a solution of 5 g of the chiral selector (*R*)-N-(3,5)-dinitrobenzoyl)-L-leucine and 5 g of the peptide-coupling agent EEDQ in tetrahydrofuran through a 150 mm × 4.6 mm I.D. column packed with 3-μm aminopropylsilica (HPLC Technology, Macclesfield, UK). The column was then washed, in turn, with tetrahydrofuran and with dichloromethane, before 100 ml of dichloromethane containing 10 g of trifluoroacetic anhydride were pumped through to derivatise any unreacted propylamine groups. The column was washed with dichloromethane before being equilibrated with the eluent.

Derivatisation procedure

The test solute was dissolved in eluent at a concentration of 0.5–2.0 mg/ml and a five-fold molar excess of 1-naphthylisocyanate was added. The solution was mixed and allowed to stand for 15 min before being injected onto the column.

RESULTS AND DISCUSSION

The conversion of β-blockers to their urea derivatives by means of isocyanates (see Fig. 1) has been previously reported by this group [2–4] and others [5–11]. The 1-naphthylurea function was identified as one likely to enhance chiral separation on Pirkle phases, so this was selected for use with nadolol for that reason. Alcohols also react with isocyanates, forming urethanes although under the conditions employed (ambient temperature, short reaction time) the naphthalenediol alcohol groups are unlikely to react.

Using an optimised mobile phase composition (as described below) the separation of the four enantiomers on the 5-μm column is almost complete (Fig. 2), with baseline resolution between

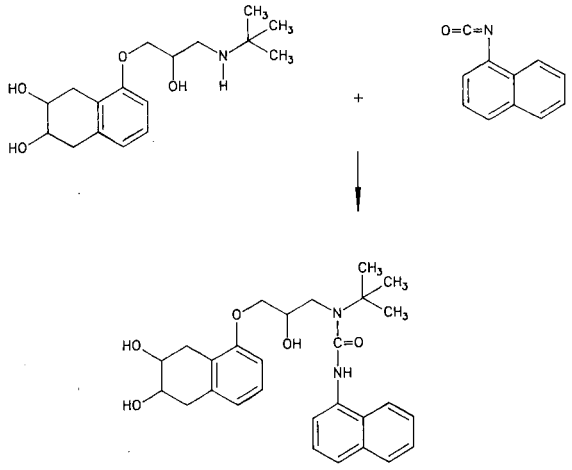

Fig. 1. Reaction between nadolol and 1-naphthylisocyanate leading to the formation of the naphthylurea derivative of the β-blocker.

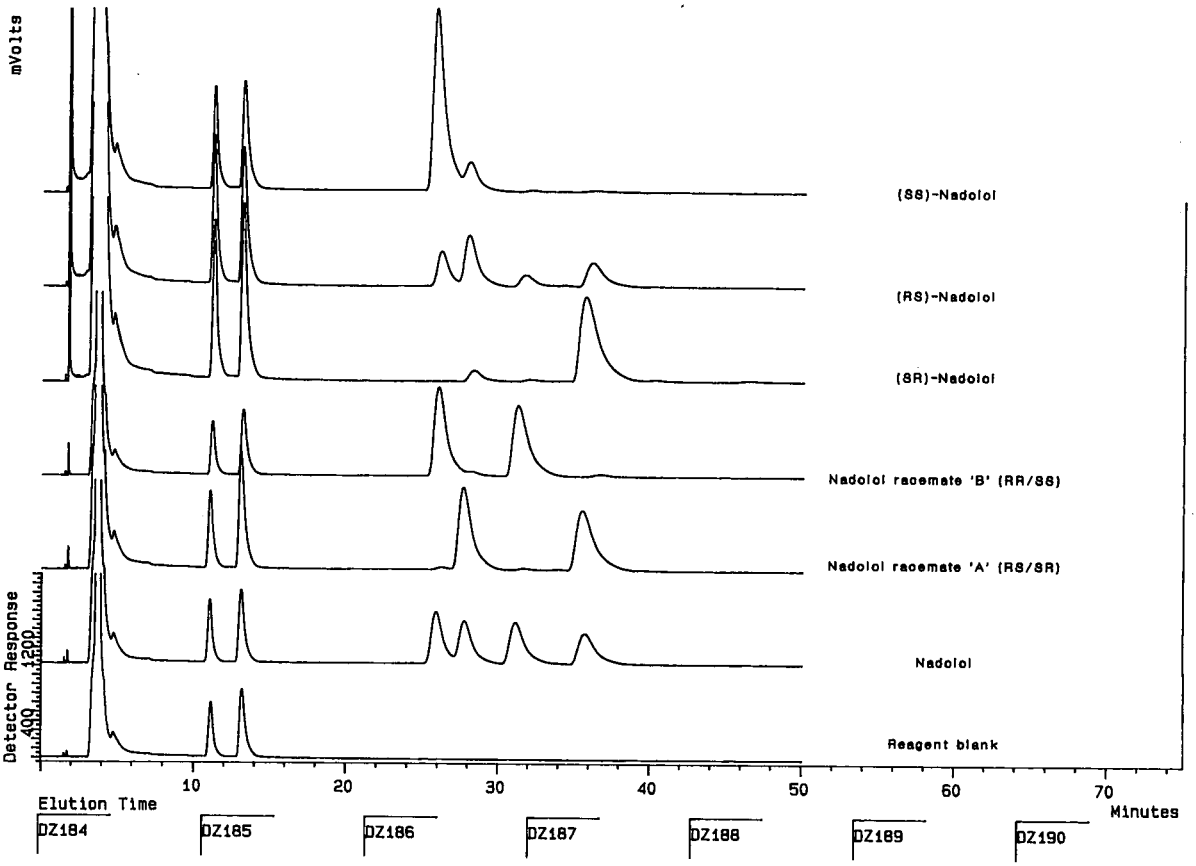

Fig. 2. Chromatograms for injections of nadolol standard materials (for details of see *Chromatographic conditions*).

peaks 2, 3 and 4 and approximately 80% separation of peaks 1 and 2. The elution order was determined using reference standard materials and is summarised in Table I. Although only three of the four isomers were available, assignment was based on a comparison with known racemic mixtures. Two system peaks are seen to elute at 11 and 13 min, neither being unreacted reagent which elutes with the solvent front. They are products of reaction between excess derivatising reagent and the eluent as they increase in size if solutions (including the blank) are left to stand for a time.

The separation achieved for the racemic sample of nadolol is sufficient for quantitation of the enantiomers, although the run time is rather long, necessitating some 40 min between injections. Preliminary attemps to optimise the separation have been undertaken based on modifications to the mo-

TABLE I

CAPACITY FACTORS FOR THE OPTICAL ISOMERS OF NADOLOL

For details see *Chromatographic conditions*.

Component	Capacity factor (k')			
	Peak 1	Peak 2	Peak 3	Peak 4
(*SS*)-Nadolol	16.2			
(*RS*)-Nadolol		17.7		
(*SR*)-Nadolol				22.8
(*RR*)-Nadolol[a]	–	–	–	–
Nadolol racemate A[b]		17.4		22.7
Nadolol racemate B[c]	16.3		19.9	
Nadolol	16.3	17.5	19.7	22.8

[a] Not available.
[b] Nadolol racemate A = (*RS*)–(*SR*)-nadolol.
[c] Nadolol racemate B = (*RR*)–(*SS*)-nadolol.

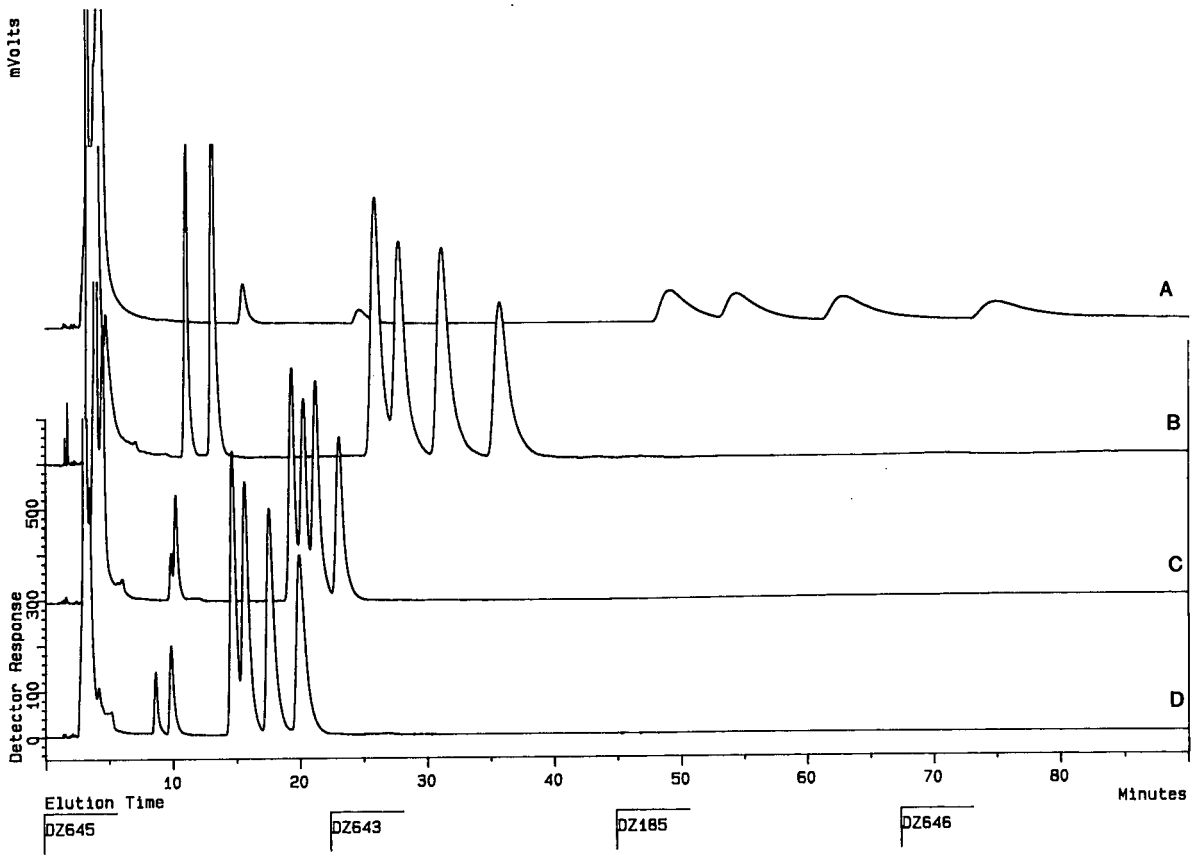

Fig. 3. Chromatograms showing effect of eluent on separation of nadolol enantiomers using (A) *n*-hexane–propan-2-ol–acetonitrile (45:5:1, v/v/v), (B) *n*-hexane–ethanol–acetonitrile (45:5:1, v/v/v), (C) as for (B) in the proportions 45:5:2.5, v/v/v and (D) as for (B) in the proportions 45:7.5:1, v/v/v.

bile phase composition. Substituting the ethanol with propan-2-ol leads to slight improvements in resolution, but with an unacceptable increase in the retention time to approximately 80 min for the slowest eluting enantiomer (Fig. 3). The use of methanol instead of ethanol leads to a two-phase eluent and although the upper (*n*-hexane) phase can be removed and used, this shows rapid elution of all components with almost total loss of resolution. Increasing the ethanol content or the acetonitrile content both speed up elution, although in the latter case there is significant loss of resolution between peaks 2 and 3 and a worsening of the overlap between peaks 1 and 2.

The separation can be improved further by reducing the particle size of the silica, as can be seen from the superior resolution observed for a given eluent on the 3-μm column (Fig. 4) compared with that for the 5-μm column with the same eluent.

This dramatic improvement should be treated with some caution, however, as the two columns may not be entirely comparable. Besides having different lengths and particle sizes, the two columns used different silica supports and were prepared in different ways. The 5-μm column was commercially packed with a chiral packing material based on Spherisorb silica whilst the 3-μm column was purchased as a commercially available achiral column (Hypersil aminopropylsilica) and then derivatised in the laboratory. However, for the 3-μm column the propan-2-ol again gave the better separation whilst the ethanol gave faster elution. Thus the choice of optimum eluent composition depends on the requirements for the speed and quality of the

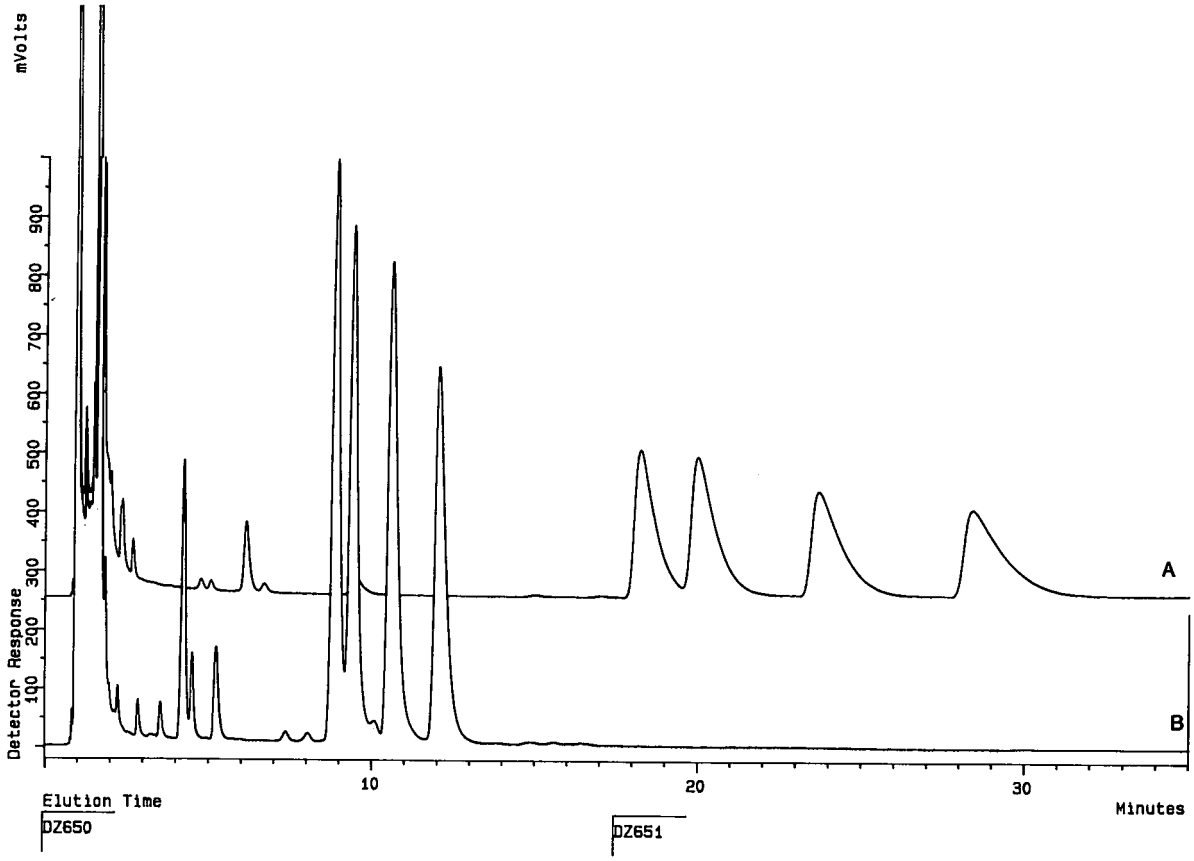

Fig. 4. Separation of nadolol enantiomers on a 3-μm column using an eluent containing (A) propan-2-ol or (B) ethanol (for details see *Chromatographic conditions*).

separation and on the particle size of the available column.

CONCLUSIONS

The separation of the four optical isomers of nadolol may be achieved on a covalent Pirkle-type CSP following conversion to their 1-naphthylurea derivatives with the achiral reagent 1-naphthylisocyanate. The separation of the optical isomers may be optimised by adjusting the choice of alcohol modifier in the eluent, as well as the relative proportions of the eluent components. The use of a smaller (3-μm) particle size silica support affords significant improvements in both speed and extent of separation. This optimised method allows the enantiomers to be accurately quantitated in an analysis time of less then 30 min.

REFERENCES

1 C. R. Lee, J.-P. Porziemsky, M.-C. Aubert and A. M. Krstulovic, *J. Chromatogr.*, 539 (1991) 55–69.
2 A. M. Dyas, M. L. Robinson and A. F. Fell, *Chromatographia*, 30 (1990) 73–79.
3 A. M. Dyas, M. L. Robinson and A. F. Fell, in D. Stevenson and I. D. Wilson (Editors), *Recent Advances in Chiral Separations*, Plenum Press, New York, 1991, pp. 31–37.
4 A.M. Dyas, A. F. Fell and M. L. Robinson, *Chirality*, 2 (1990) 120–123.
5 Q. Yang, Z-P. Sun and D-K. Liu, *J. Chromatogr.*, 447 (1988) 208–211.
6 R. J. Guttendorf, H. B. Kostenbauder and P. J. Wedlund, *J. Chromatogr.*, 489 (1989) 333–343.
7 Y. Zhou, Z-P. Sun and D-K. Liu, *J. Liq. Chromatogr.*, 13 (1990) 875–885.
8 H. G. Schaefer, H. Spahn, L. M. Lopez and H. Derendorf, *J. Chromatogr.*, 527 (1990) 351–359.
9 A. J. Sedman and J. Gal, *J. Chromatogr.*, 278 (1983) 199–203.
10 A. J. Sedman and J. Gal, *J. Chromatogr.*, 314 (1984) 275–281.
11 M. Piquette-Miller and R. T. Foster, *J. Chromatogr.*, 533 (1990) 300–303.

Journal of Chromatography, 586 (1991) 356–359
Elsevier Science Publishers B.V., Amsterdam

CHROM. 23 667

Short Communication

Retention behavior of salicylideneglycinatoaluminium(III) in reversed-phase high-performance liquid chromatography

Nobuo Uehara*, Sachie Iso and Yoshio Shijo

Department of Applied Chemistry, Faculty of Engineering, Utsunomiya University, Ishii-cho, Utsunomiya 321 (Japan)

(First received May 27th, 1991; revised manuscript received July 23rd, 1991)

ABSTRACT

The retention behavior of salicylideneglycinatoaluminium(III) was investigated. The capacity factor of the complex decreased with increasing concentration of ionic solutes and increasing water content in the eluent. The capacity factor of the complex was also smaller when an end-capped octadecylsilane column was used than when a non-end-capped octadecylsilane column was used. The complex was tightly retained with a silica gel column, but it was not retained with a polymer gel column. The complex was retained through the electrostatic interaction with the silanol groups of silica gel. It was found that the high-performance liquid chromatographic system was highly selective for aluminium(III).

INTRODUCTION

Silica-based materials have been used extensively in high-performance liquid chromatographic (HPLC) studies because of their chemical stability, rigidity and availability [1–4]. In HPLC separations using silica-based columns, residual silanol groups on the surface of packing materials often affect the retention behavior of analytes [5–7]. Silanol groups also affect the separation of metal complexes [8,9].

In a previous paper [10], we reported the determination of gallium using HPLC with salicylideneglycine and mentioned the peculiar retention behavior of salicylideneglycinatoaluminium(III). The retention behavior of the aluminium(III) complex did not obey the ordinary reversed-phase mode. We suggested that the behavior was due to the effect of the silanol groups. In this paper, this peculiar retention behavior of the aluminium(III) complex was investigated. For this purpose, the effect of the addition of various solutes in the eluent was examined. The effect of acetonitrile content and various column materials was also investigated.

EXPERIMENTAL

Reagents and apparatus

Bissalicylideneethylenediamine (BSED) was synthesized from salicylaldehyde and ethylenediamine using the method reported by Freeman and White [11]. The crude product was recrystallized from benzene, then identified by mass spectrometric analysis and elemental analysis. The BSED solution ($1 \cdot 10^{-3}$ *M*) was prepared by dissolving a fixed amount of BSED in acetonitrile. The standard solution of aluminium(III) (1000 μg ml^{-1}) was prepared by dissolving potassium aluminium sulphate in 0.05 *M* sulphuric acid. Analytical reagent-grade acetonitrile

0021-9673/91/$03.50

was distilled and filtered through a membrane filter (pore size 0.45 μm). Water was purified with a Milli-Q system after being distilled and deionized. Other reagents used were of analytical reagent-grade.

The HPLC system consisted of a Shimadzu LC-6A pump (Kyoto, Japan), a Shimadzu RF-535 fluorometric detector, a Rheodyne 7125 loop injector equipped with a 20-μl sample loop and a Shimadzu R-1231 recorder. Four Merck LiChroCART columns (125 mm × 4 mm I.D.) filled with different kinds of silica-based materials were used: (1) LiChrosorb RP-18 [7-μm irregularly shaped silica gel bonded with octadecylsilane (ODS)]; (2) LiChrospher RP-18 (5-μm spherical silica gel bonded with ODS); (3) LiChrospher RP-18(e) (end-capped LiChrospher RP-18); (4) LiChrospher Si-60 (5-μm spherical silica gel). A Tosoh TSK gel Octadecyl 4PW column (150 mm × 4.6 mm I.D.) (Tokyo, Japan) filled with 7-μm hydrophilic polymer gel bonded with octadecyl groups was also used.

Procedure

To an acidic solution containing 1.0 μg of aluminium(III) ion in a 25-ml volumetric flask, 1.0 ml of 0.5 *M* glycine solution, 1.0 ml of $1.0 \cdot 10^{-2}$ *M* BSED solution and 2.0 ml of 2 *M* acetate buffer (pH 3.5) were added, and the solution was diluted to the mark with water. The solution was heated at 60°C for 10 min. After cooling, an aliquot (20 μl) of the solution was injected into the HPLC system.

The eluent was acetonitrile–water (50:50, v/v) containing a solute to be examined. The pH of the eluent was adjusted to 3.5 by the addition of dilute hydrochloric acid prior to the addition of acetonitrile. The flow-rate was 0.8 ml min^{-1}. The temperature of the eluent was kept at 20°C ± 1°C. The excitation and emission wavelengths of the fluorometric detector were set at 350 and 455 nm, respectively.

RESULTS AND DISCUSSION

Salicylideneglycine formed from salicylaldehyde and glycine reacts with aluminium(III) to form a fluorescent complex [12]. Although the aluminium(III) complex gave maximum fluorescent intensity at pH 4.0 in a water–acetonitrile mixture, the best chromatograms were obtained at 3.5 (both eluent and sample). It has been reported [12] that the composition of the aluminium(III) complex is the metal to ligand in a ratio of 1:1, and that the salicylideneglycine acted as a diprotic acid. Therefore the aluminium(III) complex has a positive charge.

Cationic complexes are retained with ODS stationary phases through two mechanisms: the first is the hydrophobic interaction with alkyl chains bonded onto silica; the second is the ion-exchange interaction with unreacted silanol groups. If ion-exchange interaction is more dominant than hydrophobic interaction, in retaining the cationic complex, the following predictions are introduced.

(a) With increasing cation concentration in the mobile phase, the retention of the cationic complex decreases because the cation competes with the complex.

(b) With increasing acetonitrile content in the mobile phase, the retention of the complex increases, because the dielectric constant of the mobile phase decreases.

(c) With increasing content of silanol groups, the retention of complex increases.

Fig. 1 shows the chromatograms of the aluminium(III) complex in various concentrations of

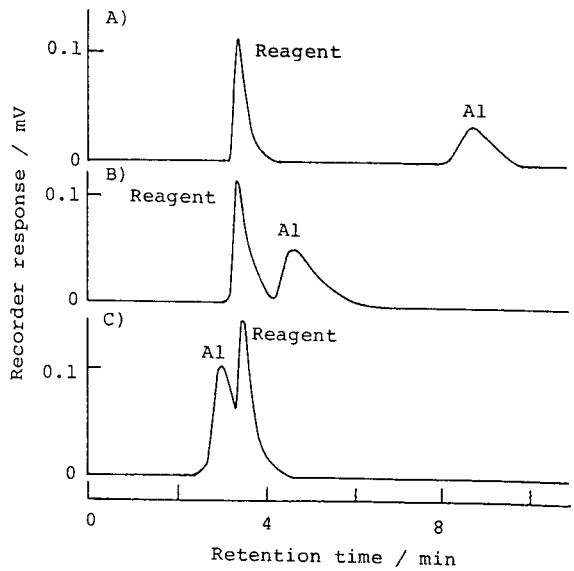

Fig. 1. Chromatograms of the aluminium complex with various sodium acetate concentrations of the eluents. (A) 0 *M*; (B) $0.33 \cdot 10^{-3}$ *M*; (C) $1.0 \cdot 10^{-3}$ *M*. Eluent: acetonitrile–water (50:50, v/v), pH 3.5; column: LiChrosorb RP-18.

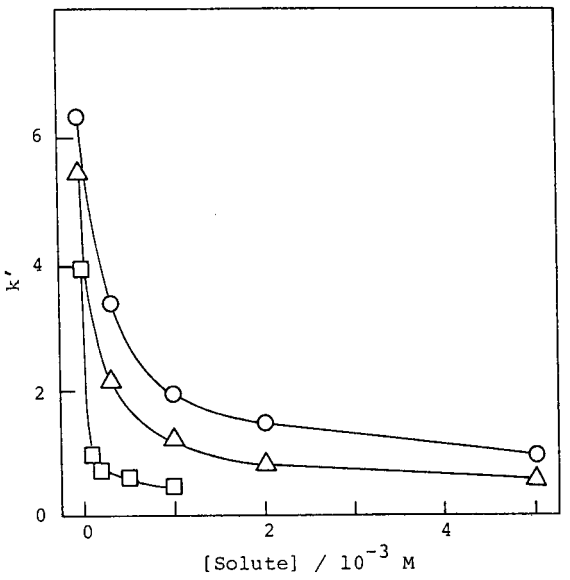

Fig. 2. Effect of ammonium salt concentration on the capacity factor. ○ = Ammonium chloride; △ = trimethylamine hydrochloride; □ = tetrabutylammonium bromide. Other conditions are the same as those in Fig. 1.

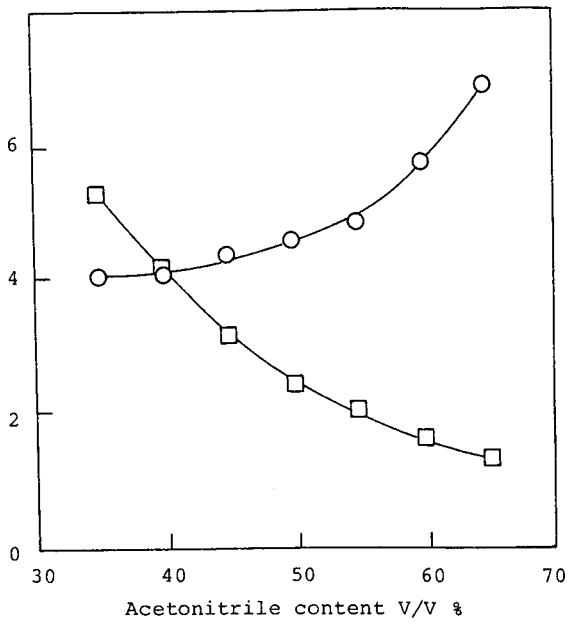

Fig. 3. Effect of acetonitrile content on the capacity factors of reagent and aluminium complex. □ = Reagent; ○ = aluminium complex. Other conditions are the same as those in Fig. 1.

sodium acetate used as buffer for the eluent. Increasing the concentration of sodium acetate decreased the retention time of the aluminium(III) complex. Other sodium carboxylates such as sodium acetate, sodium propionate and sodium *n*-butylate gave similar effects to the retention of the aluminium(III) complex. In this case, the sodium ion was the competing cation, so that the number of carbons in the carboxylates did not influence the retention. Fig. 2 shows the results of the addition of amine salts in the eluent. The effects of trimethylamine hydrochloride and tetraethylammonium chloride were not very large compared with that of ammonium chloride. As the total carbon number of the solutes used increased, the effect of the solute increased, because alkyl amines interacted with the stationary phase through hydrophobic interaction. Tetrabutylammonium bromide, which has sixteen carbons, was the most effective reagent in this work. Inorganic salts gave similar results to those of ammonium salts. The divalent salts were more effective than the monovalent salts. Non-ionic solutes gave no effects and zwitter-ionic solutes slightly affected the retention behavior.

We examined the effect of acetonitrile content in the eluent upon the capacity factor of the aluminium(III) complex. Although the capacity factor of the ligand decreased, the capacity factor of the aluminium(III) complex increased with increasing acetonitrile content, as shown in Fig. 3, which was consistent with the prediction.

There are inumerable silanol groups on the surface of silica-based materials, which act as a cation-exchange site. We used various HPLC columns in order to examine the effect of silanol groups on the retention of the aluminium(III) complex. Fig. 4 shows that the aluminium(III) complex eluted faster with the end-capped ODS column [LiChrospher RP-18(e)] than with the non-end-capped ODS column (LiChrospher RP-18). Moreover, the aluminium(III) complex was little retained on a polymer gel column (TSK gel Octadecyl 4PW) which has no silanol groups. The results show that silanol groups play an important role in retaining the aluminium(III) complex. A silica gel column (LiChrospher Si-60) did not give the peak of the aluminium(III) complex. The complex was tightly retained on the silica gel surface, but the complex was eluted when a more water-rich eluent was used.

The results obtained above support the theory

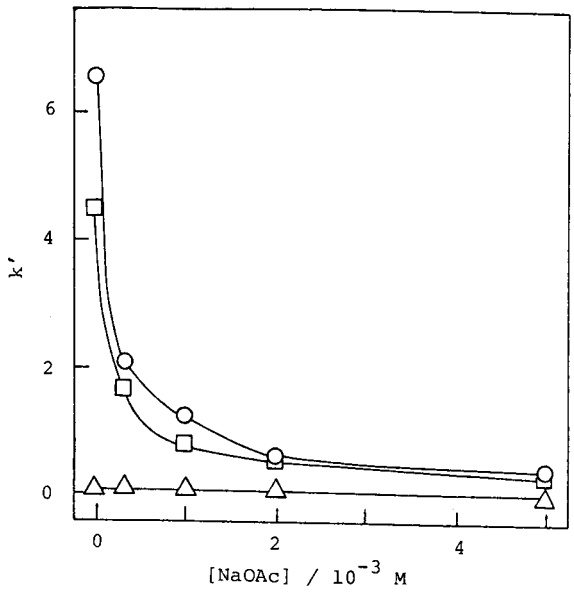

Fig. 4. Effect of column materials on the capacity factor. ○ = LiChrospher RP-18; □ = LiChrospher RP-18(e); △ = TSK gel Octadecyl 4PW. Other conditions are the same as those in Fig. 1.

that salicylideneglycinatoaluminium(III) was retained on a silica-based column through electrostatic interaction with silanol groups. The electrostatic interaction of the residual silanol groups on the ODS column was investigated by several workers [13,14]. In their cases, however, hydrophobic interaction with the stationary phase was still the dominant force in retaining the complexes. The retention of metal complexes only through ion-exchange interaction has not been reported as far as we know. We found that in the new metal complex system ion-exchange reaction with silanol groups played the dominant role in the separation of cationic complexes in the aqueous reversed-phase mode.

The HPLC system was quite selective for the aluminium(III) ion. No transitional metal ion gave a peak on the chromatogram. Nor did the alkaline earth metal ions or the indium ion give a peak. Only the peak of gallium ion appeared near the solvent front in the chromatogram. The gallium(III) complex was rarely retained on the column. The application of this finding to the determination of aumininum will be considered in further work.

REFERENCES

1 R. Rosett, *Analusis*, 15 (1987) 1.
2 I. B. Brenner, G. A. Jones, A. E. Watson and T. W. Steele, *Chem. Geol.*, 45 (1984) 135.
3 R. E. Majors, H. G. Barth and C. H. Lochmuler, *Anal. Chem.*, 54 (1982) 323R.
4 R. E. Majors, H. G. Barth and C. H. Lochmuler, *Anal. Chem.*, 56 (1984) 300R.
5 Y. Ohtsu, Y. Shiojima, T. Okumura, J. Koyama, K. Nakamura and O. Nakata, *J. Chromatogr.*, 481 (1989) 147.
6 J. Nawrocki and B. Buszewski *J. Chromatogr.*, 449 (1988) 1.
7 T. Welsh, H. Frank and G. Vigh, *J. Chromatogr.*, 506 (1990) 97.
8 M. C. Gill, Y. T. Shih and D. W. Carr, *Talanta*, 36 (1989) 293.
9 M. D. Palmieri and J. S. Fritz, *Anal. Chem.*, 60 (1988) 2244.
10 N. Uehara, M. Kasahara and Y. Shijo, *Anal. Sci.*, 6 (1990) 469.
11 D. C. Freeman, Jr. and C. E. White, *J. Am. Chem. Soc.*, 78 (1956) 2678.
12 K. Watanabe and I. Aoki, *Bunseki Kagaku*, 35 (1986) 487.
13 J. Miura, *Anal. Chem.*, 62 (1990) 1424.
14 N. Suzuki, T. Takeda and K. Saitoh, *Chromatographia*, 22 (1986) 43.

Journal of Chromatography, 586 (1991) 360–362
Elsevier Science Publishers B.V., Amsterdam

CHROM. 23 665

Short Communication

Use of mass spectrometry for the detection and identification of bromine-containing diphenyl ethers

V. G. Voinov*, Yu. N. El'kin, T. A. Kuznetsova, I. I. Mal'tsev, V. V. Mikhailov and V. A. Sasunkevich

Pacific Institute of Bioorganic Chemistry, Far East Division, Academy of Sciences of the USSR, 690022 Vladivostok (USSR)

(First received April 9th, 1991; revised manuscript received July 10th, 1991)

ABSTRACT

The gas chromatographic–resonance electron-capture mass spectrometric determination and identification of physiologically active bromine-containing compounds in the products of metabolic activity of marine symbiotic microorganisms are described. It is shown that the bacteria *Vibrio* sp. associated with the sponge *Dysidea* sp. are capable of producing brominated diphenyl esters.

INTRODUCTION

In recent years, interest in searching for new producers of physiologically active substances from microorganism has been increasing [1–3]. For a successful search for such microorganisms, it is necessary to use sensitive analytical techniques that permit the determination of small amounts (sometimes picomoles) of the necessary metabolites.

The combination of chromatography with mass spectrometry (MS) is the most reliable and sensitive technique. The use of specific detectors allows the separative capability of chromatography to be increased and an enhanced analytical resolution in the case of a poorly purified mixtures. This can be achieved by using element-selective, structure- or functional selective or property-selective detectors [4]. This applies to gas chromatography (GC)–MS. For example, if substances studied possess a high electron affinity, the use of GC–negative ion chemical ionization (NICI) MS increases the sensitivity even more.

In addition to these widely applicable methods, MS with resonance electron capture ionization (REC-MS) has been developed. In comparison with the traditional MS (including GC–MS), its characteristic feature is a greater specifity due to the energetic selectivity of ionization (the resonance character of ionization) [5]. So far REC-MS has not been used for the analysis of bioorganic compounds. In this work, REC-MS was used for the detection and identification of physiologically active bromine-containing compounds in the products of metabolic activity of the bacteria *Vibrio* sp. associated with the sponge *Dysidea* sp.

EXPERIMENTAL

Chemical and microbiological studies

Eight strains of microorganisms were isolated from microbiological samples taken from two collections (Tuluifa and Ofu, East Samoa) of the sponge *Dysidea* sp., a well known source of 3,5-dibromo-2-(3′,5′-dibromo-2′-metoxyphenoxy)phe-

0021-9673/91/$03.50

nol (TBDPE) [6]. The microorganisms were cultivated on a medium containing peptone (5 g), yeast extract (2.5 g), $MgSO_4 \cdot 7H_2O$ (0.1 g) and sea water (1 l) at 30°C for 72 h.

The culture liquid (1 l) was extracted three times with 150-ml portions of *n*-butanol. The evaporated butanol extract was separated on a silica gel (KSK) column with chloroform–ethyl acetate (20:1). The fractions obtained were tested for brominated compounds by NI-MS [electron impact (EI) 70 V, ionization by secondary electrons]. The bromine-containing fractions were combined and purified on a Sephadex LH-20 column with chloroform–ethanol (7:1), followed by UV detection at 265 nm. One of the 21 fractions obtained showed the presence of brominated compounds (monitoring by NI-MS with EI, 70 V). It was further separated using high-performance liquid chromatography (HPLC) on a Beckman–Altex Si 100 Polyol column (Serva).

Mass spectrometry

MS was carried out on an LKB 2091 mass spectrometer (able to operate in both positive and negative ion modes), combined with a Packard Model 438A gas chromatograph by the use of standard jet-type separator. For working in the REC mode, the filament power chain was modified such that the filament current stabilization could be turned off and the emission current arranged manually. GC was carried out on an SE-54 capillary column (25 m × 0.25 mm I.D.) using a solventless injection system. Helium was used as the carrier gas at a flow-rate of 2.0 ml/min. The temperature of column was increased from 200 to 300°C at 8°C/min. The temperature of the ion source, injector and separator was 250°C. With direct inlet of samples for successive sublimation of mixture components, the temperature of the direct inlet evaporator was increased from 50 to 150°C at 10°C/min. In the experiments in the EI mode, the ionization voltage was set at 70 V (for both positive and negative ions), and in the REC mode at about 4 V (which gave the maximum ion current yield of standard TBDPE isolated from an ethanol extract of the sponge *Dysidea* sp. [6]). Mass spectra were recorded with a UV oscillographic recorder. The instrumental conditions were emission current 25 μA and pressure in the analyser $1 \cdot 10^{-7}$ Torr.

RESULTS

The investigation of standard TBDPE showed that 65% of the total ion current is associated with the bromine ions of *m/z* 79 and 81 (Fig. 1) in the negative ion spectrum (EI, 70 V). We used this fact to detect the bromine-containing compounds in butanol extracts of culture liquids of eight bacterial strains isolated from the symbiotic complex of the sponge *Dysidea* sp. The analysis allowed us to select three strains of microorganisms in whose products characteristic ions with *m/z* 79 and 81 were found. One of the strains, defined as *Vibrio* sp., was used for cultivation in order to isolate the bromine-containing compounds. Successive purification of a butanol extract of culture liquid on Sephadex LH-20 silica gel and HPLC resulted in a bromine-contain-

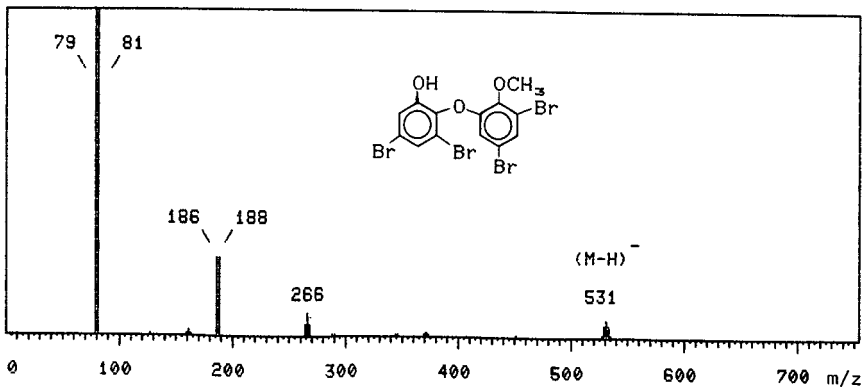

Fig. 1. Negative ion mass spectrum (EI, 70 V) of the tetrabrominated diphenyl ether TBDPE.

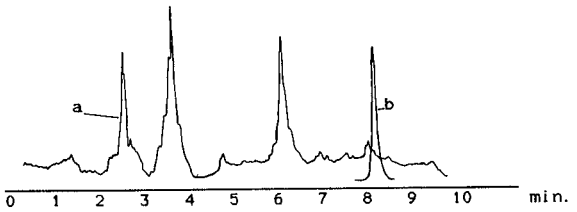

Fig. 2. Chromatograms recorded in a positive ion GC–MS run for (a) a purified butanol extract of culture liquid and (b) for standard TBDPE.

ing fraction (all the steps of the purification were monitored via the bromine ions of *m/z* 79 and 81 by NI-MS with EI, 70 V). GC showed the presence of a series of compounds (Fig. 2a), among which we failed to identify TBDPE by its retention time (Fig. 2b).

In this connection an attempt to take advantage of the energetic selectivity of REC-MS was undertaken. For this TBDPE was inserted into the ion source through a direct inlet system, and the energy of capture (of resonance) that provides the maximum yield of the total ion current was set. Then GC–MS analysis was carried out at the energy set in this way. As expected, the energetic selectivity provided an almost complete absence of ion current from compounds of other classes and allowed only two peaks to be recorded on the chromatogram (Fig. 3a). In addition to conformity with energies, the first peak also coincided with the standard according to its retention time (Fig. 3b). This allowed us to identify this peak as TBDPE. The retention time and the ionization energy of the second peak allowed it to be attributed to the same type of compound as TBDPE. The REC mass spectra recorded

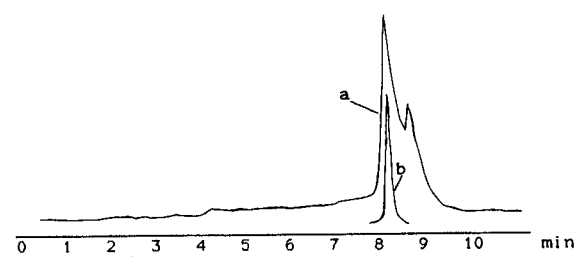

Fig. 3. Chromatograms recorded in a resonance electron-capture GC–MS run for (a) a purified butanol extract of culture liquid and (b) for standard TBDPE.

at this energy are hardly informative, because of up to 65% of the total ion current is associated with the bromine ions. However, knowing exactly the presence of brominated compounds in the sample and their retention times, we could carry out the GC–MS analysis in the positive ion mode and record both compounds. The multiplicity and relative intensities of three peak groups in the high-mass region of the spectrum of the first compound [*m/z* (%): 536 (16), 534 (65), 532 (100), 530 (70), 528 (18), 440 (14), 438 (42), 436 (43), 434 (15), 374 (9), 372 (17) and 370 (8)] coincided with the spectrum of TBDPE (it was impossible to compare the low-mass region owing to the high level of noise). The spectrum of the second compound established that its molecular mass is 72 u higher than that of TBDPE, and the multiplicity of the molecular ion region indicated the presence of four bromine atoms in this substance also. This result confirmed the inferences which were made above on the basis of the REC-MS data.

Hence the described technique allowed the removal of chemical noise and the identification of brominated diphenyl ethers in the culture liquid of the strain *Vibrio* sp. at concentrations not higher than 3–6 μl/l. Such an approach, with identification by retention time, energy of capture and masses, may be expected to be effective in the search for physiologically active substances in complex mixtures.

ACKNOWLEDGEMENT

We thank N. M. Shepetova for helping us to translate this paper.

REFERENCES

1 T. Kosuge, K. Tsuji, K. Hirai and T. Fukuyama, *Chem. Pharm. Bull.*, 33 (1985) 3059.
2 M. Yotsu, T.Yamazaki, Y. Meguro, A. Endo, M. Murata, H. Naoko and T. Yasumoto, *Toxicon*, 25 (1987) 225.
3 A. C. Stierle, J. H. Cardellina and F. L. Singleton, *Experientia*, 44 (1988) 1021.
4 P. C. Uden, Y. Yoo, T. Wang and Z. Cheng, *J. Chromatogr.*, 468 (1989) 319.
5 T. Oster, A. Kuhn and E. Illenberger, *Int. J. Mass Spectrom. Ion Processes*, 89 (1989) 1.
6 N. I. Utkina, M. V. Kazantseva and V. A. Denisenko, *Khim. Prirod. Soedin.*, 4 (1987) 603.

Journal of Chromatography, 586 (1991) 363–366
Elsevier Science Publishers B.V., Amsterdam

CHROM. 23 670

Short Communication

Determination of calcium ion in the presence of phosphate anion and collagen by capillary-type isotachophoresis

Satoru Matsushita and Masami Sugita

Technical Center for Leather, Hyogo Prefectural Institute of Industrial Research, 3 Higashigawara, Nozato, Himeji-shi, 670 (Japan)

Itaru Motooka

Department of Chemistry, Faculty of General Education, Kobe University, Tsurukabuto, Nada-ku, Kobe-shi 657 (Japan)

Yukio Kanaji

Department of Industrial Chemistry, Faculty of Engineering, Kobe University, Rokkodai-cho, Nada-ku, Kobe-shi 657 (Japan)

(First received April 23rd, 1991; revised manuscript received August 7th, 1991)

ABSTRACT

A new procedure for the determination of Ca^{2+} in the presence of phosphate anion and collagen was developed using capillary-type isotachophoresis. Ca^{2+} could be determined successfully using a leading electrolyte containing $1 \cdot 10^{-2}$ *M* potassium acetate–acetic acid (pH 5.4) and a terminating electrolyte containing $1 \cdot 10^{-2}$ *M n*-hexanoic acid in the presence of collagen. Phosphate anion influenced the determination of Ca^{2+} at pH greater than 3 but not at pH 2–3. The calcium in several calcium phosphates was determined successfully by adjusting the pH of sample solutions made from them to between 2 and 3 with hydrochloric acid.

INTRODUCTION

We are studying the synthesis of collagen–hydroxyapatite composites using the hydration [1–6] of α-tricalcium phosphate (α-TCP) in collagen solution. As the determination of Ca^{2+} in this process is influenced by phosphate anions, etc., it is necessary to pretreat samples before analysis [7]. Capillary-type isotachophoresis (ITP) has excellent selectivity [8] for each ion, but it has rarely been applied to the estimation of Ca^{2+} in calcium phosphates. Thus, we examined the determination of Ca^{2+} in the presence of phosphate anions and collagen by ITP in order to apply this method to the analysis of Ca^{2+} in the synthesis of collagen–hydroxyapatite composites and in these materials.

EXPERIMENTAL

Apparatus

A Model IP-2A Shimadzu (Kyoto, Japan) isotachophoretic analyzer equipped with a potential gradient detector was used. As the main column, a fluorinated ethylene propylene copolymer (FEP,

0021-9673/91/$03.50

TABLE I

OPERATING CONDITIONS

Parameter	Electrolyte a		Electrolyte b	
	Leading	Terminating	Leading	Terminating
Cation	H^+	Tris	K^+	H^+
Concentration	$1 \cdot 10^{-2}$ *M*	$1 \cdot 10^{-2}$ *M*	$1 \cdot 10^{-2}$ *M*	$1 \cdot 10^{-2}$ *M*
Counter ion	Cl^-	OH^-	CH_3COO^-	$CH_3(CH_2)_4COO^-$
Concentration	$1 \cdot 10^{-2}$ *M*	$1 \cdot 10^{-2}$ *M*	$1 \cdot 10^{-2}$	$1 \cdot 10^{-2}$ *M*
Solvent	Water	Water	Water (pH 5.4)	Water

Shimadzu) tube (10 cm × 0.5 mm I.D.) and as a precolumn a polytetrafluoroethylene (PTFE, Shimadzu) tube (10 cm × 1.0 mm I.D.) were used. A 2- to 10-μl aliquot of sample solution containing $5 \cdot 10^{-3}$–$1 \cdot 10^{-2}$ *M* Ca^{2+} was injected into the ITP apparatus.

To compare ITP with atomic adsorption spectrometry (AAS), we analyzed the same samples with a Model AA-180 atomic adsorption spectrometer (Nippon Jarrell-Ash, Kyoto, Japan).

Procedure

As operating conditions, the electrolytes a and b shown in Table I were examined. In electrolyte a, $1 \cdot 10^{-2}$ *M* hydrochloric acid was used as the leading electrolyte and $1 \cdot 10^{-2}$ *M* tris(hydroxymethyl)aminomethane (Tris) was used as the terminating electrolyte. The ITP of samples was carried out for 14 min at 150 μA, and then at 100 μA. In electrolyte b, $1 \cdot 10^{-2}$ *M* potassium acetate–acetic acid (pH 5.4) was used as the leading electrolyte and $1 \cdot 10^{-2}$ *M* *n*-hexanoic acid was used as the terminating electrolyte. The ITP of samples was carried out for 13 min at 200 μA, and then at 100 μA.

Materials

All solutions were prepared using guaranteed reagent-grade chemicals. The Ca^{2+} solution was obtained from calcium carbonate dried at 100°C and the phosphate anion solution was obtained from potassium dihydrogenphosphate dried at 100°C. The collagen solution was prepared by dissolving commercial pepsin-solubilized collagen (Koken, Tokyo, Japan) in $1 \cdot 10^{-3}$ *M* hydrochloric acid at 5–10°C. Sample solutions were obtained by mixing the phosphate anion solution or the collagen solution with the Ca^{2+} solution and by dissolving calcium phosphates in diluted hydrochloric acid (pH 2–3).

RESULTS AND DISCUSSION

Operating conditions

Fig. 1 shows the isotachopherograms of Ca^{2+} when 5 μl of a $5 \cdot 10^{-3}$ *M* Ca^{2+} solution were injected into the ITP apparatus. The potential unit (PU) value and the molar response in electrolyte a were larger than in electrolyte b. The calibration

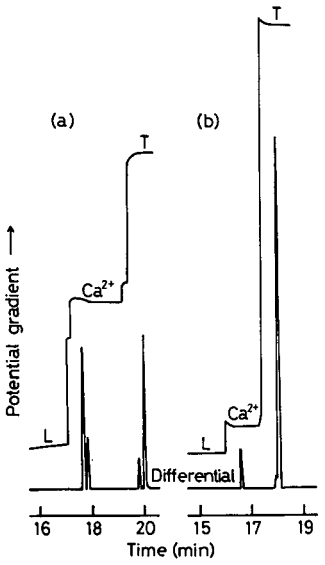

Fig. 1. Isotachopherograms of Ca^{2+}. Conditions (a) and (b) are shown in Table I. Injected sample: 5 μl of 5 m*M* Ca^{2+}. L = leading ion; T = terminating ion.

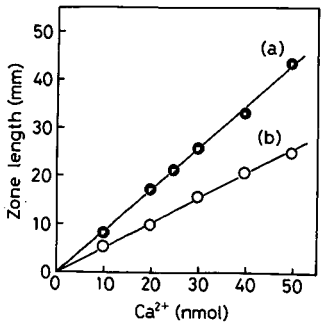

Fig. 2. Calibration curves of Ca^{2+}. Conditions (a) and (b) are shown in Table I.

curves in both conditions were linear from 10 to 50 nmol (Fig. 2). However, as the collagen could be precipitated in the analysis because of the basicity (over pH 7) of the terminating electrolyte in electrolyte a, we adopted the electrolyte system of electrolyte b in this experiment.

The reproducibility of the zone length obtained in analyses of 5 μl of a $1 \cdot 10^{-2}$ M Ca^{2+} standard solution was as follows: $\bar{x}$ (n = 26), 25.3 mm; S.D., 1.1; coefficient of variation (C.V.), 4.4%.

Influence of collagen

To examine the influence of native and denatured (heated for 30 min at 45°C) collagens on the determination of Ca^{2+}, their concentration in $5 \cdot 10^{-3}$ M Ca^{2+} solutions was varied, and the Ca^{2+} in these solutions was estimated when 5 μl of sample solution were injected. The zone length did not change with an increase in collagen concentration, whether native or denatured, when the collagen concentration was low (below about 0.1%).

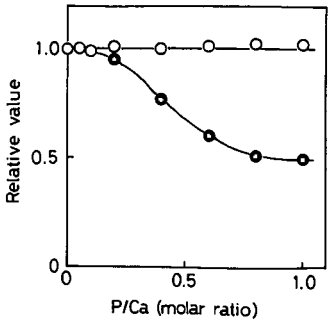

Fig. 3. Comparison of analytical methods for the determination of Ca^{2+} in the presence of phosphate anions. ○ = capillary-type isotachophoresis; ● = atomic adsorption spectrometry.

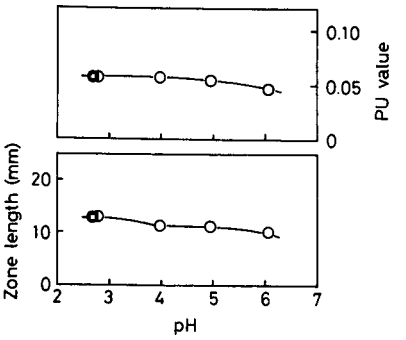

Fig. 4. Influence of pH on the zone lengths and the PU values of Ca^{2+} in the presence of phosphate anions. ○ = pH adjusted with acetic acid and ammonia, containing 0.1 M acetic acid; ● = containing 0.1 M acetic acid; ◐ = no pH adjustment.

Influence of phosphate anion

To examine the influence of the phosphate anion on the analysis of Ca^{2+}, its concentration in $5 \cdot 10^{-3}$ M solution was varied to produce an equimolar ratio (phosphorus/calcium = 1). The Ca^{2+} in these solutions was determined when 5 μl of sample solution were injected. The zone length and the PU value of the samples were the same when the phosphorus/calcium ratio was equimolar. These samples were analyzed by AAS, and the values of these samples relative to samples containing no phosphate anion were calculated for both methods.The relationship between phosphorus/calcium ratio and relative values is shown in Fig. 3. The relative values measured by ITP did not change, but those obtained with AAS decreased as the phosphorus/calcium ratio increased to 0.8, and then to about 0.5. The phosphate anion was found to influence the determination of Ca^{2+} by AAS, but not by ITP.

Influence of pH in the presence of phosphate anion

As the hydration of α-TCP occurs mainly at pH 5–6, we need to analyze the concentration of Ca^{2+} in these solutions. Thus, we examined whether the pH of solutions influences the determination of Ca^{2+} in the presence of equimolar phosphate anion. As shown in Fig. 4, the pH of solutions with no pH adjustment and containing 0.1 M acetic acid was between 2 and 3, and these zone lengths and PU values were the same. When the pH of these solutions was adjusted to 2–3 with dilute hydrochloric acid, the zone lengths and PU values recovered.

TABLE II

CALCIUM CONTENT OF SEVERAL CALCIUM PHOSPHATES

Calcium phosphate	Phosphorus/calcium ratio	Calcium content (%)	
		Measured[a]	Calculated
Calcium pyrophosphate[b]	1.00	31.6	31.5
α-Tricalcium phosphate[c]	0.67	38.3	38.7
Hydroxyapatite[d]	0.60	39.4	39.8

[a] Measured by capillary-type ITP.
[b] Synthesized by heating calcium hydrogenphosphate at 500°C for 1 h.
[c] Synthesized by heating an equimolar mixture of calcium carbonate and calcium pyrophosphate at 1300°C for 2 h.
[d] Commercial product (Isizu, Osaka, Japan).

Consequently, by adjusting the pH of solutions to 2–3, Ca^{2+} could be determined without the influence of the phosphate anion.

Determination of Ca^{2+} in calcium phosphates

We measured Ca^{2+} in sample prepared by dissolving several calcium phosphates with different phosphorus/calcium ratios in dilute hydrochloric acid, and determined their calcium content. As shown in Table II, these measured values were consistent with calculated ones.

REFERENCES

1 H. Monma and T. Kanazawa, *Yogyo-Kyokaishi*, 84 (1976) 209.
2 H. Monma and T. Kanazawa, *Yogyo-Kyokaishi*, 86 (1978) 28.
3 H. Monma and T. Kanazawa, *Yogyo-Kyokaishi*, 86 (1978) 72.
4 H. Monma, S. Ueno and M. Tsutsumi, *Gypsum Lime*, 156 (1978) 190.
5 H. Monma, S. Ueno and T. Kanazawa, *J. Chem. Techn. Biotechnol.*, 31 (1981) 15.
6 H. Monma, M. Goto and T. Kohmura, *Gypsum Lime*, 188 (1984) 11.
7 M. Yanagisawa, M. Suzuki and T. Takeuchi, *Talanta*, 14 (1967) 933.
8 *Shimadzu Capillary Type Isotachophoretic Analyzer Data Sheet*, Shimadzu, Kyoto, 1980.

Author Index

Journal of Chromatography

Request for manuscripts

Zdenek Deyl will edit a special, thematic issue of the *Journal of Chromatography* entitled "**Applications of Chromatography and Electrophoresis in Food Science**". Both reviews and research articles will be included.

Topics such as the following will be covered:

- General strategies for food analysis by chromatographic methods
- Chromatography of volatiles and odours
- Assessing food quality by chromatographic and electrophoretic methods
- Sample preparation for food analysis by chromatography and electrophoresis
- Analysis of toxic substances in food
- Analysis of food colours and dyes
- Analysis of individual food components
- Analysis of agrochemicals and drugs in food
- Analysis of compounds arising during food preparation and storage

Potential authors of reviews should contact Zdenek Deyl (Institute of Physiology, Czechoslovak Academy of Sciences, Vídeňská 1083, CS-14220 Prague, Czechoslovakia; tel.: +42-2-531267; fax: +42-2-4712253) prior to any submission. Research papers should be submitted to the above address as well.

The deadline for receipt of submissions is **January 31, 1992**. Manuscripts submitted after this deadline can still be published in the Journal, but then there is no guarantee that an accepted article will appear in the special, thematic issue. **Three** copies of the manuscript should be submitted to Zdenek Deyl. All manuscripts will be reviewed and acceptance will be based on the usual criteria for publishing in the *Journal of Chromatography*.

Vol. 586, No. 2

Journal of Chromatography

NEWS SECTION

ANNOUNCEMENTS

14TH INTERNATIONAL SYMPOSIUM ON CAPILLARY CHROMATOGRAPHY, BALTIMORE, MD, USA, MAY 25–29, 1992

The scientific program will consist of review papers, invited and submitted papers, poster sessions, and plenary and parallel discussion sessions on the latest developments in, and applications of capillary chromatography, microcolumn and microseparation techniques. Also presented will be a vendor exhibition as well as workshop type discussion sessions encompassing the latest developments in instrumentation. Techniques to be covered include: capillary GC, capillary GC–MS, capillary GC–FTIR, capillary GC–AES, micro HPLC, supercritical fluid chromatography (SFC), capillary zone electrophoresis (CZE), micellar electrokinetic chromatography (MEKC), and new columns and instrumentation. Applications to be covered are: environmental analysis, organic chemicals, pharmaceutical analysis, drug testing, petroleum and petrochemicals, flavors and fragrances, food and beverages, proteins and peptides, trace analysis, and sample preparation techniques.

The deadline for Abstracts (300 words) is November 30, 1991 and should be sent to Prof. Dr. Pat Sandra, Laboratory of Organic Chemistry, University of Ghent, Krijgslaan 281 (S4), B-9000 Ghent, Belgium. Registration costs (including proceedings and social program): prior to April 25, 1992, US$ 375, after April 25th, Full US$ 425, One-day US$ 150, Student US$ 200. Scholarships are available for young scientists.

For further information, contact: Dr. Leonard Schronk, Foundation of the ISCC, P.O. Box 663, Kennett Square, PA 19348, USA. Tel. and Fax: (+1-215) 692-4320.

ISPAC, 5TH INTERNATIONAL SYMPOSIUM ON POLYMER ANALYSIS AND CHARACTERIZATION, INUYAMA, AICHI, JAPAN, JUNE 1–4, 1992

ISPAC is a non-profit scientific organization. The purpose and scope of ISPAC are to provide an international forum for the presentation of recent advances in the field of polymer analysis and characterization methodologies.

This three-day symposium will consist of poster sessions, invited lectures, and round-table discussions and information exchange on recent advances in polymer characterization approaches, techniques, and applications. Topics will include: chromatography and other separation methods, IR, NMR, mass spectrometry, chemical characterization, light scattering rheology, microscopy, viscometry, surface analysis, thermal analysis, thermodynamics, and solution properties of polymers, as well as general con-

tributions on polymer analysis and characterization. Contributions dealing with other techniques or special classes of polymers will also be included. Invited talks will be tutorial in nature and will include state-of-the-art developments.

The deadline for submission of Abstracts is March 1, 1992.

For further information, contact: Dr. Sadao Mori, Department of Industrial Chemistry, Faculty of Engineering, Mie University, Tsu Mie, 514, Japan. Tel: (+81-592) 32-1211, ext. 3843; Fax: (+81-592) 31-2252. Dr. Howard Barth, Dupont Company, Experimental Station, P.O. Box 80228, Wilmington, DE 19880-0228, USA. Tel: (+1-302) 695-4354; Fax: (+1-302) 695-1351.

CAC-92, 5TH INTERNATIONAL CONFERENCE ON CHEMOMETRICS IN ANALYTICAL CHEMISTRY, MONTREAL, CANADA, JULY 14–17, 1992

The emphasis of this CAC '92 meeting will be on the use of chemometrical methods in the solution of practical analytical problems as well as the development of new techniques and improved chemometrical software.

The scientific program will include invited plenary speakers, contributed research papers, and a selected series of tutorials by experts to help present the basis of these techiques and their application to real world problems.

Topics to be presented will include:

- application and development of techniques of design, optimization, and evaluation of analytical methods, including sampling;
- application of chemometrics to the problems of environmental analytical chemistry;
- signal-, image-, and data-analysis/processing, optimum filtering, parameter estimation, time, series analysis, multivariate calibration and curve resolution;
- application of expert systems to the development and use of analytical methods and instruments.

The conference registration fee is expected to be about US$ 200. The official language of the conference will be English.

For further details contact: International Conference on Chemometrics in Analytical Chemistry, c/o Department of Chemistry, Clarkson University, Potsdam, NY 13699-5810, USA. Tel: (+1-315) 268-3861 (Dr. Hopke); (+1-315) 268-2394 (Dr. Lavine); Fax: (+1-315) 268-6670.

8TH INTERNATIONAL SYMPOSIUM ON CAPILLARY ELECTROPHORESIS AND ISOTACHOPHORESIS, ROME, ITALY, OCTOBER 6–9, 1992

This meeting is the eighth of a biennial series, the last one being held in High Tatras, CS. The meeting will begin with a one day workshop October 6, 1992, featuring a short course on capillary electrophoresis for young researchers who would like to start with these techniques.

Invited lectures, oral communications and poster sessions will be the basis for wide discussion during the three day symposium on October 7–9. The scientific program will cover all aspects of capillary zone electrophoresis, isotachophoresis, micellar electrokinetic chromatography, isoelectric focusing, instrumentation, gel filled capillaries, capillary technology and applications.

The deadline for submission of abstracts is April 15, 1992. The official language of the symposium will be english.

For further information contact: Dr. Salvatore Fanali, Istituto di Cromatografia del C.N.R., P.O. Box 10, 00016 Monterotondo Scalo (Rome), Italy. Tel: (+39-6) 9005328/9005836; Fax: (39-6) 9005849; Telex: 624809 CNR ML 1.

12TH INTERNATIONAL SYMPOSIUM ON HIGH-PERFORMANCE LIQUID CHROMATOGRAPHY OF PROTEINS, PEPTIDES AND POLYNUCLEOTIDES, SYDNEY, AUSTRALIA, NOVEMBER 29–DECEMBER 2, 1992

This international meeting will bring together world experts to examine new developments and applications in the areas of HPLC and other high resolution techniques for the analysis and purification of

proteins, peptides, polynucleotides and their chemical mimetics. Sessions will also include advances in biopharmaceutical, carbohydrate and lipid analysis. The program will include invited and contributed lectures, poster presentations and discussion sessions.

You are invited to submit Abstracts describing original research in areas including: electrokinetic separations, column technology and support material, protein conformation and chromatographic behaviour, polypeptide structural studies, protein purity and QC of recombinant proteins, polynucleotides, polysaccharides, membrane proteins, lipids and lipoproteins, affinity chromatography, analytical applications, sample preparation, preparative chromatography of biopolymers, high resolution electrophoresis, integrated purification systems, biospecific detectors, process monitoring, recovery of recombinant proteins, protein–surface interaction, molecular biorecognition, isolation and purification techniques, regulatory issues and quality control, detection and amplification, electrophoresis, separation and protein engineering, membrane technology and special topics. The Scientific Committee welcomes your suggestions for additional topics to be covered in the Symposium. The deadline for submission of Abstracts is June 10, 1992.

The registration fee will be A$ 495 before September 30, 1992 and includes admission to all scientific sessions, one copy of the final program and a book of abstracts, one copy of the Proceedings and social program. Students are eligble for a reduced rate at A$ 325 (Proceedings not included). After September 30, 1992 the fee will be A$ 545 full registration and A$ 365 for students.

Papers presented at the Symposium will be published in a special issue of the *Journal of Chromatography* provided the instructions issued by the Editor are carefully followed.

For further information contact: 12 ISPPP Sectretariat, GPO Box 128, Sydney, NSW 2001, Australia. Tel.: (+61-2) 262-2277; Fax: (+61-2) 262-2323.

HPLC '93, 17TH INTERNATIONAL SYMPOSIUM ON COLUMN LIQUID CHROMATOGRAPHY, HAMBURG, GERMANY, MAY 9–14, 1993

The Symposium will cover all aspects of high-performance liquid chromatography (HPLC) and related high resolution separation techniques. The sessions will address advances in: sample preparation and derivatization, various areas in both analytical separations and preparative isolation and purification, novel detectors and detections methods, hyphenated techniques, miniaturization (microbore and capillary LC), biopolymer separations, supercritical fluid chromatography, field flow fractionation, capillary electrophoresis and electrokinetic chromatography and chemometrical applications. This 5-day symposium will include invited lectures, contributed presentations, posters and panel discussions.

A planned exhibition of instruments will be integrated into the poster session. Interested exhibitors are requested to contact the secretariat for further information.

Abstracts for presentations should be submitted by July 31, 1992. The deadline for registering is March 19, 1993.

For further details contact: Gesellschaft Deutscher Chemiker, Abteilung Tagungen, P.O. Box 900440, Varrentrappstrasse 40-42, W-6000 Frankfurt am Main 90, Germany. Tel: (+49-69) 7917-360; Fax: (+49-69) 7917-475.

Announcements are included free of charge. Information on planned events should be sent well in advance (6 months) to: Journal of Chromatography, News Section, P.O. Bov 330, 1000 AH Amsterdam, Netherlands, or by Fax: (+31 20) 5862304.

CALENDAR OF FORTHCOMING EVENTS

□ **Dec. 4–5, 1991**
Wiesbaden, Germany
European Symposium on Analytical Supercritical Fluid Chromatography and Extraction
Contact: Karin Markides, Analytical Chemistry, Uppsala University, Box 531, S-751 21 Uppsala, Sweden. Tel.: (+46-18) 182500; Fax: (+46-18) 108542.

Dec. 9–11, 1991
Storlien, Sweden
EUCHEM Conference on Capillary Electroseparations
Contact: Dr. Agneta Sjögren, The Swedish National Committee for Chemistry, Wallingatan 26B, S-111 24 Stockholm, Sweden. Tel.: (+46-8) 115260; Fax: (+46-8) 106678.

Jan. 6–11, 1992
San Diego, CA, USA
1992 Winter Conference on Plasma Spectrochemistry
Contact: Dr. R. Barnes, c/o ICP Information Newsletter, Department of Chemistry, CRC Towers, University of Massachusetts, Amherst, MA 01003-0035, USA. Tel.: (413) 545-2294; Fax: (413) 545-4490; Bitnet: RBARNES@UMASS.

Feb. 9–13, 1992
Amsterdam, Netherlands
HPCE '92, 4th International Symposium on High Performance Capillary Electrophoresis
Contact: Shirley E. Schlessinger, HPCE '92, 400 East Randolph Drive, Suite 1015, Chicago, IL 60601, USA. Tel.: (312) 527-2011.

Feb. 17–18, 1992
Antwerp, Belgium
Hands-on Workshops on: Supercritical Fluid Extraction and Supercritical Fluid Chromatography; on Liquid Chromatography–Gas Chromatography; and on Hyphenated Techniques in Capillary Gas Chromatography: Mass Spectrometry, Fourier Transform Infrared Spectroscopy, Atomic Emission Detection
Contact: Dr. R. Smits, p.a. BASF Antwerpen N.V., Central Laboratory, Scheldelaan, B-2040 Antwerp, Belgium.

Feb. 18–21, 1992
Antwerp, Belgium
2nd International Symposium on Hyphenated Techniques in Chromatography
Contact: Dr. R. Smits, p.a. BASF Antwerpen N.V., Scheldelaan, B-2040 Antwerp, Belgium. Tel.: (323) 5682831; Fax: (323) 5683355; Telex: 31047 basant b.

March 9–13, 1992
New Orleans, LA, USA
43rd Pittsburgh Conference and Exposition on Analytical Chemistry and Applied Spectroscopy
Contact: Mrs. Alma Johnson, Program Secretary, The Pittsburgh Conference, 300 Penn Center Boulevard, Suite 332, Pittsburgh, PA 15235-5503, USA.

April 6–8, 1992
Atlanta, GA, USA
ANATECH '92, 3rd International Symposium on Analytical Techniques for Industrial Process Control
Contact: ANATECH '92, Infosciences Inc., 3000 Dundee Road, Suite 313, Northbrook, IL 60062, USA. Tel.: (708) 291-9161; Fax: (708) 291-0097.

April 6–8, 1992
Nancy, France
PREP-92, 9th International Symposium on Preparative and Industrial Chromatography
Contact: PREP-92 Secretary, E.N.S.I.C.-L.P.C.I., 1 rue Grandville, B.P. 451, F-54001 Nancy Cedex, France. Tel.: (+33) 83300276; Fax: (+33) 83350811.

May 5–8, 1992
Liège, Belgium
4th International Symposium on Drug Analysis
Contact: Dr. J. Crommen, Drug Analysis '92-Liège, University of Liège, Institute of Pharmacy, rue Fusch 5, B-4000 Liège, Belgium. Tel.: (+32-41) 237002; Fax: (+32-41) 221855.

May 5–8, 1992
Munich, Germany
13th International Conference on Biochemical Analysis
Contact: U. Arnold, Nymphenburger Strasse 70, D-8000 Munich 2, Germany. Tel.: (+49-89) 1234500; Fax: (+49-89) 183258.

May 12–14, 1992
La Grand Motte, France
4th European Meeting of Groupe Français de Bio-Chromatographie
Contact: Groupe Français de Bio-Chromatographie, Unité

d'Immuno Allergie, Institut Pasteur, 28 rue du Docteur Roux, 75724 Paris Cedex 15, France. Tel.: (+33-1) 45688000, ext. 7143; Fax: (+33-1) 43069835; Telex: 250609 F.

May 17–22, 1992
Kyoto, Japan
4th International Conference on Fundamentals of Adsorption
Contact: Prof. M. Suzuki, Conference Chairman, Institute of Industrial Science, University of Tokyo, 7-22-1 Roppongi, Minato-ku, Tokyo 106, Japan.

■ **May 25–29, 1992**
Baltimore, MD, USA
14th International Symposium on Capillary Chromatography
Contact: Dr. Leonard Schronk, Foundation for the ISCC, P.O. Box 663, Kennett Square, PA 19348, USA. Tel. and Fax: (+1-215) 692-4320.

■ **June 1–4, 1992**
Inuyama, Aichi, Japan
ISPAC, 5th International Symposium on Polymer Analysis and Characterization
Contact: Dr. Sadao Mori, Department of Industrial Chemistry, Faculty of Engineering, Mie University, Tsu, Mie 514, Japan. Tel: (+81-592) 32-1211, ext. 3843; Fax: (+81-592) 31-2252. Dr. Howard Barth, Dupont Company, Experimental Station, P.O. Box 80228, Wilmington, DE 19880-0228, USA. Tel: (+1-302) 695-4354; Fax: (+1-302) 695-1351.

June 9–2, 1992
Dortmund, Germany
22nd Roland W. Frei Memorial Symposium on Environmental Analytical Chemistry and Workshop on Detection in Environmental Analysis
Contact: Symposium Office IAEAC, M. Frei-Hausler, P.O. Box 46, CH-4123 Allschwil 2, Switzerland. Tel.: (+41-61) 632789; Fax: (+41-61) 4820805.

June 14–19, 1992
Baltimore, MD, USA
HPLC '92, 16th International Conference on Column Liquid Chromatography
Contact: HPLC '92, Ms. Shirley E. Schlessinger, 400 E. Randolph Drive, Suite 1015, Chicago, IL 60601, USA. Tel.: (312) 527-2011.

■ **July 14–17, 1992**
Montreal, Canada
CAC-92, 5th International Conference on Chemometrics in Analytical Chemistry
Contact: International Conference on Chemometrics in Analytical Chemistry, c/o Department of Chemistry, Clarkson University, Potsdam, NY 13699-5810, USA. Tel: (+1-315) 268-3861 (Dr. Hopke); (+1-315) 268-2394 (Dr. Lavine); Fax: (+1-315) 268-6670.

Aug. 24–27, 1992
Jena, Germany
COMPANA '92, 5th Conference on Computer Applications in Analytical Chemistry
Contact: COMPANA '92, Friedrich Schiller University Jena, Institute of Inorganic and Analytical Chemistry, Steiger 3, Haus 3, O-6900 Jena, Germany. Tel.: (+37-82) 25467 or (+37-82) 25029.

Aug. 31–Sept. 3, 1992
Cincinnati, OH, USA
106th Annual International Meeting and Exposition of the Association of Official Analytical Chemists
Contact: Margaret Ridgell, AOAC, 2200 Wilson Boulevard, Suite 400, Arlington, VA 22201-3301, USA. Tel.: (703) 522-3032; Fax: (703) 522-5468.

Sept. 13–18, 1992
Aix-en-Provence, France
19th International Symposium on Chromatography
Contact: G.A.M.S., 88 Boulevard Malesherbes, 75008 Paris, France. Tel.: (1) 45639304; Fax: (1) 49530434

■ **Oct. 5–8, 1992**
Tübingen, Germany
3rd International Symposium on Chiral Discrimination
Contact: Gesellschaft Deutscher Chemiker, Abteilung Tagungen, P.O. Box 90 04 40, D-6000 Frankfurt 90, Germany. Fax: (+49-69) 791-7475

■ **Oct. 6–9, 1992**
Rome, Italy
ITP '92, 8th International Symposium on Capillary Electrophoresis and Isotachophoresis
Contact: Dr. Salvatore Fanali, Istituto di Cromatografia del C.N.R., P.O. Box 10, 00016 Monterotondo Scalo (Rome), Italy. Tel: (+39-6) 9005328/9005836; Fax: (+39-6) 9005849; Telex: 624809 CNR ML 1.

Nov. 4–6, 1992
Montreux, Switzerland
9th Montreux Symposium on

Liquid Chromatography–Mass Spectrometry (LC–MS, SFC–MS, CZE–MS, MS–MS)

Contact: Marianne Frei, IAEAC Secretariat, P.O. Box 46, CH-4123 Allschwil, Switzerland. Tel.: (+41-61) 632789; Fax: (+41-61) 4820805.

Nov. 29–Dec. 2, 1992
Syndey, Australia
12th International Symposium on HPLC of Proteins, Peptides and Polynucleotides

Contact: 12 ISPPP Sectretariat, GPO Box 128, Sydney NSW 2001, Australia. Tel.: (+61-2) 262-2277; Fax: (+61-2) 262-2323.

■ **May 9–14, 1993**
Hamburg, Germany
17th International Symposium on Column Liquid Chromatography

Contact: Gesellschaft Deutscher Chemiker, Abteilung Tagungen, P.O. Box 900440, Varrentrappstrasse 40-42, W-6000 Frankfurt am Main 90, Germany. Tel: (+49-69) 7917-360; Fax: (+49-69) 7917-475.

Sept. 5–11, 1993
Edinburgh, UK
EUROANALYSIS VIII, 8th European Conference on Analytical Chemistry

Contact: Miss P.E. Hutchinson, Analytical Division, The Royal Society of Chemistry, Burlington House, Piccadilly, London W1V 0BN, UK. Tel.: (071) 4378656; Fax: (071) 734-1227; Telex: 268001.

June 20–24, 1994
Bournemouth, UK
20th International Symposium on Chromatography

Contact: Executive Secretary, The Chromatographic Society, Nottingham Polytechnic, Burton Street, Nottingham, NG1 4BU, UK. Tel.: (0602) 500596; Fax: (0602) 500614.

■ Indicates new or amended entry.

PUBLICATION SCHEDULE FOR 1992

Journal of Chromatography and *Journal of Chromatography, Biomedical Applications*

MONTH	O 1991	N 1991	D 1991	
Journal of Chromatography	585/1	585/2 586/1 586/2 587/1	587/2 588/1+2	The publication schedule for further issues will be published later
Cumulative Indexes, Vols. 551–600				
Bibliography Section				
Biomedical Applications				

INFORMATION FOR AUTHORS

(Detailed *Instructions to Authors* were published in Vol. 558, pp. 469–472. A free reprint can be obtained by application to the publisher, Elsevier Science Publishers B.V., P.O. Box 330, 1000 AH Amsterdam, The Netherlands.)

Types of Contributions. The following types of papers are published in the *Journal of Chromatography* and the section on *Biomedical Applications*: Regular research papers (Full-length papers), Review articles and Short Communications. Short Communications are usually descriptions of short investigations, or they can report minor technical improvements of previously published procedures; they reflect the same quality of research as Full-length papers, but should preferably not exceed five printed pages. For Review articles, see inside front cover under Submission of Papers.

Submission. Every paper must be accompanied by a letter from the senior author, stating that he/she is submitting the paper for publication in the *Journal of Chromatography*.

Manuscripts. Manuscripts should be typed in double spacing on consecutively numbered pages of uniform size. The manuscript should be preceded by a sheet of manuscript paper carrying the title of the paper and the name and full postal address of the person to whom the proofs are to be sent. As a rule, papers should be divided into sections, headed by a caption (*e.g.*, Abstract, Introduction, Experimental, Results, Discussion, etc.). All illustrations, photographs, tables, etc., should be on separate sheets.

Introduction. Every paper must have a concise introduction mentioning what has been done before on the topic described, and stating clearly what is new in the paper now submitted.

Abstract. All articles should have an abstract of 50–100 words which clearly and briefly indicates what is new, different and significant.

Illustrations. The figures should be submitted in a form suitable for reproduction, drawn in Indian ink on drawing or tracing paper. Each illustration should have a legend, all the *legends* being typed (with double spacing) together on a *separate sheet*. If structures are given in the text, the original drawings should be supplied. Coloured illustrations are reproduced at the author's expense, the cost being determined by the number of pages and by the number of colours needed. The written permission of the author and publisher must be obtained for the use of any figure already published. Its source must be indicated in the legend.

References. References should be numbered in the order in which they are cited in the text, and listed in numerical sequence on a separate sheet at the end of the article. Please check a recent issue for the layout of the reference list. Abbreviations for the titles of journals should follow the system used by *Chemical Abstracts*. Articles not yet published should be given as "in press" (journal should be specified), "submitted for publication" (journal should be specified), "in preparation" or "personal communication".

Dispatch. Before sending the manuscript to the Editor please check that the envelope contains four copies of the paper complete with references, legends and figures. One of the sets of figures must be the originals suitable for direct reproduction. Please also ensure that permission to publish has been obtained from your institute.

Proofs. One set of proofs will be sent to the author to be carefully checked for printer's errors. Corrections must be restricted to instances in which the proof is at variance with the manuscript. "Extra corrections" will be inserted at the author's expense.

Reprints. Fifty reprints of Full-length papers and Short Communications will be supplied free of charge. Additional reprints can be ordered by the authors. An order form containing price quotations will be sent to the authors together with the proofs of their article.

For Superior Chiral Separation From Analytical To Preparative.

The finest from DAICEL……

Why look beyond DAICEL? We have developed the finest CHIRALCEL, CHIRALPAK and CROWNPAK with up to 17 types of HPLC columns, all providing superior resolution of racemic compounds.

NEW CHIRALPAK AS

● CHIRALPAK AS

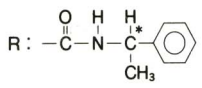

for β-Lactam antibiotics

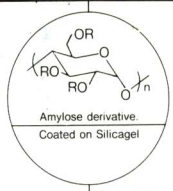

NEW CHIRALPAK AD

● CHIRALPAK AD

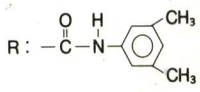

1-Acetoxy-2-azetidine

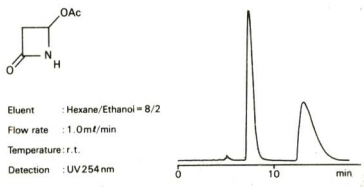

Oxyphencyclimine

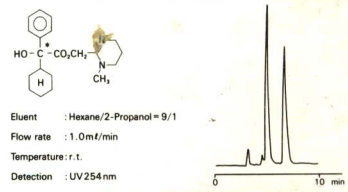

Ofloxacine methyl ester

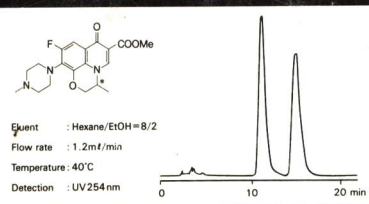

Verapamil

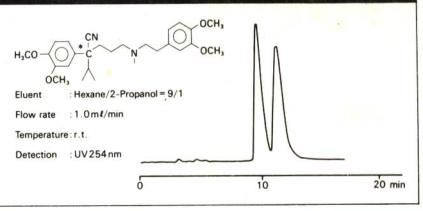

Analytical column 0.46cm × 25cm(10μm)

CHIRALCEL OA
OB
OC
OD
OJ
OF
OG
OK

CHIRALPAK AS
AD

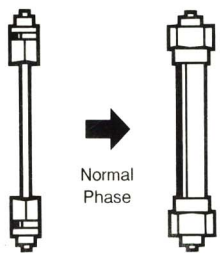

Normal Phase

Semi-preparative column 2cm × 25cm(10μm)

You can have Pure enantiomer quickly!!

■Separation Service

- A pure enantiomer separation in the amount of 100g ~ 10kg is now available.
- Please contact us for additional information regarding the manner of use and application of our chiral columns and how to procure our separation service.

DAICEL CHEMICAL INDUSTRIES, LTD.

chiral chemicals division.
8-1, Kasumigaseki 3-chome, Chiyoda-ku, Tokyo 100, Japan Phone: 03 (507) 3151 FAX: 03 (507) 3193

DAICEL(U.S.A.), INC.
Fort Lee Executive Park
Two Executive Drive, Fort Lee,
New Jersey 07024
Phone: (201) 461-4466
FAX: (201) 461-2776

DAICEL(U.S.A.), INC.
23456 Hawthorne Blvd.
Bldg. 5, Suit 130
Torrance, CA 90505
Phone: (213) 791-2030
FAX: (213) 791-2031

DAICEL(EUROPA)GmbH
Oststr. 22
4000 Düsseldorf 1, F.R. Germany
Phone: (211) 369848
Telex: (41) 8588042 DCEL D
FAX: (211) 364429

DAICEL CHEMICAL(ASIA)PTE. LTD.
65 Chulia Street #40-07
OCBC Centre, Singapore 0104
Phone: 5332511
FAX: 5326454